UCLA
UCLA Electronic Theses and Dissertations

Title
Classical Physics and Complete Gravitational Theories from Scattering Amplitudes

Permalink
https://escholarship.org/uc/item/3h07n5x5

Author
Kosmopoulos, Dimitrios

Publication Date
2022

Peer reviewed|Thesis/dissertation

UNIVERSITY OF CALIFORNIA

Los Angeles

Classical Physics and Complete Gravitational Theories from Scattering Amplitudes

A dissertation submitted in partial satisfaction

of the requirements for the degree

Doctor of Philosophy in Physics

by

Dimitrios Kosmopoulos

2022

ABSTRACT OF THE DISSERTATION

Classical Physics and Complete Gravitational Theories from Scattering Amplitudes

by

Dimitrios Kosmopoulos

Doctor of Philosophy in Physics

University of California, Los Angeles, 2022

Professor Zvi Bern, Chair

Amplitudes methods have been successfully applied to various physical situations. In this manuscript we present their application to two quite distinct problems: classical gravitational-wave physics and constraining gravitational theories beyond general relativity. In chapter 1 we develop two methods for simplifying a computationally intense step in amplitudes calculations, specifically the sum over the physical states of photons and gravitons. These methods, even though generic, are developed with the application of gravitational-wave physics in mind. In chapters 2 and 3 we compute novel corrections to the Newtonian gravitational potential experienced by two spinning objects. These corrections originate in general-relativity effects. In chapter 4 we obtain bounds on Wilson coefficients of four-dimensional gravitational effective field theories. By calculating explicit examples of consistent gravitational theories and extracting the corresponding Wilson coefficients, we find that they occupy tiny islands in the Wilson-coefficient space derived. In chapter 5 we extend this analysis to dimensions higher than four. We again construct explicit gravitational theories and observe that the corresponding Wilson coefficients land in similar regions.

The dissertation of Dimitrios Kosmopoulos is approved.

Thomas Dumitrescu

Michael Gutperle

Per J. Kraus

Zvi Bern, Committee Chair

University of California, Los Angeles

2022

To my mother, father, and sister,

who encourage me to follow my dreams regardless of how far from them they may take me.

To my wife,

whose support is one of the main reasons I believe I can make them come true.

TABLE OF CONTENTS

LIST OF FIGURES

LIST OF TABLES

ACKNOWLEDGMENTS

 I wish to thank my advisor, Zvi Bern, for guiding me towards the most interesting and relevant projects, for providing me with the resources to perform high-level research, for getting me in contact with expert scientists in the field, and most importantly for being there to address my questions and worries, whether big or small.

I thank Andrés Luna and Alexander Zhiboedov for beautiful collaborations in the early stages of my graduate career which helped me mature as a scientist and prepared me to apply for a post-doctoral position. I am also grateful to Enrico Herrmann, Radu Roiban, and Fei Teng for being great collaborators in past and current projects.

I thank Chia-Hsien Shen, Fei Teng, and especially Alexander Edison for their deep physics insights and for sharing their expertise in using computer programs necessary for calculations. I thank Mikhail Solon for our amazing collaboration and his great mentorship both on research and life in academia. I thank Michael Gutperle for his support and mentorship throughout my graduate studies. I also wish to thank the other members of our group with whom we have spent countless hours discussing physics: Callum Jones, David Chester, Eric Sawyer, Jared Claypoole, Juan Pablo Gatica, Julio Parra-Martinez, Michael Enciso, Michael Ruf, Trevor Scheopner.

I finally wish to thank my wife, Alexandra Latshaw, whose support and love helped me overcome all challenges of graduate life.

CONTRIBUTION OF AUTHORS

Chapter 1 is based on Ref. [1]. Chapter 2 is based on Ref. [2] which includes work done in collaboration with Andrés Luna. Chapter 3 reports work done in collaboration with Zvi Bern, Andrés Luna, Radu Roiban and Fei Teng and is based on Ref. [3]. Chapter 4 is based on Ref. [4] with Zvi Bern and Alexander Zhiboedov. Finally, chapter 5 includes work in collaboration with Zvi Bern, Enrico Herrmann and Radu Roiban which appeared in Ref. [5].

2016	Bachelor of Science, Physics, National and Kapodistrian University of Athens
2017	Master of Science, Physics, University of California, Los Angeles (UCLA)
2017–2020	Teaching Assistant, Physics Department, University of California, Los Angeles (UCLA)
2019–Present	Graduate Researcher, Physics Department, University of California, Los Angeles (UCLA)

PUBLICATIONS

Z. Bern, E. Herrmann, **D. Kosmopoulos**, R. Roiban, "Effective Field Theory Islands from Perturbative and Nonperturbative Four-Graviton Amplitudes,"
arXiv:2205.01655 [hep-th],

Z. Bern, **D. Kosmopoulos**, A. Luna, R. Roiban, F. Teng, "Binary Dynamics Through the Fifth Power of Spin at $\mathcal{O}(G^2)$,"
arXiv:2203.06202 [hep-th],

Z. Bern, **D. Kosmopoulos**, A. Zhiboedov, "Gravitational Effective Field Theory Islands, Low-Spin Dominance, and the Four-Graviton Amplitude,"
J. Phys. A **54**, no.34, 344002 (2021) | arXiv:2103.12728 [hep-th],

D. Kosmopoulos, A. Luna, "Quadratic-in-Spin Hamiltonian at $\mathcal{O}(G^2)$ from Scattering Amplitudes,"

JHEP **07**, 037 (2021) | arXiv:2102.10137 [hep-th],

D. Kosmopoulos, "Simplifying D-Dimensional Physical-State Sums in Gauge Theory and Gravity,"

Phys. Rev. D **105**, 056025 (2022) | arXiv:2009.00141 [hep-th].

CHAPTER 1

Simplifying D-Dimensional Physical-State Sums in Gauge Theory and Gravity

We provide two independent systematic methods of performing D-dimensional physical-state sums in gauge theory and gravity in such a way so that spurious light-cone singularities are not introduced. A natural application is to generalized unitarity in the context of dimensional regularization or theories in higher spacetime dimensions. Other applications include squaring matrix elements to obtain cross sections, and decompositions in terms of gauge-invariant tensors.

1.1 Introduction

The past years have seen remarkable advances to our ability to calculate scattering amplitudes in perturbative quantum field theory. On the one hand, much of this progress relies on choices of variables that exploit the four-dimensional nature of the kinematics, such as spinor-helicity [6, 7, 8, 9, 10] or momentum-twistor [11] variables. On the other hand, for certain problems it is favorable to work in arbitrary dimension D. For example, D-dimensional methods proved useful in the recent evaluation of the conservative two-body Hamiltonian for spinless black holes to order G^3 [12, 13], relevant to gravitational-wave physics studied by the LIGO and Virgo collaborations [14, 15].

In multiloop calculations, the preferred regularization scheme is dimensional regularization [16]. Occasionally, subtleties arise when one combines four-dimensional methods with dimensional regularization. In these instances D-dimensional methods are necessary, as

was the case for example in the recent reexamination of the two-loop counterterm of pure gravity [17]. Furthermore, we are often interested in performing a calculation in a generic dimension. The calculation of the gravitational potential between two scalar particles in arbitrary dimension at order G^2 [18] is a recent illustration.

A prominent method used in D-dimensional calculations is generalized unitarity. Generalized unitarity was orginally developed for four-dimensional computations [19, 20], but has since been extended to higher dimensions [21, 22, 23, 24, 25, 26, 27, 28, 29]. D-dimensional generalized unitarity has been employed in calculations pertaining to phenomenology at the Large Hadron Collider (LHC) (see for e.g. [30, 31]), as well as in the study of supersymmetric theories [32]. It meshes well with other modern amplitudes techniques, such as the double copy [33, 34, 35], and as such is a natural tool for computations in gravitational theories [36, 37, 38]. Recently, Ref. [39] used generalized unitarity for a worldsheet theory. These important and diverse results underline the significance of simplifying as much as possible the implementation of D-dimensional generalized unitarity.

A difficulty we encounter when we work in D dimensions is that physical-state sums for gluons and gravitons introduce spurious light-cone singularities that complicate the calculation. If we do not eliminate these spurious singularities at the level of the integrand, we have to regularize them with the Mandelstam-Leibbrandt [40, 41] or principle-value [42, 43, 44] prescription for example, which complicates integration.

In this chapter we develop two methods for performing these sums so that we do not introduce spurious singularities. Refs. [45, 12, 13, 46] showed that in certain four-point amplitudes by appropriate arrangements the spurious light-cone singularities automatically drop out in generalized-unitary cuts. Here we provide methods to systematically eliminate such spurious singularities from any generalized-unitarity cut or any sewing involving gauge-invariant quantities at any loop order.

We may apply our methods to a variety of situations, some of which we depict in Fig. 1.1. For calculations based on generalized unitarity [19, 20], while in some cases it is sufficient to compute the generalized-unitarity cuts in four-dimensions [47, 48], in others we need to know
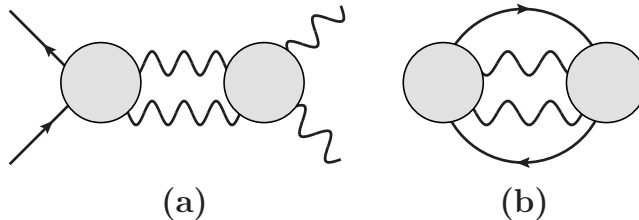
Figure 1.1: Examples of calculations where we may apply the techniques of this chapter: (a) integrand-level generalized-unitarity cut and (b) squared matrix elements for cross sections. The blobs represent amplitudes. All exposed lines are taken as on shell. The internal exposed lines indicate gauge-particle legs that we intend to sew.

them in $D = 4 - 2\epsilon$ dimensions [21, 22, 23, 24, 25, 26, 27, 28, 29]. In some cases, matrix-element squares, useful in calculations of cross sections, are calculated in D dimensions [49, 50, 51, 52]. Furthermore, a useful technique that relies on physical-state sums is the decomposition of an amplitude into gauge-invariant tensors [53, 54, 55, 56, 57, 58].

In this chapter we provide two independent methods of performing the physical-state sums so that we do not introduce spurious singularities. In the first method we identify gauge-invariant subpieces (two in gauge theory and three in gravity) of our expression and perform the physical-state sum for each subpiece separately. This allows us to substitute the physical-state projectors with replacements rules for the individual subpieces that do not contain spurious singularities. In our second method we provide a simple systematic way to make a gauge-invariant quantity obey the generalized Ward identity, such that the spurious-singularity pieces automatically drop out of the physical-state sum. We find that there are certain limitations in the applicability of the second approach, which however are not relevant for many practical purposes.

We focus on theories that contain scalars, photons, gluons and gravitons for concreteness. However, we may straightforwardly apply our techniques to theories with different matter content. Some examples are theories that contain fermions or higher-spin fields [46, 59].

We organize the remainder of the chapter as follows. In Sect. 1.2 we review a few properties that are useful for our purposes and establish our conventions. In Sect. 1.3 we

discuss our first method of performing the physical-state sums. We describe how to isolate the gauge-invariant subpieces of an expression and how to perform the physical-state sum for each one. In Sect. 1.4 we describe our second method. We explain how to bring an expression in the appropriate form and how to use that form to remove the spurious-singularity pieces from the physical-state projectors. We present our conclusions in Sect. 1.5.

1.2 Background and definitions

In this chapter we study gauge and gravitational theories. We refer to the particles associated with these theories, namely the gluon and the graviton, as gauge particles. We describe the state of a gluon by a null polarization vector ε^μ, as appropriate for circular polarization. We express the polarization tensor that describes the state of the graviton as a product of two factors of the polarization vector of the gluon, $\varepsilon^{\mu\nu} = \varepsilon^\mu \varepsilon^\nu$. This polarization tensor is traceless since the gluon polarization vectors are taken to be null. With this construction we may collectively describe the gauge particle by its polarization vector ε^μ.

We analyse the sewing of gauge-invariant quantities. By sewing we refer to performing the physical-state sum of some gauge-particle legs that belong to these quantities. We denote gauge-invariant quantities by $\mathcal{A}$ and refer to them as amplitudes. Our results, however, apply to any gauge-invariant quantities. They apply for example to higher-loop generalized-unitarity cuts [19, 20] or gauge-invariant tensors [53, 54, 55, 56, 57, 58].

When a quantity is gauge invariant, then it satisfies the Ward identity (WI) for each gauge particle. The WI states that when the polarization vector of a single gauge particle ε is replaced by the particle's momentum p, then the amplitude vanishes:

$$\mathcal{A}\big|_{\varepsilon_\mu \to p_\mu} = 0 \quad \text{(gauge theory)}, \quad \mathcal{A}\big|_{\varepsilon_\mu \varepsilon_\nu \to p_\mu q_\nu} = 0 \quad \text{(gravity)}. \tag{1.1}$$

In the gravitational case, one of the two factors of the polarization vector is replaced by the corresponding momentum, while the other one by an arbitrary vector q^ν[1]. We emphasize

---

[1]In practice, it is convenient to formally distinguish the two factors (eg. $\varepsilon^{\mu\nu} = \varepsilon^\mu \tilde{\varepsilon}^\nu$) and only set them equal ($\tilde{\varepsilon}^\mu = \varepsilon^\mu$) at the end of the calculation.

that this property is only true upon use of the on-shell conditions. In gravity we have to use the on-shell conditions both before and after the above replacement. Namely, one must use the mass-shell condition for every particle $(p_i^2 = m_i^2)$, momentum conservation $(\sum_i p_i = 0$, where we take all particles to be outgoing), and the fact that polarization vectors are null $(\varepsilon_i^2 = 0)$ and transverse $(\varepsilon_i \cdot p_i = 0)$.

When sewing gauge-invariant quantities, one is instructed to sum over the physical polarizations of the gauge particles of interest. This sum is equal to the physical-state projector. We occasionally refer to performing this sum as inserting the projector. In gauge theory we have

$$P^{\mu\nu}(p, q) = \sum_{\text{pols.}} \varepsilon^\mu(-p)\varepsilon^\nu(p) = \eta^{\mu\nu} - \frac{q^\mu p^\nu + p^\mu q^\nu}{q \cdot p}, \tag{1.2}$$

while in gravity

$$P^{\mu\nu\alpha\beta}(p, q) = \sum_{\text{pols.}} \varepsilon^{\mu\nu}(-p)\varepsilon^{\alpha\beta}(p) = \frac{1}{2}\left(P^{\mu\alpha}P^{\nu\beta} + P^{\nu\alpha}P^{\mu\beta}\right) - \frac{1}{D-2}P^{\mu\nu}P^{\alpha\beta}. \tag{1.3}$$

In both cases p is the momentum of the gauge particle in question, q is an arbitrary null vector and D is the dimension of spacetime. We observe that insertions of the physical-state projectors introduce spurious light-cone singularities $1/q \cdot p$. We call them spurious because they drop out from the final expression, appearing only in intermediate steps of calculations.

In this chapter we develop strategies that allow us to effectively[2] make the following replacement in Eqs. (1.2) and (1.3):

$$P^{\mu\nu}(p, q) \to \eta^{\mu\nu}. \tag{1.4}$$

Specifically, for gravity we effectively get

$$P^{\mu\nu\alpha\beta}(p, q) \to \frac{1}{2}\left(\eta_{\mu\alpha}\eta_{\nu\beta} + \eta_{\mu\beta}\eta_{\nu\alpha} - \frac{2}{D-2}\eta_{\mu\nu}\eta_{\alpha\beta}\right), \tag{1.5}$$

where on the right-hand side we recognize the de Donder projector. Our methods allow us to use Feynman-gauge-like and de Donder-gauge-like sewing rules, while at the same time not introduce any ghost degrees of freedom. We do not achieve this by choosing a specific gauge. Rather, we phrase the whole discussion in terms of on-shell objects.

---

[2]We use the word effectively because the replacement might also need an overall factor. We discuss the details in the following sections.
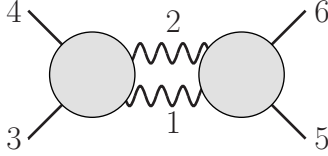
Figure 1.2: The scalar-QED generalized-unitarity cut studied in Sect. 1.3.1. The two blobs are Compton amplitudes in this theory. Solid lines correspond to scalar particles and wiggly lines correspond to photons. External momenta are taken outgoing while internal momenta flow to the right. All exposed lines are taken as on shell.

1.3 Spurious-singularity-free replacement rules

In this section we derive a set of replacement rules that may be used to perform the physical-state sums in gauge theory and gravity. These rules do not contain spurious singularities while using them is equivalent to using Eqs. (1.2) and (1.3). The only requirement for applying these rules is that the quantities being sewn obey the WI.

As a warm-up to the general case, we consider a simple example in scalar QED that demonstrates the basic idea. We proceed to discuss our method in general. Then, we provide a summary of our results. Finally, we conclude this section by studying an involved example in detail.

1.3.1 Demonstration in a simple example

Here we wish to demonstrate our method with a simple example. In particular, we compute the one-loop generalized-unitarity cut of Fig. 1.2 without introducing spurious singularities. We take the external particles to be massive scalars while the internal particles are photons. We compute the generalized-unitarity cut in question by sewing two factors of the Compton amplitude of scalar QED. At the level of the Compton amplitudes, all particles are taken as on shell. We choose to consider scalar QED due to the compactness of the expression. Refs. [45, 46] calculated corresponding cuts in gravity.
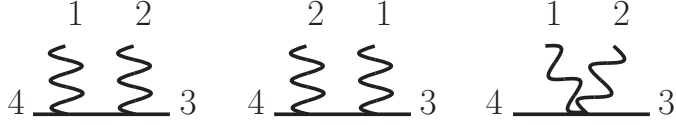
Figure 1.3: The three Feynman diagrams we need to calculate in order to get the scalar-QED amplitudes of Eq. (1.6). The solid line represents a scalar particle while the wiggly lines represent photons. We take all momenta to be outgoing.

We set the couplings to unity for convenience. We denote the two Compton amplitudes that enter our example by $\mathcal{A}_L$ and $\mathcal{A}_R$. We have

$$
\begin{aligned}
\mathcal{A}_L &= 2i \left(\frac{p_4 \cdot \varepsilon_1 p_3 \cdot \varepsilon_2}{p_1 \cdot p_4} + \frac{p_4 \cdot \varepsilon_2 p_3 \cdot \varepsilon_1}{p_1 \cdot p_3} + \varepsilon_1 \cdot \varepsilon_2 \right), \\
\mathcal{A}_R &= 2i \left(\frac{p_6 \cdot \varepsilon_{-1} p_5 \cdot \varepsilon_{-2}}{-p_1 \cdot p_6} + \frac{p_6 \cdot \varepsilon_{-2} p_5 \cdot \varepsilon_{-1}}{-p_1 \cdot p_5} + \varepsilon_{-1} \cdot \varepsilon_{-2} \right),
\end{aligned}
\tag{1.6}
$$

where $\varepsilon_i \equiv \varepsilon(p_i)$ and $\varepsilon_{-i} \equiv \varepsilon(-p_i)$. We present the Feynman diagrams needed to calculate $\mathcal{A}_L$ in Fig. 1.3. We use the on-shell conditions to reduce $\mathcal{A}_L$ to a basis of Lorentz-invariant products. Namely, we solve momentum conservation as $p_2 = -p_1 - p_3 - p_4$ and impose $\varepsilon_2 \cdot p_1 = -\varepsilon_2 \cdot p_3 - \varepsilon_2 \cdot p_4$ and $p_3 \cdot p_4 = -p_1 \cdot p_3 - p_1 \cdot p_4 - m_L^2$, where m_L is the mass of the scalar. We obtain $\mathcal{A}_R$ by the appropriate relabelling.

We wish to sew both photon-legs 1 and 2, so that we obtain the generalized-unitarity cut depicted in Fig. 1.2. We start by summing over the physical polarizations of photon-leg 1. We denote this sum as $\sum_1$. We have

$$
\sum_1 \mathcal{A}_L \mathcal{A}_R = \mathcal{C}_0^{\mu\nu} \sum_1 \varepsilon_{1\mu} \varepsilon_{-1\nu},
\tag{1.7}
$$

where

$$
\mathcal{C}_0^{\mu\nu} \equiv -4 \left(\frac{p_3 \cdot \varepsilon_2}{p_1 \cdot p_4} p_4^\mu + \frac{p_4 \cdot \varepsilon_2}{p_1 \cdot p_3} p_3^\mu + \varepsilon_2^\mu \right) \left(\frac{p_5 \cdot \varepsilon_{-2}}{-p_1 \cdot p_6} p_6^\nu + \frac{p_6 \cdot \varepsilon_{-2}}{-p_1 \cdot p_5} p_5^\nu + \varepsilon_{-2}^\nu \right).
\tag{1.8}
$$

We build $\mathcal{C}_0^{\mu\nu}$ out of the remaining momenta and polarization vectors. Importantly, it does not contain the metric $\eta^{\mu\nu}$. Observe that

$$
\mathcal{C}_0^{\mu\nu} p_{1\mu} = \mathcal{C}_0^{\mu\nu} p_{1\nu} = 0.
\tag{1.9}
$$

7

This is a consequence of the WI for particle 1, obeyed by $\mathcal{A}_L$ and $\mathcal{A}_R$. We can see this explicitly as follows. If we define $\mathcal{A}_L^\mu$ by $\mathcal{A}_L = \varepsilon_{1\mu}\mathcal{A}_L^\mu$ and similarly for $\mathcal{A}_R^\nu$, then we have

$$\mathcal{C}_0^{\mu\nu} = \mathcal{A}_L^\mu \mathcal{A}_R^\nu. \tag{1.10}$$

Then the WI for the two amplitudes (Eq. (1.1)) reads

$$p_{1\mu}\mathcal{A}_L^\mu = p_{1\nu}\mathcal{A}_R^\nu = 0. \tag{1.11}$$

We call $\mathcal{A}_L^\mu$ and $\mathcal{A}_R^\nu$ transverse because they obey the above property. We observe that in this case we may write $\mathcal{C}_0^{\mu\nu}$ as a product of two transverse objects.

Using Eq. (1.9) we may simplify the insertion of the projector. Focusing on the spurious singularity piece of the projector (Eq. (1.2)), we have

$$\left(\sum_1 \mathcal{A}_L\mathcal{A}_R\right)_{\text{spurious sing.}} = \frac{1}{p_1 \cdot q}\left(\mathcal{C}_0^{\mu\nu}p_{1\mu}q_\nu + \mathcal{C}_0^{\mu\nu}p_{1\nu}q_\mu\right) = 0. \tag{1.12}$$

Then the full expression becomes

$$\begin{aligned}
\sum_1 \mathcal{A}_L\mathcal{A}_R &= \mathcal{C}_0^{\mu\nu}\sum_1 \varepsilon_{1\mu}\varepsilon_{-1\nu} = \mathcal{C}_0^{\mu\nu}\eta_{\mu\nu} \\
&= 4\left(\frac{p_4 \cdot p_6 p_3 \cdot \varepsilon_2 p_5 \cdot \varepsilon_{-2}}{p_1 \cdot p_4 p_1 \cdot p_6} + \frac{p_4 \cdot p_5 p_3 \cdot \varepsilon_2 p_6 \cdot \varepsilon_{-2}}{p_1 \cdot p_4 p_1 \cdot p_5} - \frac{p_3 \cdot \varepsilon_2 p_4 \cdot \varepsilon_{-2}}{p_1 \cdot p_4}\right. \\
&\quad + \frac{p_3 \cdot p_6 p_4 \cdot \varepsilon_2 p_5 \cdot \varepsilon_{-2}}{p_1 \cdot p_3 p_1 \cdot p_6} + \frac{p_3 \cdot p_5 p_4 \cdot \varepsilon_2 p_6 \cdot \varepsilon_{-2}}{p_1 \cdot p_3 p_1 \cdot p_5} - \frac{p_4 \cdot \varepsilon_2 p_3 \cdot \varepsilon_{-2}}{p_1 \cdot p_3} \\
&\quad \left. + \frac{p_6 \cdot \varepsilon_2 p_5 \cdot \varepsilon_{-2}}{p_1 \cdot p_6} + \frac{p_5 \cdot \varepsilon_2 p_6 \cdot \varepsilon_{-2}}{p_1 \cdot p_5} - \varepsilon_2 \cdot \varepsilon_{-2}\right).
\end{aligned} \tag{1.13}$$

Next, we wish to sew photon-leg 2. Before we proceed, we reduce our expression to a basis of Lorentz-invariant products. Namely, we solve momentum conservation as $p_1 = -p_2 + p_5 + p_6$ and $p_3 = -p_4 - p_5 - p_6$. Any other choice would be equally valid. We impose the trasversality

conditions, $\varepsilon_{\pm 2} \cdot p_2 = 0$, and the mass-shell conditions. We find

$$\sum_1 \mathcal{A}_L \mathcal{A}_R = \mathcal{C}_0^{\mu\nu} \eta_{\mu\nu}$$

$$= 4 \Bigg(- \frac{(p_2 \cdot p_5 + p_2 \cdot p_6 + p_4 \cdot p_5)(p_4 + p_5 + p_6) \cdot \varepsilon_2 \, p_5 \cdot \varepsilon_{-2}}{p_2 \cdot p_5 \, p_2 \cdot (p_4 + p_5 + p_6)}$$

$$+ \frac{p_4 \cdot p_5 (p_4 + p_5 + p_6) \cdot \varepsilon_2 \, p_6 \cdot \varepsilon_{-2}}{p_2 \cdot p_6 \, p_2 \cdot (p_4 + p_5 + p_6)} - \frac{(p_4 + p_5 + p_6) \cdot \varepsilon_2 \, p_4 \cdot \varepsilon_{-2}}{p_2 \cdot (p_4 + p_5 + p_6)}$$

$$+ \frac{p_4 \cdot p_5 p_4 \cdot \varepsilon_2 p_5 \cdot \varepsilon_{-2}}{p_2 \cdot p_4 \, p_2 \cdot p_5} - \frac{(p_2 \cdot p_5 + p_2 \cdot p_6 + p_4 \cdot p_5) p_4 \cdot \varepsilon_2 p_6 \cdot \varepsilon_{-2}}{p_2 \cdot p_4 \, p_2 \cdot p_6}$$

$$+ \frac{p_4 \cdot \varepsilon_2 (p_4 + p_5 + p_6) \cdot \varepsilon_{-2}}{p_2 \cdot p_4} + \frac{p_6 \cdot \varepsilon_2 p_5 \cdot \varepsilon_{-2}}{p_2 \cdot p_5} + \frac{p_5 \cdot \varepsilon_2 p_6 \cdot \varepsilon_{-2}}{p_2 \cdot p_6} - \varepsilon_2 \cdot \varepsilon_{-2} \Bigg). \tag{1.14}$$

Now we may sew particle 2,

$$\sum_{1,2} \mathcal{A}_L \mathcal{A}_R = \sum_2 \mathcal{C}_0^{\mu\nu} \eta_{\mu\nu} = \tilde{\mathcal{C}}_0^{\mu\nu} \sum_2 \varepsilon_{2\mu} \varepsilon_{-2\nu} - 4 \sum_2 \varepsilon_2 \cdot \varepsilon_{-2}, \tag{1.15}$$

where

$$\tilde{\mathcal{C}}_0^{\mu\nu} = 4 \Bigg(- \frac{(p_2 \cdot p_5 + p_2 \cdot p_6 + p_4 \cdot p_5)(p_4^\mu + p_5^\mu + p_6^\mu) \, p_5^\nu}{p_2 \cdot p_5 \, p_2 \cdot (p_4 + p_5 + p_6)}$$

$$+ \frac{p_4 \cdot p_5 (p_4^\mu + p_5^\mu + p_6^\mu) \, p_6^\nu}{p_2 \cdot p_6 \, p_2 \cdot (p_4 + p_5 + p_6)} - \frac{(p_4^\mu + p_5^\mu + p_6^\mu) \, p_4^\nu}{p_2 \cdot (p_4 + p_5 + p_6)}$$

$$+ \frac{p_4 \cdot p_5 p_4^\mu p_5^\nu}{p_2 \cdot p_4 \, p_2 \cdot p_5} - \frac{(p_2 \cdot p_5 + p_2 \cdot p_6 + p_4 \cdot p_5) p_4^\mu p_6^\nu}{p_2 \cdot p_4 \, p_2 \cdot p_6}$$

$$+ \frac{p_4^\mu (p_4^\nu + p_5^\nu + p_6^\nu)}{p_2 \cdot p_4} + \frac{p_6^\mu p_5^\nu}{p_2 \cdot p_5} + \frac{p_5^\mu p_6^\nu}{p_2 \cdot p_6} \Bigg). \tag{1.16}$$

Again, $\tilde{\mathcal{C}}_0^{\mu\nu}$ is built out of the remaining momenta and does not contain the metric. One may verify that

$$\tilde{\mathcal{C}}_0^{\mu\nu} p_{2\mu} = \tilde{\mathcal{C}}_0^{\mu\nu} p_{2\nu} = 0. \tag{1.17}$$

This time this property does not straightforwardly follow from the WI of the two amplitudes (indeed, we cannot write $\tilde{\mathcal{C}}_0^{\mu\nu}$ as a product of two transverse objects). We discuss this property in detail in the next subsection. A hint about why it holds is that the whole expression obeys the WI for particle 2 and so does the term $\varepsilon_2 \cdot \varepsilon_{-2}$ by itself, since $\varepsilon_{\pm 2} \cdot p_2 = 0$.

9

Delaying its explanation, we may use the above observation to simplify the sewing of particle 2:

$$\sum_{1,2} \mathcal{A}_L \mathcal{A}_R = \tilde{\mathcal{C}}_0^{\mu\nu} \sum_2 \varepsilon_{2\mu}\varepsilon_{-2\nu} - 4\sum_2 \varepsilon_2 \cdot \varepsilon_{-2} = \tilde{\mathcal{C}}_0^{\mu\nu}\eta_{\mu\nu} - 4\sum_2 \varepsilon_2 \cdot \varepsilon_{-2}. \tag{1.18}$$

We complete our example by performing the remaining sum,

$$\sum_2 \varepsilon_2 \cdot \varepsilon_{-2} = D - 2, \tag{1.19}$$

where D is the dimension of spacetime. We obtain the above by dotting Eq. (1.2) with the metric $\eta_{\mu\nu}$. Finally,

$$\begin{aligned}
\sum_{1,2} \mathcal{A}_L \mathcal{A}_R = {} & \tilde{\mathcal{C}}_0^{\mu\nu}\eta_{\mu\nu} - 4(D-2) \\[4pt]
= {} & 4\Bigg(-\frac{(p_2 \cdot p_5 + p_2 \cdot p_6 + p_4 \cdot p_5)(p_4 + p_5 + p_6) \cdot p_5}{p_2 \cdot p_5\, p_2 \cdot (p_4 + p_5 + p_6)} \\[4pt]
& + \frac{p_4 \cdot p_5(p_4 + p_5 + p_6) \cdot p_6}{p_2 \cdot p_6 p_2 \cdot (p_4 + p_5 + p_6)} - \frac{(p_4 + p_5 + p_6) \cdot p_4}{p_2 \cdot (p_4 + p_5 + p_6)} \\[4pt]
& + \frac{p_4 \cdot p_5 p_4 \cdot p_5}{p_2 \cdot p_4 p_2 \cdot p_5} - \frac{(p_2 \cdot p_5 + p_2 \cdot p_6 + p_4 \cdot p_5)p_4 \cdot p_6}{p_2 \cdot p_4 p_2 \cdot p_6} \\[4pt]
& + \frac{p_4 \cdot (p_4 + p_5 + p_6)}{p_2 \cdot p_4} + \frac{p_6 \cdot p_5}{p_2 \cdot p_5} + \frac{p_5 \cdot p_6}{p_2 \cdot p_6} \Bigg) - 4(D-2).
\end{aligned} \tag{1.20}$$

We conclude that we may perform both sewings without introducing any spurious singularities.

1.3.2   The general case

Now we take up the discussion of the general case of summing over the physical polarizations of a gauge particle. We denote the polarization vectors and momenta of the gauge-particle legs being sewn as $\varepsilon_+ \equiv \varepsilon(p)$ and p, and $\varepsilon_- \equiv \varepsilon(-p)$ and $(-p)$ respectively. We write $\sum_{\text{pols.}}$ for the sum over the physical polarizations of the gauge particle.

Claim: Given a quantity C that obeys the Ward identity (Eq. (1.1)) for both ε_+ and ε_-, we may perform the sum

$$\sum_{\text{pols.}} C, \tag{1.21}$$

10

in terms of a set of spurious-singularity-free replacements rules. We collect these rules in Eq. (1.42) for gauge theory and Eq. (1.45) for gravity.

We proceed to prove the above claim in the cases of gauge theory and gravity separately.

1.3.2.1 Proof in gauge theory

In the case of gauge theory, the quantity C may be written as

$$C = \mathcal{C}_0^{\mu\nu} \varepsilon_{+\mu} \varepsilon_{-\nu} + \mathcal{C}_1 \varepsilon_+ \cdot \varepsilon_-, \tag{1.22}$$

where we build $\mathcal{C}_0^{\mu\nu}$ and $\mathcal{C}_1$ out of the remaining momenta and polarization vectors. We note that $\mathcal{C}_0^{\mu\nu}$ does not contain the metric $\eta^{\mu\nu}$. In other words, there is no ambiguity in splitting C into these two pieces.

At this point we reduce C to a basis of Lorentz-invariant products using momentum conservation and the on-shell conditions. Specifically, we impose the transversality condition $(\varepsilon_\pm \cdot p = 0)$. For example, if we choose to solve momentum conservation such that p is one of the independent momenta appearing in our basis, then we may decompose $\mathcal{C}_0^{\mu\nu}$ as

$$\mathcal{C}_0^{\mu\nu} = Q^{\mu\nu} + Q_+^\mu p^\nu + Q_-^\nu p^\mu + Q_0 p^\mu p^\nu. \tag{1.23}$$

Then, due to the transversality condition we have

$$\mathcal{C}_0^{\mu\nu} \varepsilon_{+\mu} \varepsilon_{-\nu} = Q^{\mu\nu} \varepsilon_{+\mu} \varepsilon_{-\nu}. \tag{1.24}$$

We note that we do not have to choose the above basis.

Next, being gauge invariant, C obeys the WI for the two legs in question:

$$C|_{\varepsilon_+ \to p} = 0, \qquad C|_{\varepsilon_- \to p} = 0. \tag{1.25}$$

We observe that so does $\varepsilon_+ \cdot \varepsilon_-$ since $\varepsilon_\pm \cdot p = 0$. We conclude that the last term must also obey the WI:

$$\mathcal{C}_0^{\mu\nu} \varepsilon_{+\mu} p_\nu = 0, \qquad \mathcal{C}_0^{\mu\nu} p_\mu \varepsilon_{-\nu} = 0. \tag{1.26}$$

We now argue that the stronger condition

$$\mathcal{C}_0^{\mu\nu} p_\nu = 0, \qquad \mathcal{C}_0^{\mu\nu} p_\mu = 0, \tag{1.27}$$

11

follows from the above. Indeed, that would not be the case only if we needed to use some of the special properties of the polarization vectors in Eq. (1.26). Those properties are

$$\varepsilon_\pm \cdot p = 0 \quad \text{and} \quad \varepsilon_\pm^2 = 0. \tag{1.28}$$

The null condition is not required, since $\mathcal{C}_0^{\mu\nu}$ does not contain $\varepsilon_\pm$. The transversality condition is also not required, since we have reduced $\mathcal{C}_0^{\mu\nu}$ to a basis of Lorentz-invariant products (this is most easily seen in a basis where p is one of the independent momenta).

Using this property we may cancel the spurious-singularity piece of the projector

$$\left(\mathcal{C}_0^{\mu\nu} \sum_{\text{pols.}} \varepsilon_{+\mu} \varepsilon_{-\nu} \right)_{\text{spurious sing.}} = \frac{1}{p \cdot q} \left(\mathcal{C}_0^{\mu\nu} p_\mu q_\nu + \mathcal{C}_0^{\mu\nu} p_\nu q_\mu \right) = 0. \tag{1.29}$$

Then we find

$$\sum_{\text{pols.}} C = \mathcal{C}_0^{\mu\nu} \sum_{\text{pols.}} \varepsilon_{+\mu} \varepsilon_{-\nu} + \mathcal{C}_1 \sum_{\text{pols.}} \varepsilon_+ \cdot \varepsilon_- = \mathcal{C}_0^{\mu\nu} \eta_{\mu\nu} + \mathcal{C}_1 (D-2), \tag{1.30}$$

where

$$\sum_{\text{pols.}} \varepsilon_+ \cdot \varepsilon_- = D - 2, \tag{1.31}$$

and D is the spacetime dimension.

From Eq. (1.30) we see that performing the physical-state sum at hand is equivalent to using the replacement rule

$$x_1^\mu x_2^\nu \sum_{\text{pols.}} \varepsilon_{+\mu} \varepsilon_{-\nu} \to x_1^\mu x_2^\nu \eta_{\mu\nu}, \tag{1.32}$$

supplemented by Eq. (1.31) in the individual terms in $\sum_{\text{pols.}} C$. By x_i we refer to the various vectors that appear in the problem. In this way, by treating the term $\varepsilon_+ \cdot \varepsilon_-$ separately we manage to sum over the physical polarizations of the gauge particle without introducing any spurious singularities.

1.3.2.2 Proof in gravity

The case of gravity follows in a similar manner. We may write

$$C = \mathcal{C}_0^{\mu\nu\alpha\beta} \varepsilon_{+\mu} \varepsilon_{+\nu} \varepsilon_{-\alpha} \varepsilon_{-\beta} + \mathcal{C}_1^{\mu\nu} \varepsilon_{+\mu} \varepsilon_{-\nu} (\varepsilon_+ \cdot \varepsilon_-) + \mathcal{C}_2 (\varepsilon_+ \cdot \varepsilon_-)^2, \tag{1.33}$$

where we build $\mathcal{C}_0^{\mu\nu\alpha\beta}$, $\mathcal{C}_1^{\mu\nu}$ and $\mathcal{C}_2$ out of the remaining momenta and polarization vectors. This splitting is unique, since $\mathcal{C}_0^{\mu\nu\alpha\beta}$ and $\mathcal{C}_1^{\mu\nu}$ do not contain any terms proportional to the metric or combinations of the metric. In writing the above we make use of the fact that the polarization vectors are null ($\varepsilon_\pm^2 = 0$). As before, we must also impose the transversality condition ($\varepsilon_\pm \cdot p = 0$).

We use the fact that C and $\varepsilon_+ \cdot \varepsilon_-$ obey the WI to deduce that all three terms individually obey the WI. Then, we may show that

$$\mathcal{C}_0^{\mu\nu\alpha\beta} p_\mu = \mathcal{C}_0^{\mu\nu\alpha\beta} p_\nu = \mathcal{C}_0^{\mu\nu\alpha\beta} p_\alpha = \mathcal{C}_0^{\mu\nu\alpha\beta} p_\beta = 0, \tag{1.34}$$

and

$$\mathcal{C}_1^{\mu\nu} p_\mu = \mathcal{C}_1^{\mu\nu} p_\nu = 0. \tag{1.35}$$

It then follows from Eq. (1.3) that

$$\mathcal{C}_0^{\mu\nu\alpha\beta} \sum_{\text{pols.}} \varepsilon_{+\mu} \varepsilon_{+\nu} \varepsilon_{-\alpha} \varepsilon_{-\beta} = \mathcal{C}_0^{\mu\nu\alpha\beta} \frac{1}{2} \left(\eta_{\mu\alpha} \eta_{\nu\beta} + \eta_{\mu\beta} \eta_{\nu\alpha} - \frac{2}{D-2} \eta_{\mu\nu} \eta_{\alpha\beta} \right), \tag{1.36}$$

and

$$\mathcal{C}_1^{\mu\nu} \sum_{\text{pols.}} \varepsilon_{+\mu} \varepsilon_{-\nu} (\varepsilon_+ \cdot \varepsilon_-) = \mathcal{C}_1^{\mu\nu} \eta_{\mu\nu} \frac{D(D-3)/2}{D-2}. \tag{1.37}$$

Finally, for $(\varepsilon_+ \cdot \varepsilon_-)^2$ we get

$$\sum_{\text{pols.}} (\varepsilon_+ \cdot \varepsilon_-)^2 = D(D-3)/2. \tag{1.38}$$

Together, our result reads

$$\sum_{\text{pols.}} C = \mathcal{C}_0^{\mu\nu\alpha\beta} \sum_{\text{pols.}} \varepsilon_{+\mu} \varepsilon_{+\nu} \varepsilon_{-\alpha} \varepsilon_{-\beta} + \mathcal{C}_1^{\mu\nu} \sum_{\text{pols.}} \varepsilon_{+\mu} \varepsilon_{-\nu} (\varepsilon_+ \cdot \varepsilon_-) + \mathcal{C}_2 \sum_{\text{pols.}} (\varepsilon_+ \cdot \varepsilon_-)^2$$

$$= \mathcal{C}_0^{\mu\nu\alpha\beta} \frac{1}{2} \left(\eta_{\mu\alpha} \eta_{\nu\beta} + \eta_{\mu\beta} \eta_{\nu\alpha} - \frac{2}{D-2} \eta_{\mu\nu} \eta_{\alpha\beta} \right) + \mathcal{C}_1^{\mu\nu} \eta_{\mu\nu} \frac{D(D-3)/2}{D-2} + \mathcal{C}_2 D(D-3)/2. \tag{1.39}$$

Eq. (1.39) suggests that performing the physical-state sum of the graviton leg in question is equivalent to using the replacement rules

$$x_1^\mu x_2^\nu x_3^\alpha x_4^\beta \sum_{\text{pols.}} \varepsilon_{+\mu} \varepsilon_{+\nu} \varepsilon_{-\alpha} \varepsilon_{-\beta} \to x_1^\mu x_2^\nu x_3^\alpha x_4^\beta \frac{1}{2} \left(\eta_{\mu\alpha} \eta_{\nu\beta} + \eta_{\mu\beta} \eta_{\nu\alpha} - \frac{2}{D-2} \eta_{\mu\nu} \eta_{\alpha\beta} \right),$$

$$x_1^\mu x_2^\nu \sum_{\text{pols.}} \varepsilon_{+\mu} \varepsilon_{-\nu} (\varepsilon_+ \cdot \varepsilon_-) \to x_1^\mu x_2^\nu \eta_{\mu\nu} \frac{D(D-3)/2}{D-2}, \tag{1.40}$$

along with Eq. (1.38) in the individual terms in $\sum_{\text{pols.}} C$. By x_i we denote the various vectors that appear in the calculation. In this way, we may avoid introducing spurious singularities if we treat the various terms separately.

1.3.3 Summary

Here we summarize our results. We emphasize that we need to reduce the gauge-invariant quantity under study to a basis of Lorentz-invariant products before we use the following replacement rules. We use the right arrow ($\rightarrow$) to indicate that the relation stated is not true term by term; but rather, when we apply it to each term, we reproduce the whole expression correctly. We emphasize that our rules are not equivalent to simply dropping the spurious-singularity pieces. For convenience we repeat Eqs. (1.2) and (1.3).

1.3.3.1 Gauge theory

The physical-state projector:

$$P^{\mu\nu}(p,q) = \sum_{\text{pols.}} \varepsilon^{\mu}(-p)\varepsilon^{\nu}(p) = \eta^{\mu\nu} - \frac{q^{\mu}p^{\nu} + p^{\mu}q^{\nu}}{q \cdot p}. \tag{1.41}$$

Equivalent spurious-singularity-free rules:

$$x_1^{\mu}x_2^{\nu} \sum_{\text{pols.}} \varepsilon_{\mu}(-p)\varepsilon_{\nu}(p) \rightarrow x_1^{\mu}x_2^{\nu}\eta_{\mu\nu},$$

$$\sum_{\text{pols.}} \varepsilon(-p) \cdot \varepsilon(p) = D - 2, \tag{1.42}$$

where the x_i refer to momenta and polarization vectors that appear in the problem.

1.3.3.2 Gravity

The physical-state projector:

$$P^{\mu\nu\alpha\beta}(p,q) = \sum_{\text{pols.}} \varepsilon^{\mu\nu}(-p)\varepsilon^{\alpha\beta}(p) = \frac{1}{2}\left(P^{\mu\alpha}P^{\nu\beta} + P^{\nu\alpha}P^{\mu\beta}\right) - \frac{1}{D-2}P^{\mu\nu}P^{\alpha\beta}, \tag{1.43}$$

where

$$\varepsilon^{\mu\nu}(-p) = \varepsilon^{\mu}(-p)\varepsilon^{\nu}(-p), \quad \varepsilon^{\alpha\beta}(p) = \varepsilon^{\alpha}(p)\varepsilon^{\beta}(p). \tag{1.44}$$

Equivalent spurious-singularity-free rules:

$$x_1^\mu x_2^\nu x_3^\alpha x_4^\beta \sum_{\text{pols.}} \varepsilon_\mu(-p)\varepsilon_\nu(-p)\varepsilon_\alpha(p)\varepsilon_\beta(p) \to x_1^\mu x_2^\nu x_3^\alpha x_4^\beta \frac{1}{2}\left(\eta_{\mu\alpha}\eta_{\nu\beta} + \eta_{\mu\beta}\eta_{\nu\alpha} - \frac{2}{D-2}\eta_{\mu\nu}\eta_{\alpha\beta}\right),$$

$$x_1^\mu x_2^\nu \sum_{\text{pols.}} \varepsilon_\mu(-p)\varepsilon_\nu(p)\Big(\varepsilon(-p)\cdot\varepsilon(p)\Big) \to x_1^\mu x_2^\nu \eta_{\mu\nu} \frac{D(D-3)/2}{D-2},$$

$$\sum_{\text{pols.}} \Big(\varepsilon(-p)\cdot\varepsilon(p)\Big)^2 = D(D-3)/2, \tag{1.45}$$

where the x_i refer to momenta and polarization vectors that appear in the problem.

1.3.4 An example in detail

In this subsection we discuss the computation of the three-loop generalized-unitarity cut depicted in Fig. 1.4. This is one of the cuts that can be used to construct the conservative two-body Hamiltonian for spinless black holes to order G^4 following the methods of Ref. [12, 13].

The solid black lines denote massive scalar particles, while the wiggly lines denote gravitons. The blobs correspond to tree-level amplitudes. We may construct them straightforwardly using the Kawai, Lewellen and Tye relations [33] or the Bern, Carrasco and Johansson double copy [34, 35] from the corresponding gauge-theory ones. The exposed lines are taken as on shell. To construct the cut, we have to sew together the tree-level amplitudes, by summing over the physical states propagating through the internal exposed lines.

We take all external particles to be outgoing. We take the internal momenta to flow upwards and to the right. The mass of the lower scalar line is m_1, while the mass of the upper one is m_2. In what follows, it is important to impose the on-shell conditions for both external and internal exposed lines.

We avoid introducing spurious singularities by taking the following steps:

- We start by sewing particle 5. To reduce our expression to a basis we, for example, solve momentum conservation as $p_{10} = -p_1 - p_5 - p_6$ and $p_{11} = -p_2 - p_5$ and impose the remaining on-shell conditions. We may then use the rules developed above.

- We continue to sew leg 6. We must use all on-shell conditions. For example, terms of

15
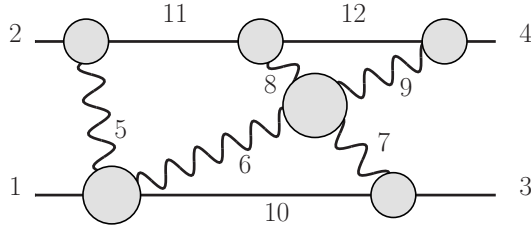
Figure 1.4: A three-loop generalized-unitarity cut relevant in the construction of the conservative two-body Hamiltonian for spinless black holes to order G^4. The blobs represent tree-level amplitudes. The solid lines correspond to scalars while the wiggly ones to gravitons. We take the external particles to be outgoing and the internal momenta to go upwards and to the right. All exposed lines are taken as on shell.

the form $\varepsilon_i \cdot p_i$ introduced by the above sewing must be set to zero, before applying the replacement rules.

- We now sew leg 7. Sewing leg 6 introduced ε_i^2, with $i = 7, 8, 9$, which must be set to zero before the sewing of leg 7. After we impose all on-shell conditions we may use the spurious-singularity-free replacement rules.

- In a similar manner we sew successively legs 8 and 9.

We have explicitly verified that this process gives the correct answer, i.e. the one we get by using the physical-state projectors. However, following our approach we do not have to introduce spurious singularities in any of the steps taken.

1.4 Generalized Ward identity

In this section we develop an alternative approach to simplifying the physical-state sums. In this approach we bring the amplitudes we wish to sew in a form in which they obey the generalized Ward identity (GWI) for the gauge-particle legs of interest. The GWI is a stronger version of the WI, where the vanishing of the amplitude when we replace a polarization vector with the corresponding momentum (Eq. 1.1) happens without using the

special properties of the remaining polarization vectors. Namely, we do not need to use the null ($\varepsilon_i^2 = 0$) and transversallity ($\varepsilon_i \cdot p_i = 0$) conditions.

We organize this section as follows. We start by demonstrating the idea in a simple example. We proceed to describe how we can manipulate any n-point amplitude into obeying the GWI for up to $(n-2)$ external gauge particles. If the external gauge particles are $(n-1)$ or less, then all of them may obey the GWI. Next, we explain how this property allows us to drop the spurious-singularity pieces when we insert the physical-state projectors (Eqs. (1.2) and (1.3)). We discuss some implementation details and limitations of our method. Finally, we conclude by repeating the analysis of the three-loop generalized-unitarity cut of the last section using this second approach.

1.4.1 Demonstration in a simple example

We wish to introduce the GWI-based approach in terms of a simple example. In contrast to the procedure described in Sect. 1.3, which targets the sewing step directly, here we manipulate the amplitude we wish to sew in order to bring it to an appropriate form. As we discuss in the following subsections, once the gauge-invariant quantity in question satisfies the GWI, we may insert the physical-state projects with the spurious singularities dropped.

Similarly to Sect. 1.3.1, we demonstrate our method using the Compton amplitude of scalar QED, due to the compactness of the expression. We show that this amplitude in a generic form does not obey the GWI. We observe that we may use momentum conservation to bring it to a form such that it does obey the GWI. Refs. [45, 46] obtained the corresponding gravitational amplitudes in such a form. That was possible due to the simplicity of the four-point amplitude at hand. Our methods, however, are systematic and applicable to any gauge-invariant quantity.

The amplitude is given by

$$\mathcal{A}_4 = 2i \left(\frac{p_4 \cdot \varepsilon_1 p_3 \cdot \varepsilon_2}{p_1 \cdot p_4} + \frac{p_4 \cdot \varepsilon_2 p_3 \cdot \varepsilon_1}{p_1 \cdot p_3} + \varepsilon_1 \cdot \varepsilon_2 \right), \tag{1.46}$$

where we set the coupling to unity for convenience. We depict the Feynman diagrams we

need in order to calculate this amplitude in Fig. 1.3. We reduce the amplitude to a basis of Lorentz-invariant products, as we discuss in Sect. 1.3.1. Specifically, we use momentum conservation to eliminate p_2 and $\varepsilon_2 \cdot p_1$ from our basis.

To discuss the GWI, it is convenient to replace the polarization vectors with generic vectors w_1 and w_2. We do not assume any special properties for w_1 and w_2. We have

$$\mathcal{A}_4^w = 2i \left(\frac{p_4 \cdot w_1 p_3 \cdot w_2}{p_1 \cdot p_4} + \frac{p_4 \cdot w_2 p_3 \cdot w_1}{p_1 \cdot p_3} + w_1 \cdot w_2 \right). \tag{1.47}$$

$\mathcal{A}_4^w$ is equivalent to the off-shell amplitude $\mathcal{A}_4^{\mu\nu}$ defined by $\mathcal{A}_4 = \mathcal{A}_4^{\mu\nu} \varepsilon_{1\mu} \varepsilon_{2\nu}$. In terms of this object the statements of the WI and the GWI for particle 1 take the form:

$$\mathcal{A}_4^w \big|_{w_1 \to p_1, w_2 \to \varepsilon_2} = 0 \quad \text{(WI)}, \quad \mathcal{A}_4^w \big|_{w_1 \to p_1} = 0 \quad \text{(GWI)}. \tag{1.48}$$

We now establish that $\mathcal{A}_4$ in this form does not obey the GWI. Indeed,

$$\mathcal{A}_4^w \big|_{w_1 \to p_1} = 2i(p_3 + p_4 + p_1) \cdot w_2 = -2i p_2 \cdot w_2 \neq 0. \tag{1.49}$$

The WI however is satisfied, since $\varepsilon_2 \cdot p_2 = 0$.

We draw the reader's attention to the fact that the replacement $w_1 \to p_1$ introduces $p_1 \cdot w_2$, a Lorentz-invariant product that is not present in our off-shell amplitude (Eq. (1.47)). Once our basis contains all products that may arise from the replacement $w_1 \to p_1$, then our amplitude will obey the GWI.

We want to change our basis so that the off-shell amplitude contains $p_1 \cdot w_2$. To do that we use $p_4 = -p_1 - p_2 - p_3$ in our on-shell amplitude. We get

$$\mathcal{A}_4 = 2i \left(\frac{(p_2 + p_3) \cdot \varepsilon_1 p_3 \cdot \varepsilon_2}{p_1 \cdot (p_2 + p_3)} - \frac{(p_1 + p_3) \cdot \varepsilon_2 p_3 \cdot \varepsilon_1}{p_1 \cdot p_3} + \varepsilon_1 \cdot \varepsilon_2 \right), \tag{1.50}$$

which then gives

$$\tilde{\mathcal{A}}_4^w = 2i \left(\frac{(p_2 + p_3) \cdot w_1 p_3 \cdot w_2}{p_1 \cdot (p_2 + p_3)} - \frac{(p_1 + p_3) \cdot w_2 p_3 \cdot w_1}{p_1 \cdot p_3} + w_1 \cdot w_2 \right). \tag{1.51}$$

We introduce the tilde to differentiate this form from the previous one. We may think of $\mathcal{A}_4^w$ and $\tilde{\mathcal{A}}_4^w$ as the off-shell amplitude calculated in different gauge choices. Now, we may confirm that this form satisfies the GWI. Indeed,

$$\mathcal{A}_4^w \big|_{w_1 \to p_1} = 2i \big(p_3 - (p_1 + p_3) + p_1 \big) \cdot w_2 = 0. \tag{1.52}$$

18

We may verify that the analysis is identical for particle 2. Also, the result would be the same if we were to solve momentum conservation as $p_3 = -p_1 - p_2 - p_4$.

Let us recap what we just did. We wrote a form of $\mathcal{A}_4$ where p_1 and p_2 are explicit. We used that form to construct the off-shell amplitude $\tilde{\mathcal{A}}_4^w$. The observation then was that replacing w_1 with p_1 does not introduce Lorentz-invariant products that were not already in the basis used to write the amplitude. We saw that this property was sufficient for our amplitude to obey the GWI.

We used the generic vectors w_1 and w_2 in this section for pedantic reasons. Namely, one may use the special properties of the polarization vectors when putting the on-shell amplitude in the appropriate form. However, one should not use them in order to check whether the GWI is satisfied. To alleviate any confusion on that point, we chose to use a different symbol.

1.4.2 The general case

In this subsection we formulate and prove a claim regarding the GWI in the context of a general amplitude. We start by obtaining a criterion on whether an amplitude satisfies the GWI. Subsequently, using this criterion we obtain a constructive proof of our claim.

We express our amplitude in terms of a basis of Lorentz-invariant products. For brevity we refer to the Lorentz-invariant products that contain at least one polarization vector as ε-products. Observe that if we perform the mapping $\varepsilon_i \to p_i$, for a given particle i, on the ε-products, then the amplitude vanishes according to the WI (Eq. (1.1)). To establish whether the amplitude obeys the GWI, we may use the following criterion:

1. If, under $\varepsilon_i \to p_i$ for a given particle i, we introduce ε-products that are not part of the basis, then the special properties of the polarization vectors are needed to ensure Eq. (1.1). The amplitude does not obey the GWI for particle i.

2. If, under $\varepsilon_i \to p_i$ for a given particle i, all ε-products introduced are part of the basis, then Eq. (1.1) is satisfied without the need to use the special properties of the

polarization vectors. The amplitude obeys the GWI for particle i.

At this point we want to comment on the gravitational case, where we have two factors of the polarization vector ε_i^μ. We use the above criterion on the individual ε-products, rather than the amplitude itself. Each ε-product contains up to one factor of each polarization vector since $\varepsilon_i^2 = 0$. Hence, we do not need to modify our criterion in order to use it in gravity.

Claim: An n-point amplitude can always be promoted to obey the GWI for up to $(n-2)$ external gauge particles. If the external gauge particles are $(n-1)$ or less, then all of them may obey the GWI.

Proof of claim: Consider first an n-point amplitude where all external particles are gauge particles. To construct our basis, we write down all possible Lorentz-invariant products and we restrict them using the on-shell conditions. First, we remove any products of the form $\varepsilon_i \cdot p_i$ or ε_i^2, due to the polarization vectors being transverse and null. Next, we choose the two particles for which the GWI will not be satisfied. Say we choose particles n and $(n-1)$. We solve momentum conservation in terms of p_n. Then, our basis does not include any products of the form $\varepsilon_i \cdot p_n$. Further, again using momentum conservation, we may eliminate $\varepsilon_n \cdot p_{n-1}$. The on-shell conditions put restrictions on momentum products as well, but those are not important for our purposes.

Now, we perform the mapping $\varepsilon_i \to p_i$ for a given particle i on our basis elements and check whether we introduce ε-products not included in our basis. Namely, we look for the elements $\varepsilon_j \cdot p_n$ for any j or $\varepsilon_n \cdot p_{n-1}$. For particles n and $(n-1)$ we find that we do introduce such elements:

$$
\begin{aligned}
\varepsilon_n \cdot \varepsilon_{n-1} &\to p_n \cdot \varepsilon_{n-1} \quad \text{under} \quad \varepsilon_n \to p_n, \\
\varepsilon_n \cdot \varepsilon_{n-1} &\to \varepsilon_n \cdot p_{n-1} \quad \text{under} \quad \varepsilon_{n-1} \to p_{n-1}.
\end{aligned}
\tag{1.53}
$$

Performing a similar check for the rest of the particles we find that all elements map to ones within the basis. Hence our amplitude obeys the GWI for the first $(n-2)$ gauge particles.

Finally, consider an n-point amplitude that has at least one particle that is not a gauge particle. We label the momenta such that this particle is the n-th particle and we solve

momentum conservation in terms of p_n. Further, since this particle is not a gauge particle, there is no product of the form $\varepsilon_n \cdot p_{n-1}$ to eliminate from our basis. Observe that this was the element blocking the amplitude with n gauge particles to obey the GWI for particle $(n-1)$ in the above setup. Therefore, in this case, the amplitude obeys the GWI for all gauge particles.

1.4.3 Simplifying the physical-state projectors using the GWI

In this subsection we formulate and prove a claim regarding the use of the GWI to drop the spurious singularities when inserting the projectors. We refer to the projectors where we have dropped the spurious-singularity pieces as *simplified projectors*. For simplicity, we look at the gauge-theory case. The discussion in gravity follows in the same way.

Claim: Consider the sewing of amplitudes $\mathcal{A}_L$ and $\mathcal{A}_R$. Assuming that $\mathcal{A}_L$ is an n_L-point amplitude and $\mathcal{A}_R$ an n_R-point one with $n_L \leq n_R$, we may use the WI and the GWI to drop the spurious singularities in up to $(n_L - 1)$ insertions of the projector.

Proof of claim: We consider the sewing of n gauge particles with $n \leq n_L - 1$. We assume that the n particles in question are labeled particle 1 through particle n. Using the process described in the previous subsection, we arrange the amplitudes such that they obey the GWI for particles 2 through n.

We first show how we may use the WI for particle 1 to drop the spurious singularities in the corresponding insertion of the projector. We then discuss the use of the GWI for particle 2 for the same purpose. Subsequent sewings follow in the same manner.

We sum over the physical polarizations of particle 1, which we denote by $\sum_1$. The amplitude $\mathcal{A}_L$ contains the polarization vector $\varepsilon(p_1) \equiv \varepsilon_1$, while $\mathcal{A}_R$ contains $\varepsilon(-p_1) \equiv \varepsilon_{-1}$. Focusing on the spurious singularity piece of the projector (Eq. (1.2)), we have

$$\left(\sum_1 \mathcal{A}_L \mathcal{A}_R \right)_{\text{spurious sing.}} = \frac{1}{p_1 \cdot q} \left(\mathcal{A}_L \big|_{\varepsilon_1 \to p_1} \mathcal{A}_R \big|_{\varepsilon_{-1} \to q} + \mathcal{A}_L \big|_{\varepsilon_1 \to q} \mathcal{A}_R \big|_{\varepsilon_{-1} \to p_1} \right) = 0, \quad (1.54)$$

due to the WI (Eq. (1.1)) of the two amplitudes. Then the complete sum over the physical

polarizations of particle 1 gives

$$\sum_1 \mathcal{A}_L \mathcal{A}_R = \left(\mathcal{A}_L \mathcal{A}_R\right)\big|_{\varepsilon_1^\mu \varepsilon_{-1}^\nu \to \eta^{\mu\nu}}. \tag{1.55}$$

It is convenient to rewrite the above as follows. We introduce D appropriately normalized vectors e_i, such that

$$\sum_{i=1}^{D} e_i^\mu e_i^\nu = \eta^{\mu\nu}. \tag{1.56}$$

Then we may write

$$\sum_1 \mathcal{A}_L \mathcal{A}_R = \sum_{i=1}^{D} \left(\mathcal{A}_L\big|_{\varepsilon_1 \to e_i} \mathcal{A}_R\big|_{\varepsilon_{-1} \to e_i}\right). \tag{1.57}$$

Next, we continue to sum over the physical polarizations of particle 2. We see that the WI of the two amplitudes is not sufficient to guarantee the vanishing of the spurious singularities. Indeed, the WI relies on the special properties of all the polarization vectors. Since the first pair of polarization vectors is replaced by the vectors e_i, the WI for the two amplitudes is not obeyed.

At this point we want to emphasize that the entire expression still obeys the WI for the remaining gauge particles. However, it is the WI of the individual amplitudes, $\mathcal{A}_L$ and $\mathcal{A}_R$, that makes the spurious-singularity pieces vanish.

We may now see why the GWI is helpful. Since it does not rely on the special properties of the polarization vectors, it still holds after we replace them with the vectors e_i. For example, if $\mathcal{A}_L$ satisfies the GWI for particle 2, we have

$$\mathcal{A}_L\big|_{\varepsilon_1 \to e_i, \varepsilon_2 \to p_2} = 0, \tag{1.58}$$

for any i. Therefore, as long as both amplitudes obey the GWI for the particle being sewn, we may drop the spurious-singularity pieces from the insertion of the projector. This concludes our proof.

We now comment on a limitation of this approach. If in the above setup we wish to sew all n_L particles, as is the case in some calculations of matrix-element squares for example, then we cannot avoid introducing spurious singularities in the last insertion of the projector.

The situation is different however if the n_L sewings involve three or more amplitudes. We take up this discussion in the next subsection.

1.4.4 Implementation details

In this subsection we comment on some details that are important for the implementation of the method developed above. We start by discussing how can we approach the sewing of three or more amplitudes, as for example is shown in Fig. 1.5. Then, we comment on when exactly should we use the special properties of the polarization vectors.

In a multiloop calculation based on generalized-unitarity we typically need to sew together multiple amplitudes. To maximize the efficiency of our method in this case we should break the process in *steps*. In any given step we should be sewing together exactly two amplitudes. We recall that by amplitude we refer to any gauge-invariant quantity.

Take for example the case depicted in Fig. 1.5a. To build the two-loop generalized-unitarity cut in question we need to sew together three tree-level amplitudes. Given that we need to sew all legs of the middle four-point amplitude, one might think that we are forced to introduce spurious singularities in one of the insertions of the physical-state projector. We circumvent that in the following way.

We start by sewing the two tree-level amplitudes on the left. We prepare them so that the legs that carry the momenta $\pm p_1$ and $\pm p_2$ obey the GWI. Then we proceed with the sewing using the simplified projectors. Next, we have to sew the one-loop quantity on the left with the tree-level amplitude on the right (Fig. 1.5b). Given that both of these objects are gauge-invariant quantities, we may again use the above method. Namely, we prepare them so that the legs that carry the momenta $\pm p_3$ and $\pm p_4$ obey the GWI. We do this by a simple change of basis, just like before. Then, we proceed with the sewing using the simplified projectors. In this way we may sew multiple amplitudes together, introducing the minimum number of spurious singularities.

An aspect that this method hinges on is the appropriate use of the special properties of
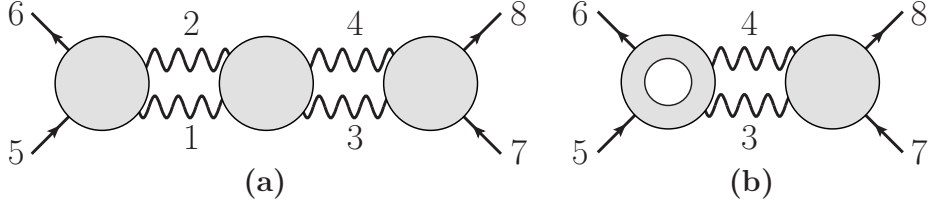
Figure 1.5: An example where we need to break the process into two steps. All exposed lines are taken as on-shell. Solid blobs represent tree-level amplitudes. In (b) the hollow blob represents the one-loop quantity we get by performing the physical-state sums for particles 1 and 2 on the two amplitudes on the left in (a).

polarization vectors. Specifically, we first manipulate the amplitudes into the appropriate form as discussed above. In doing so we should use all special properties of the polarization vectors. Then, we sew a number of legs of the amplitudes. Between these sewings we should not use any special properties of the polarization vectors, as that would interfere with the GWI of the legs left to be sewn. After all sewings of that step are completed, we should again use the special properties of the polarization vectors.

For example, referring again to Fig. 1.5, upon sewing particle 1, we introduce $\varepsilon_2 \cdot p_2$ and $\varepsilon_3 \cdot p_3$ among other terms. We should not set these terms to zero before sewing particle 2, as that would interfere with the GWI for that particle. After we complete the sewings of the left two amplitudes (i.e. the sewings of particles 1 and 2), we change our basis to make our amplitudes obey the GWI for particles 3 and 4. We should now use the special properties of the remaining polarization vectors. In our example, we should set $\varepsilon_3 \cdot p_3$ to zero, among other terms.

1.4.5   Summary

Here we briefly summarize the method developed above. The problem at hand is to organize a calculation in gauge theory or gravity where multiple D-dimensional sewings are required, as is for example typical for generalized-unitarity approaches to multiloop calculations. The conventional way of performing such a calculation is to use the physical-state projectors,

Eqs. (1.2) and (1.3), repeated here for convenience,

$$P^{\mu\nu}(p,q) = \sum_{\text{pols.}} \varepsilon^\mu(-p)\varepsilon^\nu(p) = \eta^{\mu\nu} - \frac{q^\mu p^\nu + p^\mu q^\nu}{q \cdot p}, \tag{1.59}$$

and

$$P^{\mu\nu\alpha\beta}(p,q) = \sum_{\text{pols.}} \varepsilon^{\mu\nu}(-p)\varepsilon^{\alpha\beta}(p) = \frac{1}{2}\left(P^{\mu\alpha}P^{\nu\beta} + P^{\nu\alpha}P^{\mu\beta}\right) - \frac{1}{D-2}P^{\mu\nu}P^{\alpha\beta}. \tag{1.60}$$

Our proposed method allows one to perform the sewings without introducing spurious singularities. Specifically, we bring the amplitudes to be sewn in a form such that we may replace $P^{\mu\nu}(p,q)$ with $\eta^{\mu\nu}$ in the above two equations. We refer to these projectors as simplified projectors.

To do so we first need to organize our calculation in steps. In each step we are only sewing two gauge-invariant quantities together. Before the sewing, we use momentum conservation and the on-shell conditions so that the momenta of the particles to be sewn are some of the independent momenta appearing in our expression. We may then verify that the amplitudes at hand obey the GWI for these legs. We proceed with the sewing using the simplified projectors. During a given step, between sewings, it is important not to use the on-shell conditions, as that spoils the GWI for the remaining legs to be sewn. Finally, after all sewings of a given step are completed, we may again use the on-shell conditions. If in any given step we have to sew all external particles of an amplitude and those particles are gauge-particles, then we have to introduce spurious singularities in one of the insertions of the projector.

1.4.6 An example in detail

Here we repeat the discussion of the construction of the three-loop generalized-unitarity cut depicted in Fig. 1.4 using the GWI approach. To construct the cut of Fig. 1.4 without introducing any spurious singularities we may follow these steps:

- We start by sewing particle 5. We need to verify that the associated three-point and four-point tree-level amplitudes satisfy the GWI for that particle. To do so, we choose

to use momentum conservation to eliminate momenta 10 and 11. Next, we impose the on-shell conditions. Now our amplitudes obey the GWI for particle 5 and we may proceed to sew it using the simplified projector.

- Next, we choose to sew particle 10. Since that particle is scalar, this simply amounts to multiplying the corresponding three-point amplitude with the result we got above.

- We continue by sewing particles 6 and 7. To do this we must manipulate both the expression we got so far and the four-point tree-level amplitude to obey the GWI for particles 6 and 7.

  - For the four-point amplitude we choose to solve momentum conservation as $p_9 = p_6 + p_7 - p_8$. Further, we impose $\varepsilon_9 \cdot p_8 = \varepsilon_9 \cdot p_7 + \varepsilon_9 \cdot p_6$ along with the remaining on-shell conditions. In this way we choose a basis where the momenta p_6 and p_7 are independent, turning the amplitude into obeying the GWI for the corresponding legs.

  - For the expression we got from the previous sewings, we use $p_3 = -p_1 - p_2 - p_4 - p_6 - p_7$. We impose the on-shell conditions for all exposed lines, even the ones already sewn (e.g. $p_{10}^2 - m_1^2 = p_5^2 = 0$).

We may now sew particles 6 and 7 using the simplified projector. It is important not to use any on-shell conditions between the two sewings. If we do, after sewing particle 6 for example, we spoil the GWI for particle 7. Namely, sewing particle 6 introduces $\varepsilon_7 \cdot p_7$ and ε_7^2. We do not set these terms to zero at this point, as they are essential in reproducing the correct result.

- We may now proceed to sew leg 8 and then leg 9, following a similar approach. Alternatively, we may multiply the remaining three-point amplitudes together to build a four-point quantity, which we then sew to the expression we got so far. We choose to do the latter in order to emphasize that we may sew any gauge-invariant quantity with the proposed method. Again, we should make sure that the two quantities obey the GWI for particles 8 and 9.

- For the four-point quantity, we choose to solve momentum conservation as $p_{11} = p_8 + p_9 - p_3$.

- For the expression we got so far we use $p_{11} = -p_1 - p_2 - p_4 - p_8 - p_9$. We should also choose one of the p_6, p_7 and p_{10} as our loop momentum and solve for the other two in terms of it. Then we impose the on-shell conditions. A new feature that appears here is the introduction of ε_8^2 and ε_9^2 from sewing particles 6 and 7. At this stage we should use the null condition and set them to zero.

After these manipulations we may sew the final two legs using the simplified projectors.

We comment again on the subtle point that we should not use the special properties of the polarization vectors between sewings of a given step, but we have to use them in order to make a quantity obey the GWI. This is why we do not set ε_7^2 to zero after sewing particle 6 but we do set ε_8^2 and ε_9^2 to zero after sewing particles 6 and 7.

We have explicitly verified that this process correctly reproduces the answer we get by using the full projector. We emphasize once more that we do not have to introduce spurious singularities at any of the steps taken.

1.5 Conclusions

D-dimensional approaches are useful in a variety of problems. Specifically, they are natural in the context of dimensional regularization [16]. In this setup it is often the case that we need to perform a physical-state sum of a gluon or graviton leg. An important example where such sums appear is calculations based on D-dimensional generalized unitarity [19, 20, 21, 22, 23, 24, 25, 26, 27, 28, 29]. Other examples include D-dimensional matrix-element squares for cross sections [49, 50, 51, 52], and the decomposition of an amplitude into gauge-invariant tensors [53, 54, 55, 56, 57, 58].

In general, these physical-state sums introduce spurious light-cone singularities. These spurious singularities unnecessarily complicate the expressions, especially in the gravitational

case. Further, if we do not eliminate them prior to phase-space or loop integration, the spurious singularities require nontrivial prescriptions to make them well defined. Hence, with new generalized-unitarity based calculations [12, 13, 46] pushing the frontier of relativistic gravitational-wave physics, there is a specific need for methods that avoid introducing these spurious singularities.

In this chapter we achieve this goal by providing two independent methods that allow us to perform the physical-state sums so that we do not introduce spurious singularities. Our methods are applicable to any gauge-invariant quantities, at tree or loop level. In our first method we identify gauge-invariant subpieces in our expression. We observe that we may perform the physical-state sum for each piece without introducing spurious singularities. In this way we derive a set of replacement rules that do not contain spurious singularities and are equivalent to the physical-state projectors. In our second method we use momentum conservation to bring our gauge-invariant quantities in a form such that they obey the generalized Ward identity for the legs to be sewn. In this form, the spurious singularities automatically drop out of the physical-state sums. We identify certain limitations on the applicability of this approach.

Spurious singularities also appear in physical-state sums of massive vector bosons, spin-3/2 particles, or other higher-spin fields. We are confident that we can tackle these problems with methods similar to the ones developed in this chapter. We hope that our methods will help simplify future calculations involving D-dimensional physical-state sums in gauge theory and gravity.

CHAPTER 2

Quadratic-in-Spin Hamiltonian at $\mathcal{O}(G^2)$ from Scattering Amplitudes

We obtain the quadratic-in-spin terms of the conservative Hamiltonian describing the interactions of a binary of spinning bodies in General Relativity through $\mathcal{O}(G^2)$ and to all orders in velocity. Our calculation extends a recently-introduced framework based on scattering amplitudes and effective field theory to consider non-minimal coupling of the spinning objects to gravity. At the order that we consider, we establish the validity of the formula proposed in [46] that relates the impulse and spin kick in a scattering event to the eikonal phase.

2.1   Introduction

The detection of gravitational waves by the LIGO and Virgo collaborations [60, 61] promises intriguing new discoveries. The main sources of gravitational waves are binary systems of compact astrophysical objects. Therefore, the great experimental advances also press for the development of high-precision theoretical tools for the modeling of the evolution of such systems. In the present chapter we consider the inspiral phase of the evolution of the binary. A well-developed theoretical tool to study this phase is the post-Newtonian (PN) approximation. This approach consists of an expansion in small velocities and weak gravitaional field. Several methods based on General Relativity (GR) [62, 63] as well as effective field theory (EFT) [64] have been developed in this direction. We instead choose to use the post-Minkowskian (PM) approximation, an expansion in Newton's constant G which

yields the exact velocity dependence. The PM approximation has a long history in GR [65] but has gained prominence recently (see e.g. [66, 67, 68]) due in part to the successful adaptation of modern scattering-amplitudes techniques.

The application of quantum-field-theory (QFT) methods to the study of the two-body problem dates back to the 1970's [69]. However, it was recently that Ref. [70] proposed the application of the well-established scattering-amplitudes toolkit to the derivation of gravitational potentials (see Refs. [71, 72, 73] for reviews on the modern amplitudes program). Along these lines, Ref. [74] developed an EFT of non-relativistic scalar fields which allowed the construction of the 2PM[1] canonical Hamiltonian from a one-loop scattering amplitude. This Hamiltonian was equivalent to the one of Ref. [65]. Refs. [12, 13, 75] later implemented this approach to obtain novel results at 3PM order. Ref. [76] followed up shortly after to compare these results against numerical relativity in terms of the energetics of the binary. Very recently, Ref. [77] obtained the conservative binary potential at 4PM order.

Besides making use of a non-relativistic EFT, various approaches have been developed to extract the dynamics of compact non-spinning objects from scattering data. Refs. [78, 79] established a formalism to obtain physical observables from unitarity cuts. Refs. [80, 81] made use of the Lippman-Schwinger equation. Refs. [82, 83] developed a boundary-to-bound (B2B) dictionary, and Refs. [84, 85] implemented a worldline PM EFT. Ref. [86] introduced a worldline QFT. Ref. [77] discovered an amplitude-action relation that allows the calculation of physical observables directly from the scattering amplitude.

The techniques mentioned above have been extended in multiple directions in recent years. Indeed, Refs. [87, 88, 89] applied similar methods to supergravity. Ref. [90] studied three-body dynamics, while Refs. [91, 92, 93, 94, 95] incorporated the radiation emitted by the binary into their analysis. Refs. [96, 97, 98, 99, 100, 101, 102] considered tidal deformations of the astrophysical objects. In the present chapter we explore a different direction and focus on effects due to the spin of the compact objects.

When considering intrinsic angular momentum in the problem of a binary of compact

---

[1]The nPM order corresponds to $\mathcal{O}(G^n)$.

astrophysical objects, one assumes that the spin of the objects is subdominant to the angular momentum of the system. In this way, we organize the effects we consider in a systematic expansion in the spin of the objects. Along these lines, there has been great progress in incorporating spin effects in the PN approximation. Refs. [103, 104, 105, 106, 107] approached these effects with traditional GR techniques. Ref. [108] extended the worldline EFT methods of Ref. [64] in this direction, and since then there have been substantial developments [109, 110, 111, 112, 113, 114, 115, 116, 117, 118, 119, 120, 121, 122, 123, 124, 125] (see Refs. [126, 127] for reviews).

The current state-of-the-art results at the 5PN[2] order include the linear-in-spin [128] and quadratic-in-spin [129] interactions at next-to-next-to-next-to-leading order and the cubic-in-spin [130] and quartic-in-spin [131] interactions at next-to-leading order. The PM literature on the other hand is less developed. Refs. [132, 133] recently obtained results at the 1PM and 2PM orders for effects linear in the spin of the objects via GR considerations. Ref. [134] treated the black hole (BH) case at 1PM order and exactly in the spin by matching an effective action to the linearized Kerr solution. Refs. [135, 136] obtained the 2PM-order scattering angle in the special kinematic configuration where the spins of the BHs are aligned to the orbital angular momentum of the binary.

Similarly to the non-spinning case, we may use scattering amplitudes to study the gravitational potential between spinning objects. Indeed, Ref. [137] calculated a one-loop amplitude using Feynman rules, which allowed them to obtain a 2PM-order potential by means of a Born iteration. Following the approach of [70], Ref. [138] reproduced Hamiltonians describing the interactions between spinning BHs by considering spinning particles minimally coupled to gravity. Later, Ref. [139] used the generalization of minimal-coupling amplitudes of [140] and the holomorphic classical limit of [141] to show that amplitudes encode information about BHs that is exact in spin. Refs. [142, 143] used the massive spinor-helicity formalism of [140] to study 2PM-order gravitational scattering from a one-loop amplitude.

---

[2]The nPN order corresponds to $\mathcal{O}(G^a v^{2b} S^c)$ with $a + b + c = n + 1$, where v is the relative velocity of the binary system and S corresponds collectively to the spins of the objects.

Furthermore, Ref. [144] related classical observables of a scattering process between spinning particles directly to the scattering amplitude, extending the formalism of [78]. Using this formalism, Refs. [145, 146, 147] obtained a 1PM-order Hamiltonian that reproduced the result of [134]. Finally, Ref. [46] obtained the conservative 2PM-order potential that is bilinear in the spin of the objects and valid for arbitrary spin orientations.

Studies of the classical physics of spinning particles have also revealed double copy structures. Refs. [148, 149, 150, 151, 152, 153] applied the definition of minimal coupling of [140] to classical solutions. In this way they made contact with the classical double copy of Ref. [154] and with an effective theory of on-shell heavy spinning particles [155]. The latter generalizes the heavy black hole effective theory of Ref. [156], whose amplitudes are known to double copy [157].

A suprising structure that emerged from the calculation of Ref. [46] is the expression of the observables in a scattering event in terms of the eikonal phase [158]. Similar relations already existed in the non-spinning case [158, 159, 160, 161, 45, 18, 162, 163, 88, 89]. In the spinning case there was evidence for such a relation in the special kinematic configuration where the spins of the particles are parallel to the angular momentum of the system [142, 135, 136]. The formula of [46] was the first example of such a relation for arbitrary orientations of the spins. This striking observation potentially implies that all physical observables are obtainable via simple manipulations of the scattering amplitude.

The goal of the present chapter is to obtain a 2PM-order Hamiltonian that describes the dynamics between a binary of generic spinning objects in GR including effects that are up to quadratic in the spin. We take the masses of the two objects to be m_1 and m_2 and the rest-frame spin three vectors to be $\boldsymbol{S}_1$ and $\boldsymbol{S}_2$. We denote the relative distance between the objects as $\boldsymbol{r}$ and the momentum three vector in the center-of-mass frame as $\boldsymbol{p}$. The

Hamiltonian then reads

$$H = \sqrt{\boldsymbol{p}^2 + m_1^2} + \sqrt{\boldsymbol{p}^2 + m_2^2} + V^{(0)}(\boldsymbol{r}^2, \boldsymbol{p}^2) + V^{(1,1)}(\boldsymbol{r}^2, \boldsymbol{p}^2)\frac{\boldsymbol{L} \cdot \boldsymbol{S}_1}{\boldsymbol{r}^2} + V^{(1,2)}(\boldsymbol{r}^2, \boldsymbol{p}^2)\frac{\boldsymbol{L} \cdot \boldsymbol{S}_2}{\boldsymbol{r}^2}$$

$$+ V^{(2,1)}(\boldsymbol{r}^2, \boldsymbol{p}^2)\frac{(\boldsymbol{r} \cdot \boldsymbol{S}_1)(\boldsymbol{r} \cdot \boldsymbol{S}_2)}{\boldsymbol{r}^4} + V^{(2,2)}(\boldsymbol{r}^2, \boldsymbol{p}^2)\frac{\boldsymbol{S}_1 \cdot \boldsymbol{S}_2}{\boldsymbol{r}^2} + V^{(2,3)}(\boldsymbol{r}^2, \boldsymbol{p}^2)\frac{(\boldsymbol{p} \cdot \boldsymbol{S}_1)(\boldsymbol{p} \cdot \boldsymbol{S}_2)}{\boldsymbol{r}^2}$$

$$+ V^{(2,4)}(\boldsymbol{r}^2, \boldsymbol{p}^2)\frac{(\boldsymbol{r} \cdot \boldsymbol{S}_1)^2}{\boldsymbol{r}^4} + V^{(2,5)}(\boldsymbol{r}^2, \boldsymbol{p}^2)\frac{\boldsymbol{S}_1^2}{\boldsymbol{r}^2} + V^{(2,6)}(\boldsymbol{r}^2, \boldsymbol{p}^2)\frac{(\boldsymbol{p} \cdot \boldsymbol{S}_1)^2}{\boldsymbol{r}^2} + \dots \,, \tag{2.1}$$

where $\boldsymbol{L} = \boldsymbol{r} \times \boldsymbol{p}$ is the orbital angular momentum, and the ellipsis stands for terms of higher order in the spin. Note that we omit terms quadratic in $\boldsymbol{S}_2$ as they are obtained from the ones quadratic in $\boldsymbol{S}_1$ via appropriate relabeling. The terms in Eq. (2.1) take the form

$$V^A(\boldsymbol{r}^2, \boldsymbol{p}^2) = \frac{G}{|\boldsymbol{r}|}c_1^A(\boldsymbol{p}^2) + \left(\frac{G}{|\boldsymbol{r}|}\right)^2 c_2^A(\boldsymbol{p}^2) + \mathcal{O}(G^3) \,, \tag{2.2}$$

where the label A takes the values indicated in Eq. (2.1).

Our task is to determine the coefficients c_i^A appearing in Eq. (2.2). For simplicity, and since the bilinear-in-spin interactions were given in Ref. [46], we may consider one of the bodies to be non spinning. This amounts to formally setting $\boldsymbol{S}_2 = 0$ in Eq. (2.1). We have explicitly verified that the results of this chapter do not change if we take into account all the terms in Eq. (2.1).

Following Refs. [74, 46], we obtain the potential coefficients in question via a matching calculation. First, we calculate a one-loop scattering amplitude in our so-called full theory. This is a theory that describes particles of arbitrary spin coupled to gravity. Specifically, it captures minimal and non-minimal coupling of the particles to gravity. In terms of our Lagrangian, we include all possible operators that are up to quadratic in the spin of the massive particle and up to linear in the curvature. Then, we calculate the corresponding amplitude in an EFT of spinning particles interacting via the Hamiltonian of Eq. (2.1). Our EFT generalizes that of Refs. [74, 46] to consider effects quadratic in the spin of one of the particles.

In obtaining these amplitudes we restrict to the piece that captures the classical dynamics. We implement the classical limit by rescaling $q \to \lambda q$, $S_1 \to (1/\lambda)S_1$ and expanding in λ, where q denotes graviton momenta and S_1 the covariant spin of the spinning particle. Finally, we fix the desired coefficients by matching the two computed amplitudes.
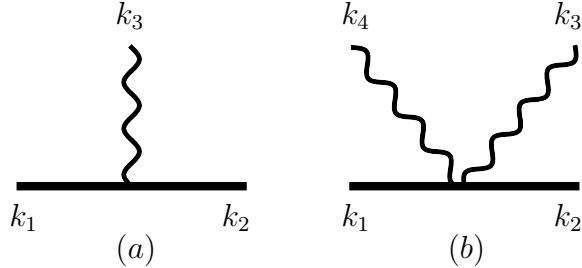
Figure 2.1: The Feynman vertices used to compute full-theory amplitudes. The three-particle vertex (a) determines the $\mathcal{O}(G)$ dynamics. The Compton amplitude, which requires the contact vertex (b), captures the $\mathcal{O}(G^2)$ dynamics. The straight lines correspond to the spinning particle, while the wiggly lines correspond to gravitons.

The remainder of this chapter is structured as follows: In Sec. 2.2 we review some aspects of the spin formalism introduced in [46] that we use throughout the chapter. Namely, we describe our field-theory approach to higher spin and its classical limit. We compute the necessary full-theory tree and one-loop amplitudes in Sec. 2.3. We adopt the method of generalized unitarity [164, 165, 166] to produce the loop-level amplitude, using tree-level amplitudes as building blocks. We then express the amplitudes in the center-of-mass frame, which facilitates the matching to the EFT. Sec. 2.4 contains the setup of the EFT, along with the computation of the EFT amplitudes. By equating the full-theory and EFT amplitudes, we obtain the desired two-body Hamiltonian. We compare our result against PN [167] and test-body [168] Hamiltonians in the literature. Finally, in Sec. 2.5 we use the derived Hamiltonian to compute scattering observables. We then establish that the conjecture of Ref. [46], which directly relates these observables to the eikonal phase [158], holds unaltered when we include the quadratic-in-spin effects. We present our concluding remarks in Sec. 5.7.

2.2 Review of Spin Formalism

In this section, we review the aspects of the higher-spin formalism that we use in the chapter. For further details, we refer the reader to Ref. [46].

We identify spinning compact astrophysical objects with higher-spin particles. We de-

scribe these massive particles of integer-spin s by real symmetric traceless rank-s tensor fields ϕ_s. For brevity, we suppress the indices of ϕ_s, implying matrix multiplication when necessary.

We use a Lagrangian to organize the interactions of higher-spin fields with gravity. Ref. [59] obtained such a Lagrangian using auxiliary fields to eliminate all but the spin-s representation of the $SO(3)$ rotation group. Here we relax this requirement, and interpret the theory as a relativistic effective theory that captures all spin-induced multipole moments of spinning objects coupled to gravity. We write the higher-spin Lagrangian $\mathcal{L}$ and action S as

$$\mathcal{L} = \mathcal{L}_{\min} + \mathcal{L}_{\mathrm{nonmin}} , \qquad S = \int d^4x \sqrt{-g}\mathcal{L} . \tag{2.3}$$

The minimal Lagrangian contains terms with up to two derivatives,

$$\mathcal{L}_{\min} = -R(e,\omega) + \frac{1}{2}g^{\mu\nu}\nabla(\omega)_\mu \phi_s \nabla(\omega)_\nu \phi_s - \frac{1}{2}m^2 \phi_s \phi_s . \tag{2.4}$$

The covariant derivative is

$$\nabla(\omega)_\mu \phi_s \equiv \partial_\mu \phi_s + \frac{i}{2}\omega_{\mu ef}M^{ef}\phi_s , \tag{2.5}$$

where ω is the spin connection, and M^{ab} are the Hermitian Lorentz generators. The gravitational field is described in the vielbein formulation. The non-minimal Lagrangian containing all the terms linear in the graviton and bilinear in the higher-spin field is

$$\mathcal{L}_{\mathrm{non\text{-}min}} = \sum_{n=1}^{\infty} \frac{(-1)^n}{(2n)!}\frac{C_{ES^{2n}}}{m^{2n}}\nabla(\omega)_{f_{2n}}\cdots\nabla(\omega)_{f_3}R_{f_1 a f_2 b}\nabla(\omega)^a \phi_s \, \mathbb{S}^{(f_1}\ldots\mathbb{S}^{f_{2n})}\nabla(\omega)^b \phi_s \tag{2.6}$$

$$-\sum_{n=1}^{\infty} \frac{(-1)^n}{(2n+1)!}\frac{C_{BS^{2n}}}{m^{2n+1}}\nabla(\omega)_{f_{2n+1}}\cdots\nabla(\omega)_{f_3}\frac{1}{2}\epsilon_{ab(c|f_1}R^{ab}{}_{|d)f_2}\nabla(\omega)^c \phi_s \mathbb{S}^{(f_1}\ldots\mathbb{S}^{f_{2n+1})}\nabla(\omega)^d \phi_s .$$

where we use an off-shell analog of the Pauli-Lubanski vector

$$\mathbb{S}^a \equiv -\frac{i}{2m}\epsilon^{abcd}M_{cd}\nabla(\omega)_b . \tag{2.7}$$

The operators in Eq. (3.3) are in direct correspondence to the non-minimal couplings in the worldline spinning-particle action of Ref. [169]. One could, in principle, include terms with dependence on higher powers of the curvature, but we do not attempt to do so in the present

chapter. Since our objective is to describe the dynamics up to spin squared, we focus on the first non-minimally coupled term,

$$\mathcal{L}_{ES^2} = -\frac{C_{ES^2}}{2m^2} R_{f_1 a f_2 b} \nabla^a \phi_s \, \mathbb{S}^{(f_1} \mathbb{S}^{f_2)} \nabla^b \phi_s. \tag{2.8}$$

Ref. [108] first studied the effects captured by this operator at leading order in the PN approximation. The extensions to next-to-leading and next-to-next-to-leading orders were considered in Refs. [111] and [167] respectively, while Ref. [170] studied its contributions to higher orders in spin. We instead consider its effects in the PM approximation.

To extract Feynman rules, we define the graviton as the fluctuation of the metric around Minkowski space. We determine the spin connection ω as the solution of the vielbein postulate, $\nabla_\mu(\omega) e_\nu{}^a = 0$. This yields the following expansions for the needed quantities

$$g_{\mu\nu} = \eta_{\mu\nu} + h_{\mu\nu}, \qquad e_\mu{}^a = \delta_\mu^a + \frac{1}{2} h_\mu{}^a - \frac{1}{8} h_{\mu\rho} h^{a\rho} + \mathcal{O}(h^3),$$

$$\omega(e)_{\mu cb} = -\partial_{[c} h_{b]\mu} - \frac{1}{4} h^\rho{}_{[c} \partial_\mu h_{b]\rho} + \frac{1}{2} h^\rho{}_{[c} \partial_\rho h_{b]\mu} - \frac{1}{2} h^\rho{}_{[c} \partial_{b]} h_{\mu\rho} + \mathcal{O}(h^3). \tag{2.9}$$

After substituting this expansion into the Lagrangian of Eq. (2.8), we follow a straightforward procedure to obtain the Feynman vertices in Fig. 2.1. These are the vertices necessary to determine the dynamics through $\mathcal{O}(G^2)$.

We describe the state of the higher-spin particles by their momentum p and polarization tensor $\varepsilon(p)$. To take the classical limit of expectation values, we choose "spin coherent states" [171], whose defining property is that they minimize the standard deviation of observables. Following [172, 173], we relate the classical spin tensor and Lorentz generators via

$$\varepsilon(\tilde{p}) M^{\mu_1 \nu_1} \varepsilon(p) = S(p)^{\mu_1 \nu_1} \varepsilon(\tilde{p}) \cdot \varepsilon(p) + \dots,$$

$$\varepsilon(\tilde{p}) \{ M^{\mu_1 \nu_1}, M^{\mu_2 \nu_2} \} \varepsilon(p) = S(p)^{\mu_1 \nu_1} S(p)^{\mu_2 \nu_2} \varepsilon(\tilde{p}) \cdot \varepsilon(p) + \dots, \tag{2.10}$$

where $\{A, B\} \equiv \frac{1}{2}(AB + BA)$ and $\tilde{p} \equiv -p - q$ (note that we use the all-outgoing convention). We can also write analogous expressions for products with higher powers of the Lorentz generator. Throughout the chapter we omit terms that do not contribute to the classical potential in ellipsis. These include terms that do not survive in the classical limit and terms that cancel in the matching between full-theory and EFT amplitudes.

36

Importantly, one can only interpret the symmetric product of Lorentz generators as a product of spin tensors. However, it is always possible to decompose a product of Lorentz generators into a sum of completely symmetric products by means of the Lorentz algebra,

$$[M^{\mu_1\nu_1}, M^{\mu_2\nu_2}] = i(\eta^{\mu_3\mu_1} M^{\mu_4\mu_2} + \eta^{\mu_2\mu_3} M^{\mu_1\mu_4} - \eta^{\mu_4\mu_1} M^{\mu_3\mu_2} - \eta^{\mu_2\mu_4} M^{\mu_1\mu_3}). \tag{2.11}$$

We take the spin tensor to obey the so-called covariant spin supplementary condition,

$$p_\mu S(p)^{\mu\nu} = 0. \tag{2.12}$$

We define the Pauli-Lubanski spin vector by

$$S^\alpha(p) = -\frac{1}{2m}\epsilon^{\alpha\beta\gamma\delta} p_\beta S_{\gamma\delta}(p). \tag{2.13}$$

Using the on-shell condition for the spinning particle $p^2 = m^2$ and Eq. (2.12), we find

$$S^{\alpha\beta}(p) = -\frac{1}{m}\epsilon^{\alpha\beta\gamma\delta} p_\gamma S_\delta(p). \tag{2.14}$$

For this choice of the spin vector we have

$$S(p)^\mu = \left(\frac{\boldsymbol{p}\cdot\boldsymbol{S}}{m}, \boldsymbol{S} + \frac{\boldsymbol{p}\cdot\boldsymbol{S}}{m(E+m)}\boldsymbol{p}\right), \tag{2.15}$$

where $\boldsymbol{S}$ is the three-dimensional rest-frame spin of the particle and $p = -(E, \boldsymbol{p})$. I.e. we obtain the covariant spin vector by boosting its rest-frame counterpart. Finally, by writing the polarization tensors as boosts of rest-frame coherent states [171], we have

$$\varepsilon(\tilde{p})\cdot\varepsilon(p) = \exp\left[-\frac{\boldsymbol{L}_q\cdot\boldsymbol{S}}{m(E+m)}\right] + \dots, \tag{2.16}$$

where $\boldsymbol{L}_q \equiv i\boldsymbol{p}\times\boldsymbol{q}$, and the ellipsis stand for terms that do not contribute to the classical potential.

2.3 Full theory amplitudes

In this section we calculate the scattering amplitudes needed to construct the desired Hamiltonian. Specifically, we obtain the relevant pieces of the tree-level and one-loop two-to-two
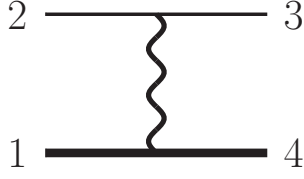
Figure 2.2: The tree-level amplitude that captures the $\mathcal{O}(G)$ spin interactions. The thick (thin) straight line represents the spinning (scalar) particle, while the wiggly line corresponds to the exchanged graviton.
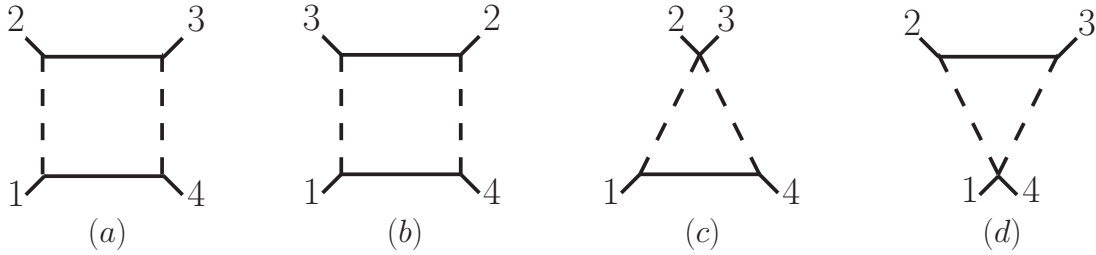
Figure 2.3: The one-loop scalar box integrals $I_\square$ (a) and $I_{\bowtie}$ (b) and the corresponding triangle integrals $I_\triangle$ (c) and $I_\triangledown$ (d). The bottom (top) solid line corresponds to a massive propagator of mass m_1 (m_2). The dashed lines denote massless propagators.

scattering amplitude between a scalar and a spinning particle. For the tree-level amplitudes we use the Feynman rules derived in the previous section. We use the generalized unitarity method [164, 165, 166] for the one-loop amplitude. Anticipating the comparison to the EFT amplitudes, we specialize our results to the center-of-mass frame.

2.3.1   Constructing the full-theory amplitudes

The information to determine the $\mathcal{O}(G)$ Hamiltonian is contained in the tree-level amplitude shown in Fig. 2.2. We take the incoming momentum of the spinning (scalar) particle to be $-p_1$ ($-p_2$) and its outgoing momentum to be p_4 (p_3). Using the Feynman rules obtained above, we find

$$\mathcal{M}^{\text{tree}} = -\frac{4\pi G}{q^2}\,\varepsilon_1 \cdot \varepsilon_4 \left(\alpha_1^{(0)} + \alpha_1^{(1,1)}\mathcal{E}_1 + \alpha_1^{(2,4)}(q \cdot S_1)^2\right) + \dots, \tag{2.17}$$

38

where $\mathcal{E}_1 \equiv i\epsilon^{\mu\nu\rho\sigma}p_{1\mu}p_{2\nu}q_\rho S_{1\sigma}$, and the labeling scheme for α_i^A follows that for c_i^A in Eq. (2.2). In the ellipsis we omit terms that do not contribute to the classical limit, along with pieces proportional to q^2, since they cancel the propagator and do not yield long-range contributions. The coefficients α_1^A take the explicit form

$$\alpha_1^{(0)} = 4m^4\nu^2(2\sigma^2 - 1)\,, \qquad \alpha_1^{(1,1)} = \frac{8m^2\nu\sigma}{m_1}\,, \qquad \alpha_1^{(2,4)} = \frac{2C_{ES^2}m^4\nu^2(2\sigma^2 - 1)}{m_1^2}\,, \qquad (2.18)$$

where we use the variables

$$\sigma = \frac{p_1 \cdot p_2}{m_1 m_2}\,, \qquad m = m_1 + m_2\,, \qquad \nu = \frac{m_1 m_2}{m^2}\,. \qquad (2.19)$$

In order to construct the $\mathcal{O}(G^2)$ Hamiltonian we further need the corresponding one-loop amplitude. We may express any one-loop amplitude as a linear combination of scalar box, triangle, bubble and tadpole integrals [174]. Refs. [74, 13] showed that the bubble and tadpole integrals do not contribute to the classical limit. Dropping these pieces we may write

$$i\mathcal{M}^{\text{1-loop}} = d_\square I_\square + d_{\bowtie} I_{\bowtie} + c_\triangle I_\triangle + c_\triangledown I_\triangledown\,, \qquad (2.20)$$

where the coefficients $d_\square$, $d_{\bowtie}$, $c_\triangle$ and $c_\triangledown$ are rational functions of external momenta and polarization tensors. The integrals $I_\square$, $I_{\bowtie}$, $I_\triangle$ and $I_\triangledown$ are shown in Fig. 2.3. The triangle integrals take the form [74]

$$I_{\triangle,\triangledown} = -\frac{i}{32m_{1,2}}\frac{1}{\sqrt{-q^2}} + \cdots\,. \qquad (2.21)$$

The box contributions do not contain any novel $\mathcal{O}(G^2)$ information. They correspond to infrared-divergent pieces that cancel out when we equate the full-theory and EFT amplitudes [74, 13]. In this sense, the explicit values for the box coefficients serve only as a consistency check of our calculation and we do not show them. Instead, we give the result for

$$i\mathcal{M}^{\triangle+\triangledown} \equiv c_\triangle I_\triangle + c_\triangledown I_\triangledown\,. \qquad (2.22)$$

We use the generalized-unitarity method [164, 165, 166, 175] to obtain the integral coefficients of Eq. (2.20). We start by calculating the gravitational Compton amplitude for
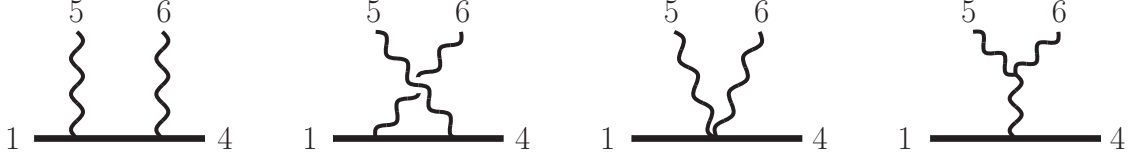
Figure 2.4: The Compton-amplitude Feynman diagrams. The straight line corresponds to the spinning particle. The wiggly lines correspond to gravitons.
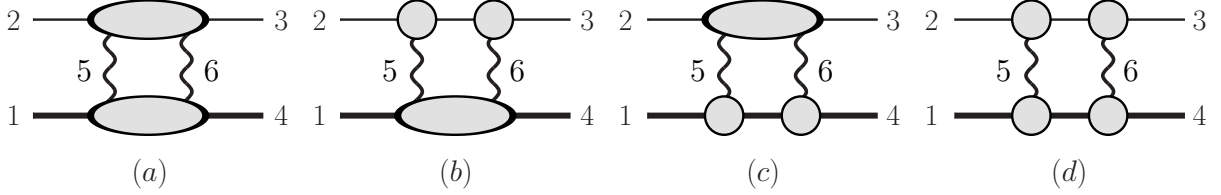
Figure 2.5: Appropriate residues of the two-particle cut (a) give the triple cuts (b) and (c), and the quadruple cut (d). The thick straight line corresponds to the spinning particle, the thin straight line to the scalar, and the wiggly lines to the exchanged gravitons. All exposed lines are taken on-shell.

the spinning particle, using the Feynman rules derived in the previous section. We depict the relevant Feynman diagrams in Fig. 2.4. Subsequently, we construct the two-particle cut depicted in Fig. 2.5(a) by gluing the Compton amplitude for the spinning particle with that for a scalar. The latter is a well-known amplitude. The residue of the two-particle cut on the scalar-matter pole gives the triple cut in Fig. 2.5(b), while the one on the spinning-matter pole gives the triple cut in Fig. 2.5(c). Localizing both matter poles gives the quadruple cut in Fig. 2.5(d). Finally, following Refs. [176, 177, 28], we obtain the box and triangle coefficients from the quadruple and triple cuts respectively. Our result reads

$$
\mathcal{M}^{\triangle + \triangledown} = \frac{2\pi^2 G^2 \varepsilon_1 \cdot \varepsilon_4}{\sqrt{-q^2}} \left[\alpha_2^{(0)} + \alpha_2^{(1,1)} \mathcal{E}_1 + \alpha_2^{(2,4)} (q \cdot S_1)^2 + \alpha_2^{(2,5)} q^2 S_1^2 + \alpha_2^{(2,6)} q^2 (p_2 \cdot S_1)^2 \right] + \dots ,
$$

where the coefficients are given by

$$\alpha_2^{(0)} = 3m^5\nu^2(5\sigma^2 - 1)\,, \qquad \alpha_2^{(1,1)} = \frac{m^2(4m_1 + 3m_2)(5\sigma^2 - 3)\nu\sigma}{m_1(\sigma^2 - 1)}\,,$$

$$\alpha_2^{(2,4)} = -\frac{m_2^2}{16(\sigma^2 - 1)}\Big[-4m_2\big(-\sigma^2 + 1 + C_{ES^2}(30\sigma^4 - 29\sigma^2 + 3)\big)$$
$$- m_1\big(35\sigma^4 - 30\sigma^2 - 5 + C_{ES^2}(155\sigma^4 - 174\sigma^2 + 35)\big)\Big]\,,$$

$$\alpha_2^{(2,5)} = -\frac{m_2^2}{16(\sigma^2 - 1)}\Big[4m_2\big(15\sigma^4 - 17\sigma^2 + 2 + C_{ES^2}(15\sigma^4 - 13\sigma^2 + 2)\big)$$
$$+ m_1\big(95\sigma^4 - 102\sigma^2 + 7 + C_{ES^2}(95\sigma^4 - 102\sigma^2 + 23)\big)\Big]\,,$$

$$\alpha_2^{(2,6)} = -\frac{1}{8(\sigma^2 - 1)^2}\Big[2m_2\big(15\sigma^4 - 14\sigma^2 - 1 + C_{ES^2}(15\sigma^4 - 10\sigma^2 + 3)\big)$$
$$+ m_1\big(65\sigma^4 - 66\sigma^2 + 1 + C_{ES^2}(65\sigma^4 - 66\sigma^2 + 17)\big)\Big]\,. \qquad (2.23)$$

We note here that the relation $\alpha_2^{(2,4)} = -\alpha_2^{(2,5)}$, which was expected following a pattern observed in Refs. [156, 46], is broken for generic values of C_{ES^2}. We recover this relation for $C_{ES^2} = 1$, which corresponds to the Kerr black hole [134]. This is in line with a recent observation in Ref. [97], that this equality fails to hold in the presence of tidal finite-size effects.

2.3.2   The amplitudes in the center-of-mass frame

In preparation for the matching procedure in the following section, we specialize our expressions to the center-of-mass frame. In this frame, the independent four-momenta read

$$p_1 = -(E_1, \boldsymbol{p})\,, \qquad p_2 = -(E_2, -\boldsymbol{p})\,, \qquad q = (0, \boldsymbol{q})\,, \qquad \boldsymbol{p} \cdot \boldsymbol{q} = \boldsymbol{q}^2/2\,. \quad (2.24)$$

Using Eq. (2.15), we have

$$q \cdot S_1 = \boldsymbol{q} \cdot \boldsymbol{S}_1 - \frac{\boldsymbol{q}^2 \boldsymbol{p} \cdot \boldsymbol{S}_1}{2m_1(E_1 + m_1)}\,, \qquad i\epsilon^{\mu\nu\rho\sigma}p_{1\mu}p_{2\nu}q_\rho S_{1\sigma} = E\,\boldsymbol{L}_q \cdot \boldsymbol{S}_1\,,$$
$$p_2 \cdot S_1 = -\frac{E}{m_1}\boldsymbol{p} \cdot \boldsymbol{S}_1\,. \qquad (2.25)$$

Furthermore, Eq. (2.16) becomes

$$\varepsilon_1 \cdot \varepsilon_4 = 1 - \frac{\boldsymbol{L}_q \cdot \boldsymbol{S}_1}{m_1(E_1 + m_1)} + \frac{(\boldsymbol{L}_q \cdot \boldsymbol{S}_1)^2}{2m_1^2(E_1 + m_1)^2} + \dots\,. \qquad (2.26)$$

41

Using the above expressions, our amplitudes take the form

$$\frac{\mathcal{M}^{\text{tree}}}{4E_1 E_2} = \frac{4\pi G}{\boldsymbol{q}^2}\left[a_1^{(0)} + a_1^{(1,1)}\boldsymbol{L}_q \cdot \boldsymbol{S}_1 + a_1^{(2,4)}(\boldsymbol{q}\cdot\boldsymbol{S}_1)^2\right], \qquad (2.27)$$

$$\frac{\mathcal{M}^{\triangle+\triangledown}}{4E_1 E_2} = \frac{2\pi^2 G^2}{|\boldsymbol{q}|}\left[a_2^{(0)} + a_2^{(1,1)}\boldsymbol{L}_q \cdot \boldsymbol{S}_1 + a_2^{(2,4)}(\boldsymbol{q}\cdot\boldsymbol{S}_1)^2 + a_2^{(2,5)}\boldsymbol{q}^2\,\boldsymbol{S}_1^2 + a_2^{(2,6)}\boldsymbol{q}^2\,(\boldsymbol{p}\cdot\boldsymbol{S}_1)^2\right].$$

The coefficients a_i^A are given in terms of the α_i^A of Eqs. (2.18) and (2.23) by[3]

$$a_i^{(0)} = \frac{\alpha_i^{(0)}}{4m^2\gamma^2\xi}, \qquad a_i^{(1,1)} = \frac{\alpha_i^{(1,1)}}{4m\gamma\xi} - \frac{1}{m_1^2(\gamma_1+1)}\frac{\alpha_i^{(0)}}{4m^2\gamma^2\xi},$$

$$a_i^{(2,j)} = \frac{\alpha_i^{(2,j)}\tilde\zeta^{(j)}}{4m^2\gamma^2\xi} - \frac{\zeta^{(j)}}{m_1^2(\gamma_1+1)}\frac{\alpha_i^{(1,1)}}{4m\gamma\xi} + \frac{\zeta^{(j)}}{m_1^4(\gamma_1+1)^2}\frac{\alpha_i^{(0)}}{8m^2\gamma^2\xi}, \qquad (2.28)$$

where $i = 1, 2$ and the structure-dependent coefficients are given by

$$\zeta^{(4)} = -\zeta^{(5)} = \boldsymbol{p}^2, \qquad \zeta^{(6)} = 1, \qquad \tilde\zeta^{(4)} = \tilde\zeta^{(5)} = 1, \qquad \tilde\zeta^{(6)} = -\frac{E^2}{m_1^2}. \qquad (2.29)$$

In addition to the definitions in Eq. (2.19) we use

$$\gamma = \frac{E}{m}, \qquad \gamma_1 = \frac{E_1}{m_1}, \qquad E = E_1 + E_2, \qquad \xi = \frac{E_1 E_2}{E^2}. \qquad (2.30)$$

2.4 Hamiltonian from effective field theory

We now turn our attention to the task of translating the scattering amplitudes of higher-spin fields to a two-body conservative Hamiltonian. We do this by matching the scattering amplitude computed in the last section to the two-to-two amplitude of an EFT of the positive-energy modes of higher-spin fields. Ref. [74] developed this matching procedure for higher orders in G and all orders in velocity, while Ref. [46] extended the formalism to include spin degrees of freedom. We conclude this section by comparing our answer with previous results in the literature.

---

[3]Note that unlike Ref. [46] we do not introduce the coefficients a_{cov}. This means that factors of the spin in Eq. (2.27) appear both because we specialize in the center-of-mass frame and due to Eq. (2.26).

2.4.1 EFT scattering amplitudes

The action of the effective field theory for the higher-spin fields ξ_1 and ξ_2 is given by

$$S = \int_{\boldsymbol{k}} \sum_{a=1,2} \xi_a^\dagger(-\boldsymbol{k}) \left(i\partial_t - \sqrt{\boldsymbol{k}^2 + m_a^2} \right) \xi_a(\boldsymbol{k}) - \int_{\boldsymbol{k},\boldsymbol{k}'} \xi_1^\dagger(\boldsymbol{k}')\xi_2^\dagger(-\boldsymbol{k}') \, V(\boldsymbol{k}',\boldsymbol{k},\hat{\boldsymbol{S}}_1) \, \xi_1(\boldsymbol{k})\xi_2(-\boldsymbol{k}) \,,$$

$$(2.31)$$

where $\int_{\boldsymbol{k}} = \int \frac{d^{D-1}\boldsymbol{k}}{(2\pi)^{D-1}}$, and the interaction potential $V(\boldsymbol{k}',\boldsymbol{k},\hat{\boldsymbol{S}}_1)$ is a function of the incoming and outgoing momenta $\boldsymbol{k}$ and $\boldsymbol{k}'$, and the spin operator $\hat{\boldsymbol{S}}_1$. We consider kinematics in the center-of-mass frame. As in the full theory side, we choose the field ξ_2 to be a scalar, while the asymptotic states of ξ_1 are taken to be spin coherent states. We obtain the classical rest-frame spin vector as the expectation value of the spin operator with respect to these on-shell states.

We build the most general potential containing only long-range classical contributions, up to quadratic order in spin. In momentum space, a minimal basis of interactions in the on-shell scheme is given by the operators

$$\hat{\mathbb{O}}^{(0)} = \mathbb{I} \,, \quad \hat{\mathbb{O}}^{(1,1)} = \boldsymbol{L}_{\hat{q}} \cdot \hat{\boldsymbol{S}}_1 \,, \quad \hat{\mathbb{O}}^{(2,4)} = \left(\hat{\boldsymbol{q}} \cdot \hat{\boldsymbol{S}}_1 \right)^2 \,, \quad \hat{\mathbb{O}}^{(2,5)} = \hat{\boldsymbol{q}}^2 \, \hat{\boldsymbol{S}}_1^2 \,, \quad \hat{\mathbb{O}}^{(2,6)} = \hat{\boldsymbol{q}}^2 \left(\boldsymbol{k} \cdot \hat{\boldsymbol{S}}_1 \right)^2 \,,$$

$$(2.32)$$

where[4] $\hat{\boldsymbol{q}} \equiv \boldsymbol{k} - \boldsymbol{k}'$ and $\boldsymbol{L}_{\hat{q}} \equiv i\boldsymbol{k} \times \hat{\boldsymbol{q}}$. Their expectation values with respect to spin coherent states are in one-to-one correspondence with the monomials in the full theory amplitude, Eq. (2.27). The labeling scheme for the operators follows the conventions of Eq. (2.1). We use the following ansatz for the potential operator

$$V(\boldsymbol{k}',\boldsymbol{k},\hat{\boldsymbol{S}}_1) = \sum_A V^A(\boldsymbol{k}',\boldsymbol{k}) \, \hat{\mathbb{O}}^A \,, \tag{2.33}$$

where A runs over the superscripts of the operators in Eq. (2.32). $V^A(\boldsymbol{k}',\boldsymbol{k})$ are free coefficients with the same structure as the spin-independent potential of Refs. [13, 12],

$$V^A(\boldsymbol{k}',\boldsymbol{k}) = \frac{4\pi G}{\hat{\boldsymbol{q}}^2} d_1^A \left(\hat{\boldsymbol{p}}^2 \right) + \frac{2\pi^2 G^2}{|\hat{\boldsymbol{q}}|} d_2^A \left(\hat{\boldsymbol{p}}^2 \right) + \mathcal{O}(G^3) \,, \tag{2.34}$$

---

[4]The three-vectors $\hat{\boldsymbol{q}}$ and $\hat{\boldsymbol{p}}$ are not to be confused with unit-norm vectors.

where $\hat{\boldsymbol{p}}^2 \equiv (\boldsymbol{k}^2 + \boldsymbol{k}'^2)/2$. At the $\mathcal{O}(G)$ level, the operators containing a factor of $\hat{\boldsymbol{q}}^2$ can be ignored, as they lead to contact terms. Therefore we choose

$$d_1^{(2,5)} = d_1^{(2,6)} = 0 \,. \tag{2.35}$$

However, the factor of $\hat{\boldsymbol{q}}^2$ does not cancel out with the $\mathcal{O}(G^2)$ denominator, so we need to keep $d_2^{(2,5)}$ and $d_2^{(2,6)}$.

We now evaluate the EFT two-to-two scattering amplitude. To this end we use the Feynman rules derived from the EFT action (Eq. (2.31)),

$$\frac{(E, \boldsymbol{k})}{\ } = \frac{i\,\mathbb{I}}{E - \sqrt{\boldsymbol{k}^2 + m^2} + i\epsilon}\,, \qquad = -iV(\boldsymbol{k}', \boldsymbol{k}, \hat{\boldsymbol{S}}_1)\,. \tag{2.36}$$

Using these rules we compute the amplitude up to $\mathcal{O}(G^2)$ directly evaluating the relevant Feynman diagrams, omitting terms that do not contribute to long range interactions. The spin-dependent vertices must be treated as operators, and thus their ordering is important. After carrying out the energy integration, we obtain an expression for the amplitude

$$\mathcal{M}^{\mathrm{EFT}} = - V(\boldsymbol{p}', \boldsymbol{p}, \boldsymbol{S}_1) - \int_{\boldsymbol{k}} \frac{V(\boldsymbol{p}', \boldsymbol{k}, \boldsymbol{S}_1)\, V(\boldsymbol{k}, \boldsymbol{p}, \boldsymbol{S}_1)}{E_1 + E_2 - \sqrt{\boldsymbol{k}^2 + m_1^2} - \sqrt{\boldsymbol{k}^2 + m_2^2}}\,. \tag{2.37}$$

Similarly to the full theory, in order to extract the classical limit, one needs to first decompose products of the spin vector into irreducible representations of the rotation group, by repeated use of the $SO(3)$ algebra.

At $\mathcal{O}(G)$ the EFT amplitude receives a contribution only from the first term of Eq. (2.37),

$$\mathcal{M}_{1PM}^{EFT} = \frac{4\pi G}{\boldsymbol{q}^2} \left[a_1^{(0)} + a_1^{(1,1)} \boldsymbol{L}_q \cdot \boldsymbol{S}_1 + a_1^{(2,4)} (\boldsymbol{q} \cdot \boldsymbol{S}_1)^2 \right]\,. \tag{2.38}$$

The a_1^A are given directly in terms of the momentum-space potential coefficients,

$$a_1^A = -d_1^A\,. \tag{2.39}$$

The EFT amplitude at $\mathcal{O}(G^2)$ receives contributions from both terms in Eq. (2.37) and

can be written as

$$\mathcal{M}_{2PM}^{EFT} = \frac{2\pi^2 G^2}{|\boldsymbol{q}|}\left[a_2^{(0)} + a_2^{(1,1)}\boldsymbol{L}_q \cdot \boldsymbol{S}_1 + a_2^{(2,4)}(\boldsymbol{q}\cdot\boldsymbol{S}_1)^2 + a_2^{(2,5)}\boldsymbol{q}^2\,\boldsymbol{S}_1^2 + a_2^{(2,6)}\boldsymbol{q}^2\,(\boldsymbol{p}\cdot\boldsymbol{S}_1)^2\right]$$
$$+ (4\pi G)^2\,a_{iter}\int\frac{d^{D-1}\boldsymbol{\ell}}{(2\pi)^{D-1}}\frac{2\xi E}{\boldsymbol{\ell}^2(\boldsymbol{\ell}+\boldsymbol{q})^2(\boldsymbol{\ell}^2+2\boldsymbol{p}\cdot\boldsymbol{\ell})}\,,$$

(2.40)

where $\boldsymbol{\ell} = \boldsymbol{k} - \boldsymbol{p}$ and we only keep terms that are relevant in the classical limit. The above coefficients are given by

$$a_2^{(0)} = -d_2^{(0)} + \frac{1}{2\xi E}\tilde{A}_0\left[\left(d_1^{(0)}\right)^2\right],$$

(2.41)

$$a_2^{(1,1)} = -d_2^{(1,1)} + \frac{1}{2\xi E}\tilde{A}_2\left[d_1^{(0)}d_1^{(1,1)}\right],$$

$$a_2^{(2,4)} = -d_2^{(2,4)} + \frac{3}{8\xi E}\tilde{A}_{4/3}\left[d_1^{(0)}d_1^{(2,4)}\right] + \frac{\boldsymbol{p}^2}{16\xi E}\tilde{A}_4\left[\left(d_1^{(1,1)}\right)^2\right] + \frac{\xi E}{4}d_1^{(1,1)}d_1^{(2,4)},$$

$$a_2^{(2,5)} = -d_2^{(2,5)} - \frac{1}{8\xi E}\tilde{A}_4\left[d_1^{(0)}d_1^{(2,4)}\right] - \frac{\boldsymbol{p}^2}{8\xi E}\tilde{A}_4\left[\left(d_1^{(1,1)}\right)^2\right] + \frac{\xi E}{4}d_1^{(1,1)}d_1^{(2,4)},$$

$$a_2^{(2,6)} = -d_2^{(2,6)} + \frac{\xi E}{\boldsymbol{p}^4}d_1^{(0)}d_1^{(2,4)} + \frac{1}{8\xi E}\tilde{A}_4\left[\left(d_1^{(1,1)}\right)^2\right] - \frac{\xi E}{\boldsymbol{p}^2}d_1^{(1,1)}d_1^{(2,4)},$$

where we define the function

$$\tilde{A}_j[X] = \left[(1-3\xi) + \frac{j\xi^2 E^2}{\boldsymbol{p}^2} + 2\xi^2 E^2\partial\right]X,$$

(2.42)

and the derivative is taken with respect to the square of the center-of-mass momentum $\partial = \partial/\partial\boldsymbol{p}^2$. The second term in Eq. (2.40) is infrared divergent and should cancel out when we equate the full-theory and EFT amplitudes. We have explicitly verified this cancellation at leading order in the classical expansion.

2.4.2 Conservative spin Hamiltonian

As mentioned in Sec. 5.1, our final result is the position-space Hamiltonian,

$$H = \sqrt{\boldsymbol{p}^2 + m_1^2} + \sqrt{\boldsymbol{p}^2 + m_2^2} + V^{(0)}(\boldsymbol{r}^2, \boldsymbol{p}^2) + V^{(1,1)}(\boldsymbol{r}^2, \boldsymbol{p}^2)\frac{\boldsymbol{L}\cdot\boldsymbol{S}_1}{\boldsymbol{r}^2}$$
$$+ V^{(2,4)}(\boldsymbol{r}^2, \boldsymbol{p}^2)\frac{(\boldsymbol{r}\cdot\boldsymbol{S}_1)^2}{\boldsymbol{r}^4} + V^{(2,5)}(\boldsymbol{r}^2, \boldsymbol{p}^2)\frac{\boldsymbol{S}_1^2}{\boldsymbol{r}^2} + V^{(2,6)}(\boldsymbol{r}^2, \boldsymbol{p}^2)\frac{(\boldsymbol{p}\cdot\boldsymbol{S}_1)^2}{\boldsymbol{r}^2} + \dots. \quad (2.43)$$

45

The potentials take the form

$$V^A(\boldsymbol{r}^2, \boldsymbol{p}^2) = \frac{G}{|\boldsymbol{r}|} c_1^A(\boldsymbol{p}^2) + \left(\frac{G}{|\boldsymbol{r}|}\right)^2 c_2^A(\boldsymbol{p}^2) + \mathcal{O}(G^3) \,. \tag{2.44}$$

We obtain the position-space Hamiltonian by taking the Fourier transform of the momentum-space Hamiltonian with respect to the momentum transfer $\boldsymbol{q}$, which is the conjugate of the separation between the particles $\boldsymbol{r}$. In this way, we express the position-space coefficients c_i^A in terms of the momentum-space coefficients d_i^A via linear relations dictated by the $\boldsymbol{q}$-dependence of the spin operators,

$$c_1^{(0)} = d_1^{(0)} \,, \quad c_1^{(1,1)} = -d_1^{(1,1)} \,, \quad c_1^{(2,4)} = -3d_1^{(2,4)} \,, \quad c_1^{(2,5)} = d_1^{(2,4)} \,, \qquad c_1^{(2,6)} = 0 \,, \tag{2.45}$$

$$c_2^{(0)} = d_2^{(0)} \,, \quad c_2^{(1,1)} = -2d_2^{(1,1)} \,, \quad c_2^{(2,4)} = -8d_2^{(2,4)} \,, \quad c_2^{(2,5)} = 2d_2^{(2,4)} - 2d_2^{(2,5)} \,, \quad c_2^{(2,6)} = -2d_2^{(2,6)} \,.$$

We determine the momentum-space coefficients d_i^A in terms of the amplitudes coefficients a_i^A by the relations in Eqs. (2.39) and (2.41). We may now obtain a_i^A by demanding that the EFT amplitude matches the full-theory one,

$$\mathcal{M}_{\mathrm{1PM}}^{\mathrm{EFT}} = \frac{\mathcal{M}^{\mathrm{tree}}}{4E_1 E_2} \,, \qquad \mathcal{M}_{\mathrm{2PM}}^{\mathrm{EFT}} = \frac{\mathcal{M}^{\mathrm{1\text{-}loop}}}{4E_1 E_2} \,, \tag{2.46}$$

where the factors of the energy account for the non-relativistic normalization of the EFT amplitude. Using Eq. (2.28) we relate a_i^A to α_i^A, which are explicitly shown in Eqs. (2.18) and (2.23). Putting everything together, we obtain novel expressions for the position-space coefficients c_i^A.

2.4.3 Comparison to the literature

In order to ensure the validity of our result, we compare it with existing Hamiltonians in the General Relativity literature. Specifically, we compare with overlapping results in Ref. [167], which obtained the next-to-next-to-leading order post-Newtonian Hamiltonian, and in Ref. [168], which calculated the test-body Hamiltonian. Both references included interactions of up to quadratic order in the spins.

One way to establish the equivalence of two Hamiltonians is to construct a canonical transformation that extrapolates between them. Alternatively, we may compare the gauge invariant scattering amplitudes calculated from the two Hamiltonians by means of the EFT. We take the latter approach here. To do so, we promote the spin vector in the classical Hamiltonians to the spin operator, and we account for the non-isotropic terms according to the conventions of [74, 12, 13].

In this way we obtain EFT amplitudes in the form of Eqs. (2.38) and (2.40). The relevant coefficients for our purposes obtained using the Hamiltonian of Ref. [167] read

$$a_1^{(2,4)} = \frac{m_2 C_{ES^2}}{2m_1} - \frac{8m_1 m_2 + 7m_2^2 - C_{ES^2}\left(6m_1^2 + 16m_1 m_2 + 6m_2^2\right)}{8m_1^3 m_2} \boldsymbol{p}^2 \tag{2.47}$$
$$- \frac{3m_2^2(7m_1^2 + 4m_1 m_2 - 2m_2^2) + C_{ES^2}(5m_1^4 - 18m_1^2 m_2^2 + 5m_2^4)}{16m_1^5 m_2^3} \boldsymbol{p}^4 + \dots,$$

and

$$a_2^{(2,4)} = \frac{m_1 m_2^3 C_{ES^2}}{4(m_1 + m_2)\boldsymbol{p}^2} + \frac{m_2\left(10m_1^2 - 7m_1 m_2 - 13m_2^2 + C_{ES^2}(32m_1^2 + 61m_1 m_2 + 29m_2^2)\right)}{16m_1(m_1 + m_2)}$$
$$+ \frac{15m_1^4 - 73m_1^3 m_2 - 361m_1^2 m_2^2 - 343m_1 m_2^3 - 82m_2^4}{64m_1^3 m_2(m_1 + m_2)} \boldsymbol{p}^2$$
$$+ \frac{C_{ES^2}(93m_1^4 + 467m_1^3 m_2 + 707m_1^2 m_2^2 + 397m_1 m_2^3 + 64m_2^4)}{64m_1^3 m_2(m_1 + m_2)} \boldsymbol{p}^2 + \dots,$$

$$a_2^{(2,5)} = -\frac{m_1 m_2^3 C_{ES^2}}{4(m_1 + m_2)\boldsymbol{p}^2} - \frac{m_2\left(22m_1^2 + 19m_1 m_2 + m_2^2 + C_{ES^2}(20m_1^2 + 35m_1 m_2 + 15m_2^2)\right)}{16m_1(m_1 + m_2)}$$

$$\tag{2.48}$$

$$- \frac{51m_1^4 + 115m_1^3 m_2 - 53m_1^2 m_2^2 - 155m_1 m_2^3 - 50m_2^4}{64m_1^3 m_2(m_1 + m_2)} \boldsymbol{p}^2$$
$$- \frac{C_{ES^2}(57m_1^4 + 279m_1^3 m_2 + 399m_1^2 m_2^2 + 209m_1 m_2^3 + 32m_2^4)}{64m_1^3 m_2(m_1 + m_2)} \boldsymbol{p}^2 + \dots,$$

$$a_2^{(2,6)} = \frac{m_1 m_2^3 C_{ES^2}}{2(m_1 + m_2)\boldsymbol{p}^4} + \frac{m_2\left(8m_1^2 + 8m_1 m_2 + m_2^2 + C_{ES^2}(7m_1^2 + 11m_1 m_2 + 4m_2^2)\right)}{4m_1(m_1 + m_2)\boldsymbol{p}^2}$$
$$+ \frac{33m_1^4 + 97m_1^3 m_2 + 13m_1^2 m_2^2 - 73m_1 m_2^3 - 28m_2^4}{32m_1^3 m_2(m_1 + m_2)}$$
$$+ \frac{C_{ES^2}(39m_1^4 + 185m_1^3 m_2 + 245m_1^2 m_2^2 + 115m_1 m_2^3 + 16m_2^4)}{32m_1^3 m_2(m_1 + m_2)} + \dots,$$

where the ellipsis stands for higher orders in $\boldsymbol{p}$. These coefficients are in complete agreement with the velocity expansion of our amplitudes. The Hamiltonian of Ref. [168] produces the

coefficients

$$a_1^{(2,4)} = \frac{m_2 \left(C_{ES^2} \left(2\gamma_1{}^3 + 2\gamma_1{}^2 - \gamma_1 - 1 \right) - 2\gamma_1{}^3 - 2\gamma_1{}^2 + 3\gamma_1 + 1 \right)}{2\gamma_1(\gamma_1 + 1)m_1} , \qquad (2.49)$$

and

$$a_2^{(2,4)} = \frac{m_2{}^2 \left(C_{ES^2} \left(30\gamma_1{}^4 - 29\gamma_1{}^2 + 3 \right) - 30\gamma_1{}^4 + 59\gamma_1{}^2 - 24\gamma_1 - 5 \right)}{16\gamma_1 \left(\gamma_1{}^2 - 1 \right) m_1} ,$$

$$a_2^{(2,5)} = -\frac{m_2{}^2 \left(C_{ES^2} \left(15\gamma_1{}^4 - 13\gamma_1{}^2 + 2 \right) - 15\gamma_1{}^4 + 43\gamma_1{}^2 - 24\gamma_1 - 4 \right)}{16\gamma_1 \left(\gamma_1{}^2 - 1 \right) m_1} ,$$

$$a_2^{(2,6)} = \frac{m_2{}^2 \left(C_{ES^2} \left(15\gamma_1{}^4 - 10\gamma_1{}^2 + 3 \right) - 15\gamma_1{}^4 + 46\gamma_1{}^2 - 24\gamma_1 - 7 \right)}{16\gamma_1 \left(\gamma_1{}^2 - 1 \right)^2 m_1{}^3} , \qquad (2.50)$$

$$a_2^{(2,\tilde{4})} = \frac{\left(95\gamma_1{}^4 - 102\gamma_1{}^2 + 15 \right) m_1}{32\gamma_1 \left(\gamma_1{}^2 - 1 \right)} , \qquad a_2^{(2,\tilde{5})} = \frac{95\gamma_1{}^4 m_1 - 102\gamma_1{}^2 m_1 + 15 m_1}{32\gamma_1 - 32\gamma_1{}^3} ,$$

$$a_2^{(2,\tilde{6})} = \frac{65\gamma_1{}^4 - 66\gamma_1{}^2 + 9}{16\gamma_1 \left(\gamma_1{}^2 - 1 \right)^2 m_1} ,$$

where the coefficients $a_2^{(2,j)}$ correspond to the spinning particle as the test body, while $a_2^{(2,\tilde{j})}$ correspond to the scalar particle as the test body. These coefficients exactly reproduce the test body expansion of our amplitudes.

2.5   Observables from the eikonal phase

The conservative Hamiltonian we obtained in the previous section enables the calculation of physical observables for a binary of compact objects interacting through gravity. On the one hand, one may calculate quantities that describe bound trajectories of the binary, as the bound-state energy. On the other hand, observables pertaining to unbound orbits have received a surge of attention. The main reason for this is that these observables serve as input to important phenomenological models, as the effective one-body Hamiltonian [178, 179, 180, 181, 182, 183]. Recently, there has been great progress in obtaining these observables directly from the scattering amplitude [78, 144, 67, 81]. Moreover, in the non-spinning case, Refs. [82, 83] developed a dictionary between observables for unbound and bound orbits.

One prominent connection between physical observables and the scattering amplitude is made via the eikonal phase [158]. There are several studies of this connection, especially

in the non-spinning case [158, 159, 160, 161, 45, 18, 162, 163, 88, 89]. Refs. [142, 135, 136] verified the applicability of this approach for spinning particles in the special configuration where the spins of the particles are orthogonal to the scattering plane. More recently, Ref. [46] conjectured a formula that expresses physical observables in terms of derivatives of the eikonal phase for arbitrary orientation of the spin vectors.

In this section we extend the analysis of Refs. [142, 135, 136] and [46]. Specifically, we start by obtaining the eikonal phase via a fourier transform of our amplitudes. By restricting to the aligned-spin configuration we obtain a scattering angle which matches that of Ref. [142, 135, 136] when we specialize to the black-hole case. Then, we verify the conjecture of Ref. [46] by solving Hamilton's equations for the impulse and spin kick, and relating them to derivatives of the eikonal phase.

The eikonal phase $\chi = \chi_1 + \chi_2 + \mathcal{O}(G^3)$ is given by

$$
\chi_1 = \frac{1}{4m_1 m_2 \sqrt{\sigma^2 - 1}} \int \frac{d^2 \boldsymbol{q}}{(2\pi)^2} e^{-i\boldsymbol{q}\cdot\boldsymbol{b}} \mathcal{M}^{tree}(\boldsymbol{q}) \,,
$$
$$
\chi_2 = \frac{1}{4m_1 m_2 \sqrt{\sigma^2 - 1}} \int \frac{d^2 \boldsymbol{q}}{(2\pi)^2} e^{-i\boldsymbol{q}\cdot\boldsymbol{b}} \mathcal{M}^{\triangle+\triangledown}(\boldsymbol{q}) \,. \tag{2.51}
$$

Using our amplitudes expressed in the center-of-mass frame (see Eq. (2.27)) we find

$$
\chi_1 = \frac{\xi E G}{|\boldsymbol{p}|} \left[-a_1^{(0)} \ln \boldsymbol{b}^2 - \frac{2a_1^{(1,1)}}{\boldsymbol{b}^2} (\boldsymbol{p} \times \boldsymbol{S}_1) \cdot \boldsymbol{b} + a_1^{(2,4)} \left(\frac{2}{\boldsymbol{b}^2} \boldsymbol{S}_{1\perp}^2 - 4 \frac{(\boldsymbol{S}_{1\perp} \cdot \boldsymbol{b})^2}{\boldsymbol{b}^4} \right) \right] \,,
$$
$$
\chi_2 = \frac{\pi \xi E G^2}{|\boldsymbol{p}|} \left[\frac{a_2^{(0)}}{|\boldsymbol{b}|} - \frac{a_2^{(1,1)}}{|\boldsymbol{b}|^3} (\boldsymbol{p} \times \boldsymbol{S}_1) \cdot \boldsymbol{b} + a_2^{(2,4)} \left(\frac{1}{|\boldsymbol{b}|^3} \boldsymbol{S}_{1\perp}^2 - 3 \frac{(\boldsymbol{S}_{1\perp} \cdot \boldsymbol{b})^2}{|\boldsymbol{b}|^5} \right) \right.
$$
$$
\left. - \left(a_2^{(2,5)} \boldsymbol{S}_1^2 + a_2^{(2,6)} (\boldsymbol{p} \cdot \boldsymbol{S}_1)^2 \right) \frac{1}{|\boldsymbol{b}|^3} \right] \,, \tag{2.52}
$$

where we define $\boldsymbol{S}_{\perp 1} \equiv \boldsymbol{S}_1 - \frac{\boldsymbol{S}_1 \cdot \boldsymbol{p}}{\boldsymbol{p}^2} \boldsymbol{p}$.

We may now use the eikonal phase to obtain certain classical observables. We start by considering the aligned-spin kinematics of Ref. [142, 135, 136]. Specifically, we take the spin to be parallel to the orbital angular momentum, and hence orthogonal to the scattering plane. This implies the relations

$$
\boldsymbol{S}_1 \cdot \boldsymbol{b} = \boldsymbol{S}_1 \cdot \boldsymbol{p} = 0. \tag{2.53}
$$

Since the scattering process is confined to a plane, it can be described by one scattering angle $\theta = \theta_1 + \theta_2 + \mathcal{O}(G^3)$, which we obtain as a derivative of the eikonal phase [158]

$$\theta_i = -\frac{E}{m_1 m_2 \sqrt{\sigma^2 - 1}} \partial_b \chi_i \,, \quad i = 1,\, 2\,, \tag{2.54}$$

where $b = |\boldsymbol{b}|$. The novel piece of the 2PM angle we obtain is quadratic in spin and given by

$$\theta_{2,\, \boldsymbol{S}_1^2} = \frac{3E\pi G^2 \boldsymbol{S}_1^2}{32 m_1^2 b^4 (\sigma^2 - 1)^2} \Big\{ m_2 \left(6(5\sigma^4 - 6\sigma^2 + 1) + 2C_{ES^2}(45\sigma^4 - 42\sigma^2 + 5) \right)$$

$$+ m_1 \left((65\sigma^4 - 66\sigma^2 + 1) + C_{ES^2}(125\sigma^4 - 138\sigma^2 + 29) \right) \Big\}\,. \tag{2.55}$$

By specializing to the black-hole case ($C_{ES^2} = 1$) we reproduce the result of Ref. [142].

Ref. [46] conjectured a formula that directly relates observables in a scattering event with arbitrary spin orientations to the eikonal phase. The observables in question are the impulse $\Delta \boldsymbol{p}$ and spin kick $\Delta \boldsymbol{S}_1$, where

$$\boldsymbol{p}(t = \infty) = \boldsymbol{p} + \Delta \boldsymbol{p}\,, \qquad \boldsymbol{p}(t = -\infty) = \boldsymbol{p}\,,$$

$$\boldsymbol{S}_1(t = \infty) = \boldsymbol{S}_1 + \Delta \boldsymbol{S}_1\,, \quad \boldsymbol{S}_1(t = -\infty) = \boldsymbol{S}_1\,. \tag{2.56}$$

Specifically, by obtaining the impulse and spin kick through $\mathcal{O}(G^2)$ using Hamilton's equations, we find that they may be written as

$$\Delta \boldsymbol{p}_\perp = -\{\boldsymbol{p}_\perp, \chi\} - \frac{1}{2}\{\chi, \{\boldsymbol{p}_\perp, \chi\}\} - \mathcal{D}_{SL}\left(\chi, \{\boldsymbol{p}_\perp, \chi\}\right) + \frac{1}{2}\{\boldsymbol{p}_\perp, \mathcal{D}_{SL}\left(\chi, \chi\right)\}\,,$$

$$\Delta \boldsymbol{S}_1 = -\{\boldsymbol{S}_1, \chi\} - \frac{1}{2}\{\chi, \{\boldsymbol{S}_1, \chi\}\} - \mathcal{D}_{SL}\left(\chi, \{\boldsymbol{S}_1, \chi\}\right) + \frac{1}{2}\{\boldsymbol{S}_1, \mathcal{D}_{SL}\left(\chi, \chi\right)\}\,. \tag{2.57}$$

In Eq. (2.57) we use the definitions

$$\{\boldsymbol{p}_\perp, f\} \equiv -\frac{\partial f}{\partial \boldsymbol{b}}\,, \qquad \{\boldsymbol{S}_1, f\} \equiv \frac{\partial f}{\partial \boldsymbol{S}_1} \times \boldsymbol{S}_1\,, \qquad \mathcal{D}_{SL}\left(f, g\right) \equiv -\boldsymbol{S}_1 \cdot \left(\frac{\partial f}{\partial \boldsymbol{S}_1} \times \frac{\partial g}{\partial \boldsymbol{L}_b} \right)\,, \tag{2.58}$$

where $\boldsymbol{L}_b \equiv \boldsymbol{b} \times \boldsymbol{p}$. In the above we decompose the impulse as

$$\Delta \boldsymbol{p} = \Delta p_\parallel \frac{\boldsymbol{p}}{|\boldsymbol{p}|} + \Delta \boldsymbol{p}_\perp\,. \tag{2.59}$$

Eq. (2.57) does not give $\Delta p_\parallel$. Instead, we obtain $\Delta p_\parallel$ from the on-shell condition $(\boldsymbol{p} + \Delta \boldsymbol{p})^2 = \boldsymbol{p}^2$.

Our calculation establishes the conjecture of Ref. [46] at the quadratic-in-spin level. The fact that the relation holds without modification when we include these higher-in-spin terms is strong indication for its validity in general. Our calculation further serves as evidence in favor of the surprisingly compact all-order formula that relates the scattering observables to the eikonal phase,

$$\Delta \mathcal{O} = i e^{-i\chi \mathcal{D}}\{\mathcal{O}, e^{i\chi \mathcal{D}}\}\,, \tag{2.60}$$

where for our case $\mathcal{O} = \boldsymbol{p}_\perp$ or $\boldsymbol{S}_1$, and $\chi \mathcal{D} g \equiv \chi g + i \mathcal{D}_{SL}(\chi, g)$.

2.6 Conclusions

In this chapter we obtained the 2PM-order Hamiltonian that describes the conservative dynamics of two spinning compact objects in General Relativity up to interactions quadratic in the spin of one of the objects. We followed the approach of Refs. [46, 74] which was based on scattering amplitudes and EFT. Along with the results of [46] for the bilinear-in-the-spins interactions, this completes the $\mathcal{O}(G^2)$ analysis of quadratic-in-spin effects not including tidal effects.

To construct the Hamiltonian we followed a matching procedure. Ref. [74] developed this procedure for non-spinning particles, while Ref. [46] extended it to the spinning case. Specifically, we calculated and matched two amplitudes, one in our full theory and one in an EFT. Ref. [46] introduced the full theory to describe the minimal and non-minimal coupling of particles of arbitrary spin to gravity. The Lagrangian contains operators that are in one-to-one correspondence with those of the worldline EFT of [169]. The EFT we used captures the dynamics of non-relativistic spinning particles interacting via a potential with unfixed coefficients. This EFT extended the one of [46] to include operators quadratic in the spin of one of the particles. By matching the amplitudes computed in these two theories, we fixed these coefficients and hence determined the desired Hamiltonian.

In our calculation we considered effects up to quadratic in the spin of one of the particles, while we took the other particle to be non-spinning. In terms of our full theory,

51

we included the first non-minimal-coupling operator along with the corresponding arbitrary Wilson coefficient C_{ES^2}. Unlike the linear-in-spin results, the effects of this operator are not universal and generic bodies are described by different values of C_{ES^2}. As a specific example, $C_{ES^2} = 1$ describes the Kerr black hole. For arbitrary values of C_{ES^2}, we found that the amplitude depends on $q^2 S_1^2$ and $(q \cdot S_1)^2$ independently, rather than on the linear combination $q^2 S_1^2 - (q \cdot S_1)^2$. The latter was expected based on an observation in Refs. [156, 46]. Recently, Ref. [97] also remarked that finite-size effects spoil the above expectation. Interestingly, for the Kerr black-hole case ($C_{ES^2} = 1$) the amplitude indeed depends on the linear combination $q^2 S_1^2 - (q \cdot S_1)^2$.

The produced conservative Hamiltonian enables the calculation of observables pertaining to binary systems of spinning black holes or neutron stars. For example, one may study bound states of the binary by choosing suitable initial conditions. In this chapter we chose to compute scattering observables instead, which may be used in the construction of important phenomenological models as the effective one-body Hamiltonian [178, 179, 180, 181, 182, 183]. Specifically, by solving Hamilton's equations we obtained the relevant impulse and spin kick. In this way we verified the conjecture of Ref. [46], which expresses these observables in terms of the eikonal phase via the simple compact formula in Eq. (2.60). The existence of such a formula has intriguing implications in classical mechanics. Specifically, it hints towards a formalism that bypasses using Hamilton's equations, and directly expresses the observables in terms of derivatives of a single function of the kinematics.

In order to establish the validity of our result for the quadratic-in-spin two-body Hamiltonian, we performed several checks against the literature. We did this by comparing at the level of the gauge-invariant amplitudes in the regime where they overlap. Firstly, we verified that our amplitude expanded in velocity matches the one calculated using the Hamiltonian of Ref. [167], which was obtained in the PN approximation. Secondly, by expanding our amplitude in the test-body limit we found agreement with the amplitude obtained by the Hamiltonian of Ref. [168]. As a third check, we computed the scattering angle for the kinematic configuration where the spin vector is aligned with the orbital angular momentum of

the system and confirmed that it reproduces the one of Ref. [142] for the BH case, $C_{ES^2} = 1$. Finally, we compared the impulse in Eq. (2.57) with the one given in Ref. [184] in covariant form and found agreement.

Our calculation serves as evidence that the formalism of Ref. [46] can capture the effects of non-minimal coupling to gravity. Therefore, an obvious future direction is to extend this analysis to include more powers of spin. Moreover, a number of pressing questions remain interesting and unanswered. These include the extension of these methods to higher PM orders, the proof of the relation between classical scattering observables and the eikonal phase, along with potential extensions of this relation to bound-orbit observables.

CHAPTER 3

Binary Dynamics Through the Fifth Power of Spin at $\mathcal{O}(G^2)$

We use a previously developed scattering-amplitudes-based framework to determine the two-body Hamiltonian for generic binary systems with arbitrary spin S. By construction this formalism bypasses difficulties with unphysical singularities or higher-time derivatives. This framework has been previously used to determine the exact velocity dependence of the $\mathcal{O}(G^2)$ quadratic-in-spin two-body Hamiltonian. We first evaluate the S^3 scattering angle and two-body Hamiltonian at this order in G, including not only all operators corresponding to the usual worldline operators, but also an additional set due to an interesting subtlety. We then evaluate S^4 and S^5 contributions at $\mathcal{O}(G^2)$ which we confirm by comparing against aligned-spin results. We conjecture that a certain shift symmetry together with a constraint on the high-energy growth of the scattering amplitude specify the Wilson coefficients for the Kerr black hole to all orders in the spin and confirm that they reproduce the previously-obtained results through S^4.

3.1 Introduction

The landmark detection of gravitational waves by the LIGO/Virgo collaboration [14, 15] heralds an era of remarkable discoveries in astronomy, cosmology and perhaps even particle physics. The increasing precision of forthcoming detectors [185, 186, 187] will demand equally precise theoretical predictions which include detailed properties of gravitational-wave sources such as their spin [62].

In this chapter we use the post-Minkowskian (PM) framework [188, 189, 190, 191, 192, 193, 194, 65, 195, 66], which has been previously applied to the two-body problem of spinning particles [132, 196, 144, 147, 146, 139, 135, 156, 155, 134, 142, 143, 145, 46, 2, 184, 197, 198]. This Lorentz-invariant framework, within which we apply amplitudes methods, resums the velocity expansion present in the post-Newtonian approach [199, 200, 201, 202, 203, 108, 103, 104, 105, 106, 112, 107, 204, 205, 206, 114, 116, 115, 117, 207, 208, 209, 210, 211, 170, 138, 212, 213, 214, 109, 215, 113, 111, 118, 169, 119, 120, 167, 130, 131, 128, 129, 216, 121, 122, 217, 218]. Vines [134] obtained the energy-momentum tensor of a Kerr black hole at $\mathcal{O}(G)$ with the full spin and velocity dependence and derived the corresponding two-body Hamiltonian. This stress tensor was shown [142, 143, 147, 145] to be equivalent with the minimal amplitudes of Ref. [140]; these amplitudes were used [146] to recover the Hamiltonian of Ref. [134]. At $\mathcal{O}(G^2)$, a PM spin-orbit Hamiltonian is known [132, 196]. There has also been progress at this order on obtaining PM higher-spin interactions [142, 143, 147, 145, 139, 135, 156, 155], including the complete quadratic-in-spin interactions for the inspiral phase of generic compact objects [46, 2, 184]. Recently, quartic-in-spin results have been given for binary Kerr black holes [198].

High orders in the spin bring a number of subtleties. Among them is the complete categorization of all independent interactions. To do so in the worldline-effective-field-theory formalism [118, 169, 119, 120, 167, 130, 131, 128, 129, 216] one must systematically eliminate all terms with higher time derivatives [219, 220, 118] that appear in the Lagrangian. The amplitudes-based approaches using massive spinor helicity [140] can introduce unphysical singularities beyond the quartic-in-spin order [145, 198]. At spin-5/2 and beyond, Compton amplitudes free of such singularities were constructed in Refs. [221, 222, 223]. With a local Lagrangian starting point, the amplitudes-based formalism of Ref. [46] bypasses these issues to all orders in spin. This formalism has been tested for quadratic in spin contributions at $\mathcal{O}(G^2)$ in Refs. [46, 2] and confirmed using the worldline [184] and worldline-quantum-field-theory [197] formalisms.

Amplitudes-based methods [69, 224, 225, 226, 227, 137, 70, 228, 80, 81, 229, 230, 74, 78]

established the state of the art in the PM expansion by producing the first conservative spinless two-body Hamiltonian at $\mathcal{O}(G^3)$ and $\mathcal{O}(G^4)$ [12, 13, 77, 231], with various aspects confirmed in a number of studies [232, 75, 233, 234, 235, 85, 236, 237, 238]. Such methods led to new results that include spin [141, 143, 142, 147, 145, 135, 156, 155, 198] and tidal effects [239, 84, 100, 96, 99, 102, 101, 97]. They also led to the discovery of new structures such as the double-copy relation between gauge and gravity theories [33, 240, 34, 35, 73] and a conjecture that a single scalar function—the eikonal phase—determines both spinning and spinless classical observables [46].

In this chapter we illustrate the applicability of the amplitudes-based field-theory formalism of Ref. [46] through the fifth power of spin. As part of this study we present results for classes of operators at the cubic and quartic-in-spin order, describing arbitrary compact astrophysical objects including black holes.

The Hamiltonian at $\mathcal{O}(G)$ for binary Kerr black holes is known to all orders in spin [134]. Ref. [198] obtained a binary Hamiltonian at $\mathcal{O}(G^2)$ through S^4 from amplitudes expected to describe Kerr black holes. By calculating through fifth order in spin and making use of a symmetry of the $\mathcal{O}(G)$ Hamiltonian of Ref. [134] and an additional assumption, we formulate a conjecture for the structure of the two-body Hamiltonian for Kerr black holes to all orders in spin and determine the Hamiltonian at S^5. Here we will consider a variety of independent interactions sufficient for matching to this conjecture and for illustrating various features, and leave a systematic study of all possible interactions to future studies.

3.2 Review of Formalism

In the classical limit of a scattering process, the momentum transfer $\boldsymbol{q}$ is much smaller than the rest mass, $|\boldsymbol{q}| \ll m$, while the rest-frame spin is large, $\boldsymbol{q} \cdot \boldsymbol{S}/m \sim \mathcal{O}(1)$. Products of classical spin tensors are related [46] to symmetric products of Lorentz generators,

$$\varepsilon(p_1)\{M^{a_1 b_1} M^{a_2 b_2} \ldots M^{a_j b_j}\}\varepsilon(p_2) \tag{3.1}$$
$$= S(p_1)^{a_1 a_1} S(p_1)^{a_2 b_2} \cdots S(p_1)^{a_j b_j} \, \varepsilon(p_1) \cdot \varepsilon(p_2) + \cdots,$$

where {...} indicates the symmetric product, $\varepsilon(p_1)$ and $\varepsilon(p_2)$ are boosted spin coherent states describing the incoming and outgoing polarization tensors of a higher-spin particle, and the ellipsis stand for subleading terms in the classical limit. Antisymmetric combinations of M^{ab} are simplified using the Lorentz algebra. The spin tensor is obtained by boosting the one in the rest frame, so it respects the covariant spin supplementary condition (SSC) $p_a S^{ab} = 0$. The classical spin vector follows from $S^{ab} \equiv -\epsilon^{abcd} p_c S_d / m$, which holds under this SSC.

We work in a field-theory framework with a Lagrangian starting point; causality-based no-go theorems for the quantum consistency of higher-spin interactions [241, 242] are avoided by interpreting it as an effective theory, valid only in the classical regime, which simply gives a covariantization of all the spin-induced multipole moments. See Ref. [243] for a connection between resolvability of the time delay and the range of validity of an EFT. We first describe operators that have on-shell three-point vertices. Following Ref. [46] we separate the Lagrangian into a minimal and non-minimal part, $\mathcal{L} = \mathcal{L}_{\min} + \mathcal{L}_{\text{non-min}}$. The former has two or fewer derivatives,

$$
\begin{aligned}
\mathcal{L}_{\min} = -R + \frac{1}{2}\eta^{ab}\nabla_a \phi_s \nabla_b \phi_s - \frac{1}{2}m^2 \phi_s \phi_s \\
+ \frac{H_2}{8} R_{abcd}\, \phi_s M^{ab} M^{cd} \phi_s + \dots ,
\end{aligned}
\tag{3.2}
$$

where we use only tangent-space indices, H_2 is a free parameter, and the ellipsis stands for terms that vanish on shell. We take the higher-spin field ϕ_s to be in a real representation of the Lorentz group. We do not require it to be transverse, so this representation is reducible and contains spins ranging from 0 to s [46]. The covariant derivative is $\nabla_a \phi_s \equiv e_a^\mu (\partial_\mu \phi_s + \frac{i}{2}\omega_{\mu ab} M^{ab} \phi_s)$, where e_a^μ is the (inverse) vielbein, $\omega_{\mu ab}$ is the spin connection, and M^{ab} are Lorentz generators in this representation.

We consider two classes of higher-derivative operators in the non-minimal Lagrangian,

$\mathcal{L}_{\text{non-min}} = \mathcal{L}_C + \mathcal{L}_H$. The first one is

$$\mathcal{L}_C = \sum_{n=1}^{\infty} \frac{(-1)^n}{(2n)!} \frac{C_{\text{ES}^{2n}}}{m^{2n}} \nabla_{f_{2n}} \dots \nabla_{f_3} R_{af_1 bf_2}$$

$$\times \nabla^a \phi_s \, \mathbb{S}^{(f_1} \mathbb{S}^{f_2} \dots \mathbb{S}^{f_{2n})} \nabla^b \phi_s \tag{3.3}$$

$$- \sum_{n=1}^{\infty} \frac{(-1)^n}{(2n+1)!} \frac{C_{\text{BS}^{2n+1}}}{m^{2n+1}} \nabla_{f_{2n+1}} \dots \nabla_{f_3} \widetilde{R}_{(a|f_1|b)f_2}$$

$$\times \nabla^a \phi_s \mathbb{S}^{(f_1} \mathbb{S}^{f_2} \dots \mathbb{S}^{f_{2n+1})} \nabla^b \phi_s \,,$$

where $\mathbb{S}^a \equiv \frac{-i}{2m} \epsilon^{abcd} M_{cd} \nabla_b$ is the Pauli-Lubanski vector, and $\widetilde{R}_{abcd} \equiv \frac{1}{2} \epsilon_{abij} R^{ij}{}_{cd}$ is the dual Riemann tensor. These operators are in one-to-one correspondence to the non-minimal operators in the worldline action of Ref. [169].

The second family of higher-derivative operators generalizes the H_2 term in the minimal Lagrangian Eq. (3.2) [1],

$$\mathcal{L}_H = - \sum_{n=1}^{\infty} \frac{(-1)^n(2n-1)}{(2n)!(2n+1)} \frac{H_{2n}}{m^{2n-2}} \nabla_{f_{2n}} \dots \nabla_{f_3} R^{(a}{}_{f_1}{}^{b)}{}_{f_2}$$

$$\times \phi_s M_a{}^{(f_1} M_b{}^{f_2} \mathbb{S}^{f_3} \dots \mathbb{S}^{f_{2n})} \phi_s$$

$$+ \sum_{n=1}^{\infty} \frac{(-1)^n n}{(2n+1)!(n+1)} \frac{H_{2n+1}}{m^{2n-1}} \nabla_{f_{2n+1}} \dots \nabla_{f_3} \widetilde{R}^{(a}{}_{f_1}{}^{b)}{}_{f_2}$$

$$\times \phi_s M_a{}^{(f_1} M_b{}^{f_2} \mathbb{S}^{f_3} \dots \mathbb{S}^{f_{2n+1})} \phi_s \,. \tag{3.4}$$

The normalization is such that H_i appear as $C_{2n} \equiv C_{\text{ES}^{2n}} + H_{2n}$ and $C_{2n+1} \equiv C_{\text{BS}^{2n+1}} + H_{2n+1}$ in three-point amplitudes upon using the covariant SSC. Comparison with Ref. [134] fixes the values of the C_n combinations to

$$C_n = 1, \quad n = 2, 3, \dots \tag{3.5}$$

for a Kerr black hole. A standard EFT Lagrangian does not include multiple operators with identical on-shell matrix elements because their difference can be absorbed by higher-point contact operators. The equality here however relies on the SSC rather than on the equation

---

[1] Note that the H_2 operator in Eq. (3.4) is written in a form different from that in Eq. (3.2). The equivalence can be proved by using Bianchi identities.

of motion. As we will see, $\mathcal{L}_C$ and $\mathcal{L}_H$ contribute differently to the gravitational Compton amplitude even in the classical limit.

The covariant SSC is imposed only on amplitudes in the classical limit. We may therefore introduce in the Lagrangian terms containing $\nabla_a \phi_s M^{ab}$ as the off-shell covariantization of $p_a S^{ab}$,

$$\mathcal{L}_{\text{SSC}} \supset D_n \dots \nabla_a \phi_s M^{ab} \dots \phi_s \,, \tag{3.6}$$

where D_n are their Wilson coefficients and the index n indicates that the ellipsis contain further $(n-1)$ Lorentz generators in addition to a single Riemann tensor. In the classical limit their three-point matrix elements are proportional to $p_a S^{ab}(p)$ and thus vanish under covariant SSC. As we will discuss, these operators have nonzero four-point classical matrix elements starting at S^{n+1}, even after the use of the covariant SSC. Here we will, however, not include such operators in our Lagrangian. [2]

The non-minimal Lagrangian $\mathcal{L}_{\text{non-min}}$ can be further extended with infinite sequences of operators with higher powers of the Riemann tensor and its derivatives. They first contribute at S^4 and can also encode tidal effects. Our conjectured structure of the two-body Hamiltonian of Kerr black holes suggests that such terms are necessary starting at S^5. While many others exist, for our purposes in order to define the Kerr black hole it is sufficient to include

$$
\begin{aligned}
\mathcal{L}_{R^2} = \\
\frac{1}{1800 m^7} & (E_1 R_{af_1 bf_2} \nabla_{f_5} \widetilde{R}_{cf_3 df_4} + E_2 \nabla_{f_5} R_{af_1 bf_2} \widetilde{R}_{cf_3 df_4}) \nabla^{(a} \nabla^{c)} \phi_s \mathbb{S}^{(f_1} \mathbb{S}^{f_2} \mathbb{S}^{f_3} \mathbb{S}^{f_4} \mathbb{S}^{f_5)} \nabla^{(b} \nabla^{d)} \phi_s \\
+ \frac{1}{1800 m^5} & (E_3 R_{af_1 bf_2} \nabla_{f_5} \widetilde{R}_{cf_3 df_4} + E_4 \nabla_{f_5} R_{af_1 bf_2} \widetilde{R}_{cf_3 df_4}) \nabla^c \phi_s M^{a(f_1} M^{|b|f_2} \mathbb{S}^{f_3} \mathbb{S}^{f_4} \mathbb{S}^{f_5)} \nabla^d \phi_s \\
+ \frac{1}{1800 m^7} & (2 E_5 R_{eabf_1} \nabla_{f_2} \widetilde{R}^e{}_{cdf_3} + E_6 R_{aebf_1} \nabla^e \widetilde{R}_{cf_2 df_3} + \\
& E_7 \nabla_{f_2} R_{eabf_1} \widetilde{R}^e{}_{cdf_3}) \nabla^{(a} \nabla^{c)} \phi_s \mathbb{S}^m \mathbb{S}_m \mathbb{S}^{(f_1} \mathbb{S}^{f_2} \mathbb{S}^{f_3)} \nabla^{(b} \nabla^{d)} \phi_s \,, \tag{3.7}
\end{aligned}
$$

where $E_1, \dots, E_7$ are Wilson coefficients. For generic bodies one would need a complete list of all independent such operators.

---

[2] These extra operators are not needed when matching our Wilson-coefficient dependent aligned-spin scattering angles through S^4 with those computed from a worldline formalism [244].

Having specified the Lagrangian, the four-point Compton amplitude is straightforwardly obtained using Feynman rules. The generalized unitarity method [19, 20] then gives the one-loop integrand with four external higher-spin states. The relevant generalized cut at $\mathcal{O}(G^2)$ is

$$\text{Cut}_{\text{t-channel}} = \quad \text{} \quad , \tag{3.8}$$

where the blobs represent on-shell gravitational Compton amplitudes. By adjusting terms that vanish on shell, the Compton amplitudes can be chosen to satisfy generalized gauge invariance, so the physical-state projectors are manifestly Lorentz invariant and independent of reference momenta [1]. Apart from inclusion of higher powers of the spin vector, the construction of the integrand follows the discussion in Ref. [46] so we will not detail it here. We then use FIRE [245, 246] as well as Forde's method [176, 177, 28] to extract the coefficients of the scalar triangle integrals which determine the classical amplitude.

3.3 Results

In general the amplitude is a sum of scalar box, triangle and bubble-integral contributions. The box integrals correspond to iteration of lower-order terms and carry no new information. The bubble integrals contain purely quantum information and are hence dropped. The new classical information at this order is encoded in the triangle integrals and their coefficients [230, 74], whose structure is

$$\mathcal{M}^{\triangle+\triangledown} = \frac{2\pi^2 G^2 \varepsilon_1 \cdot \varepsilon_4 \varepsilon_2 \cdot \varepsilon_3}{\sqrt{-q^2}} \sum_n \sum_i \alpha^{(n,i)} \mathcal{O}^{(n,i)} . \tag{3.9}$$

Here n is the number of spin vectors and the index i labels their independent contractions. For brevity, we include here explicitly only the $S_1^n S_2^0$ terms with $n = 2$ through $n = 5$. The relevant operators $\mathcal{O}^{(n,i)}$ are given in Table 3.1, while an ancillary file contains the full amplitudes [247]. We use the shorthand notation $\mathcal{E}_j = -i\epsilon^{\mu\nu\rho\tau} u_{1\mu} u_{2\nu} q_\rho a_{j\tau}$, as well as $u_i^\mu = p_i^\mu/m_i$, $a_i^\mu = S_i^\mu/m_i$ and $\sigma = u_1 \cdot u_2$.

60

	i		i		i	
$\mathcal{O}^{(2,i)}$	1	$\mathcal{E}_1^2$	2	$q^2(u_2{\cdot}a_1)^2$	3	$(q{\cdot}a_1)^2$
$\mathcal{O}^{(4,i)}$	1	$\mathcal{E}_1^4$	2	$q^2(u_2{\cdot}a_1)^2\mathcal{E}_1^2$	3	$q^4(u_2{\cdot}a_1)^4$
	4	$(q{\cdot}a_1)^2\mathcal{E}_1^2$	5	$q^2(q{\cdot}a_1)^2(u_2{\cdot}a_1)^2$	6	$(q{\cdot}a_1)^4$

Table 3.1: The independent $S_1^2 S_2^0$ and $S_1^4 S_2^0$ structures are given in the table. The $S_1^3 S_2^0$ and $S_1^5 S_2^0$ structures follow from these via $\mathcal{O}^{(3,i)} = \mathcal{E}_1 \mathcal{O}^{(2,i)}$ and $\mathcal{O}^{(5,i)} = \mathcal{E}_1 \mathcal{O}^{(4,i)}$.

We parametrize the coefficients $\alpha^{(n,i)}$ in Eq. (3.9) as

$$\alpha^{(2,i)} = \frac{m_1^2 m_2^2}{16(-1+\sigma^2)^2}(\gamma^{(2,i)}m_1 + \delta^{(2,i)}m_2)\,,$$

$$\alpha^{(3,i)} = \frac{m_1^2 m_2^2 \sigma}{8(-1+\sigma^2)^2}(\gamma^{(3,i)}m_1 + 2\delta^{(3,i)}m_2)\,,$$

$$\alpha^{(4,i)} = \frac{m_1^2 m_2^2}{1536(-1+\sigma^2)^3}\left(\gamma^{(4,i)}m_1 + \frac{8}{5}\delta^{(4,i)}m_2\right),$$

$$\alpha^{(5,i)} = \frac{m_1^2 m_2^2 \sigma}{768(-1+\sigma^2)^3}\left(\gamma^{(5,i)}m_1 + \frac{1}{75}\delta^{(5,i)}m_2\right), \tag{3.10}$$

where $\gamma^{(k,i)}$ and $\delta^{(k,i)}$ are polynomials in σ^2. They correspond to the probe limits $m_2 \ll m_1$ and $m_1 \ll m_2$, respectively. We list the coefficients $\gamma^{(k,i)}$ in Table 3.2 in terms of combinations $Z_{k,j}$ of Wilson coefficients, which we collect in Table 3.3.

We parametrize the polynomials $\delta^{(k,i)}$ that govern the limit $m_1 \ll m_2$ as

$$\delta^{(k,i)} = \sum_{\ell=0}^{5} \delta_\ell^{(k,i)}\sigma^{2\ell}\,. \tag{3.11}$$

The coefficients $\delta_\ell^{(k,i)}$ determining $\delta^{(2,i)}$ and $\delta^{(3,i)}$ are given in Table 3.4. We note that while $\delta_\ell^{(2,i)}$ depends only on the combination C_2 of Wilson coefficients, $\delta_\ell^{(3,i)}$ depends separately on C_2 and H_2. The coefficients of the polynomials $\delta^{(4,i)}$ and $\delta^{(5,i)}$ are given in Table V of Ref. [3] and depend separately on C_n, H_n and E_n.

For Kerr black holes, the coefficients $C_n = 1$ set to zero all the $\gamma^{(k,i)}$ coefficients in the second column of Tables 3.2 and 3.3. The remaining operators in Table 3.1 with nonzero $\gamma^{(k,i)}$

i	$\gamma^{(2,i)}$	i	$\gamma^{(2,i)}$
1	$7 + 23C_2 - Z_{2,1}\sigma^2(102 - 95\sigma^2)$	3	$12Z_{2,2}(\sigma^2 - 1)^2(5\sigma^2 - 1)$
2	$5 - 11C_2 + 5Z_{2,1}\sigma^2(6 - 7\sigma^2)$		

i	$\gamma^{(3,i)}$	i	$\gamma^{(3,i)}$
1	$Z_{3,1}(5 - 9\sigma^2)$	3	$4Z_{3,2}(\sigma^2 - 1)(5\sigma^2 - 3)$
2	$Z_{3,1}(7\sigma^2 - 3)$		

i	$\gamma^{(4,i)}$	i	$\gamma^{(4,i)}$
1	$44C_3 + 59Z_{4,2} - Z_{4,1}\sigma^2(250 - 239\sigma^2)$	4	$12Z_{4,3}(1 - \sigma^2)(23 - 102\sigma^2 + 95\sigma^4)$
2	$72C_3 - 78Z_{4,2} + Z_{4,1}\sigma^2(276 - 294\sigma^2)$	5	$12Z_{4,3}(\sigma^2 - 1)(11 - 30\sigma^2 + 35\sigma^4)$
3	$28C_3 - 9Z_{4,2} + 7Z_{4,1}\sigma^2(2 - 3\sigma^2)$	6	$24Z_{4,4}(\sigma^2 - 1)^3(5\sigma^2 - 1)$

i	$\gamma^{(5,i)}$	i	$\gamma^{(5,i)}$
1	$Z_{5,1}(7 - 13\sigma^2)$	4	$12Z_{5,2}(\sigma^2 - 1)(9\sigma^2 - 5)$
2	$2Z_{5,1}(11\sigma^2 - 5)$	5	$12Z_{5,2}(\sigma^2 - 1)(3 - 7\sigma^2)$
3	$Z_{5,1}(3\sigma^2 - 1)$	6	$8Z_{5,3}(\sigma^2 - 1)^2(3 - 5\sigma^2)$

Table 3.2: The $\gamma^{(m,i)}$ polynomials for $S_1^m S_2^0$ where the $Z_{i,j}$ are defined in Table 3.3.

coefficients have, up to quantum-suppressed terms $p_i \cdot q = \pm q^2/2 \to 0$, the shift symmetry

$$a_i^\mu \to a_i^\mu + \xi_i q^\mu/q^2, \quad i = 1, 2 , \tag{3.12}$$

where ξ_i are arbitrary constants and q^2 was included so the classical q scaling is uniform. Inspection of the binary Kerr-black-hole Hamiltonian of Ref. [134] reveals that it exhibits the same symmetry. We therefore conjecturally *define* the black-hole limit as the values of the Wilson coefficients which realize this symmetry. It will be interesting to see if this definition holds to all orders in G.

This definition is consistent with the vanishing of $\delta^{(2,3)}$ for $C_2 = 1$. Requiring that $\delta^{(3,3)}$ vanishes further sets $H_2 = 1$, which is consistent with the value for this coefficient fixed by requiring that the Compton amplitude has good high-energy properties [248, 249, 250]. The worldline formalism fixes this value for general bodies, not just for the Kerr black hole,

$Z_{2,1} = C_2 + 1$	$Z_{2,2} = C_2 - 1$
$Z_{3,1} = 3C_2 + C_3$	$Z_{3,2} = C_2 - C_3$
$Z_{4,1} = 3C_2^2 + 4C_3 + C_4$	$Z_{4,3} = C_2^2 - C_4$
$Z_{4,2} = 3C_2^2 + C_4$	$Z_{4,4} = 3C_2^2 - 4C_3 + C_4$
$Z_{5,1} = 10C_2C_3 + 5C_4 + C_5$	$Z_{5,2} = 2C_2C_3 - C_4 - C_5$
	$Z_{5,3} = 2C_2C_3 - 3C_4 + C_5$

Table 3.3: Useful combinations of Wilson coefficients.

i	$\delta_0^{(2,i)}$	$\delta_1^{(2,i)}$	$\delta_2^{(2,i)}$	$\delta_3^{(2,i)}$
1	$8Z_{2,1}$	$-(68 + 52C_2)$	$60Z_{2,1}$	0
2	$4(3 - C_2)$	$-12Z_{2,1}$	0	0
3	$-4Z_{2,2}$	$68Z_{2,2}$	$-124Z_{2,2}$	$60Z_{2,2}$

i	$\delta_0^{(3,i)}$		$\delta_1^{(3,i)}$	
1	$3(H_2 - 2)H_2 - (C_2 - 8)C_2$		$C_2(2C_2 - 13) - 2C_3 - 3(H_2 - 2)H_2$	
2	$C_2(4C_2 - 5) + 2C_3 - 5(H_2 - 2)H_2$		$5(C_2 - H_2)(2 - C_2 - H_2)$	
3	$(5 - 2C_2)C_2 - 2C_3 + (H_2 - 2)H_2$		$2\big[C_2(3C_2 - 8) + 4C_3 - (H_2 - 2)H_2\big]$	
	$\delta_2^{(3,1)} = \delta_2^{(3,2)} = 0 \,,$		$\delta_2^{(3,3)} = (11 - 4C_2)C_2 - 6C_3 + (H_2 - 2)H_2$	

Table 3.4: Coefficients of the polynomials $\delta^{(2,i)}$ and $\delta^{(3,i)}$.

by requiring that the equation of motion is invariant under the change of SSC [168]. See Ref. [109, 215, 113, 111] for an alternative perspective. In contrast, string theory predicts state-dependent values for H_2, perhaps due to the spectrum containing more than a single massive higher-spin state [249].

Imposing that $\delta^{(4,4)}, \delta^{(4,5)}$ and $\delta^{(4,6)}$ vanish fixes $H_4 = 0$, which recovers the amplitude obtained in [198] and, notably, leaves H_3 undetermined. The proposed symmetry Eq. (3.12) and the resulting values for Wilson coefficients are consistent with the $S_1^m S_2^{4-m}$ amplitude included in the ancillary file [247].

$\frac{1}{r^2}\boldsymbol{L}\cdot\boldsymbol{S}_1$	$\frac{1}{r^4}(\boldsymbol{r}\cdot\boldsymbol{S}_1)^2$	$\frac{1}{r^2}\boldsymbol{S}_1^2$
$\frac{1}{r^2}(\boldsymbol{p}\cdot\boldsymbol{S}_1)^2$	$\frac{1}{r^4}(\boldsymbol{p}\cdot\boldsymbol{S}_1)^2\boldsymbol{L}\cdot\boldsymbol{S}_1$	$\frac{1}{r^6}(\boldsymbol{r}\cdot\boldsymbol{S}_1)^2\boldsymbol{L}\cdot\boldsymbol{S}_1$
$\frac{1}{r^4}\boldsymbol{S}_1^2\boldsymbol{L}\cdot\boldsymbol{S}_1$	$\frac{1}{r^4}(\boldsymbol{p}\cdot\boldsymbol{S}_1)^4$	$\frac{1}{r^6}(\boldsymbol{r}\cdot\boldsymbol{S}_1)^2(\boldsymbol{p}\cdot\boldsymbol{S}_1)^2$
$\frac{1}{r^8}(\boldsymbol{r}\cdot\boldsymbol{S}_1)^4$	$\frac{1}{r^8}(\boldsymbol{r}\cdot\boldsymbol{S}_1)^4$	$\frac{1}{r^4}(\boldsymbol{p}\cdot\boldsymbol{S}_1)^2\boldsymbol{S}_1^2$
$\frac{1}{r^6}(\boldsymbol{r}\cdot\boldsymbol{S}_1)^2\boldsymbol{S}_1^2$	$\frac{1}{r^4}\boldsymbol{S}_1^4$	$\frac{1}{r^6}(\boldsymbol{p}\cdot\boldsymbol{S}_1)^4\boldsymbol{L}\cdot\boldsymbol{S}_1$
$\frac{1}{r^6}\boldsymbol{S}_1^4\boldsymbol{L}\cdot\boldsymbol{S}_1$	$\frac{1}{r^{10}}(\boldsymbol{r}\cdot\boldsymbol{S}_1)^4\boldsymbol{L}\cdot\boldsymbol{S}_1$	$\frac{1}{r^6}(\boldsymbol{p}\cdot\boldsymbol{S}_1)^2\boldsymbol{S}_1^2\boldsymbol{L}\cdot\boldsymbol{S}_1$
$\frac{1}{r^8}(\boldsymbol{r}\cdot\boldsymbol{S}_1)^2\boldsymbol{S}_1^2\boldsymbol{L}\cdot\boldsymbol{S}_1$		$\frac{1}{r^8}(\boldsymbol{r}\cdot\boldsymbol{S}_1)^2(\boldsymbol{p}\cdot\boldsymbol{S}_1)^2\boldsymbol{L}\cdot\boldsymbol{S}_1$

Table 3.5: The Hamiltonian spin structures for the first five orders in $\boldsymbol{S}_1$.

Requiring the presence of the symmetry Eq. (3.12), or equivalently that $\delta^{(5,4)}, \delta^{(5,5)}$ and $\delta^{(5,6)}$ vanish, determines $H_3 = 3/2$ and shows that H_5 is degenerate with R^2 terms at this order. It however leaves undetermined certain R^2 Wilson coefficients. The combination appearing in the amplitude can be fixed by requiring that, as at lower powers of the spin, the amplitude does not grow faster than the spin-independent part at large σ, where we take $\mathcal{E}_{1,2} \sim \sigma$ because of its momentum dependence. Equivalently, one may require that the classical part of the one-loop amplitude does not grow faster at high energies than the tree-level amplitude. The polynomials $\delta^{(5,i)}$ are then uniquely fixed, given below together with $\gamma^{(5,i)}$,

$$
\begin{aligned}
\gamma_{\text{Kerr}}^{(5,1)} &= 16(7 - 13\sigma^2)\,, & \frac{1}{75}\delta_{\text{Kerr}}^{(5,1)} &= 24(1 - 4\sigma^2)\,, \\
\gamma_{\text{Kerr}}^{(5,2)} &= 32(11\sigma^2 - 5)\,, & \frac{1}{75}\delta_{\text{Kerr}}^{(5,2)} &= 48(2 + \sigma^2)\,, \\
\gamma_{\text{Kerr}}^{(5,3)} &= 16(3\sigma^2 - 1)\,, & \frac{1}{75}\delta_{\text{Kerr}}^{(5,3)} &= 8(12 - 16\sigma^2 + 7\sigma^4)\,.
\end{aligned}
\tag{3.13}
$$

These results are collected in an attached Mathematica text file [247]. It is interesting to understand if the symmetry Eq. (3.12) and the high-energy scaling are sufficient to determine all Wilson coefficients for all powers of the spin at $\mathcal{O}(G^2)$ and perhaps beyond when supplemented with other information such as tree-level matching Eq. (3.5).

Following the detailed description in Ref. [46] the amplitude coefficients can be directly converted to real-space Hamiltonian coefficients, in terms of a set of spin structures. In

Table 3.5 we display the ones that depend only on $\boldsymbol{S}_1$. We express the real-space Hamiltonian in terms of 2, 9, 18, 43, 86 $\boldsymbol{S}^n$ structures, keeping both $\boldsymbol{S}_1$ and $\boldsymbol{S}_2$ for $n = 1$, 2, 3, 4, 5, respectively. A list of these as well as the Hamiltonian coefficients are included in the attached files of this manuscript [247]. Using this Hamiltonian, which depends only on canonical variables, any physical observable, whether for a bound or unbound system can be determined straightforwardly using Hamilton's equations. This Hamiltonian has terms containing $1/\boldsymbol{p}^2$, but interestingly all singularities cancel for Kerr black holes.

We compared the scattering angle through S^4 in the aligned-spin limit with the results of Ref. [213, 135] for Kerr black holes and found complete agreement. We also found that our scattering angle for generic bodies is consistent with a generalization of Ref. [136] that departs from Kerr geometry [244]. Interestingly, the coefficients of R^2 operators in the framework of Ref. [136] are related to quadratic combinations of our C_n coefficients.

Finally, let us comment on the operators in Eq. (3.6) whose three-point matrix elements in the classical limit vanish, being proportional to the SSC $p_a S^{ab} = 0$. The higher-point matrix elements of these operators are more subtle, and indeed explicit calculations show that these operators contribute nontrivial contact terms to the amplitude. More generally, explicit calculations show that equality upon use of the SSC of three-point matrix elements of covariant operators does not guarantee equality of four- or higher-point matrix elements, nor does it guarantee that the difference can be absorbed into curvature-square operators. Interestingly, all contributions linear in D_n to the classical amplitude are also proportional to $(H_2 - 1)$, which vanishes if $H_2 = 1$; this is however no longer the case for the nonlinear dependence on D_n.

3.4 Conclusions

In this chapter we constructed the $\mathcal{O}(G^2)$ 2PM two-body Hamiltonian for general compact objects, including Kerr black holes. We did so by extracting it from a variety of new amplitudes computed in the field-theory approach of Ref. [46]. Our explicit results are included

in the ancillary material [247]. Here we comment on two new and unexpected features that we identified and require further investigation.

We encountered a larger number of operators with independent Wilson coefficients at each order in spin; they include all those of the worldline approach, and others that either have fixed coefficients or do not have an obvious counterpart in the worldline approach [244]. An example is the gravitational quadrupole operator, whose coefficient H_2 is fixed to unity by requiring that the equations of motion are invariant under change of the SSC [168]. It is important to understand the origin of this additional freedom in our formalism, for example, whether it is a consequence of the unconstrained nature of the higher-spin field we use, and whether it corresponds to astrophysical phenomena beyond the current worldline description. To this end it would be very useful to categorize all independent interactions in both the worldline and field-theory approaches and to systematically compare results.

Based on our explicit results and the observation of a spin shift symmetry, we also conjectured that certain spin-dependent structures characterize the Kerr-black-hole interactions to all orders in spin and perhaps even to all orders in Newton's constant. We proposed this together with the requirement that the amplitude grows no worse than the spin-independent part of $\mathcal{M}$ at high energies as a field-theory *definition* of the Kerr black hole limit. It would be important to understand the physical interpretation of the shift symmetry and whether these constraints properly single out an effective field theory that describes the Kerr black hole of general relativity and study their consequences.

We expect that the issues raised in this chapter will be resolved with further computations at high orders in spin and a systematic comparison with the worldline and other general-relativity approaches.

CHAPTER 4

Gravitational Effective Field Theory Islands, Low-Spin Dominance, and the Four-Graviton Amplitude

We analyze constraints from perturbative unitarity and crossing on the leading contributions of higher-dimension operators to the four-graviton amplitude in four spacetime dimensions, including constraints that follow from distinct helicity configurations. We focus on the leading-order effect due to exchange by massive degrees of freedom which makes the amplitudes of interest infrared finite. In particular, we place a bound on the coefficient of the R^3 operator that corrects the graviton three-point amplitude in terms of the R^4 coefficient. To test the constraints we obtain nontrivial effective field-theory data by computing and taking the large-mass expansion of the one-loop minimally-coupled four-graviton amplitude with massive particles up to spin 2 circulating in the loop. Remarkably, we observe that the leading EFT coefficients obtained from both string and one-loop field-theory amplitudes lie in small islands. The shape and location of the islands can be derived from the dispersive representation for the Wilson coefficients using crossing and assuming that the lowest-spin spectral densities are the largest. Our analysis suggests that the Wilson coefficients of weakly-coupled gravitational physical theories are much more constrained than indicated by bounds arising from dispersive considerations of $2 \to 2$ scattering. The one-loop four-graviton amplitudes used to obtain the EFT data are computed using modern amplitude methods, including generalized unitarity, supersymmetric decompositions and the double copy.

4.1 Introduction

Remarkably, systematic bounds can be placed on possible corrections to Einstein gravity [251, 252, 253, 254, 255, 256, 257, 258, 259, 260, 261, 262, 263, 264, 265, 266, 267, 268, 269, 270, 271]. Such corrections naturally appear due to the presence of heavy particles in the theory. To leading order in Newton's constant G, such particles can be exchanged at tree-level, as in string theory, or at one-loop, as in the case of matter minimally coupled to gravity. By expanding such amplitudes at low energies and matching to a low-energy effective field theory one finds an infinite series of higher-derivative corrections to Einstein gravity. The coefficients in front of these higher-derivative operators, or Wilson coefficients, satisfy various bounds due to unitarity and causality of the underlying amplitude [251, 252, 253, 254, 255, 256, 257, 258, 259, 260, 261, 262, 263, 264, 265, 266]. In this paper, we focus on the leading corrections to Einstein gravity.[1] A central question, which we investigate in this paper, is to understand if there are principles that can greatly restrict the values of physically allowed Wilson coefficients.

Consistency bounds on the Wilson coefficients received a lot of attention recently in the context of $2 \to 2$ scattering, which is also the subject of our paper. The basic tool to derive such bounds is given by dispersion relations which express low-energy Wilson coefficients as weighted sums of the discontinuity of the amplitude. Unitarity constrains the form of the discontinuity of the amplitude which can be further used to derive the bounds. The simplest examples of this type constrain the sign of Wilson coefficients. More interesting bounds arise when one accommodates constraints coming from crossing symmetry. Including those leads to the two-sided bounds on the Wilson coefficients [267, 268, 269, 270]. In this way the ultraviolet (UV) complete theories form bounded regions in the space of couplings. Ref. [269] also analyzed a few examples of physical EFTs in the context of scattering of scalars and noted that they lie near the boundaries of the allowed region due to the importance of low-spin contributions to the partial-wave expansions (see Sect. 10.3 and Appendix D of

---

[1]In particular, higher-loop effects do not affect the discussion in this paper since by assumption gravity is weakly coupled and we are focusing on the leading-order effect.

Ref. [269]).

In the context of physical theories, especially gravitational ones, it is then natural to ask the following question:

Is it possible that the Wilson coefficients of physical theories live in much smaller regions than the bounds coming from considerations of $2 \to 2$ scattering suggest?

By physical theories in this paper we mean perturbatively consistent S-matrices that satisfy unitarity, causality, and crossing for any $n \to m$ scattering processes. Constructing such S-matrices is far beyond the scope of bootstrap methods that focus on $2 \to 2$ scattering, but such examples are provided to us by string theory and matter minimally coupled to gravity.[2] We can then imagine that consistency of the full S-matrix is reflected back on the $2 \to 2$ scattering through more stringent constraints on Wilson coefficients that one would naively have found by analyzing $2 \to 2$ scattering. In this paper we present data extracted from field-theory and string-theory $2 \to 2$ scattering amplitudes that suggest that the above assertion is indeed true and we identify a principle behind it. This principle is *low-spin dominance* (LSD), which, if fundamentally correct, might be traced back to the consistency of the full gravitational S-matrix, beyond $2 \to 2$ scattering. However, demonstrating this is beyond the scope of the present paper.

The universal nature of gravity together with the strict consistency requirements that graviton scattering obeys make such an assertion plausible. It is a well-known fact that scattering of massless spinning particles is very constrained [272]. In fact, massless particles of spin larger than two do not admit a non-trivial S-matrix [273, 274]. Gravitons, being massless spin-two particles, are thus expected to have an especially constrained S-matrix, and the assertion made in the previous paragraph is thus particularly plausible for graviton scattering which is the subject of the present paper.

---

[2]Perturbatively consistent S-matrices occupy a somewhat intermediate position between fully non-perturbatively consistent quantum gravities (often referred to as landscape) and consistency of $2 \to 2$ scattering studied by bootstrap methods.

Firstly, we use the techniques of Ref. [269] to derive bounds between low-energy couplings of the same dimensionality in gravitational scattering.[3] We focus on the first few corrections to Einstein gravity. We then ask where do the Wilson coefficients obtained from string theory and from the low-energy limit of the one-loop minimally-coupled amplitudes land in the space allowed by the general bounds. Remarkably, in all cases studied here we find that both the string and field-theory coefficients land on a small *theory island*, which to a good approximation is a thin line segment in the space of EFT coefficients. (See, for example, Fig. 4.9 and Fig. 4.12 in Sect. 4.5).[4] The location of this island can be found by assuming that lowest-spin partial waves dominate the dispersive representation of the low-energy couplings, which is the LSD principle. See Sect. 4.5.2 for the precise mathematical formulation. More generally, we show how one can combine an assumed hierarchy among the spectral densities of various spins with crossing symmetry to systematically derive stronger bounds on the Wilson coefficients. We impose crossing symmetry via the use of null constraints [267, 268].

The idea that LSD is a true property of physical theories can be traced back to causality, or the statement that the amplitude cannot grow too fast in the Regge limit. Otherwise we could have simply added a tree-level exchange by a large-spin particle which would contribute to a given spin partial wave. Due to causality we cannot do this (see e.g. Ref. [241]). The situation is particularly dramatic in gravity. In this case the only particle that can be exchanged at tree-level in graviton scattering without violating causality is the graviton itself. Moreover, its self-coupling has to be the one of Einstein gravity Ref. [241, 276, 277, 278] . Alternatively, particles of all spins have to be exchanged at tree level to preserve causality, which is the mechanism realized in string theory. It is important to emphasize that at the level of $2 \to 2$ scattering LSD does not follow from causality and we do not prove it in this paper, rather we use it as a principle to organize the known data, and suggest that it may hold more generally. It would be interesting to understand if it follows from considerations

---

[3]It would be very interesting to generalize our analysis to include bounds that relate couplings of different dimensionality along the lines of Refs. [267, 268, 271].

[4]In Ref. [275] the string-theory island was interpreted in terms of unitarity constraints coupled with world-sheet monodromy constraints.

on the consistency of $n \to m$ graviton scattering.

Alternatively, it is also possible that our finding of LSD could be special for the models considered here and bears little significance for more general gravitational models. This possibility, which we cannot exclude, would be still very interesting. Indeed, as we demonstrate, any such violation is an indication for non-stringy, non-weakly-coupled-matter physics. For example, it would be very interesting to see if one can somehow violate LSD by making the matter sector strongly coupled, e.g. by considering large-N QCD coupled to gravity [279].

Curiously, the phenomenon of LSD generates hierarchies between different Wilson coefficients in the absence of any symmetry. We call this phenomenon *hierarchy from unitarity* and it is something that could have puzzled an unassuming low-energy physicist. We find that specific combinations of Wilson coefficients whose dispersive representation does not involve the lowest-spin partial waves can be much smaller than their counterparts that do have them in their definitions.

Secondly, we apply the dispersive sum rules [280, 268] to amplitudes with various helicity configurations of the external gravitons.[5] We derive various bounds on the inelastic scattering (the one in which the final and initial state gravitons have different helicities) in terms of the elastic one (see e.g. Ref. [281]). We also place a precise bound on the R^3 coefficient in terms of the R^4 coefficient (see Eq. (4.200)). Such a bound translates the problem of making the analysis of Ref. [241] quantitatively precise to the problem of the bounding the leading R^4 contact coefficient in terms of the gap of the theory. This has been recently done in Ref. [271] in a similar perturbative setting for $D = 10$ maximal supergravity; see also Ref. [282] for the nonperturbative analysis of the same problem. It would, of course, be very interesting to generalize these studies to more general cases of graviton scattering.

In order to provide data for checking and understanding the derived constraints, we first compute the one-loop four-graviton scattering amplitude with the gravitons minimally coupled to massive matter up to spin 2. Amplitudes corresponding to the ones discussed here,

---

[5]Flat space superconvergence considered in Ref. [278] is a particular example of these more general sum rules.

but with massless particles circulating in the loop were obtained a while ago in Ref. [283] and corresponding gauge-theory amplitudes with massive particles in the loop were computed in Ref. [22]. We use the same type of organization of the amplitude in terms of supersymmetric multiplets as applied in the earlier calculations, since they naturally group contributions according to their analytic properties.

To evaluate the amplitudes, we make use of standard tools including the unitarity method [19, 20] and the Bern-Carrasco-Johansson (BCJ) [34, 35, 73] double copy, which gives gravity integrands in terms of corresponding gauge-theory ones. We build on the D-dimensional version of the unitarity method of Ref. [22] in order to fix the rational terms in the amplitudes. At four points gauge-theory tree-level amplitudes automatically satisfy the duality between color and kinematics, so the associated double-copy relations also hold automatically on the unitarity cuts. We use this to express the cuts of the gravity loop integrands directly in terms of the corresponding gauge-theory ones. By using the double copy our computation parallels the corresponding gauge-theory one [22] allowing us to import many of the same steps into the gravitational amplitude calculations.

A complication with massive amplitudes is that there is a class of terms that depend on the mass but do not have branch cuts in any kinematic variable. This makes their construction tricky in the context of the unitarity method. Ref. [284] introduced an approach to this problem. Here we instead solve the problem differently by making use of a special property of the scattering amplitudes under study that exploits their simple dependence on the mass of the particle circulating in the loop. In our case (i.e. a single mass circulating in the loop) we instead use knowledge of the ultraviolet properties of the amplitudes to fix all remaining functions in the amplitude not determined by unitarity. This procedure is greatly aided by arranging the amplitude in terms of integrals that have no mass or spacetime dependence in their coefficients. To ensure the veracity of our amplitudes we perform a number of nontrivial checks on the mass dependence, and infrared and ultraviolet properties. Related to this, we also note a simple relation between ultraviolet divergences of appropriate spacetime dimension shifts of the amplitudes and the terms in the large-mass

expansion in four dimensions (see Eq. (4.65)).

We analyze our amplitudes in the large-mass limit and match to a low-energy effective field theory. In this way we systematically obtain corrections to Einstein gravity due to the presence of a heavy spinning particle. These corrections are organized in inverse powers of the particle's mass. As already noted not only are our results for the Wilson coefficients fully consistent with the general analysis of bounds on gravitational scattering, but are restricted to small islands.

Since we focus on the leading effect due to heavy particles in the weakly coupled setting neither IR divergences, nor logarithms due to the loops of massless particles make an appearance in our analysis. Taking these into consideration is an important task which we leave for the future.

Our paper naturally consists of two parts: In the first part we explain in detail the construction of the one-loop massive amplitudes used to provide theoretical data that we interpret in the second part in terms of bounds on coefficients of gravitational EFTs. Readers who are interested in the EFT constraints can skip Sect. 4.2 on the construction of the one-loop amplitudes. Particularly important plots that illustrate the theory islands and the concept of low-spin dominance in the partial-wave expansion are given in Figs. 4.9-4.12.

In more detail, the sections are organized as follows: In Sect. 4.2 we describe our construction of the one-loop four-graviton amplitude with massive matter up to spin 2 in the loop. In Sect. 4.3 we compute graviton scattering in a general low-energy effective theory. By expanding our amplitudes in the low-energy limit, we extract the Wilson coefficients of the effective field theory. In Sect. 4.4 we describe the general properties of the gravitational amplitudes stemming from unitarity and causality. In Sect. 4.5 we derive two-sided bounds on Wilson coefficients that follow from a single helicity configuration that describes elastic scattering; comparing to known data from string theory and our computed one-loop amplitude, we show that the results fall into small islands. We trace the position of these islands using low-spin dominance of partial waves. In Sect. 4.6 we obtain bounds that arise from considering multiple helicities. We bound the low-energy expansion coefficients of inelas-

tic amplitudes in terms of elastic ones. We also derive a bound for the coefficient of the R^3 operator in terms of the R^4 coefficient. Finally, we provide our concluding remarks in Sect. 4.7. We include various appendices. In Appendix 4.A we describe in some detail our definition of minimal coupling of gravity to a massive spinning particle. In Appendix 4.B we collect tree-level graviton four-point amplitudes in various string theories. In Appendix 4.C we present details on the derivation of some low-energy bounds that are not listed in the main text of the paper. In Appendix 4.D we analyze an amplitude function with an accumulation point in the spectrum that partially violates low-spin dominance, but show that the corresponding low-energy coefficients still land on the small islands. Appendix 4.E collects the Wigner d-matrices used throughout the paper. In Appendix 4.F we present our results for the one-loop amplitudes. We give the expressions for one-loop integrals in terms of which the amplitudes are expressed in Appendix 4.G. Finally, in Appendix 4.H we expand these results to high orders in the large-mass expansion.

4.2   Construction of one-loop four-graviton scattering amplitudes

In this section we describe the construction of the one-loop four-graviton amplitudes with massive matter up to spin 2 in the loop. We collect the results in Appendix 4.F. We first briefly review the methods used to obtain the amplitudes. Then, following the generalized-unitarity method we build the integrand-level generalized-unitarity cuts. We describe a natural and efficient organization of the unitarity cuts and the amplitudes motivated by supersymmetry. This organization also meshes well with the double-copy construction which we use to obtain gravitational unitarity cuts from gauge-theory ones. Having obtained the unitarity cuts we describe the necessary integral reduction and cut merging into the amplitudes. This process fixes all but a few pieces of the amplitudes, which we obtain by exploiting the known ultraviolet properties of the amplitudes. After calculating the amplitudes, we comment on some interesting ultraviolet properties we observe. Finally, we conclude this section by listing the consistency checks we performed on our calculation.

74

4.2.1 Basic methods

Spinor helicity

We use the spinor-helicity method [6, 7, 8, 9, 10] to describe the external graviton states of amplitudes (for reviews see Refs. [285, 71, 71]). The natural quantities in this formalism are two component Weyl spinors

$$(\lambda_i)_\alpha \equiv [u_+(k_i)]_\alpha \,, \qquad (\tilde{\lambda}_i)_\alpha \equiv [u_-(k_i)]_\alpha \,, \tag{4.1}$$

which we write in a 'bra' and 'ket' notation as

$$|k_i^+\rangle = |\,i\,\rangle = \lambda_i \,, \qquad |k_i^-\rangle = |\,i\,] = \tilde{\lambda}_i \,, \qquad \langle k_i^-| = \langle\,i\,| = \lambda_i \,, \qquad \langle k_i^+| = [\,i\,| = \tilde{\lambda}_i \,. \tag{4.2}$$

where k_i^μ refers to the null momentum of the i-th external particle, while the '$\pm$' superscript refers to the helicity of the corresponding state. The spinor inner products are defined using the antisymmetric tensors $\varepsilon^{\alpha\beta}$ and $\varepsilon^{\dot\alpha\dot\beta}$,

$$\langle k_i^- | k_j^+\rangle = \langle ij\rangle = \varepsilon^{\alpha\beta}(\lambda_i)_\alpha(\lambda_j)_\alpha \,, \qquad \langle k_i^+ | k_j^-\rangle = [ij] = -\varepsilon^{\dot\alpha\dot\beta}(\tilde{\lambda}_i)_{\dot\alpha}(\tilde{\lambda}_i)_{\dot\alpha} \,. \tag{4.3}$$

These spinor products are antisymmetric in their arguments and we choose a convention where they satisfy $\langle ij\rangle[ij] = 2k_i \cdot k_j$.

In order to construct amplitudes with external gravitons, our starting point is the corresponding ones with external gluons. For calculations involving external gluons the helicity polarization vectors are defined as

$$\varepsilon_\mu^+(k_i; q_i) = \frac{\langle q_i|\gamma_\mu|i]}{\sqrt{2}\langle iq_i\rangle} \,, \qquad \varepsilon_\mu^-(k_i; q_i) = \frac{[q_i|\gamma_\mu|i\rangle}{\sqrt{2}[iq_i]} \,, \tag{4.4}$$

where q_i are arbitrary null 'reference momenta' which drop out of the final gauge-invariant amplitudes. Note that we do not use a shorthand notation for the spinors corresponding to the reference momenta. The polarization tensors for gravitons are simply given in terms of products of gluon polarization vectors,

$$\varepsilon_{\mu\nu}^+(k; q) = \varepsilon_\mu^+(k; q)\,\varepsilon_\nu^+(k; q) \,, \qquad \varepsilon_{\mu\nu}^-(k; q) = \varepsilon_\mu^-(k; q)\,\varepsilon_\nu^-(k; q) \,, \tag{4.5}$$

which automatically satisfy the graviton tracelessness condition, due to the Fierz identity. When these polarization vectors are contracted into external momenta k_i^μ or loop momenta ℓ^μ we define,

$$k_1 \cdot \varepsilon_2^+ = \frac{\langle q_2 | \slashed{k}_1 | 2]}{\sqrt{2}\langle q_2 2 \rangle} \equiv \frac{\langle q_2 | 1 | 2]}{\sqrt{2}\langle q_2 2 \rangle}, \qquad \ell \cdot \varepsilon_2^+ = \frac{\langle q_2 | \slashed{\ell} | 2]}{\sqrt{2}\langle q_2 2 \rangle} \equiv \frac{\langle q_2 | \ell | 2]}{\sqrt{2}\langle q_2 2 \rangle}, \quad \text{etc.,} \qquad (4.6)$$

where we also use the abbreviation $\varepsilon_2^+ \equiv \varepsilon^+(k_2; q_2)$.

We note that, in general, for loop calculations some care is needed when using dimensional regularization. To take advantage of the spinor-helicity formulation in a one-loop calculation we need to choose an appropriate version of dimensional regularization. Specifically, instead of taking the external polarization tensors and momenta to be $(4 - 2\epsilon)$-dimensional as in conventional dimensional regularization [16], we use the so called four-dimensional helicity (FDH) scheme [286, 287, 47, 288, 289] where both external and loop state counts are kept in four dimensions and only the loop momentum is continued to $4 - 2\epsilon$ dimensions. Because the massive one-loop amplitudes that we obtain here are neither ultraviolet nor infrared divergent, the precise distinction between the different versions of dimensional regularization drops out from the final results for the amplitudes. We do, however, need to regularize intermediate steps because individual loop integrals are ultraviolet divergent, with the divergence canceling in final results.

Generalized unitarity

In order to construct the loop integrands we use the generalized-unitarity method [19, 20]. This method systematically builds complete loop-level integrands using as input on-shell tree-level amplitudes. A central advantage is that simplifications and features of the latter are directly imported into the former. Reviews of the generalized-unitarity methods are found in Refs. [164, 165].

In general, the task of computing an amplitude is to reduce it to a linear combination of known scalar integrals. Using standard integral-reduction techniques (see e.g. Refs. [174, 290, 246]) any four-point one-loop amplitude can be written as a linear combination of box,
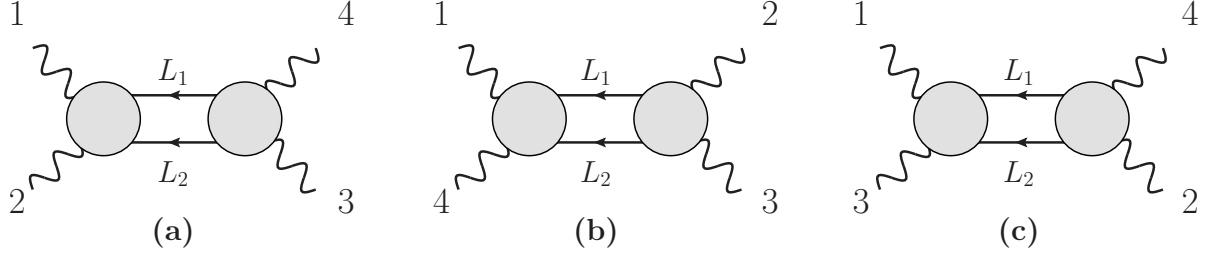
Figure 4.1: The (a) s-, (b) t- and (c) u-channel two-particle cuts of a one-loop four-point amplitude. The exposed lines are all on shell and the blobs represent tree-level amplitudes.

triangle, bubble and tadpole integrals,

$$\mathcal{M}_4^{\text{1-loop}} = \left(d_{s,t}I_4(s,t) + c_s I_3(s) + b_s I_2(s) + \text{perms.}\right) + b_0 I_2(0) + a_0 I_1, \tag{4.7}$$

where the permutations run over distinct relabelings of the integrals. At the four-point level there are a total of 11 coefficients. These coefficients depend on polarization vectors, momenta, masses and the dimensional-regularization parameter ϵ. We define the basis integrals appearing in Eq. (4.7) by

$$I_4(s,t) = \int \frac{d^D L}{(2\pi)^D} \frac{-i(4\pi)^{D/2}}{(L^2 - m^2)((L+k_1)^2 - m^2)((L+k_1+k_2)^2 - m^2)((L-k_4)^2 - m^2)},$$

$$I_3(s) = \int \frac{d^D L}{(2\pi)^D} \frac{i(4\pi)^{D/2}}{(L^2 - m^2)((L+k_1)^2 - m^2)((L+k_1+k_2)^2 - m^2)},$$

$$I_2(s) = \int \frac{d^D L}{(2\pi)^D} \frac{-i(4\pi)^{D/2}}{(L^2 - m^2)((L+k_1+k_2)^2 - m^2)},$$

$$I_1 = \int \frac{d^D L}{(2\pi)^D} \frac{i(4\pi)^{D/2}}{(L^2 - m^2)}, \tag{4.8}$$

where $D = 4 - 2\epsilon$, $s = (k_1 + k_2)^2$, $t = (k_2 + k_3)^2$ and $u = (k_1 + k_3)^2$. We obtain the remaining integrals in Eq. (4.7) by permuting the external legs. The unitarity method efficiently targets the coefficients of the integrals in Eq. (4.7). The integrals $I_2(0)$ and I_1 are respectively bubble on external leg and tadpole contributions, and are independent of kinematic variables. As we discuss below, because they lack dependence on kinematic variables, these latter integrals require special treatment to determine their coefficients.

Traditionally, unitarity of the scattering matrix is implemented at the integrated level via dispersion relations (see e.g. Ref. [291]). However, for our purposes, it is much more

convenient to use an integrand-level version of unitarity [19, 20]. This is based on the concept of a generalized-unitarity cut that reduces an integrand to a sum of products of tree-level amplitudes. For example, for the s-channel cut displayed in Fig. 4.1(a),

$$i\mathcal{M}_4^{\text{1-loop}}\Big|_{s\text{-cut}} = \int \frac{d^{4-2\epsilon}L}{(2\pi)^{4-2\epsilon}} \frac{1}{L_1^2 - m^2} \frac{1}{L_2^2 - m^2}$$
$$\sum_{\text{states}} \mathcal{M}_4^{tree}(1, 2, L_1, L_2) \mathcal{M}_4^{tree}(-L_1, -L_2, 3, 4)\Big|_{s\text{-cut}}, \qquad (4.9)$$

where $L_1 = L$ and $L_2 = -L - k_1 - k_2$ represent the two cut legs, and $\mathcal{M}_4^{tree}$ denote the tree-level amplitudes. The sum runs over all intermediate physical states that contribute for a given set of external states. The three generalized-unitarity cuts of the one-loop four-point amplitude are shown in Fig. 4.1. In this figure the exposed lines are all on shell and the blobs represent on-shell tree-level amplitudes.

To obtain the full one-loop amplitude we must combine the unitarity cuts. One possibility is to carry this out prior to integration by finding a single integrand with the correct unitarity cuts in all channels [292]. Some non-trivial examples where this approach was implemented are high-loop computations in super-Yang-Mills and supergravity (see e.g. Refs. [293, 294, 295]). On the other hand, in high-multiplicity QCD calculations (see e.g. Ref. [176, 296]) the cuts are usually combined after reducing to a basis of integrals. We apply the latter approach here. We do so by promoting each cut propagator to a Feynman propagator, and each cut to a Feynman integral. We then use FIRE6 [245, 245, 246] to reduce each Feynman integral to the scalar integrals appearing in Eq. (4.7). In each cut channel we only determine coefficients of basis integrals with cuts in that channel. By systematically evaluating each cut we determine all coefficients except for those of integrals without kinematic dependence, i.e. $I_2(0)$ and I_1. In the case of gauge theory, the corresponding coefficients are determined by imposing the known ultraviolet behavior of the amplitudes [22]. Below, we describe an analogous procedure for the case of gravitational amplitudes.

Double copy

To efficiently obtain the unitarity cuts of the four-graviton amplitude, we use the double-
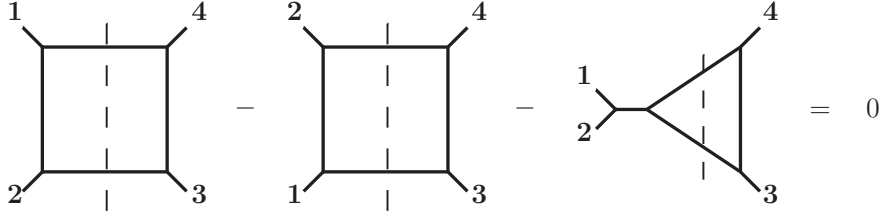
Figure 4.2: Example of a color or numerator relation for the one-loop four-point amplitudes. Here the diagram represent either color or kinematic numerators. We use these relations on the generalized-unitarity cuts, as indicated by the dashed lines. The relations are effectively tree-level ones except that the state and color sums on the cut legs are carried out.

copy construction [33, 34, 35] which expresses gravitational scattering amplitudes directly in terms of gauge-theory ones. Here we use the BCJ form of the double-copy relations [34, 35, 73], which is more natural when organizing expressions in terms of diagrams.

To apply the BCJ double copy, we start by writing a four-point one-loop gauge-theory amplitude in the following form:

$$i\mathcal{A}_4^{\text{1-loop}} = g^4 \sum_i \int \frac{d^{4-2\epsilon}L}{(2\pi)^{4-2\epsilon}} \frac{1}{S_i} \frac{n_i c_i}{D_i} \, . \tag{4.10}$$

The sum runs over all distinct four-point one-loop graphs with trivalent vertices. We denote the gauge-theory coupling constant by g. We label each graph by an integer i. The S_i are the symmetry factors of the graphs. The color factor c_i of each graph is obtained by dressing each vertex by a structure constant $\tilde{f}^{abc}$, since we take all particles to be in the adjoint representation. Our normalization of the structure constants follows that of Ref. [34, 35]. The denominator D_i contains the propagators of each graph. Finally, we capture all non-trivial kinematic dependence by the numerator n_i.

The color factors obey color-algebra relations of the type

$$c_i - c_j - c_k = 0 \, , \tag{4.11}$$

where i, j and k are some graphs. These relations follow from the Jacobi identity obeyed by the structure constants $\tilde{f}^{abc}$. For a representation obeying color-kinematics duality, the

numerators satisfy the same Jacobi relations, i.e.

$$\tilde{n}_i - \tilde{n}_j - \tilde{n}_k = 0 \,. \tag{4.12}$$

The tildes on the numerators signify that these numerators do not have to be the same as the ones appearing in Eq. (4.10), but as noted in Ref. [34, 35] these can be kinematic numerators from a different theory. Given such a representation we may obtain the corresponding gravitational amplitude simply by replacing the color factor with the corresponding kinematic numerator,

$$c_i \to \tilde{n}_i \,, \tag{4.13}$$

so that

$$i\mathcal{M}_4^{\text{1-loop}} = \left(\frac{\kappa}{2}\right)^4 \sum_i \int \frac{d^{4-2\epsilon}L}{(2\pi)^{4-2\epsilon}} \frac{1}{S_i} \frac{n_i \tilde{n}_i}{D_i} \,, \tag{4.14}$$

where κ is the gravitational coupling constant, which is given in terms of Newton's constant by,

$$\kappa^2 = 32\pi G \,. \tag{4.15}$$

The matter content of the resulting gravitational theory is determined by the choice of the numerators n_i and $\tilde{n}_i$. We use this to control the type of particle circulating in the loop.

While the BCJ double copy is usually formulated at the level of the full integrand, since we extract the final answer directly from the cuts it is more convenient to use it at the level of generalized-unitarity cuts. In Fig. 4.2 we depict an example of a color relation in terms of cut graphs. In this way we can ignore duality relations that contain diagrams without support on the given cut. For duality relations with support on the cut, the particles of each tree-level amplitude entering the cut remain on the same side of the cut for all three diagrams, as is the case in Fig. 4.2. Effectively this amounts to using the duality relations for the two tree-level amplitudes on each side of the cut (see e.g. Fig. 4.3). The tree-level relations are sufficient to ensure that for the cut diagram, the double-copy replacement formula Eq. (4.13) holds.
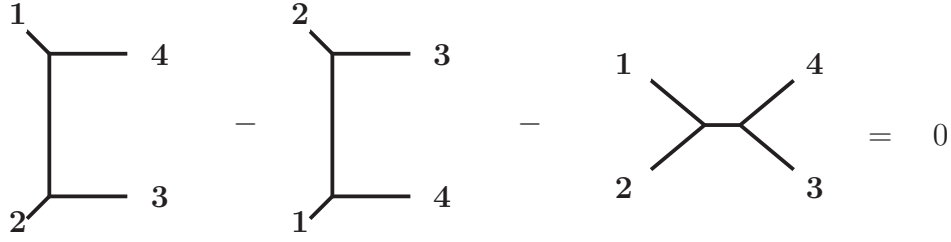
Figure 4.3: The tree-level four-point color or numerator Jacobi identity. This can be used to set the numerator of one of the diagrams to zero.

We also take advantage of a property of four-point tree-level amplitudes noted in the original BCJ paper [34, 35], which states that we can effectively set one of the three numerators to zero. In this way the duality relation implies that the other two numerators must be equal (up to a possible sign). In order to achieve that, we absorb the propagator of the diagram whose numerator is set to zero into the numerators of the other two diagrams. Specifically, consider the four-point all-gluon tree-level amplitude,

$$i\mathcal{A}_4^{\text{tree}} = g^2 \left(\frac{n_s c_s}{s} + \frac{n_t c_t}{t} + \frac{n_u c_u}{u} \right). \tag{4.16}$$

Using the color Jacobi identity depicted in Fig. 4.3, $c_s = c_t - c_u$, we can eliminate c_s in favor of the other two color factors, so that

$$i\mathcal{A}_4^{\text{tree}} = g^2 \left(\frac{n_t' c_t}{t} + \frac{n_u' c_u}{u} \right), \tag{4.17}$$

where

$$n_t' = n_t + n_s \frac{t}{s}, \qquad n_u' = n_u - n_s \frac{u}{s}. \tag{4.18}$$

Demanding that the numerators n_t' and n_u' (and $n_s' = 0$) satisfy the duality relation of Fig. 4.3 then implies that

$$n_t' = n_u'. \tag{4.19}$$

The analysis is identical in the presence of matter.

81

4.2.2 Setup of the calculation

Our goal is to obtain the four-point one-loop amplitude with external gravitons and with minimally-coupled massive spinning particles up to spin 2 circulating in the loop. Following the generalized-unitarity method we first build the integrand-level generalized-unitarity cuts in Eq. (4.9). For the one-loop four-point amplitude there are three independent cuts, labeled by the Mandelstam invariant that can be build out of the external graviton momenta on the tree-level amplitudes, i.e. s-, t- and u-channel cuts. We consider all spins up to spin 2 for the massive particles and we denote their mass by m. While these masses can be different for each particle since only a single particle at a time circulates in the loop there is no need to put an index labeling the massive particle. We take the massive particles to be real.

We note that there is an ambiguity in the definition of the minimal coupling of a spin 2 particle to gravity. In this paper, we fix this ambiguity by demanding that we recover pure gravity in the appropriate massless limit. This choice also preserves tree-level unitarity [297, 248, 249, 298, 250] and causality [299]. We discuss this ambiguity and the choice we make in this paper in Appendix 4.A.

For the amplitude in question there exist three independent helicity configurations. Specifically, we calculate

$$\mathcal{M}_4^{\text{1-loop}}(1^+, 2^-, 3^-, 4^+), \qquad \mathcal{M}_4^{\text{1-loop}}(1^+, 2^+, 3^-, 4^+), \qquad \mathcal{M}_4^{\text{1-loop}}(1^+, 2^+, 3^+, 4^+). \quad (4.20)$$

We refer to these configurations respectively as *double-minus*, *single-minus* and *all-plus*. All other amplitudes are related to these via relabelings and parity.

We build the generalized-unitarity cuts from four-point tree-level gravity amplitudes. The double copy implies that these tree-level amplitudes can be directly obtained from the corresponding gauge-theory ones, which can be described by the three diagrams shown in Fig. 4.3. As we discussed in the previous section we can use the color Jacobi identity in the gauge-theory case to remove one diagram, at the expense of other diagrams obtaining numerators that are nonlocal in the external kinematic invariants. The net effect is that after multiplying and dividing by appropriate propagators every contribution to the cut can
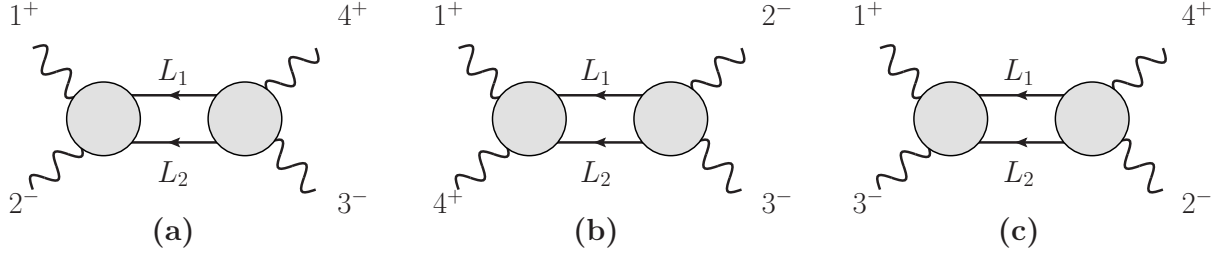
Figure 4.4: The (a) s-, (b) t- and (c) u-channel two-particle cuts of a one-loop four-point amplitude with two negative- and two positive-helicity external gluons or gravitons (double-minus configuration). The internal lines represent massive spinning particles. The exposed lines are all on shell and the blobs represent tree-level amplitudes.

be assigned to cut box diagrams. Moreover, on the generalized cuts the four-point tree-level BCJ numerator relations set the remaining numerators equal to each other, as noted in Eq. (4.19).

For example, for the four-point gauge-theory amplitude the s-channel cut in Fig. 4.4(a) is of the form,

$$i\mathcal{A}_4\Big|_{s\text{-cut}} = g^4 \int \frac{d^{4-2\epsilon}L}{(2\pi)^{4-2\epsilon}} \, n_{\text{g},s} \left(\frac{c_{1234}}{D_{1234}} + \frac{c_{1342}}{D_{1342}} \right) \Big|_{s\text{-cut}}. \tag{4.21}$$

The box color factor (see Fig. 4.5) is given by

$$c_{abcd} = \tilde{f}^{e_a g_1 g_4} \, \tilde{f}^{e_b g_2 g_1} \, \tilde{f}^{e_c g_3 g_2} \, \tilde{f}^{e_d g_4 g_3} \,, \tag{4.22}$$

where $abcd$ takes in the values indicated in Eq. (4.21). As usual, repeated indices are summed. The denominators are given by products of the usual Feynman propagators,

$$D_{abcd} = \left(L^2 - m^2\right)\left((L + k_a)^2 - m^2\right)\left((L + k_a + k_b)^2 - m^2\right)\left((L + k_a + k_b + k_c)^2 - m^2\right), \tag{4.23}$$

where the k_a are external momenta. Finally, $n_{\text{g},s}$ is a gauge-theory kinematic factor common to both box diagrams.

The gravitational cuts are similar. For example, the s-channel cut is of the form,

$$i\mathcal{M}_4\Big|_{s\text{-cut}} = \left(\frac{\kappa}{2}\right)^4 \int \frac{d^{4-2\epsilon}L}{(2\pi)^{4-2\epsilon}} \, n_{\text{GR},s} \left(\frac{1}{D_{1234}} + \frac{1}{D_{1342}} \right) \Big|_{s\text{-cut}}, \tag{4.24}$$

83
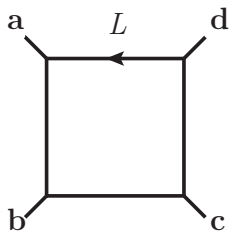
Figure 4.5: Generic box diagram whose color factor and denominator are given by Eqs. (4.22) and (4.23) respectively. The external momenta are taken incoming while the direction of the loop momentum is indicated by the arrow.

where $n_{\mathrm{GR},s}$ is the single s-channel gravitational kinematic numerator. As we noted in Sect. 4.2.1, the gravity amplitudes follow from replacing the color factor with a gauge-theory kinematic numerator. As we describe in more detail below, the particle content circulating in the loop is determined by the choice of the gauge-theory numerators.

As can be seen from Figs. 4.4(a) and 4.4(c), for the indicated helicity configuration, the u-channel cut is obtained by relabeling the momenta and spinors in the s-channel cut: $k_2 \leftrightarrow k_3$ and $\langle 2| \leftrightarrow \langle 3|$. For the single-minus and all-plus configurations, all three cuts are given by appropriate relabelings of a single cut.

4.2.3 Supersymmetric decompositions

We are interested in the problem of minimally-coupled massive matter circulating in the loop. A convenient way to organize this calculation is by following the massless case where each particle can be described as a linear combination of supersymmetric multiplets circulating in the loop. Our organization is in direct correspondence to this supersymmetric decomposition [300, 301, 283, 302]. This allows us to recycle the results of the calculation of the lower-spin particles circulating in the loop into contributions for the higher-spin particles. It also has the advantage of grouping together terms that contain integrals of the same tensor rank. For the gauge-theory case such a decomposition has already been used to organize the contributions of massive spin 0, 1/2 and 1 particles circulating in the loops [302, 22]. The double-copy construction will allow us to import this into minimally-coupled gravitational

theories with up to spin-2 massive particles.

Gauge theory

We start by examining the corresponding amplitudes in gauge theory. For the case of one-loop four-point amplitudes with external gluons and massive matter circulating in the loop, Ref. [302] showed that[6]

$$
\begin{aligned}
\mathcal{A}_4^{S=0} &= \mathcal{A}_4^{\{0\}} \,, \\
\mathcal{A}_4^{S=1/2} &= -2\mathcal{A}_4^{\{0\}} + \mathcal{A}_4^{\{1/2\}} \,, \\
\mathcal{A}_4^{S=1} &= 3\mathcal{A}_4^{\{0\}} - 4\mathcal{A}_4^{\{1/2\}} + \mathcal{A}_4^{\{1\}} \,.
\end{aligned}
\tag{4.25}
$$

where the notation $\mathcal{A}_4^{\{S\}}$ denotes the new piece we need to calculate at spin-S. In this way we express the amplitudes with a given spinning particle circulating in the loop in terms of the simpler-to-calculate new pieces. Inverting the above equations, we may think of the new pieces as amplitudes with multiplets circulating in the loop. These massive multiplets have the same degrees of freedom as the corresponding massless ones. Hence, in terms of on-shell supersymmetric representation theory they satisfy the BPS condition [303, 304, 305]. For recent calculations involving massive supersymmetric multiplets in gauge theory see Refs. [306, 307, 308, 309, 310, 311, 312, 313, 314].

Before turning to the corresponding gravitational decomposition it is useful to first look at the massless limit. For the gauge theory case we have that as $m \to 0$,

$$
\begin{aligned}
\mathcal{A}_4^{S=0} &\to \mathcal{A}_4^{S=0,\, m=0} \,, \\
\mathcal{A}_4^{S=1/2} &\to \mathcal{A}_4^{S=1/2,\, m=0} \,, \\
\mathcal{A}_4^{S=1} &\to \mathcal{A}_4^{S=1,\, m=0} + \mathcal{A}_4^{S=0,\, m=0} \,,
\end{aligned}
\tag{4.26}
$$

where we see that the $S = 1$ case is nontrivial, which follows from the mismatch in the number of degrees of freedom in a massive and massless vector boson.

Background field gauge

---

[6]We combine the 'gauge boson' and 'scalar' contributions of Ref. [302] into the massive $S = 1$ result.

A nice way to understand the above supersymmetric decomposition is in terms of background field gauge [164]. While we do not use background field gauge to compute the amplitudes, it does offer useful insight into the structure of the amplitude. For the different particles circulating in the loop we can write the effective action as

$$\Gamma_{S=0}[A] = \ln \det{}_{[0]}^{-1/2}\left(D^2 + m^2\right),$$

$$\Gamma_{S=1/2}[A] = \ln \det{}_{[1/2]}^{1/4}\left(D^2\,\mathbb{I} + m^2\,\mathbb{I} - g\frac{1}{2}\sigma^{\mu\nu}F_{\mu\nu}\right), \tag{4.27}$$

$$\Gamma_{S=1}[A] = \ln \det{}_{[1]}^{-1/2}\left(D^2\mathbb{I} + m^2\mathbb{I} - g\Sigma^{\mu\nu}F_{\mu\nu}\right) + \ln \det{}_{[0]}\left(D^2 + m^2\right) + \ln \det{}_{[0]}^{-1/2}\left(D^2 + m^2\right),$$

where $\mathbb{I}$ is the identity matrix, $\sigma_{\mu\nu}/2$ is the spin-1/2 Lorentz generator and $\Sigma_{\mu\nu}$ is the spin-1 Lorentz generator. Ignoring the $F_{\mu\nu}$ terms and focusing on the $(D^2 + m^2)$ term, each state corresponds to a power to which the determinant is raised: $-1/2$ for a bosonic state and $+1/2$ for a fermionic state. For a massive real scalar there is precisely one bosonic state corresponding the $-1/2$ power to which the first determinant is raised. For the $S = 1/2$ fermion the determinant is raised to the $1/4$ power to account for the 4×4 Dirac determinant, effectively leaving a single power that corresponds to the two states of a Majorana fermion. Similarly, for the $S = 1$ vector, the determinant is over a 4×4 Lorentz generator space so the exponent of $-1/2$ in the first term in $\Gamma_{S=1}[A]$ corresponds to 4 bosonic states. This is then reduced to two states by the ghost determinant corresponding to the second term and increased by one state from the scalar longitudinal degree of freedom required by a massive vector boson corresponding to the third term. This extra degree of freedom is incorporated into Eq. (4.25) as well. To make the supersymmetric cancellations more manifest we rewrite the Dirac determinant as a product of determinants so that the similarity to the bosonic case is clear,

$$\det{}_{[1/2]}^{1/2}(\slashed{D} + im)\det{}_{[1/2]}^{1/2}(\slashed{D} - im) = \det{}_{[1/2]}^{1/4}(\slashed{D}^2 + m^2)$$

$$= \det{}_{[1/2]}^{1/4}(D^2 + m^2 - g\frac{1}{2}\sigma^{\mu\nu}F_{\mu\nu}), \tag{4.28}$$

where $\slashed{D}^2 = \frac{1}{2}\{\slashed{D}, \slashed{D}\} + \frac{1}{2}[\slashed{D}, \slashed{D}]$. This corresponds to using the second order formalism for fermions described in Ref. [315]. The fact that the mass enters into Eq. (4.27) in such a

simple manner can also be understood in terms of a Kaluza-Klein reduction of the massless case from five dimensions, truncated to keeping only the lowest massive state in the loop.

The effective-action determinants Eq. (4.27) can be straightforwardly applied to show that the supersymmetric decomposition organizes contributions in terms of power counting of the resulting diagrams. The terms with leading power of loop momenta come from the D^2 terms in Eq. (4.27), because $F_{\mu\nu}$ contains only the external gluon momenta. If we set the $F_{\mu\nu}$ terms to zero then in all supersymmetric combinations the balance between the bosons and fermions implies the leading powers of loop momentum cancel. Subleading terms in supersymmetric combinations come from using one or more factors of $F_{\mu\nu}$ when generating a graph; each $F_{\mu\nu}$ reduces the maximum power of momentum by one. Terms with a lone $F_{\mu\nu}$ vanish, thanks to $\mathrm{Tr}(\sigma^{\mu\nu}) = \mathrm{Tr}(\Sigma^{\mu\nu}) = 0$. This reduces the leading power in an m-point one-particle-irreducible diagram from ℓ^m down to ℓ^{m-2}. For $\mathcal{A}_m^{\{1\}}$, a comparison of the traces of products of two and three $\sigma^{\mu\nu}$ and $\Sigma_{\mu\nu}$ shows that further cancellations reduce the leading behavior all the way down to ℓ^{m-4}. In gauges other than Feynman background field gauge, these cancellations would be more more obscure.

Gravity

Now consider the gravitational case. In the $m \to 0$ limit we again have a mismatch in the number of degrees of freedom for $S \geq 1$ between the massive and massless cases,

$$
\begin{aligned}
\mathcal{M}_4^{S=0} &\to \mathcal{M}_4^{S=0,\,m=0}, \\
\mathcal{M}_4^{S=1/2} &\to \mathcal{M}_4^{S=1/2,\,m=0}, \\
\mathcal{M}_4^{S=1} &\to \mathcal{M}_4^{S=1,\,m=0} + \mathcal{M}_4^{S=0,\,m=0}, \\
\mathcal{M}_4^{S=3/2} &\to \mathcal{M}_4^{S=3/2,\,m=0} + \mathcal{M}_4^{S=1/2,\,m=0}, \\
\mathcal{M}_4^{S=2} &\to \mathcal{M}_4^{S=2,\,m=0} + \mathcal{M}_4^{S=1,\,m=0} + \mathcal{M}_4^{S=0,\,m=0}.
\end{aligned}
\tag{4.29}
$$

In the massless case with spinning particles circulating in the loop we can again decompose

the amplitudes in terms of ones with supermultiplets circulating in the loop [283],

$$
\begin{aligned}
\mathcal{M}_4^{S=0,\,m=0} &= \mathcal{M}_4^{\{0\},\,m=0}\,, \\
\mathcal{M}_4^{S=1/2,\,m=0} &= -2\mathcal{M}_4^{\{0\},\,m=0} + \mathcal{M}_4^{\{1/2\},\,m=0}\,, \\
\mathcal{M}_4^{S=1,\,m=0} &= 2\mathcal{M}_4^{\{0\},\,m=0} - 4\mathcal{M}_4^{\{1/2\},\,m=0} + \mathcal{M}_4^{\{1\},\,m=0}\,, \\
\mathcal{M}_4^{S=3/2,\,m=0} &= -2\mathcal{M}_4^{\{0\},\,m=0} + 9\mathcal{M}_4^{\{1/2\},\,m=0} - 6\mathcal{M}_4^{\{1\},\,m=0} + \mathcal{M}_4^{\{3/2\},\,m=0}\,, \\
\mathcal{M}_4^{S=2,\,m=0} &= 2\mathcal{M}_4^{\{0\},\,m=0} - 16\mathcal{M}_4^{\{1/2\},\,m=0} + 20\mathcal{M}_4^{\{1\},\,m=0} - 8\mathcal{M}_4^{\{3/2\},\,m=0} \\
&\quad + \mathcal{M}_4^{\{2\},\,m=0}\,.
\end{aligned}
\tag{4.30}
$$

The $\{S\}$ pieces in each case are in direct correspondence to the supermultiplets circulating in the loop, as defined in Ref. [283][7]. For example,

$$
\mathcal{M}_4^{\{1/2\},\,m=0} = \mathcal{M}_4^{\mathcal{N}=1,\,m=0}\,,
\tag{4.31}
$$

where $\mathcal{N} = 1$ denotes the chiral multiplet consisting of a Weyl fermion and two real scalars.

Using the relation between the massive and massless amplitudes in Eq. (4.29) and the massless supersymmtric decomposition in Eq. (4.30), we can organize our computation in a similar way as for gauge theory in Eq. (4.25). Specifically, we have

$$
\begin{aligned}
\mathcal{M}_4^{S=0} &= \mathcal{M}_4^{\{0\}}\,, \\
\mathcal{M}_4^{S=1/2} &= -2\mathcal{M}_4^{\{0\}} + \mathcal{M}_4^{\{1/2\}}\,, \\
\mathcal{M}_4^{S=1} &= 3\mathcal{M}_4^{\{0\}} - 4\mathcal{M}_4^{\{1/2\}} + \mathcal{M}_4^{\{1\}}\,, \\
\mathcal{M}_4^{S=3/2} &= -4\mathcal{M}_4^{\{0\}} + 10\mathcal{M}_4^{\{1/2\}} - 6\mathcal{M}_4^{\{1\}} + \mathcal{M}_4^{\{3/2\}}\,, \\
\mathcal{M}_4^{S=2} &= 5\mathcal{M}_4^{\{0\}} - 20\mathcal{M}_4^{\{1/2\}} + 21\mathcal{M}_4^{\{1\}} - 8\mathcal{M}_4^{\{3/2\}} + \mathcal{M}_4^{\{2\}}\,.
\end{aligned}
\tag{4.32}
$$

The massive multiplets circulating in the loop are 'short', i.e. they have the same degrees of freedom as the corresponding massless ones. Hence, they obey the BPS condition [303, 304, 305]. While we have not tried directly embedding these amplitudes into supergravity theories, it is an interesting question to do so. Here we use the relation to supermultiplets for

---

[7]We use a real scalar while Ref. [283] used a complex one. Hence there is relative factor of $1/2$ for that contribution.

a more modest aim of reorganizing the contributions, so that as the spin increases the new pieces become simpler. Examples of supergravity calculations involving massive multiplets are given in Ref. [316, 317, 318, 319].

We note that in general, care is required when using dimensional regularization in conjunction with helicity methods and supersymmetric decompositions. To allow for different choices of regularization scheme, we would need to correct the last line of Eq. (4.25) to be [302]

$$\mathcal{A}_4^{S=1} = (3 - 2\delta_R\epsilon)\mathcal{A}_4^{\{0\}} - 4\mathcal{A}_4^{\{1/2\}} + \mathcal{A}_4^{\{1\}}, \tag{4.33}$$

where $\delta_R = 0$ in the FDH scheme [286] and $\delta_R = 1$ in either conventional dimensional regularization [16] or the 't Hooft-Veltman scheme [320]. One may then propagate this correction to the gravitational amplitudes through the double copy. While the correction is of $\mathcal{O}(\epsilon)$, it can interfere with infrared or ultraviolet singularities to give nontrivial contributions. However, for the massive amplitudes that we are computing here, the distinction between different schemes is not important because the four-graviton amplitudes with massive matter in the loop are both ultraviolet and infrared finite (see Sects. 4.2.6 and 4.2.8).

We also note that the coefficient of the scalar ($\mathcal{M}_4^{\{0\}}$) counts the degrees of freedom of the particle in question, modulo a minus sign for the fermions. Recall that all particles are taken to be real. Also, given the general setup of our amplitudes (Eqs. (4.21) and (4.24)), we get a similar decomposition for the corresponding numerators $n_{\mathrm{g},\alpha}$ and $n_{\mathrm{GR},\alpha}$.

Finally, the supersymmetric decomposition is simplified in the case of the single-minus and all-plus configurations. In these cases, supersymmetric Ward identities [321, 322, 323, 324] show that only the $\mathcal{M}_4^{\{0\}}$ piece gives a nonzero contribution for each spin particle in the

loop. Using this observation, Eq. (4.32) becomes

$$\mathcal{M}_4^{S=0}(1^\pm, 2^+, 3^+, 4^+) = \mathcal{M}_4^{\{0\}}(1^\pm, 2^+, 3^+, 4^+),$$

$$\mathcal{M}_4^{S=1/2}(1^\pm, 2^+, 3^+, 4^+) = -2\mathcal{M}_4^{\{0\}}(1^\pm, 2^+, 3^+, 4^+),$$

$$\mathcal{M}_4^{S=1}(1^\pm, 2^+, 3^+, 4^+) = 3\mathcal{M}_4^{\{0\}}(1^\pm, 2^+, 3^+, 4^+), \tag{4.34}$$

$$\mathcal{M}_4^{S=3/2}(1^\pm, 2^+, 3^+, 4^+) = -4\mathcal{M}_4^{\{0\}}(1^\pm, 2^+, 3^+, 4^+),$$

$$\mathcal{M}_4^{S=2}(1^\pm, 2^+, 3^+, 4^+) = 5\mathcal{M}_4^{\{0\}}(1^\pm, 2^+, 3^+, 4^+).$$

Therefore for these two helicity configurations, it is sufficient to calculate the $S = 0$ amplitude where only a scalar circulates in the loop.

4.2.4   Kinematic numerators through the double copy

Following the double-copy construction we can directly obtain the gravitational unitarity-cut numerators from gauge-theory ones. We may express the double copy in terms of spinning particles or new pieces (Eq. (4.32)) circulating in the loop. In the latter case, we find an especially compact representation for the numerators.

Taking the product of gauge-theory kinematic numerators we decompose them into cut numerators of the gravitational case. In terms of spin we have

$$n_{g,\alpha}^{\tilde{S}} n_{g,\alpha}^{S=0} = n_{\text{GR},\alpha}^{\tilde{S}}, \qquad \text{for } \tilde{S} = 0, 1/2, 1,$$

$$n_{g,\alpha}^{S=1/2} n_{g,\alpha}^{S=1/2} = n_{\text{GR},\alpha}^{S=1} + n_{\text{GR},\alpha}^{S=0},$$

$$n_{g,\alpha}^{S=1} n_{g,\alpha}^{S=1/2} = n_{\text{GR},\alpha}^{S=3/2} + n_{\text{GR},\alpha}^{S=1/2}, \tag{4.35}$$

$$n_{g,\alpha}^{S=1} n_{g,\alpha}^{S=1} = n_{\text{GR},\alpha}^{S=2} + n_{\text{GR},\alpha}^{S=1} + n_{\text{GR},\alpha}^{S=0},$$

where α denotes the cut under consideration. These are in direct correspondence to the Clebsch-Gordan decomposition. In terms of the new pieces in Eq. (4.32),

$$n_{g,\alpha}^{\{S\}} n_{g,\alpha}^{\{0\}} = n_{\text{GR},\alpha}^{\{S\}}, \qquad \text{for } S = 0, 1/2, 1,$$

$$n_{g,\alpha}^{\{1/2\}} n_{g,\alpha}^{\{1/2\}} = n_{\text{GR},\alpha}^{\{1\}},$$

$$n_{g,\alpha}^{\{1\}} n_{g,\alpha}^{\{1/2\}} = n_{\text{GR},\alpha}^{\{3/2\}}, \tag{4.36}$$

$$n_{g,\alpha}^{\{1\}} n_{g,\alpha}^{\{1\}} = n_{\text{GR},\alpha}^{\{2\}}.$$

Observe that the gauge-theory numerator $n_{g,\alpha}^{S=0}$ along with either $n_{g,\alpha}^{S=1/2}$ or $n_{g,\alpha}^{S=1}$ are sufficient to construct all the gravitational numerators up to spin 2. We explicitly verified that both constructions yield the same result. Refs. [302, 22] calculated the corresponding amplitudes $\mathcal{A}_4^{S=0}$, $\mathcal{A}_4^{S=1/2}$ and $\mathcal{A}_4^{S=1}$, from which we may extract the desired kinematic numerators. As a consistency check, we match $\mathcal{A}_4^{\{1\}}$, which was calculated in Ref. [314].

From the above construction we find a remarkably simple form for the kinematic numerators. For the double-minus gauge-theory numerators we have,

$$n_{g,\alpha}^{\{S\}} = \left([14]\langle 23\rangle\right)^2 (\psi_\alpha)^{2-2S}, \tag{4.37}$$

while for the corresponding gravity numerators we have,

$$n_{GR,\alpha}^{\{S\}} = \left([14]\langle 23\rangle\right)^4 (\psi_\alpha)^{4-2S}, \tag{4.38}$$

where

$$\psi_s \equiv \frac{\langle 2|\ell|1]\langle 3|\ell|4]}{s[14]\langle 23\rangle}, \qquad \psi_t \equiv \frac{(m^2+\mu^2)}{t}, \qquad \psi_u \equiv \frac{\langle 3|\ell|1]\langle 2|\ell|4]}{u[14]\langle 32\rangle}. \tag{4.39}$$

For the single-minus and all-plus configurations it is sufficient to calculate the numerators for a scalar circulating in the loop. For the single-minus configuration for gauge theory and gravity we find

$$n_{g,s}^{S=0} = \frac{(m^2+\mu^2)}{s}\frac{[12]}{\langle 12\rangle}\langle 3|\ell|4]^2, \qquad n_{GR,s}^{S=0} = \frac{(m^2+\mu^2)^2}{s^2}\frac{[12]^2}{\langle 12\rangle^2}\langle 3|\ell|4]^4, \tag{4.40}$$

while for the all-plus configuration we have

$$n_{g,s}^{S=0} = (m^2+\mu^2)^2\frac{[12][34]}{\langle 12\rangle\langle 34\rangle}, \qquad n_{GR,s}^{S=0} = (m^2+\mu^2)^4\left(\frac{[12][34]}{\langle 12\rangle\langle 34\rangle}\right)^2. \tag{4.41}$$

For these two configurations, we obtain the numerators for the t- and u-channel cuts by appropriate relabelings.

Following the conventions of Ref. [22], we break the $(4-2\epsilon)$-dimensional loop momentum L into a four-dimensional part ℓ and a (-2ϵ)-dimensional part μ. We write $L = (\ell, \mu)$. Using this notation we have for example

$$\ell^2 = m^2 + \mu^2, \tag{4.42}$$

91

when the cut condition $L^2 = m^2$ is satisfied. We take $\epsilon < 0$ so that we can break the loop momentum in this fashion. Further, whenever a four-dimensional vector $v \equiv (v, 0)$ is contracted with the $(4 - 2\epsilon)$-dimensional loop momentum, the (-2ϵ)-dimensional part is projected out,

$$v \cdot L = v \cdot \ell \,. \tag{4.43}$$

Ref. [140] (Eqs. (5.20) and (5.36)) calculated Compton amplitudes for a massive particle in four dimensions of up to spin 1 in gauge theory and up to spin 2 in gravity. We find similar spin dependence in our double-minus numerators as for these Compton amplitudes.

4.2.5 Integral reduction and cut merging

In this subsection we use standard integration-by-parts (IBP) methods to reduce the generalized-unitarity cuts we calculated in the previous section in terms of a basis of master integrals. This allows us to fix all integral coefficients in Eq. (4.7) other than those of the tadpole and the bubble on external leg. We discuss these remaining pieces in Sect. 4.2.6. We show details for the double-minus configuration with a scalar in the loop; the remaining helicity configurations and particle-in-the-loop contributions are similar. In order to keep the expressions concise, we do not include the helicity labels.

The general strategy for constructing the full amplitudes is to evaluate the cuts one by one in terms of the master integrals appearing in Eq. (4.7). If a given integral has a generalized cut in the channel being evaluated then that channel fully determines its coefficient. By stepping through the three channels in Fig. 4.1 we obtain the coefficients of all master integrals except $I_2(0)$ and I_1. The box integrals each have cuts in two channels so consistency requires that they give the same coefficient.

We start with the s-channel cut of the $S = 0$ double-minus helicity configuration defined in Eq. (4.20). The discussion for the u-channel cut follows in the same way, since it is given

by a relabeling of the s-channel one. We have

$$i\mathcal{M}_4^{S=0}\Big|_{s\text{-cut}} = \left(\frac{\kappa}{2}\right)^4 (\langle 23\rangle[14])^4 \int \frac{d^{4-2\epsilon}L}{(2\pi)^{4-2\epsilon}} \left(\frac{\langle 2|\ell|1\rangle\langle 3|\ell|4\rangle}{s[14]\langle 23\rangle}\right)^4 \left(\frac{1}{D_{1234}} + \frac{1}{D_{1342}}\right)\Big|_{s\text{-cut}}.$$

(4.44)

We define

$$v_1^\mu = \langle 2|\gamma^\mu|1], \qquad\qquad v_2^\mu = \langle 3|\gamma^\mu|4], \qquad (4.45)$$

which live in the four-dimensional subspace so that the v_i effectively project out the $(4-2\epsilon)$-dimensional components. This implies that $v_i \cdot \ell = v_i \cdot L$, as follows from the prescription [22] that $\epsilon < 0$. Next, we lift the cut condition and regard our expression as part of the full integrand that we would have obtained by Feynman rules,

$$i\mathcal{M}_4^{S=0,\,s\text{-channel}} = \left(\frac{\kappa}{2}\right)^4 (\langle 23\rangle[14])^4 \int \frac{d^{4-2\epsilon}L}{(2\pi)^{4-2\epsilon}} \left(\frac{\langle 2|L|1\rangle\langle 3|L|4\rangle}{s[14]\langle 23\rangle}\right)^4 \left(\frac{1}{D_{1234}} + \frac{1}{D_{1342}}\right), \quad (4.46)$$

keeping in mind that it is only valid for contributions that have an s-channel cut. We apply IBP identities [325] in $4-2\epsilon$ dimensions to reduce the above integrals to the master integrals in Eq. (4.7), using the software FIRE6 [245, 245, 246]. Upon reducing to master integrals we remove the ones that have no s-channel cut.

Next, we turn to the t-channel cut. We have

$$i\mathcal{M}_4^{S=0}\Big|_{t\text{-cut}} = \left(\frac{\kappa}{2}\right)^4 (\langle 23\rangle[14])^4 \int \frac{d^4\ell}{(2\pi)^4} \frac{d^{-2\epsilon}\mu}{(2\pi)^{-2\epsilon}} \left(\frac{(m^2+\mu^2)}{t}\right)^4 \left(\frac{1}{D_{1234}} + \frac{1}{D_{1423}}\right)\Big|_{t\text{-cut}},$$

(4.47)

where we subdivide the integration into four- and (-2ϵ)-dimensional parts

$$\int \frac{d^{4-2\epsilon}L}{(2\pi)^{4-2\epsilon}} = \int \frac{d^4\ell}{(2\pi)^4} \frac{d^{-2\epsilon}\mu}{(2\pi)^{-2\epsilon}}. \qquad (4.48)$$

As for the s channel, we lift the cut conditions and regard our expression as part of the full integrand,

$$i\mathcal{M}_4^{S=0,\,t\text{-channel}} = \left(\frac{\kappa}{2}\right)^4 (\langle 23\rangle[14])^4 \int \frac{d^4\ell}{(2\pi)^4} \frac{d^{-2\epsilon}\mu}{(2\pi)^{-2\epsilon}} \left(\frac{(m^2+\mu^2)}{t}\right)^4 \left(\frac{1}{D_{1234}} + \frac{1}{D_{1423}}\right).$$

(4.49)

93

As we discuss in Appendix 4.G.2, the integrals with the (-2ϵ)-dimensional components of loop-momentum μ in the numerators can be expressed directly in terms of the master integrals defined in Eq. (4.8). After reducing our expression we eliminate master integrals that vanish on the t-channel cut.

As noted above, an important consistency condition arises from the fact that the box integrals have cuts in two channels, so we can determine their coefficients from either channel. We explicitly verified that the coefficients we obtain for the box integrals from looking at the different channels are the same. In this way we are able to extract all coefficients of Eq. (4.7) other than a_0 and b_0, since the corresponding integrals have no cuts in any channel; we obtain these remaining two integral coefficients in Sect. 4.2.6.

4.2.6 Ultraviolet behavior and rational pieces

Analyzing the different generalized-unitarity cuts we obtain all the coefficients in Eq. (4.7) other than a_0 and b_0. Tadpoles and bubbles on external legs (see Fig. 4.6) vanish on any cut, therefore their coefficients are not accessible through generalized unitarity. In this subsection we use the known UV properties of the amplitude to obtain these coefficients. Similarly to Sect. 4.2.5, we discuss the double-minus configuration as a specific example. The other configurations follow in the same manner.

First, we observe that simply neglecting these two integrals leads to an inconsistent answer. Expanding to leading order in ϵ we get

$$\mathcal{M}_4^{S=0}\Big|_{a_0\to 0,\, b_0\to 0} = (\langle 23\rangle[14])^4 \frac{m^2 \tilde{Q}(s,t,m)}{\epsilon} + \mathcal{O}(\epsilon^0)\,, \tag{4.50}$$

where $\tilde{Q}(s,t,m)$ is some rational function. We note that we expect no UV divergence to appear in the four-graviton amplitude since the only counterterm that we could write to absorb it is the Gauss-Bonnet term, which is evanescent in four dimensions [326]. Also, the UV divergence not coming out local hints that we neglected to include some integrals.

We use the vanishing of the UV divergence to obtain the remaining coefficients a_0 and b_0. Note that since a_0 and b_0 are rational functions of ϵ, it seems that we do not have enough
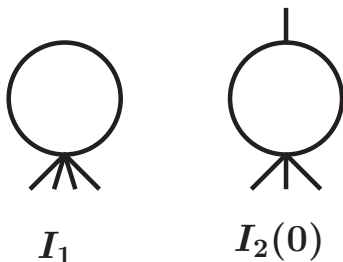
Figure 4.6: The tadpole and bubble-on-external-leg integrals.

information to fully fix them. We surpass this difficulty by realizing that our problem admits a second integral basis where the integral coefficients do not depend on ϵ and m. This basis is overcomplete in that it contains $(4-2\epsilon)$- and higher-dimensional integrals, while the one introduced in Eq. (4.7) only includes $(4-2\epsilon)$-dimensional integrals. We discuss this basis in detail and provide an algorithmic way of switching between the two bases in Appendix 4.G.2.

We start by bringing the quantity we get from cut merging to the basis containing higher-dimensional integrals. In doing so, we remove any integrals that vanish on all cuts. We refer to this piece expressed in this basis as the 'on-shell-constructable' piece. Then, we need to figure out which integrals without unitarity cuts we need to include in our expression, since in principle one could add infinitely many higher-dimensional integrals.

We consider the pieces that would arise in a Feynman-rules calculation. For the amplitude at hand we would find integrals up to quartically divergent. After we IBP reduce them and express them in the basis that contains the higher-dimensional integrals, we would in principle find all scalar integrals up to quartically divergent appearing. Hence we need to consider:

$$ I_1, \qquad I_2(k^2), \qquad I_1^{6-2\epsilon}, \qquad I_2^{6-2\epsilon}(k^2), \qquad I_2^{8-2\epsilon}(k^2), \qquad (4.51) $$

where we imagine the limiting case $k^2 \to 0$. For our definition of higher-dimensional integrals see Eq. (4.275). These are all the integrals that have no unitarity cuts and are up to quartically divergent. The reason why we consider the above limiting case is because the coefficients of these integrals might have a $1/k^2$ pole.

Then, the unknown piece in our amplitude up to normalization takes the form

$$\lim_{k^2 \to 0} \left(\beta_1 I_1 + \beta_2 I_2(k^2) + \beta_3 I_1^{6-2\epsilon} + \beta_4 I_2^{6-2\epsilon}(k^2) + \beta_5 I_2^{8-2\epsilon}(k^2) \right) = \gamma_1 I_1 + \gamma_2 I_2(0) + \gamma_3 I_1^{6-2\epsilon},$$

(4.52)

where we use

$$I_2^{6-2\epsilon}(k^2) = I_1 + \frac{k^2}{6} I_2(0) + \mathcal{O}(k^4), \qquad I_2^{8-2\epsilon}(k^2) = I_1^{6-2\epsilon} + \frac{k^2}{6} I_1 + \mathcal{O}(k^4),$$

(4.53)

following Appendix B of Ref. [22]. The unknown coefficients γ_i are rational functions of the kinematics that do not contain ϵ or m dependence. In writing this expression we assume that the coefficients of the integrals are at worse divergent as $1/k^2$ and that the expression is finite in the $k^2 \to 0$ limit when a massive particle is circulating in the loop.[8]

Upon these considerations, our amplitude takes the form

$$\mathcal{M}_4^{S=0} = \mathcal{M}_4^{S=0}\Big|_{\text{on-shell-constr.}} + \frac{1}{(4\pi)^{2-\epsilon}} \left(\frac{\kappa}{2} \right)^2 \mathcal{M}_4^{\text{tree}} \left(\gamma_1 I_1 + \gamma_2 I_2(0) + \gamma_3 I_1^{6-2\epsilon} \right),$$

(4.54)

where the γ_i are coefficients are determined from the requirement that ultraviolet divergences cancel, the integrals I_1 and I_2 are given in Eqs. (4.276) and (4.278), and

$$\mathcal{M}_4^{\text{tree}} \equiv \mathcal{M}_4^{\text{tree}}(1^+, 2^-, 3^-, 4^+) = \left(\frac{\kappa}{2} \right)^2 \frac{(\langle 23 \rangle [14])^4}{stu}.$$

(4.55)

The Mandelstam variables are defined below Eq. (4.8). Note that the little-group scaling for the unknown terms is fixed to be $(\langle 23 \rangle [14])^4$. Since the γ_i are rational functions of the kinematics, we are free to multiply and divide by (stu) to introduce $\mathcal{M}_4^{\text{tree}}$.

Next, demanding that the amplitude has no UV divergence and that all three γ_i are independent of the mass m uniquely fixes γ_1 and γ_3 to nonzero values while setting $\gamma_2 = 0$. The results for the amplitudes collected in Appendix 4.F the values of the γ_i are all chosen to make the amplitudes UV finite.

As a simple consistency check, we repeat this analysis adding integrals that have no unitarity cuts and are divergent worse than quartically (namely $(8-2\epsilon)$- and higher-dimensional

---

[8]We drop ill-defined 'cosmological constant' tadpole diagrams with a $1/\left(\sum_{i=1}^4 k_i \right)^2$ propagator.

tadpoles). We verify that the answer is the same, i.e. the coefficients of these new integrals are set to zero.

We now briefly comment on the $m \to 0$ limit. In this limit, both I_1 and $I_2(0)$ vanish, and the amplitude has no UV divergence, as can be seen from Eq. (4.50). Hence our amplitude has the correct UV behavior in this limit as well. Moreover, all integrals that have no unitarity cuts become scaleless and hence zero in dimensional regularization. Therefore, there are no unfixed coefficients and our construction based on the unitarity cuts captures the full amplitude.

Finally, we want to clarify why we chose the overcomplete basis with higher-dimensional integrals. The coefficients a_0 and b_0 are in principle arbitrary rational functions of ϵ and m, and of the kinematic variables s and t. The existence of a basis where the integral coefficients do not contain ϵ or m significantly restricts the functional dependence of a_0 and b_0 on ϵ and m. The existence of such a basis is a nontrivial fact that may be understood via analyzing the calculation in a covariant gauge, as we explain in Appendix 4.G.2. In this way the two integral bases are not completely equivalent, since the latter one is exploiting more of the specific properties of the problem at hand.

4.2.7 Further ultraviolet properties

Quadratic and quartic divergence

Next, we want to analyze the quadratic and quartic divergence of our amplitude. In dimensional regularization, the signature of these divergences are poles around $\epsilon = 1$ and $\epsilon = 2$ in the final answer. Since we compute our amplitude to all order in ϵ we may probe these poles. We tackle this question in the basis that contains only $(4 - 2\epsilon)$-dimensional integrals. In the basis that includes higher-dimensional integrals, many of the integrals are quadratically or quartically divergent, which obscures the analysis. We discuss the double-minus configuration for a spin-0 particle in the loop; the other cases are similar. As we demonstrate, our amplitude has no quadratic or quartic divergences.

We start with the quadratic divergence. In the chosen basis the only quadratically divergent integral is the tadpole. However, the coefficient of the tadpole is linear in $(\epsilon - 1)$, hence there is no contribution to the quadratic divergence from it. It then suffices to expand all coefficients around $\epsilon = 1$ and only keep the divergent piece. We get

$$\mathcal{M}_4^{S=0} = -\frac{1}{(4\pi)^{2-\epsilon}} \left(\frac{\kappa}{2}\right)^2 \mathcal{M}_4^{\text{tree}} \frac{su}{(\epsilon - 1)t^6} (3s^2 u^2 + 10m^2 stu + 6m^4 t^2)\Big(\iota_2(s) + \iota_2(u)\Big)$$
$$+ \mathcal{O}\Big((\epsilon - 1)^0\Big), \tag{4.56}$$

where we introduced

$$\iota_2(s) = s\big(2m^2 I_3(s) - I_2(s)\big). \tag{4.57}$$

Note that $I_n \equiv I_n^{4-2\epsilon} = I_n^{2-2(\epsilon-1)}$. It appears that our amplitude has a quadratic divergence which is non local due to the $1/t^6$ factor. However, using Eq. (4.285) with $D = 2 - 2(\epsilon - 1)$ we get

$$I_3^{4-2(\epsilon-1)}(s) = \frac{1}{2(\epsilon - 1)}\big(-2m^2 I_3^{2-2(\epsilon-1)}(s) + I_2^{2-2(\epsilon-1)}(s)\big), \tag{4.58}$$

which gives

$$\iota_2(s) = -2s(\epsilon - 1)I_3^{4-2(\epsilon-1)}(s). \tag{4.59}$$

Since $I_3^{4-2(\epsilon-1)}(s)$ is finite as $\epsilon \to 1$, we see that there is no quadratic divergence.

The analysis of the quartic divergence follows in a similar manner. In this basis there are no quartically-divergent integrals. We expand our result around $\epsilon = 2$ to get

$$\mathcal{M}_4^{S=0} = \frac{1}{(4\pi)^{2-\epsilon}} \left(\frac{\kappa}{2}\right)^2 \mathcal{M}_4^{\text{tree}} \frac{su}{(\epsilon - 2)t^5} (5su + 6m^2 t)\Big(\iota_4(s) + \iota_4(u)\Big) + \mathcal{O}\Big((\epsilon - 2)^0\Big), \tag{4.60}$$

where

$$\iota_4(s) = 2sI_1 + s(s - 6m^2)I_2(s) + 4m^4 s I_3(s). \tag{4.61}$$

Using Eq. (4.285) two consecutive times we get

$$\iota_4(s) = -4s(\epsilon - 2)I_3^{4-2(\epsilon-2)}(s), \tag{4.62}$$

which shows that there is no quartic divergence.

In our problem we demonstrated that the coefficients of the integrals which have no unitarity cuts in Eq. (4.54) contain no m dependence. This property was crucial in order to fix them using the vanishing of the (logarithmic) UV divergence. In a more general situation we expect this property to no longer be true. In such a scenario, analyzing the higher UV divergences offers an alternative method for obtaining these coefficients. For example, if we demand the vanishing of the quadratic and quartic divergences along with the logarithmic one for our problem, we may fix the coefficients γ_i to the values we found above, without needing to impose that they do not contain m dependence.

Ultraviolet divergences in higher dimensions

We can also inspect the ultraviolet properties in higher dimensions. This is straightforward because we obtain expressions for the amplitudes valid to all orders in ϵ. In the calculations we keep the external kinematics and helicities fixed in four dimensions. In addition, we use the FDH scheme [286, 287] which keeps the number of physical states circulating in the loop fixed at their four-dimensional values. However, we can still analytically continue the loop momentum to any dimension and study the divergence properties. We can use this as a rather nontrivial check on our expressions and also to point out a simple relation between appropriately defined divergences in higher dimensions and coefficients of terms in the large-mass expansion. We discuss the double-minus configuration with a scalar in the loop for concreteness, however our results hold for all cases considered in this paper.

Since our expressions are valid to all orders in the dimensional-regularization parameter ϵ, we may shift the spacetime dimension of the loop momentum by 2σ via $\epsilon \to \epsilon - \sigma$. For example for $\sigma = 1$ the spacetime dimension is shifted to $D = 6 - 2\epsilon$. In the shifted dimension we define the coefficients of the ultraviolet divergences as

$$\mathcal{M}_4^{S=0}\big|_{\epsilon \to \epsilon - \sigma} = \frac{1}{(4\pi)^\sigma} \frac{1}{(\sigma - 1)!} \frac{1}{\epsilon} \sum_{n=0}^{\sigma-1} \left(m^2\right)^n \delta_{\sigma, n}^{UV}(s, t) + \mathcal{O}\left(\epsilon^0\right), \qquad (4.63)$$

where we choose the normalization in a particular way to account for the angular loop-

integration in different dimensions. Note that there is no UV divergence for $\sigma = 0$, corresponding to $D = 4 - 2\epsilon$, due to the lack of a corresponding counterterm matrix element. For $\sigma = 1$ the counterterm is an R^3-type operator. In this case, up to a numerical factor the coefficient of the divergence matches the tree amplitude generated from an R^3 insertion, which we describe in Sect. 4.3. For convenience we restrict ourselves to even dimensions (for $\epsilon \to 0$) because in these cases the dimension-shifting formulas (Eq. (4.285)) bring the higher-dimensional integrals back to four dimensions. For $2 \leq \sigma \leq 6$ we have explicitly confirmed that the divergences are local and therefore correspond to appropriate derivatives of R^4-type operators, as expected. We note that because individual integrals have nonlocal coefficients the fact that the divergences are local provides a rather nontrivial check on our expressions. Furthermore, starting at $D = 8 - 2\epsilon$ all the integrals are divergent, so their coefficients feed into this check.

Finally, we point out a relation between the ultraviolet divergences in Eq. (4.63) and terms in the large-mass expansion in four dimensions. Specifically, defining

$$\mathcal{M}_4^{S=0} = \sum_{n=1}^{\infty} \frac{\delta_n^{IR}(s,t)}{m^{2n}} , \qquad (4.64)$$

we have explicitly checked through $\sigma = 4$ or equivalently $D = 12 - 2\epsilon$ that

$$\delta_{\sigma,0}^{UV} = \delta_\sigma^{IR} . \qquad (4.65)$$

Similarly, we find that $\delta_{\sigma,n}^{UV}$ is proportional to $\delta_{\sigma-n,0}^{UV} = \delta_{\sigma-n}^{IR}$ with a common proportionality constant for all multiplets. For this correspondence to hold it is important to keep both the external and internal states at their four dimensional value; only the loop momentum is analytically continued to higher spacetime dimensions. It is quite remarkable that such simple relations exist between the coefficients of the divergences in higher dimensions and the terms in the large-mass expansion of the amplitudes in four dimensions.

4.2.8 Consistency checks

We have carried out a variety of checks on our amplitudes. Basic self-consistency checks are that ultraviolet and infrared or mass singularities be of the right form.

Ultraviolet singularities must be local. In general this is nontrivial and happens only after the ultraviolet singularities are combined. In our case, the coefficient of the divergences vanishes. We also verified that the $1/(\epsilon - 1)$ pole cancels, consistent with the fact that the Ricci-scalar counterterm vanishes by the equation of motion. Similarly for the $1/(\epsilon - 2)$ pole, the expression is not only local but it vanishes. Further, we verified that the divergences obtained by analytically continuing the loop momentum to higher dimensions while keeping the state counts and external kinematics to their four-dimensional values are also local.

Another nontrivial check comes from looking at the $m \to 0$ limit. Since the internal lines are massive, there is no IR divergence for our amplitude. However, we may regard the mass of the internal lines as an infrared regulator for the corresponding massless amplitude and study the IR divergence as $m \to 0$. In gravity the infrared singularities are quite simple since there are only soft singularities and no collinear or mass singularities [273, 274, 327, 328]. The soft singularities arise only from gravitons circulating in the loop. This implies that as $m \to 0$ all contributions must be infrared finite except for the $\mathcal{M}_4^{\{2\}}$ piece (corresponding to $\mathcal{N} = 8$ supergravity in the massless limit), since this is the only piece that has a graviton circulating in the loop in this limit.

To carry out this check we start with the on-shell-constructable piece. We start from the $(4 - 2\epsilon)$-dimensional integral basis, where only the boxes and the triangles have IR singularities. The triangles only contain simple logarithms (see Eq. (4.280)) while the boxes contain both logarithms and dilogarithms (see Eq. (4.281)). To simplify the check we use Eq. (4.285) to trade the boxes for triangles and $(6 - 2\epsilon)$-dimensional boxes. Importantly, the latter have no IR singularities. In this form the infrared singularities are all pushed into triangle integrals, hence it suffices to verify that their coefficients vanish as $m \to 0$, which we confirm for all but the $\mathcal{M}_4^{\{2\}}$ piece. Next we look at the contributions with no unitarity cuts. These pieces are zero if we take $m \to 0$ before we expand in ϵ. On the other hand, divergent terms appear if we first expand in ϵ and then take $m \to 0$. However, given that the ultraviolet divergence vanishes in four-dimensions these infrared divergent $\log(m)$ pieces also cancel among themselves. For the $\mathcal{M}_4^{\{2\}}$ piece there is indeed a infrared singularity that

develops as $m \to 0$. In this case, we recover the known infrared divergence of pure Einstein gravity [273, 274, 327, 328].

As another check, we have explicitly verified that as $m \to 0$ our massive results match the massless ones given in Ref. [283], up to an overall sign in $\mathcal{M}_4^{\{1/2\}}$, as noted in Ref. [329]. One simple way to implement this check is to start with the expressions for the amplitudes in the $(4 - 2\epsilon)$-dimensional integral basis, set $m \to 0$ in the integral coefficients, and replace the massive integrals with massless ones.

Finally, we note that contributions from individual integrals do not decay at large mass as required by decoupling, while the amplitudes have the required property. This involves nontrivial cancellation between the pieces, providing yet another check.

4.3 Amplitudes in the low-energy effective field theory

In this section we study four-graviton scattering in a general parity-even low-energy EFT. Such EFTs start from the Einstein-Hilbert action and extend to systematically include higher-dimension operators. We include a massless scalar field to our analysis, corresponding to the dilaton found in string theory.

We match this EFT to the one-loop amplitudes determined in Sect. 4.2 and collected in Appendix 4.F. In this context, the EFT is valid for energies significantly smaller than the mass of the spinning particle in the loop. In this way we determine the modification to the low-energy theory of gravity due to the presence of a heavy particle. We take this as a nontrivial model of ultraviolet physics feeding into low-energy physics.

For the lowest-dimension operators, we calculate the four-point tree-level amplitudes in this EFT and compare them to the expansion of our one-loop amplitudes in the large-mass limit in order to obtain their Wilson coefficients. More generally, since we later put bounds on the coefficients appearing in the amplitudes themselves, there is no need to relate these back to a Lagrangian. For comparison to the bounds derived in subsequent sections we also present the one-loop scattering amplitudes expanded in the large-mass limit. In

Appendix 4.H we present the expansions to much higher orders, which should be useful for further studies of the bounds.

Finally, we obtain the Regge limits of our one-loop amplitudes. These are useful later in analyzing low-energy coefficients via dispersion relations.

4.3.1 Setup of the effective field theory

The first few terms of the EFT describing low-energy gravitational scattering are

$$S_{\text{EFT}} = \int d^4x \sqrt{-g} \left[-\frac{2}{\kappa^2} R + \frac{1}{2} \partial_\mu \phi \partial^\mu \phi + \frac{2\beta_\phi}{\kappa^2} \phi\, C + \frac{8}{\kappa^3} \frac{\beta_{R^3}}{3!} R^3 + \frac{2\beta_{R^4}}{\kappa^4} C^2 + \frac{2\tilde{\beta}_{R^4}}{\kappa^4} \tilde{C}^2 + \dots \right], \tag{4.66}$$

where R is the Ricci scalar, κ is given in terms of Newton's constant G via $\kappa^2 = 32\pi G$, and the metric is $g_{\mu\nu} = \eta_{\mu\nu} + \kappa h_{\mu\nu}$ in terms of the graviton field $h_{\mu\nu}$. To describe the most general parity-even theory that captures low-energy four-graviton scattering, we include the massless scalar field ϕ. The factors of $\frac{1}{\kappa}$ are chosen to normalize the kinetic term canonically and to remove the factors of κ that would appear in the three-point tree-level amplitudes built out of a single insertion of $\phi\, C$ or R^3 and the four-graviton tree-level amplitudes built out of a single insertion of C^2 or $\tilde{C}^2$. The β_ϕ, β_{R^3}, β_{R^4} and $\tilde{\beta}_{R^4}$ are Wilson coefficients that depend on the details of the UV physics. The composite operators are defined by

$$R^3 \equiv R^{\mu\nu\kappa\lambda} R_{\kappa\lambda\alpha\gamma} R^{\alpha\gamma}{}_{\mu\nu}\,, \qquad C \equiv R^{\mu\nu\kappa\lambda} R_{\mu\nu\kappa\lambda}\,, \qquad \tilde{C} \equiv \frac{1}{2} R^{\mu\nu\alpha\beta} \epsilon_{\alpha\beta}{}^{\gamma\delta} R_{\gamma\delta\mu\nu}\,, \tag{4.67}$$

where $R_{\lambda\mu\nu\kappa}$ is the Riemann tensor. One can systematically add higher-dimension operators; we choose not to do so here since our later analysis is at the amplitude level, so the mapping back to Lagrangian coefficients is not necessary.

In writing the effective action Eq. (4.66) we apply the equations of motion and integrate by parts to reduce the number of terms to a minimum independent set. In particular, in constructing the higher-dimensional operators we replace instances of the Ricci scalar and tensor, R and $R_{\mu\nu}$, with appropriate contractions of the matter stress-energy tensor. We drop such terms since they give rise to higher-point matter interactions, which do not affect our

analysis. For example, we do not include R^2-type terms because the squares of R and $R_{\mu\nu}$ do not contribute due to the equations of motion, while the contraction of two Riemann tensors C can be traded for the Gauss-Bonnet contribution, which is equal to a total derivative in four dimensions [326]. Furthermore, we do not include operators that our calculation is not sensitive to. Specifically, we do not consider the other possible contraction of three Riemann tensors, since it does not contribute to four-graviton scattering [330, 331]. We restrict ourselves to parity-even interactions and neglect the parity-odd operators $\phi\tilde{C}$ and $C\tilde{C}$ [332, 333]. The possible parity-even contractions of four Riemann tensors were obtained in Ref. [334]. Recent studies that use similar Lagrangians are found in Refs. [333, 335, 336, 337, 338].

4.3.2 Scattering amplitudes in the effective field theory

To describe the amplitudes it is useful to extract overall dependence on the spinors, leaving only functions of s, u with simple crossing properties. Specifically, for the independent helicity configurations we define,

$$
\begin{aligned}
\mathcal{M}_4(1^+, 2^-, 3^-, 4^+) &= (\langle 23 \rangle [14])^4 \, f(s, u) \,, \\
\mathcal{M}_4(1^+, 2^+, 3^-, 4^+) &= ([12][14]\langle 13 \rangle)^4 \, g(s, u) \,, \\
\mathcal{M}_4(1^+, 2^+, 3^+, 4^+) &= \left(\frac{[12][34]}{\langle 12 \rangle \langle 34 \rangle} \right)^2 h(s, u) \,,
\end{aligned}
\tag{4.68}
$$

corresponding to the *double-minus*, *single-minus* and *all-plus* helicity configurations. As usual we do not include the overall i that normally would appear in Feynman diagrams. All other amplitudes are given by permutations and complex conjugation,

$$
\mathcal{M}_4(1^{h_1}, 2^{h_2}, 3^{h_3}, 4^{h_4}) = \mathcal{M}_4^*(1^{-h_1}, 2^{-h_2}, 3^{-h_3}, 4^{-h_4}) \,.
\tag{4.69}
$$

where we define the complex conjugation to not act on the $i\epsilon$ prescription.[9] In parity-preserving theories complex conjugation acts only on the spinors swapping the positive and

---

[9]More precisely, given complex conjugation $\gamma : z \mapsto z^*$, we define $f^*(z)$ as $f^* \equiv \gamma \circ f \circ \gamma : z \mapsto (f(z^*))^*$. For identical scalar particles Eq. (4.69) becomes the familiar hermitian analyticity.

negative helicity spinors,

$$\mathcal{M}_4(1^{h_1}, 2^{h_2}, 3^{h_3}, 4^{h_4}) = \mathcal{M}_4(1^{-h_1}, 2^{-h_2}, 3^{-h_3}, 4^{-h_4})\Big|_{\lambda_i \leftrightarrow \tilde{\lambda}_i}, \tag{4.70}$$

so that the f, g and h functions are unaltered.

In general relativity the leading-order results for the amplitudes above take the form

$$f_{\text{GR}}(s, u) = \left(\frac{\kappa}{2}\right)^2 \frac{1}{stu} + \dots, , \tag{4.71}$$

$$g_{\text{GR}}(s, u) = \frac{1}{(4\pi)^2} \left(\frac{\kappa}{2}\right)^4 \frac{1}{s^2 t^2 u^2} \frac{s^2 + t^2 + u^2}{360} + \dots, \tag{4.72}$$

$$h_{\text{GR}}(s, u) = -\frac{1}{(4\pi)^2} \left(\frac{\kappa}{2}\right)^4 \frac{s^2 + t^2 + u^2}{120} + \dots. \tag{4.73}$$

Below we do not consider loop effects in general relativity itself (due to gravitons circulating in the loops) but focus on the properties of the higher-derivative operators in the gravitational EFT generated by integrating out massive degrees of freedom. For the same reason IR divergences are not an issue for our analysis since the corrections of interest are manifestly IR finite.

Permutation symmetry of the amplitudes plays a crucial role in our analysis and manifests itself in the following crossing relations

$$f(s, u) = f(u, s), \tag{4.74}$$

$$g(s, u) = g(u, s) = g(s, t), \tag{4.75}$$

$$h(s, u) = h(u, s) = h(s, t). \tag{4.76}$$

where $s + t + u = 0$.

With our normalizations the three-point amplitude arising from the Einstein term is[10]

$$\mathcal{M}_3^{\text{GR}}(1^+, 2^+, 3^-) = \frac{\kappa}{2} \left(\frac{[12]^3}{[23][31]}\right)^2. \tag{4.77}$$

The three-points amplitudes with an insertion of the ϕC or the R^3 operator are [331]

$$\mathcal{M}_3^{\phi C}(1^+, 2^+, 3^\phi) = \beta_\phi [12]^4, \quad \mathcal{M}_3^{R^3}(1^+, 2^+, 3^+) = \beta_{R^3} \Big([12][23][31]\Big)^2, \tag{4.78}$$

---

[10]We implicitly use complex momenta so that the three-point amplitude does not vanish from kinematic constraints.

where β_ϕ and β_{R^3} are the Wilson coefficient for these operators appearing in Eq. (4.66).

At four points ϕC contributes to the double-minus and all-plus configurations,

$$\mathcal{M}_4^{\phi C}(1^+, 2^+, 3^+, 4^+) = -3(\beta_\phi)^2 stu \left(\frac{[12][34]}{\langle 12\rangle\langle 34\rangle}\right)^2,$$

$$\mathcal{M}_4^{\phi C}(1^+, 2^-, 3^-, 4^+) = -(\beta_\phi)^2 \frac{(\langle 23\rangle[14])^4}{t}. \tag{4.79}$$

On the other hand, there are two independent helicity configurations, the all-plus and the single-minus configurations, that contain a single insertion of R^3. We obtain these amplitudes following Ref. [331]. We find

$$\mathcal{M}_4^{R^3}(1^+, 2^+, 3^-, 4^+) = \beta_{R^3}\left(\frac{\kappa}{2}\right)\frac{1}{stu}\left([12][14]\langle 13\rangle\right)^4, \tag{4.80}$$

and

$$\mathcal{M}_4^{R^3}(1^+, 2^+, 3^+, 4^+) = 10\beta_{R^3}\left(\frac{\kappa}{2}\right)stu\left(\frac{[12][34]}{\langle 12\rangle\langle 34\rangle}\right)^2, \tag{4.81}$$

which is slightly rearranged compared to Ref. [331]. We build a double-minus contribution out of two insertions of R^3 [266],

$$\mathcal{M}_4^{R^3}(1^+, 2^-, 3^-, 4^+) = (\beta_{R^3})^2 \frac{su}{t}\left(\langle 23\rangle[14]\right)^4. \tag{4.82}$$

For the R^4-type operators the amplitudes are [337]

$$\mathcal{M}_4^{R^4}(1^+, 2^+, 3^+, 4^+) = \beta_{R^4}^- \frac{(s^2 + t^2 + u^2)^2}{2}\left(\frac{[12][34]}{\langle 12\rangle\langle 34\rangle}\right)^2,$$

$$\mathcal{M}_4^{R^4}(1^+, 2^-, 3^-, 4^+) = \beta_{R^4}^+\left(\langle 23\rangle[14]\right)^4, \tag{4.83}$$

where by $\mathcal{M}_4^{R^4}$ we refer to the amplitudes build out of both C^2 and $\tilde{C}^2$, with

$$\beta_{R^4}^\pm \equiv \beta_{R^4} \pm \tilde{\beta}_{R^4}, \tag{4.84}$$

Using these four-point amplitudes we may extract the coefficients β_{R^3}, β_{R^4} and $\tilde{\beta}_{R^4}$ by matching to our one-loop calculation in the large-mass limit. Since we did not include the massless scalar field in the construction of our one-loop amplitudes, we have $\beta_\phi = 0$ in this case.

Next, we bring our one-loop amplitudes in a form suitable to compare to the EFT amplitudes listed above. We start with the double-minus amplitude. As usual, we organize the contributions according to the supersymmetric decomposition Eq. (4.32),

$$\mathcal{M}_4^{\{S\}}(1^+, 2^-, 3^-, 4^+) = (\langle 23 \rangle [14])^4 \, f^{\{S\}}(s, u) \,. \tag{4.85}$$

In the large-mass limit, for the double-minus amplitudes we have,

$$f^{\{0\}} = \mathcal{K} \left(\frac{1}{6300m^4} + \frac{t}{41580m^6} + \frac{81(s^2 + u^2) + 155su}{15135120m^8} + \frac{\left(161(s^2 + u^2) + 324su\right)t}{151351200m^{10}} + \cdots \right),$$

$$f^{\{1/2\}} = \mathcal{K} \left(\frac{1}{1120m^4} + \frac{t}{8400m^6} + \frac{15(s^2 + u^2) + 28su}{554400m^8} + \frac{\left(153(s^2 + u^2) + 313su\right)t}{30270240m^{10}} + \cdots \right),$$

$$f^{\{1\}} = \mathcal{K} \left(\frac{1}{180m^4} + \frac{t}{1680m^6} + \frac{22(s^2 + u^2) + 39su}{151200m^8} + \frac{\left(20(s^2 + u^2) + 43su\right)t}{831600m^{10}} + \cdots \right),$$

$$f^{\{3/2\}} = \mathcal{K} \left(\frac{1}{24m^4} + \frac{t}{360m^6} + \frac{9(s^2 + u^2) + 14su}{10080m^8} + \frac{\left(8(s^2 + u^2) + 21su\right)t}{75600m^{10}} + \cdots \right),$$

$$f^{\{2\}} = \mathcal{K} \left(\frac{1}{2m^4} + \frac{s^2 + su + u^2}{120m^8} + \frac{stu}{504m^{10}} + \cdots \right), \tag{4.86}$$

where

$$\mathcal{K} = \frac{1}{(4\pi)^2} \left(\frac{\kappa}{2} \right)^4 \,. \tag{4.87}$$

For the all-plus and single-minus configurations it suffices to give the result for the spin-0 contribution since we obtain the remaining amplitudes via Eq. (4.34). For the single-minus configuration we have

$$\mathcal{M}_4^{S=0}(1^+, 2^+, 3^-, 4^+) = ([12]\langle 13 \rangle [14])^4 \, g(s, u) \,, \tag{4.88}$$

where

$$g(s, u) = \mathcal{K} \left(\frac{1}{5040m^2 stu} + \frac{1}{6306300m^8} + \frac{(s^2 + su + u^2)}{441080640m^{12}} + \cdots \right). \tag{4.89}$$

Finally, for the all-plus configuration we have,

$$\mathcal{M}_4^{S=0}(1^+, 2^+, 3^+, 4^+) = \left(\frac{[12][34]}{\langle 12 \rangle \langle 34 \rangle} \right)^2 h(s, u) \,, \tag{4.90}$$

where

$$h(s, u) = \mathcal{K}\bigg(\frac{stu}{504m^2} + \frac{(s^2 + su + u^2)^2}{3780m^4} + \frac{(s^2 + su + u^2)stu}{7920m^6}$$

$$+ \frac{75(s^6 + u^6) + 225(s^5 u + su^5) + 559(s^4 u^2 + s^2 u^4) + 743 s^3 u^3}{7207200m^8}$$

$$+ \frac{3(s^2 + su + u^2)^2 stu}{400400m^{10}} + \dots \bigg). \tag{4.91}$$

The fact that the highest power of m appearing in the large-mass expansion is m^{-2} may be contrasted to the high powers of the m in the coefficients of the integrals in the $(4 - 2\epsilon)$-dimensional integral basis (see Eqs. (4.264), (4.269) and (4.270)). It is a nontrivial consistency check that our amplitudes vanish in the large-mass limit, as expected from decoupling. Indeed, the above large-mass behavior hinges on nontrivial cancellations between all pieces of the amplitude.

Now consider the matching and extraction of the Wilson coefficients β_{R^3}, β_{R^4} and $\tilde{\beta}_{R^4}$ (or, equivalently, β_{R^3} and $\beta_{R^4}^{\pm}$). Since the relation between the Wilson coefficients and the amplitudes is linear, the Wilson coefficients satisfy the supersymmetric decomposition (Eq. (4.32)). Hence, we may organize our results in terms of the multiplets circulating in the loop. One may then assemble the corresponding coefficients for any spinning particle circulating in the loop using Eq. (4.32).

Since the all-plus and single-minus amplitudes are nonzero only for the $\{0\}$ piece, we have

$$(\beta_{R^3})^{\{0\}} = \frac{1}{(4\pi)^2} \left(\frac{\kappa}{2} \right)^3 \frac{1}{m^2} \frac{1}{5040}, \qquad (\beta_{R^4}^-)^{\{0\}} = \frac{1}{(4\pi)^2} \left(\frac{\kappa}{2} \right)^4 \frac{1}{m^4} \frac{1}{7560},$$

$$(\beta_{R^3})^{\{S\} \neq 0} = (\beta_{R^4}^-)^{\{S\} \neq 0} = 0. \tag{4.92}$$

where our notation $(\beta_X)^{\{S\}}$ means the value of β_X as determined by the data for the new piece for a given spin S. The double-minus configuration is nonzero for any multiplet circulating

in the loop. We find

$$(\beta_{R^4}^+)^{\{0\}} = \frac{1}{(4\pi)^2} \left(\frac{\kappa}{2}\right)^4 \frac{1}{m^4} \frac{1}{6300}, \qquad (\beta_{R^4}^+)^{\{1/2\}} = \frac{1}{(4\pi)^2} \left(\frac{\kappa}{2}\right)^4 \frac{1}{m^4} \frac{1}{1120},$$

$$(\beta_{R^4}^+)^{\{1\}} = \frac{1}{(4\pi)^2} \left(\frac{\kappa}{2}\right)^4 \frac{1}{m^4} \frac{1}{180}, \qquad (\beta_{R^4}^+)^{\{3/2\}} = \frac{1}{(4\pi)^2} \left(\frac{\kappa}{2}\right)^4 \frac{1}{m^4} \frac{1}{24},$$

$$(\beta_{R^4}^+)^{\{2\}} = \frac{1}{(4\pi)^2} \left(\frac{\kappa}{2}\right)^4 \frac{1}{m^4} \frac{1}{2}. \tag{4.93}$$

4.3.3 Regge limits of the amplitudes

For our analysis of the amplitudes with dispersion relations in the next sections, we need the behavior of the amplitudes for $t \to \infty$ and $s \in \mathbb{R}$ fixed, with $|s| < 4m^2$ and for $s \to \infty$ and $t \in \mathbb{R}$ fixed, with $|t| < 4m^2$. We extract these directly from the explicit values of the amplitudes in Appendix 4.H.

We start with the $t \to \infty$ limit. For the new-pieces in the supersymmetric decomposition we have

$$f^{\{S\}}(s, u) \sim \frac{\log(t)}{t^2}, \qquad S = 0, \ 1/2, \ 1,$$

$$f^{\{3/2\}}(s, u) \sim \frac{\log^2(t)}{t^2}, \qquad f^{\{2\}}(s, u) \sim \frac{1}{t},$$

$$g^{\{0\}}(s, u) \sim \frac{1}{t^2}, \qquad h^{\{0\}}(s, u) \sim t^2, \tag{4.94}$$

where the f, g, and h function are related to the amplitude via Eq. (4.68). Using Eq. (4.32) we assemble the contributions for each particle of a given spin,

$$f^S(s, u) \sim \frac{\log(t)}{t^2}, \qquad S = 0, \ 1/2, \ 1,$$

$$f^{3/2}(s, u) \sim \frac{\log^2(t)}{t^2}, \qquad f^2(s, u) \sim \frac{1}{t},$$

$$g^S(s, u) \sim \frac{1}{t^2}, \qquad h^S(s, u) \sim t^2, \qquad S = 0, \ 1/2, \ 1, \ 3/2, \ 2. \tag{4.95}$$

For the f^S functions corresponding to the case of no helicity flips between incoming and incoming states the spin 2 contribution dominates as expected.

Next, we consider the $s \to \infty$ limit. We find

$$f^{\{S\}}(s, u) \sim \frac{1}{s}, \qquad S = 0,\ 1/2,\ 1,\ 3/2,\ 2,$$

$$g^{\{0\}}(s, u) \sim \frac{1}{s^2}, \qquad h^{\{0\}}(s, u) \sim s^2, \tag{4.96}$$

which gives

$$f^{S}(s, u) \sim \frac{1}{s}, \qquad g^{S}(s, u) \sim \frac{1}{s^2}, \qquad h^{S}(s, u) \sim s^2, \qquad S = 0,\ 1/2,\ 1,\ 3/2,\ 2. \tag{4.97}$$

Note that the limits of the functions g^S and h^S in Eqs. (4.96) and (4.97) follow from those in Eqs. (4.94) and (4.95), since these functions are crossing symmetric.

4.4   Properties of gravitational amplitudes

We now turn to the properties of the low-energy effective field theory, arising from taking the large-mass expansion of the one-loop four-graviton amplitudes calculated in Sect. 4.2. Here we do not consider loop effects in general relativity itself (due to gravitons circulating in the loops) but focus on the properties of the leading-order higher-derivative operators in a weakly-coupled gravitational EFT generated by integrating out massive degrees of freedom. For the same reason IR divergences are not an issue for our analysis since the corrections of interest are manifestly IR finite. We also note that we do not need to deal with UV divergences, since the one-loop four graviton amplitude with polarization tensors restricted to four dimensions considered here is UV finite [326].

To make the analysis more complete we also include the example of tree-level graviton scattering in string theory (see Appendix 4.B). As recently discussed in [339], in this case the scattering amplitudes have a great degree of universality; e.g. to leading order considered here they do not depend on the details of the string compactification.

A general question we ask in this paper is the following: where do physical theories land in the space of couplings that satisfy the bounds from causality, unitarity and crossing? In this section we review general properties of the gravitational amplitudes relevant for the derivation of the bounds. In subsequent sections we then proceed with the derivation of

various bounds on the Wilson coefficients, following the recent developments of Refs. [267, 268, 269, 340, 270]. Finally, we check that the results presented in the paper satisfy the expected bounds and analyze the region in the space of couplings covered by known theories.

4.4.1 Low-energy expansion

The functions f, g and h defined in Eq. Eq. (4.68) correspond to the independent helicity configurations. We consider their low-energy expansion[11]

$$f(s,u) = \left(\frac{\kappa}{2}\right)^2 \frac{1}{stu} + |\beta_{R^3}|^2 \frac{su}{t} - |\beta_\phi|^2 \frac{1}{t} + \sum_{i=0}^{\infty} f_{2i,i} s^i u^i + \sum_{i=1}^{\infty} \sum_{j=0}^{[\frac{i}{2}]} f_{i,j}(s^{i-j}u^j + s^j u^{i-j}),$$

$$g(s,u) = \left(\frac{\kappa}{2}\right) \frac{\beta_{R^3}}{stu} + \sum_{p,q=0}^{\infty} g_{2p+3q,q} \sigma_2^p \sigma_3^q,$$

$$h(s,u) = [10\left(\frac{\kappa}{2}\right)\beta_{R^3} - 3\beta_\phi^2]stu + \sum_{p,q=0,2p+3q\geq4}^{\infty} h_{2p+3q,q}\sigma_2^p\sigma_3^q, \qquad (4.98)$$

where $[x]$ means the integer part of x, and we introduced

$$\sigma_k \equiv (-1)^k \frac{s^k + t^k + u^k}{k}. \qquad (4.99)$$

In Eq. (4.98) we explicitly write the massless exchange poles and assume that the rest of the amplitude admits a simple low-energy expansion. This is a structure expected from integrating out massive degrees of freedom and indeed, the amplitudes analyzed in the present paper are of this type. It does not however capture correctly the structure of the amplitude once the loops involving massless particles are included. For example, consider the case of the one-loop correction due to gravitons circulating in the loop; see Eq. Eq. (4.71) and Appendix 4.F.4. In this case, we see that for the all-plus amplitude one-loop Einstein gravity generates a non-zero $h_{2,0}$. Similarly, for the single-minus amplitude $g(s,u)$ the one-loop result in Einstein gravity has poles in each of the Mandelstam variables. Finally, the double-minus amplitude $f(s,u)$, see Eq. Eq. (4.273), contains IR divergences, logarithms, as well as higher-order singularities in $1/t$ compared to the formulas above. In the present paper we focus on

---

[11]Here we allowed for parity-odd and parity-violating effects which render certain coefficients in the low-energy expansion complex.

the effect produced by integrating out massive degrees of freedom and do not analyze the effects from one-loop massless exchanges. Mathematically, this is simply due to the fact that at leading order that we are interested in, the two effects lead to additive contributions to the scattering amplitude and can be analyzed separately. Moreover, the corrections to graviton scattering due to integrating out massive degrees of freedom satisfy all the basic properties that we discuss later in the section and as such the low-energy expansion generated in this way satisfies consistency bounds. Physically, integrating out massive degrees of freedom leads to effects that are localized in the impact parameter space $b \lesssim 1/m_{\mathrm{gap}}$, which are encoded via higher-derivative operators in a gravitational EFT, whereas the one-loop effect due to graviton exchange contributes at any impact parameter, which also manifests itself through the fact that such corrections do not admit the representation Eq. (4.98). It would be very interesting to develop a systematic and unified approach to treat both effects in the context of gravitational scattering, but this is beyond the scope of the present paper and we leave it for future work.

In writing Eq. (4.98) we take into account the crossing relations Eq. (4.74). Note that $\sigma_3 = -stu$ for $u = -s-t$. In the expansion Eq. (4.98) $f_{i,j}$ are real. For parity-preserving theories $h_{k,j}$ and $g_{k,j}$ are real as well. In the formulas above β_{R^3} encodes the unique non-minimal correction to the three-point amplitude of gravitons as defined in Eq. (4.78). Similarly β_ϕ encodes the non-minimal coupling of a scalar to two gravitons. In parity-preserving theories these are real.

For completeness we take into account the possibility of non-minimal coupling to a massless scalar in the amplitude above with the three-point amplitude given in Eq. (4.78). Curiously the non-minimal correction to the three-point graviton amplitude and the non-minimal coupling to a massless scalar mix in the first term in the low-energy expansion of $h(s, u)$ Eq. (4.98). This point was discussed in detail in Ref. [331].

We list the explicit results for these functions obtained for the amplitudes considered in the present paper as an expansion in large mass in Eqs. Eq. (4.86), Eq. (4.89) and Eq. (4.91), as well as in Appendix 4.H. The exact form of the amplitudes is found in Appendix 4.F.

4.4.2 Unitarity constraints

Here we consider the constraints that arise from unitarity. Since the gravitational EFTs of interest are weakly coupled, we limit ourselves to perturbative unitarity as discussed for example in Refs. [140, 269]. It would be of course be very interesting to implement unitarity nonperturbatively along the lines of Refs. [341, 342]. In four dimensions this would also require understanding the constraints of unitarity at the level of IR-finite observables; see e.g. Refs. [343, 342] for a recent discussion. Luckily, for our purpose of investigating the leading-order corrections to the gravitational EFT these subtle but important issues are irrelevant. Here we primarily follow the discussion of Ref. [269] but modify it to account for differing helicity configurations.

To discuss the constraints coming from unitarity we note that the general incoming two-graviton state is a superposition of amplitudes with different helicities. In total there are four choices for the incoming and four choices for the outgoing states. We therefore consider the following matrix of possible amplitudes

$$
\begin{pmatrix}
\mathcal{M}_{(+,-,-,+)} & \mathcal{M}_{(+,-,-,-)} & \mathcal{M}_{(-,-,-,+)} & \mathcal{M}_{(-,-,-,-)} \\
\mathcal{M}_{(+,-,+,+)} & \mathcal{M}_{(+,-,+,-)} & \mathcal{M}_{(-,-,+,+)} & \mathcal{M}_{(-,-,+,-)} \\
\mathcal{M}_{(+,+,-,+)} & \mathcal{M}_{(+,+,-,-)} & \mathcal{M}_{(-,+,-,+)} & \mathcal{M}_{(-,+,-,-)} \\
\mathcal{M}_{(+,+,+,+)} & \mathcal{M}_{(+,+,+,-)} & \mathcal{M}_{(-,+,+,+)} & \mathcal{M}_{(-,+,+,-)}
\end{pmatrix},
\tag{4.100}
$$

where we labeled the helicities of the gravitons using an all-incoming convention.

Consider now scattering in the physical t-channel $14 \to 23$. To describe this situation we consider the center-of-mass frame and choose helicity spinors as follows [140, 269]

$$
\lambda_1 = t^{1/4} \begin{pmatrix} 1 \\ 0 \end{pmatrix}, \quad \lambda_4 = t^{1/4} \begin{pmatrix} 0 \\ 1 \end{pmatrix},
$$

$$
\lambda_2 = it^{1/4} \begin{pmatrix} \cos\frac{\theta}{2} \\ \sin\frac{\theta}{2} \end{pmatrix}, \quad \lambda_3 = it^{1/4} \begin{pmatrix} \sin\frac{\theta}{2} \\ -\cos\frac{\theta}{2} \end{pmatrix}.
\tag{4.101}
$$

Since we consider particles 1 and 4 to be incoming we take $\tilde{\lambda}_{1,4} = \lambda_{1,4}^*$. Particles 2 and 3 are outgoing, therefore $\tilde{\lambda}_{2,3} = -\lambda_{2,3}^*$. With this choice we get $t = \langle 14 \rangle [14]$, $s = \langle 12 \rangle [12] =$

$-t\sin^2\frac{\theta}{2}$, so that $\cos\theta = 1 + \frac{2s}{t}$. Evaluating the matrix (4.100) for this kinematics we obtain

$$
\mathcal{M}(s,t) \equiv \begin{pmatrix}
t^4 f(s,u) & s^2 t^2 u^2 g^*(s,u) & s^2 t^2 u^2 g^*(s,u) & h^*(s,u) \\
s^2 t^2 u^2 g(s,u) & u^4 f(s,t) & s^4 f(t,u) & s^2 t^2 u^2 g^*(s,u) \\
s^2 t^2 u^2 g(s,u) & s^4 f(t,u) & u^4 f(s,t) & s^2 t^2 u^2 g^*(s,u) \\
h(s,u) & s^2 t^2 u^2 g(s,u) & s^2 t^2 u^2 g(s,u) & t^4 f(s,u)
\end{pmatrix}. \tag{4.102}
$$

Unitarity restricts the form of the discontinuity of various amplitudes. We introduce the t-channel discontinuity as

$$
\text{Disc}_t \mathcal{M}(s,t) \equiv \frac{\mathcal{M}(s,t+i\epsilon) - \mathcal{M}(s,t-i\epsilon)}{2i}. \tag{4.103}
$$

Through the optical theorem or unitarity, the discontinuity Eq. (4.103) is related to the square of the $2 \to n$ amplitude where we insert a complete set of intermediate states. It is convenient to decompose intermediate states into the irreducible representation of the Poincare group, which are therefore labeled by the total energy $\sqrt{t}$, spin J and potentially other quantum numbers i. The simplest example is when we have an exchange by a single particle of mass $\sqrt{t}$ and spin J. In this case Eq. (4.103) produces the square of the corresponding three-point couplings multiplied by a kinematical polynomial.[12] A slightly more general situation is when we have an exchange by multiple particles of the same mass and spin. In this case the discontinuity produces Eq. (4.103) a sum over the products of the corresponding three-point couplings. Finally, we can also have a multi-particle state as an intermediate state of total energy $\sqrt{t}$ and spin J. It is convenient to think about it again as a single-particle state with the continuous label for the species (which corresponds to the distribution of the total energy among the constituent particles). The result is always the same: we can write Eq. Eq. (4.103) as a sum of kinematical polynomials multiplied by various *spectral densities* $\rho_J(t)$ which encode the sum over the products of couplings to the intermediate states of energy $\sqrt{t}$ and J in a given theory. What we just said is simply a restatement of the standard partial-wave expansion in a language which is perhaps slightly

---

[12]In the case of external scalars these are familiar Legendre polynomials. For spinning particles the analogous polynomials in $D = 4$ are Wigner d-functions, which are written explicitly below.

more intuitive. For a more complete and detailed derivation see Refs. [341, 342]. In this way we can write the discontinuity in terms of the spectral density. For example,

$$\mathrm{Disc}_t \mathcal{M}_{(+,-,-,+)}(s,t) = \sum_{J=0}^{\infty} \frac{1+(-1)^J}{2} \rho_J^{++}(t) d_{0,0}^J(x) \,. \tag{4.104}$$

Applying this to all helicity configurations in the matrix of amplitudes Eq. (4.102) we get

$$\mathrm{Disc}_t \mathcal{M}(s,t)$$

$$= \sum_{J=0}^{\infty} \frac{1+(-1)^J}{2} \begin{pmatrix} \rho_J^{++}(t) d_{0,0}^J(x) & 0 & 0 & \left[\tilde{\rho}_J^{++}(t)\right]^* d_{0,0}^J(x) \\ 0 & 0 & 0 & 0 \\ 0 & 0 & 0 & 0 \\ \tilde{\rho}_J^{++}(t) d_{0,0}^J(x) & 0 & 0 & \rho_J^{++}(t) d_{0,0}^J(x) \end{pmatrix}$$

$$+ \sum_{J=4}^{\infty} \begin{pmatrix} 0 & 0 & 0 & 0 \\ 0 & \rho_J^{+-}(t) d_{4,4}^J(x) & \rho_J^{+-}(t)(-1)^J d_{4,-4}^J(x) & 0 \\ 0 & \rho_J^{+-}(t)(-1)^J d_{4,-4}^J(x) & \rho_J^{+-}(t) d_{4,4}^J(x) & 0 \\ 0 & 0 & 0 & 0 \end{pmatrix}$$

$$+ \sum_{J=4}^{\infty} \frac{1+(-1)^J}{2} \begin{pmatrix} 0 & \left[\tilde{\rho}_J^{+-}(t)\right]^* d_{4,0}^J(x) & \left[\tilde{\rho}_J^{+-}(t)\right]^* d_{4,0}^J(x) & 0 \\ \tilde{\rho}_J^{+-}(t) d_{4,0}^J(x) & 0 & 0 & \left[\tilde{\rho}_J^{+-}(t)\right]^* d_{4,0}^J(x) \\ \tilde{\rho}_J^{+-}(t) d_{4,0}^J(x) & 0 & 0 & \left[\tilde{\rho}_J^{+-}(t)\right]^* d_{4,0}^J(x) \\ 0 & \tilde{\rho}_J^{+-}(t) d_{4,0}^J(x) & \tilde{\rho}_J^{+-}(t) d_{4,0}^J(x) & 0 \end{pmatrix} \,, $$

$$\tag{4.105}$$

where we introduced $x \equiv \cos\theta = 1 + \frac{2s}{t}$ and we used Wigner d-matrices $d_{\lambda,\lambda'}^J(x)$ which we list explicitly in Appendix 4.E. The formula above can be derived by explicitly analyzing the effect of an exchange by a particle, or equivalently an irreducible representation, of given mass $\sqrt{t}$ and spin J. The relevant three-point amplitudes are fixed up to a number and their products are encoded in the various spectral densities $\rho_J(m^2)$. The indices $++$ and $+-$ denote the helicities of the corresponding incoming gravitons.

To discuss dispersion relations we also need to understand the properties of the u-channel

discontinuity which is defined as

$$\text{Disc}_u\mathcal{M}(s,t) \equiv \frac{\mathcal{M}(s,-s-t-i\epsilon) - \mathcal{M}(s,-s-t+i\epsilon)}{2i}. \qquad (4.106)$$

By the same argument it takes the following form[13]

$$\text{Disc}_u\mathcal{M}(s,t)$$

$$= \sum_{J=0}^{\infty} \frac{1+(-1)^J}{2} \begin{pmatrix} 0 & 0 & 0 & \left[\tilde{\rho}_J^{++}(u)\right]^* d_{0,0}^J(\tilde{x}) \\ 0 & \rho_J^{++}(u)d_{0,0}^J(\tilde{x}) & 0 & 0 \\ 0 & 0 & \rho_J^{++}(u)d_{0,0}^J(\tilde{x}) & 0 \\ \tilde{\rho}_J^{++}(u)d_{0,0}^J(\tilde{x}) & 0 & 0 & 0 \end{pmatrix}$$

$$+ \sum_{J=4}^{\infty} \begin{pmatrix} \rho_J^{+-}(u)d_{4,4}^J(\tilde{x}) & 0 & 0 & 0 \\ 0 & 0 & \rho_J^{+-}(u)(-1)^J d_{4,-4}^J(\tilde{x}) & 0 \\ 0 & \rho_J^{+-}(u)(-1)^J d_{4,-4}^J(\tilde{x}) & 0 & 0 \\ 0 & 0 & 0 & \rho_J^{+-}(u)d_{4,4}^J(\tilde{x}) \end{pmatrix}$$

$$+ \sum_{J=4}^{\infty} \frac{1+(-1)^J}{2} \begin{pmatrix} 0 & \left[\tilde{\rho}_J^{+-}(u)\right]^* d_{4,0}^J(\tilde{x}) & \left[\tilde{\rho}_J^{+-}(u)\right]^* d_{4,0}^J(\tilde{x}) & 0 \\ \tilde{\rho}_J^{+-}(u)d_{4,0}^J(\tilde{x}) & 0 & 0 & \left[\tilde{\rho}_J^{+-}(u)\right]^* d_{4,0}^J(\tilde{x}) \\ \tilde{\rho}_J^{+-}(u)d_{4,0}^J(\tilde{x}) & 0 & 0 & \left[\tilde{\rho}_J^{+-}(u)\right]^* d_{4,0}^J(\tilde{x}) \\ 0 & \tilde{\rho}_J^{+-}(u)d_{4,0}^J(\tilde{x}) & \tilde{\rho}_J^{+-}(u)d_{4,0}^J(\tilde{x}) & 0 \end{pmatrix},$$

$$(4.107)$$

where $\tilde{x} = 1 + \frac{2s}{u}$.

The spectral densities that enter the unitarity relation are given in terms of the product of the couplings to the corresponding intermediate states. The diagonal terms being given by the absolute value square of the couplings are nonnegative

$$\rho_J^{++}(m^2) \geq 0, \quad \rho_J^{+-}(m^2) \geq 0. \qquad (4.108)$$

---

[13]We thank Alessandro Vichi for pointing out a typo in Eq. (4.107) of an earlier version of the paper.

The off-diagonal terms satisfy simple Cauchy-Schwartz inequalities[14]

$$|\tilde{\rho}_J^{+-}(m^2)|^2 \le \rho_J^{++}(m^2)\rho_J^{+-}(m^2), \quad |\tilde{\rho}_J^{++}(m^2)| \le \rho_J^{++}(m^2). \tag{4.109}$$

Below we discuss bounds on the possible form of the low-energy coefficients stemming from unitarity and growth of the amplitude at infinity. In particular, it is convenient for us to consider combinations of amplitudes that have nonnegative semi-definite discontinuities both in the t- and u-channel. We consider the following convenient choices that are sufficient for our purposes

$$\mathcal{M}_h(s,t) \equiv \begin{pmatrix} t^4 f(s,u) + u^4 f(s,t) - s^4 f(t,u) & h^*(s,u) \\ h(s,u) & t^4 f(s,u) + u^4 f(s,t) - s^4 f(t,u) \end{pmatrix}, \tag{4.110}$$

$$\mathcal{M}_g(s,t) \equiv \begin{pmatrix} t^4 f(s,u) + u^4 f(s,t) & 2s^2 t^2 u^2 g^*(s,u) \\ 2s^2 t^2 u^2 g(s,u) & t^4 f(s,u) + u^4 f(s,t) \end{pmatrix}. \tag{4.111}$$

These matrices are t–u crossing symmetric

$$\mathcal{M}_{h,g}(s,t) = \mathcal{M}_{h,g}(s,u). \tag{4.112}$$

Using the form of the discontinuity dictated by unitarity above together with the Cauchy-Schwartz inequalities Eq. (4.109) one can check that

$$\partial_s^n \mathrm{Disc}_t \mathcal{M}_{h,g}|_{s=0} = \partial_s^n \mathrm{Disc}_u \mathcal{M}_{h,g}|_{s=0} \succeq 0, \qquad n \ge 0, \tag{4.113}$$

where the notation '$\succeq 0$' means that the matrix is positive semi-definite.[15] We obtain these inequalities from the following properties of the Wigner d-matrices together with Eq. (4.109)

$$\partial_s^n d_{0,0}^J(x)|_{s=0} \ge 0, \tag{4.114}$$

$$\partial_s^n \left(d_{4,4}^J(x) - (-1)^J d_{4,-4}^J(x) \right)|_{s=0} \ge 0, \tag{4.115}$$

$$\partial_s^n \left(\rho_J^{++}(t) d_{0,0}^J(x) + \rho_J^{+-}(t) d_{4,4}^J(x) - 2|\tilde{\rho}_J^{+-}(t)| d_{4,0}^J(x) \right)|_{s=0} \ge 0, \tag{4.116}$$

---

[14]In terms of couplings to the intermediate state of energy $\sqrt{t}$ and spin J these inequalities simply state that $\left|\sum_i \lambda_{++i}\lambda_{+-i}^*\right|^2 \le (\sum_i |\lambda_{++i}|^2)(\sum_i |\lambda_{+-i}|^2)$ and $|\sum_i \lambda_{++i}^2| \le \sum_i |\lambda_{++i}|^2$ respectively.

[15]A hermitian $n \times n$ matrix M is called positive semi-definite if $z^* M z \ge 0$ for all $z \in \mathbb{C}^n$.

where $s = 0$ corresponds to $x = 1$ (see definition of x below Eq. (4.105)). The first property Eq. (4.114) is a well-known property of Legendre polynomials. We have not attempted to prove Eq. (4.115) and Eq. (4.116) that rely on the properties of the relevant $d^J_{\lambda,\lambda'}(x)$, however we checked them explicitly up to $J = 30$. We also checked using formulas from Appendix 4.E the conditions above for any J and $n = 0, 1, 2$; these are the cases that we consider below in more detail. For forward scattering a closely related discussion can be found in Ref. [281].

The matrices above admit simple eigenvectors in the parity-preserving case, where we have $g(s, u) = g^*(s, u)$ and $h(s, u) = h^*(s, u)$. In this case the matrices above have eigenvalues

$$\mathcal{M}_{h,\pm}(s, t) = u^4 f(s, t) + t^4 f(s, u) - s^4 f(t, u) \pm h(s, u),$$

$$\mathcal{M}_{g,\pm}(s, t) = u^4 f(s, t) + t^4 f(s, u) \pm 2s^2 t^2 u^2 g(s, u). \tag{4.117}$$

Unitarity Eq. (4.113) then becomes the statement about nonnegativity of the discontinuity of Eq. (4.117). In this case we can apply dispersion relations directly to the functions Eq. (4.117).

4.4.3 Causality

Causality and unitarity put constraints on the high-energy behavior of the amplitude. The corresponding bounds are well known in the case of gapped QFTs [344], but are on a less-rigorous footing in gravitational theories.

At tree level the gravitational amplitudes are expected to satisfy

$$\lim_{|t| \to \infty} |\mathcal{M}_{\text{tree}}(s, t)| \le t^2, \qquad s < 0. \tag{4.118}$$

This result is very intuitive but hard to establish rigorously. It naturally emerges from various considerations [241, 345, 346].

The situation is less clear nonperturbatively, however the simple qualitative picture of high-energy scattering in gravity together with unitarity and causality again imply that a similar bound exists. The bound is usually assumed to be

$$\lim_{|t| \to \infty} |\mathcal{M}_{\text{full}}(s, t)| < t^2, \qquad s < 0. \tag{4.119}$$

This can be used to write dispersion relations in $D \geq 5$ where the amplitudes are IR finite and make sense nonperturbatively. In $D = 4$ the situation is less clear due to the IR divergences, but presumably a similar bound exists for the IR safe observables. It is also possible to satisfy Eq. (4.119) at tree level but this requires an infinite number of particles of arbitrary high spin to be exchanged. A famous example of this type is given by the tree-level string amplitudes.

In this paper, we are interested in particular in the properties of the one-loop scattering amplitudes in $D = 4$. These do not have to satisfy Eq. (4.118) or Eq. (4.119), therefore we do not use them. Indeed, let us imagine that the bound Eq. (4.118) is saturated at tree-level. This corresponds to exchange of a particle of spin 2. When we go to one-loop we can exchange a pair of spin-2 particles and the resulting amplitude will grow like t^3. Therefore it is natural that the following bound holds at one loop

$$\lim_{|t| \to \infty} |\mathcal{M}_{1-\text{loop}}(s,t)| \leq t^3, \qquad s < 0. \tag{4.120}$$

The explicit amplitudes computed in the paper indeed satisfy Eq. (4.120). Below, in writing dispersion relations we assume the Regge bound to be as given in Eq. (4.120) and choose the number of subtractions accordingly. Note that since Eq. (4.120) is weaker than Eq. (4.118), bounds derived in this way apply both to the tree and one-loop amplitudes. They also apply to full nonperturbative amplitudes in $D \geq 5$.

It is a special feature of gravitational amplitudes that an infinite number of particles has to be exchanged at tree-level in order for the amplitudes to satisfy Eq. (4.118). This follows from the fact that such exchanges at tree-level correspond to non-minimal couplings, which are known to lead to violations of Eq. (4.118) [241, 277, 278]. The only exception to this rule is general relativity, which corresponds to the minimal self-coupling of the graviton.

The tree-level Regge growth bound Eq. (4.118) is the reason why it is so hard to construct tree-level gravitational amplitudes different from the ones of general relativity. This famous achievement of string theory leads to causal and unitarity amplitudes with infinitely many poles that corresponds to exchanges of infinitely many particles of arbitrarily large spin. In

fact, every such modification must contain strings [347].[16]

4.4.4 Dispersive sum rules

Given the gravitational amplitudes that satisfy unitarity and the Regge bounds we can consider various dispersion relations. One class of dispersion relations that we find useful recasts the vanishing of the (subtracted) amplitude in the Regge limit in terms of its discontinuity.

Such relations are known as superconvergence relations [278], or dispersive sum rules [280]. We follow the latter terminology and consider the following integrals

$$B_k^+(s) = \oint_\infty \frac{dt}{2\pi i} \mathcal{M}(s,t) \frac{1}{t} \frac{1}{(t(s+t))^k} = 0, \qquad k \geq 2, \qquad (4.121)$$

where the condition $k \geq 2$ originates from the Regge bound (4.120) and guarantees that the arc at infinity produces a vanishing contribution.

By deforming the contour we get the following formula

$$B_k^+(s) : \oint_{t_0} \frac{dt}{2\pi i} \mathcal{M}(s,t) \frac{1}{t} \frac{1}{(t(s+t))^k} \qquad (4.122)$$
$$= \int_{m_{gap}^2}^\infty \frac{dt}{\pi} \frac{1}{(t(s+t))^k} \left(\frac{1}{t} \mathrm{Disc}_t \mathcal{M}(s,t) + \frac{1}{s+t} \mathrm{Disc}_u \mathcal{M}(s,t) \right),$$

where the integrals are depicted in Fig. 4.7.

We evaluate the LHS of Eq. (4.122) using the low-energy expansion, and we use the RHS to establish some nontrivial properties that the coefficients of the low-energy expansion should satisfy. More precisely, we consider the expansion of (4.122) around $s = 0$.

A few comments are in order. Firstly, note that the minimal tree-level graviton-exchange term in $f(s,u) \sim \frac{1}{stu}$ does not contribute to the sum rules of interest here, $B_{k \geq 2}^+(s)$. In particular, we are able to expand the sum rules in powers of s. Assuming a more stringent Regge bound, $B_1^+(s)$ can be studied [271] and used to bound various coefficients in terms of G. We do not consider this sum rule in the present paper. Secondly, the non-minimal

---

[16]Curiously, as explained in some detail in Appendix 4.D, if we allow for accumulation points in the spectrum we can consider much simpler amplitude functions. These functions, however, contain an infinite number of particles of a given mass.
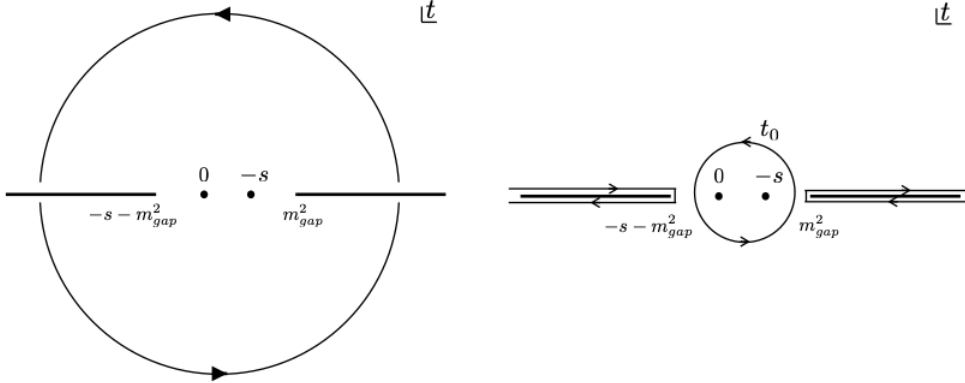
Figure 4.7: The vanishing of the arc integral at infinity on the left panel, cf. Eq. (4.121), can be restated as an equality of the integrals on the right panel (see Eq. (4.122).)

coupling β_{R^3} contributes to B_2^+ and we utilize this fact in Sect. 4.6.2 in order to bound β_{R^3} in terms of other EFT data.

4.4.5 The theory islands

What is the space of gravitational EFTs that admit a consistent UV completion? Answering this question nonperturbatively is a formidable task, but we can consider the simpler question of understanding perturbatively in G possible consistent UV completions of gravity. It is in this spirit that in this paper we focus on the leading-order-in-G correction to general relativity.

Imagine that we label all possible perturbatively consistent theories of gravity by an index i so that the four-graviton scattering amplitudes in a given theory are given by the matrix $\mathcal{M}_i$ (see Eq. (4.100)).[17] It is clear then that by taking a superposition of such amplitudes

---

[17]For simplicity we keep the index discrete, but of course it can be continuous, e.g. denoting the mass of

with non-negative coefficients we again get an amplitude that satisfies all the constraints discussed in the sections above

$$\mathcal{M}_{\text{theory}} = \sum_i c_i \mathcal{M}_i, \qquad c_i \geq 0. \tag{4.123}$$

By expanding such amplitudes at low energies, as in Sect. 4.4.1, we get a set of higher-derivative corrections. The low-energy Wilson coefficients then form a convex cone which we can think of as the *t*heory space,[18] which is generated by vectors $\mathcal{M}_i$.[19]

It has been recently established that causality, crossing and unitarity constrain Wilson coefficients both from above and from below [267, 268, 269, 270]. In the space of couplings formed by weakly-coupled theories it is thus natural to talk about *t*he theory island, namely the region spanned by known perturbative UV completions of gravity. By definition we have

$$\text{Theory island} \subseteq \text{EFThedron}, \tag{4.124}$$

where by the EFThedron we call the set of amplitudes satisfying the constraints reviewed in this section (in particular we only impose perturbative unitarity). It is interesting to ask to what extent we can populate the space of allowed couplings by known perturbative UV completions. Recall that by a perturbative UV completion we call an S-matrix that satisfies unitarity, causality and crossing perturbatively in Newton's constant G and for any process $m \to n$.

There are two classes of perturbative UV completions we consider here: tree-level corrected theories and one-loop corrected theories. In tree-level corrected theories the leading-order correction to general relativity enters at tree-level, in other words the higher-derivative corrections in the Lagrangian are suppressed by a new scale, e.g. string scale, which can be much lower than the Planck scale. Perturbative string theories are famous examples of this

---

the particle exchanged in the loop. It does not affect the discussion.

[18]A convex cone is a subset of vector space closed under linear combinations with positive coefficients.

[19]Nonperturbatively in G, Eq. (4.123) is not necessarily consistent since is can violate nonperturbative unitarity $|S_J| \leq 1$. Since we are interested in the leading-order correction in the regime when gravity is weakly coupled, this issue is irrelevant.

type. It is a well-known fact that gravitational amplitudes in string theory have a great degree of universality, as discussed recently in Ref. [339]. In Appendix 4.B we review the cases of superstring, heterotic and bosonic strings at tree level.[20] Alternatively, we can consider theories where the higher-derivative operators come with an extra power of G. The one-loop amplitudes computed in the present paper are precisely of this type. By choosing the mass spectrum and spins of the particles propagating in the loop we can get various amplitudes.

Combining these two examples we consider the following set of amplitudes in the present paper

$$\mathcal{M}^{\text{here}}_{\text{theory}} = c_{\text{(ss)}}\mathcal{M}^{\text{(ss)}}_{\text{tree}} + c_{\text{(hs)}}\mathcal{M}^{\text{(hs)}}_{\text{tree}} + c_{\text{(bs)}}\mathcal{M}^{\text{(bs)}}_{\text{tree}} + \sum_{S=0,\frac{1}{2},1,\frac{3}{2},2} c_S \mathcal{M}^{1-\text{loop}}_S . \qquad (4.125)$$

Obviously, we do not claim that this space is complete. Let us emphasize that in the analysis below we allow taking arbitrary superpositions of string amplitudes with various tensions as well as one-loop amplitudes with arbitrary choices of the masses and spins, $S \leq 2$, of particles circulating in the loop.

On the string side, for example we can consider the ϵ deformation of the superstring amplitude discussed in the conclusions of Ref. [269]. It is not clear however that these deformations can be promoted to fully consistent perturbative S-matrices. Moreover, we checked that adding this correction does not affect the theory island considered in the present paper in a noticeable way.

On the field-theory side we can consider gapped strongly-coupled theories of matter coupled to gravity. One interesting example is large-N QCD coupled to gravity [279]. In this case we expect the tree-level corrections due to non-minimally coupled glueballs and one-loop corrections due to minimally-coupled glueballs to both enter at the same order G^2. Finally, we do not discuss here amplitudes in models with extra dimensions [348, 349, 350]. Of course, it would be very interesting to extend our analysis to include these examples as well.

---

[20]Strictly speaking the bosonic string is not part of the theory space due to the presence of the tachyon in the spectrum, but it is useful to keep it to check various formulas.

In writing the contribution of matter we can imagine integrating out a multiple number of particles of given spin with various masses. For the constraints discussed below one can check that the effect of this freedom can be absorbed into rescaling of the coefficients c_S. In particular, the bounds that we describe below hold for any choice of masses and number of species for particles that we integrate out.

In the following sections we use these amplitudes to populate the theory island. Surprisingly, we find that

$$\text{Theory island} \ll \text{EFThedron}, \tag{4.126}$$

in a sense that should become clear below. In other words, the set of known weakly-coupled theories occupy a much smaller space in the space of couplings than is allowed by the general constraints coming from the analysis of $2 \to 2$ scattering. This is, of course, in accord with the ongoing landscape vs swampland debate but is also different from that. Indeed, the theory island as defined here does not guarantee the existence of the nonperturbative completion of gravity. We only study the consistency of the leading-order corrections to the Einstein-Hilbert theory perturbatively in G and already in this setting we seem to find a much smaller space of possibilities than follows from general constraints.

4.5 Deriving bounds: elastic amplitude

In this section we analyze bounds on the low-energy expansion of the elastic amplitude $f(s, u)$ using the techniques of Ref. [269] and [267, 268].[21] We focus on couplings of the same dimensionality and derive two-sided bounds on them by explicitly identifying the facets of the relevant polytopes and then taking their crossing-symmetric section.

As observed in Ref. [269], identifying the relevant boundaries are particularly simple in case of the one-channel dispersion relations when the polytopes in question are cyclic.[22]

---

[21]See also Ref. [351, 352, 352] for a closely related discussion.

[22]We refer the reader to Ref. [269] for the definition of this term.

In case of the two-channel dispersion relations the cyclicity property is lost. However, as Ref. [269] observed, a set of new boundaries that appear in this case involve low-spin partial waves and can be explicitly identified upon inspection. This is indeed what we observed in the examples below. To the best of our knowledge there is no proof that the list of boundaries obtained in this way is complete (and therefore that the bounds are optimal), and we do not attempt such a proof in the present work.

We will not attempt to relate couplings of different dimensionality to each other either. This problem was recently analyzed in Ref. [267, 268, 270] and the expected dimensional-analysis scaling of various couplings with order $\mathcal{O}(1)$ coefficients was rigorously established. It would be very interesting to apply these techniques to the gravitational amplitudes discussed here but we defer this to the future.

4.5.1   Strategy

We first briefly describe the basic strategy to derive bounds [269]. We consider the vector of low-energy couplings of the same dimensionality $\vec{F}$ which via dispersion relations is given by the sum of s- and u-channel partial waves

$$\vec{F} = \sum_J \left(c_{J,s} \vec{V}_{J,s} + c_{J,u} \vec{V}_{J,u} \right), \qquad c_{J,s}, c_{J,u} \geq 0\,. \tag{4.127}$$

In this formula $c_{J,s}$ and $c_{J,u}$ encode spectral densities discussed in Sect. 4.4.2 and $\vec{V}_{J,s}$, $\vec{V}_{J,u}$ are known functions related to partial waves—see e.g. Eq. (4.134) for the precise formula. However for the present discussion we can simply think of $\vec{V}_{J,s}$ and $\vec{V}_{J,u}$ as some abstract, given vectors and $c_{J,s}$, $c_{J,u}$ being non-negative numbers. We would like to characterize the space Eq. (4.127), which is a polytope. A convenient way to do it is by identifying its facets

$$\vec{F} \cdot \vec{W}_i \geq 0\,, \tag{4.128}$$

where $\vec{W}_i$ is a normal to a given facet. From Eq. (4.127) we see that all the facets are of the form[23]

$$(W_i)_{I_0} = \epsilon_{I_0 I_1 ... I_d} V_{a_1}^{I_1} ... V_{a_d}^{I_d} , \qquad (4.129)$$

where we assumed that the vectors $\vec{V}_a$ are $(d+1)$-dimensional and we contracted them using the $(d+1)$-dimensional ϵ-tensor.[24] The index a labels both spin and channel. Therefore, we can characterize the space Eq. (4.127) by a set of determinants $\langle F, a_1, ..., a_d \rangle \geq 0$. The task is then to find all $(a_1, ..., a_d)$, such that Eq. (4.128) holds. In general, this is a formidable task since the space of vectors in Eq. (4.127) is infinite dimensional.

As explained in Ref. [269], remarkably, the set of vectors $\vec{V}_{J,s}$ defines a cyclic polytope, which for us simply means that the set of its boundaries can be written down explicitly very easily. They essentially take the form of determinants built out of pairs of consecutive vectors in the sum over spins. For example, for $d = 4$ the relevant determinants take the form $(i, i+1, j, j+1)$ with $j > i$, where i and j label various spins in the sum Eq. (4.127).

The cyclicity property is lost when considering the sum of the s- and u-channel as in Eq. (4.127). By inspecting the resulting polytope Ref. [269] observed that it is "almost cyclic" in the sense that the only boundaries which are not of the type $(i, i+1, j, j+1)$ in the example considered above involve low-spin partial waves in Eq. (4.127) and can be found by direct inspection. This is what we also find and this is the strategy of finding bounds that we follow in this paper. In particular, we do not prove that the set of bounds found in this way is complete (even though we suspect it to be the case). It would be very interesting to rigorously demonstrate this.

After the allowed region Eq. (4.128) is identified we impose crossing symmetry, which is

---

[23]Strictly speaking, this statement is only true for finite-dimensional sums in Eq. (4.127). For infinite-dimensional sums we can also have limiting points. For us the limiting point is $J = \infty$. We find, however, that its existence does not play a role in the analysis in the following sections. The reason for it is that in practice we search for the boundaries Eq. (4.128) by first truncating the sum over spins up to some J_{max} and then extrapolating to $J_{max} = \infty$.

[24]Here d has nothing to do with the dimensionality of spacetime. Instead, it is the dimensionality of the relevant subset of the low-energy couplings that we would like to bound.

the subspace defined by linear relations between various components of the coupling vector $\vec{F}$. By taking the crossing-symmetric slice of the allowed space of couplings we get two-sided bounds on the low-energy Wilson coefficients.

4.5.2 Non crossing-symmetric dispersive representation of low-energy couplings

Consider again the double-minus amplitude

$$\mathcal{M}_4(1^-, 2^-, 3^+, 4^+) = (\langle 12 \rangle [34])^4 \, f(t, u) \,. \tag{4.130}$$

Following Ref. [269], we introduce the expansion[25]

$$f(t, u) = f(t, -s - t) = \left(\frac{\kappa}{2}\right)^2 \frac{1}{stu} + |\beta_{R^3}|^2 \frac{tu}{s} - |\beta_\phi|^2 \frac{1}{s} + \sum_{k \geq j \geq 0} a_{k,j} s^{k-j} t^j \,. \tag{4.131}$$

From Eq. (4.131) we see that for fixed k all $a_{k,j}$ have the same dimensionality. Crossing symmetry $f(t, u) = f(u, t)$ leads to linear relations among $a_{k,j}$ which will play an important role below.

Of course, in Eq. (4.98) we are expanding the same function, so the $f_{i,j}$ introduced there and the $a_{k,j}$ in Eq. (4.131) are all related to each other in a trivial fashion. We get for the first few coefficients

$$a_{0,0} = f_{0,0} \,, \qquad a_{1,0} = -f_{1,0} \,, \qquad a_{1,1} = 0 \,. \tag{4.132}$$

The vanishing of $a_{1,1}$ is a consequence of t–u crossing symmetry of $f(t, u)$ which is not manifest in Eq. (4.131).

The function of interest $f(t, u)$ admits a simple dispersive representation

$$f(t, -s - t) = \oint \frac{ds'}{2\pi i} \frac{f(t, -s' - t)}{s - s'} = \left(\frac{\kappa}{2}\right)^2 \frac{1}{stu} + |\beta_{R^3}|^2 \frac{tu}{s} - |\beta_\phi|^2 \frac{1}{s}$$

$$- \int_{m_{gap}^2}^\infty \frac{dm^2}{\pi} \left(\sum_{J=0}^\infty \frac{1 + (-1)^J}{2} \frac{\rho_J^{++}(m^2) d_{0,0}^J (1 + \frac{2t}{m^2})}{m^8} \frac{1}{s - m^2} \right.$$

$$\left. + \sum_{J=4}^\infty \frac{\rho_J^{+-}(m^2) d_{4,4}^J \left(1 + \frac{2t}{m^2}\right)}{(t + m^2)^4} \frac{1}{-s - t - m^2} \right) \,. \tag{4.133}$$

---

[25]Note that we performed an $s \leftrightarrow t$ transformation compared to Eq. (4.98).

In deriving (4.133) we used the Regge bound (4.120) to drop the arcs at infinity. When applied to Eq. (4.130) it implies that $|f(t, -s - t)| \leq 1/|s|$ at large s and fixed t. Indeed, this is the case for all the one-loop amplitudes that we consider.

An important feature of Eq. (4.133) is that crossing symmetry $f(t, u) = f(u, t)$ is not manifest (hence the title of this section). Therefore imposing it leads to interesting constraints. In fact, as we will see below it leads to two-sided bounds on the couplings.

By expanding Eq. (4.133) at small s and t we get the dispersive representations for the couplings $a_{k,j}$. They take the following form

$$a_{k,j} = \int_{m_{gap}^2}^{\infty} \frac{dm^2}{\pi} \frac{1}{(m^2)^{k+1}} \left(\sum_{J=0}^{\infty} \frac{1 + (-1)^J}{2} \frac{\rho_J^{++}(m^2)}{m^8} P_{++}^j(\mathcal{J}^2) + \sum_{J=4}^{\infty} \frac{\rho_J^{+-}(m^2)}{m^8} P_{+-}^{k,j}(\mathcal{J}^2) \right),$$

(4.134)

where we introduced the spin Casimir $\mathcal{J}^2 = J(J + 1)$. We call Eq. (4.134) the dispersive representation of low-energy couplings. We again emphasize that crossing symmetry leads to linear relations among $a_{k,j}$ which are not manifest in Eq. (4.134).

In the formula above we introduced polynomials $P_{++}^j(\mathcal{J}^2)$ and $P_{+-}^{k,j}(\mathcal{J}^2)$ which have the following properties[26]

$$P_{++}^0(\mathcal{J}^2) = 1, \qquad P_{+-}^{k,0}(\mathcal{J}^2) = (-1)^k,$$
$$P_{++}^1(\mathcal{J}^2) = \mathcal{J}^2, \qquad P_{+-}^{k,1}(\mathcal{J}^2) = (-1)^{k+1}(\mathcal{J}^2 - 20 - k),$$
$$\lim_{J \to \infty} P_{++}^j(\mathcal{J}^2) = \frac{1}{\Gamma(j+1)^2} \mathcal{J}^{2j} + \dots, \qquad \lim_{J \to \infty} P_{+-}^{k,j}(\mathcal{J}^2) = \frac{(-1)^{k+j}}{\Gamma(j+1)^2} \mathcal{J}^{2j} + \dots. \quad (4.135)$$

Based on the formulas above we see that couplings $a_{k,j}$ written in Eq. (4.134) roughly probe the k'th moment of the spectral density with respect to m^2 and $(2j)$'th moment with respect to spin. In particular, we expect that higher-j coefficients to be more sensitive to higher-spin spectral densities and higher-k couplings to have the large $\frac{m^2}{m_{gap}^2}$ region more suppressed. This is indeed what we will find in the explicit examples below.

---

[26]In the ++ channel the closed-form expression takes the form $P_{++}^j(\mathcal{J}^2) = \frac{1}{\Gamma(j+1)^2} \prod_{n=1}^{j}(\mathcal{J}^2 - n(n-1))$.

Crossing symmetry leads to the set of sum rules which were dubbed null constraints in Ref. [268]. Effectively, they express the low-spin partial-wave data in terms of the higher-spin data. Consider for example the relation $a_{1,1} = 0$, listed in Eq. (4.132). Using the formulas above we can write it as follows

$$\int_{m_{\text{gap}}^2}^{\infty} \frac{dm^2}{(m^2)^2} \frac{\rho_4^{+-}(m^2)}{m^8} =$$
$$\int_{m_{\text{gap}}^2}^{\infty} \frac{dm^2}{(m^2)^2} \left(\sum_{J=2}^{\infty} \frac{1+(-1)^J}{2} \frac{\rho_J^{++}(m^2)}{m^8} \mathcal{J}^2 + \sum_{J=5}^{\infty} \frac{\rho_J^{+-}(m^2)}{m^8} (\mathcal{J}^2 - 21) \right), \qquad (4.136)$$

where all the terms in the RHS of Eq. (4.136) are non-negative. In other words, crossing symmetry allows us to express the moment of $\rho_4^{+-}(m^2)$ in terms of all other spectral densities.

Let us next describe the first few bounds for $k \leq 6$. We do not attempt to derive the bounds across the couplings of different dimensionalities as it was done in Ref. [267, 268, 270, 271]. Instead we focus on the geometry of couplings of the same dimensionality as was studied in Ref. [269]. For $k = 1, 3, 5$ we do not get any nontrivial bounds. For even k the results are presented below.

k = 0:

We first start with $k = 0$. From (4.133) it immediately follows that

$$a_{0,0} \geq 0. \qquad (4.137)$$

Moreover, we have

$$a_{k,0} = \frac{1}{\pi} \int_{m_{\text{gap}}^2}^{\infty} \frac{dm^2}{m^{2k+10}} \left(\sum_{J=0}^{\infty} \frac{1+(-1)^J}{2} \rho_J^{++}(m^2) + (-1)^k \sum_{J=4}^{\infty} \rho_J^{+-}(m^2) \right). \qquad (4.138)$$

This immediately implies that $a_{k,0}$ for even k can be interpreted as even moments μ_k

$$\mu_k \equiv \frac{1}{\pi} \int_{m_{\text{gap}}^2}^{\infty} \frac{dm^2}{m^{2k+10}} \left(\sum_{J=0}^{\infty} \frac{1+(-1)^J}{2} \rho_J^{++}(m^2) + \sum_{J=4}^{\infty} \rho_J^{+-}(m^2) \right). \qquad (4.139)$$

As a result the bounds of Ref. [353] apply. For odd k, we obviously have $|a_k| \leq \mu_k$.

k = 2:

Next consider $k = 2$. Here the couplings of the same dimensionality are $\mathbf{a}_2 = (a_{2,0}, a_{2,1}, a_{2,2})$. One obvious constraint is

$$a_{2,0} \geq 0 \,. \tag{4.140}$$

On top of that we get the following list of constraints which specify the boundary of the region of allowed couplings,[27]

$$\{\langle \mathbf{a}_2, i_s, i_s + 2 \rangle_{i_s \geq 2} \,, \qquad \langle \mathbf{a}_2, (i_u + 1)^{(2)}, i_u^{(2)} \rangle_{i_u \geq 4} \,, \qquad \langle \mathbf{a}_2, 4_u^{(2)}, 2_s \rangle\} \geq 0 \,. \tag{4.141}$$

Here we follow the notation of Ref. [269], which is defined as

$$\langle \mathbf{a}_2, i, j \rangle \equiv \det \begin{pmatrix} a_{2,0} & v_{i,0} & v_{j,0} \\ a_{2,1} & v_{i,1} & v_{j,1} \\ a_{2,2} & v_{i,2} & v_{j,2} \end{pmatrix} \,, \tag{4.142}$$

where we also define the following vectors

$$v_{J,m}^{(s)} = (J_s)_m \equiv \frac{1}{m!} \partial_t^m d_J^{0,0}(1 + 2t)|_{t=0} \,, \tag{4.143}$$

$$v_{J,k,m}^{(u)} = (J_u^{(k)})_m \equiv \frac{1}{m!} \partial_t^m \frac{1}{(k-m)!} \partial_s^{k-m} \frac{1}{(1+s+t)} \frac{d_J^{4,4}(1+2t)}{(1+t)^4}|_{s,t=0} \,, \tag{4.144}$$

where in the formula above we set the arbitrary mass scale $m^2 = 1$ since it leads to trivial overall rescaling of the vectors that enter into the determinant Eq. (4.142) and as such does not affect the positivity bounds Eq. (4.141). Note that the vector $v_{i,k}^{(u)}$ depends on the order k of the corrections that we are studying, which we denote by $i_u^{(k)}$. For example, to evaluate (4.141) we should set $k = 2$ in Eq. (4.144). The constraints Eq. (4.141) have an intuitive explanation. By plugging the dispersive representation of the couplings into the determinant $\langle \mathbf{a}_2, i, j \rangle$ we get a sum over partial waves where the coefficients of partial wave i and j are zero. The plane $\langle \mathbf{a}_2, i, j \rangle$ then separates the region in the coupling space where these coefficients are positive and negative.

---

[27]The constraint Eq. (4.140) can be understood as arising from the limiting point when i_s or $i_u \to \infty$.

130
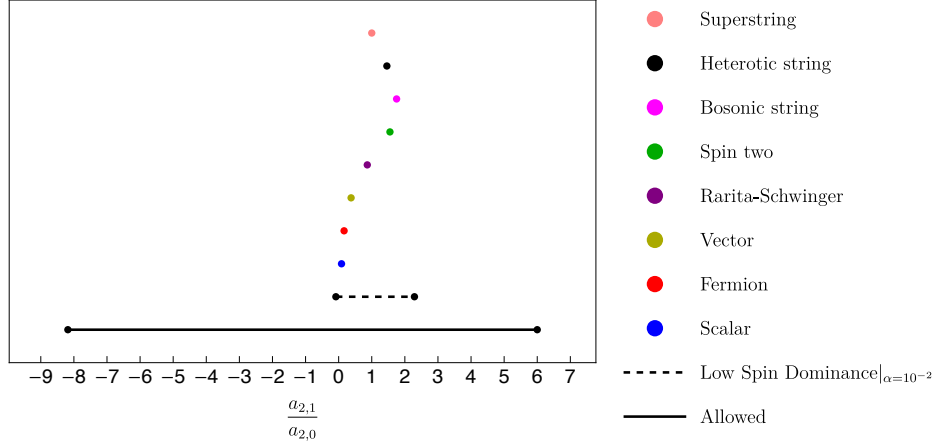
Figure 4.8: The allowed region for $\frac{a_{2,1}}{a_{2,0}}$ given by Eq. (4.146) is depicted in black. The explicit amplitudes that emerge from integrating out the one-loop matter or tree-level string theories are depicted in various colors. Assuming LSD in the form Eq. (4.152) with $\alpha = 10^2$ one can derive stronger bounds which we depict by the dashed line.

We see that Eq. (4.141) involves cyclic constraints from the s-channel $\langle \mathbf{a}_2, i_s, i_s + 2 \rangle_{i_s \geq 2}$, similarly from the u-channel $\langle \mathbf{a}_2, (i_u+1)^{(2)}, i_u^{(2)} \rangle_{i_u \geq 4}$, as well as a mixed constraint $\langle \mathbf{a}_2, 4_u^{(2)}, 2_s \rangle$ that involves low-spin partial waves. This phenomenon observed in Ref. [269] continues to hold for higher k as well. It allows us to easily identify the set of conditions that carve out the region of allowed couplings analytically rather straightforwardly by inspecting the low-spin boundaries. Of course, in practice we only look for possible boundaries up to some finite spin $J_{\max}$ and assume that the observed pattern continues all the way to $J_{\max} = \infty$.

In deriving the bounds above we did not impose crossing symmetry. At the level $k = 2$ we are working it implies that

$$\text{Crossing}: \quad a_{2,1} = a_{2,2}. \tag{4.145}$$

Taking the crossing-symmetric slice of the constraints Eq. (4.141) gives the two-sided bound on the Wilson coefficients

$$-\frac{90}{11} \leq \frac{a_{2,1}}{a_{2,0}} = \frac{a_{2,2}}{a_{2,0}} \leq 6. \tag{4.146}$$

It is very striking that for the explicit UV completions studied here we find a much narrow window of possibilities that we depict in Fig. 4.8. We now try to understand the origin of

131

this fact. To do this it will be useful to use the null constraint $a_{2,1} - a_{2,2} = 0$ to derive a bound similar to Eq. (4.146). By adding the null constraint to the dispersive representations for $a_{2,1}$ and $a_{2,2}$ it is straightforward to show that

$$-\frac{108}{13} \frac{\langle \rho_5^{+-} \rangle_2}{\langle \rho_0^{++} \rangle_2 + \langle \rho_4^{+-} \rangle_2 + \langle \rho_5^{+-} \rangle_2} \leq \frac{a_{2,1}}{a_{2,0}} = \frac{a_{2,2}}{a_{2,0}} \leq \frac{6\langle \rho_2^{++} \rangle_2 + \frac{16}{7}\langle \rho_4^{+-} \rangle_2}{\langle \rho_0^{++} \rangle_2 + \langle \rho_4^{+-} \rangle_2 + \langle \rho_2^{++} \rangle_2}, \qquad (4.147)$$

where we introduced $\langle \ldots \rangle$ for the relevant integrals over intermediate energies m^2

$$\langle \rho_J \rangle_k \equiv \frac{1}{\pi} \int_{m_{gap}^2}^{\infty} \frac{dm^2}{m^{2k+10}} \rho_J(m^2) \,. \qquad (4.148)$$

To derive the upper bound in Eq. (4.147) we used the dispersive representation for $a_{2,1} - \frac{2}{7}(a_{2,2} - a_{2,1})$. To derive the lower bound we considered $a_{2,1} + \frac{4}{13}(a_{2,2} - a_{2,1})$.

The bound Eq. (4.147) is rigorous. Its advantage however is that it only contains low-spin spectral densities. By adding the null constraint $a_{2,1} - a_{2,2} = 0$ with an appropriate coefficient we made sure that all the higher-spin contributions are sign-definite and the bound Eq. (4.147) then follows. It is clear then how can we come close to the saturation of the bounds Eq. (4.146). The upper bound saturation requires that $\langle \rho_2^{++} \rangle_2$ is dominant, whereas the lower-bound saturation requires that $\langle \rho_5^{+-} \rangle_2$ dominates. Note that each of these is not the minimal spin that appears in the corresponding channel, which are $\langle \rho_0^{++} \rangle_2$ and $\langle \rho_4^{+-} \rangle_2$ correspondingly.

This is not what happens in the known physical theories as we will show in more detail. In the examples that we analyze in this paper the higher-spin contributions to the spectral densities are suppressed compared to the minimal spin ones. The fact that at large spin the spectral densities decay exponentially in spin is something familiar from the fact that the scattering is local in the impact parameter space. Analyzing the concrete examples we see that this hierarchy continues all the way to minimal spin. We call this phenomenon *low-spin dominance* (LSD) of partial wave and mathematically we can express it as follows:

$$\text{Low-spin dominance (weak)}: \quad \langle \rho_4^{+-} \rangle_k \geq \langle \rho_{J>4}^{+-} \rangle_k, \quad \langle \rho_0^{++} \rangle_k \geq \langle \rho_{J>0}^{++} \rangle_k \,. \qquad (4.149)$$

In fact, Eq. (4.149) is very conservative and in the explicit examples the suppression of higher-spin partial waves is much stronger than Eq. (4.149). Nevertheless, already using

Eqs. (4.149) and (4.147) we can strengthen the bound Eq. (4.146) to obtain

$$(4.147) + (4.149): \quad -\frac{54}{13} \leq \frac{a_{2,1}}{a_{2,0}} = \frac{a_{2,2}}{a_{2,0}} \leq 3. \tag{4.150}$$

We clarify that here we derived Eq. (4.150) to illustrate the point that LSD implies stronger bounds. We have not tried to find the optimal bound that follows from Eq. (4.149) and dispersive representations of the couplings. It would be interesting to study this more systematically.

It is also instructive to see what happens if we assume LSD in the strong form

$$\text{Low-spin dominance (strong):} \quad \langle \rho_4^{+-} \rangle_k \gg \langle \rho_{J>4}^{+-} \rangle_k, \quad \langle \rho_0^{++} \rangle_k \gg \langle \rho_{J>0}^{++} \rangle_k. \tag{4.151}$$

We will discuss in more detail the expected form of the hierarchy below in the section dedicated to spectral densities, but for now it is sufficient to say that we will find that Eq. (4.151) correctly captures the region occupied by the known theories. To make Eq. (4.151) more precise let us introduce its quantitative version

$$\text{Low-spin dominance (α-factor):} \quad \langle \rho_4^{+-} \rangle_k \geq \alpha \langle \rho_{J>4}^{+-} \rangle_k, \quad \langle \rho_0^{++} \rangle_k \geq \alpha \langle \rho_{J>0}^{++} \rangle_k. \tag{4.152}$$

For illustrating bounds, below we choose for concreteness $\alpha = 10^2$. This choice is not accidental as the perturbative examples considered in this paper, tree-level string amplitudes and one-loop matter amplitudes, happen to be of this type.[28]

Let us now consider the bounds coming from Eq. (4.147) with the additional assumption of $\alpha = 10^2$ LSD Eq. (4.152). In this way we obtain

$$(4.147) + (4.152)|_{\alpha=10^2}: \quad -0.083 \leq \frac{a_{2,1}}{a_{2,0}} = \frac{a_{2,2}}{a_{2,0}} \leq 2.286. \tag{4.153}$$

It is also interesting to consider what happens if we consider $\alpha \to \infty$. In this case one can again use the trick of adding a null constraint $(a_{2,2} - a_{2,1})$ with some non-zero coefficient to dispersive representation of the couplings to show that

$$\text{LSD}_{\alpha\to\infty}: \quad 0 \leq \frac{a_{2,1}}{a_{2,0}} = \frac{a_{2,2}}{a_{2,0}} \leq 2. \tag{4.154}$$

---

[28] One exception is the heterotic string amplitude where we have $\langle \rho_2^{++} \rangle_k \sim \frac{1}{10} \langle \rho_0^{++} \rangle_k$.

Remarkably, we find that the region occupied by known theories in Fig. 4.8 lies inside Eq. (4.153) and even Eq. (4.154). We will see below that the phenomenon of the data being well explained by the strong version of LSD continues for higher k's as well.

k = 4:

For $k = 4$ we first consider a subset of couplings $\hat{\mathbf{a}}_4 = (a_{4,0}, a_{4,1}, a_{4,2})$. From the dispersive representation of the couplings it immediately follows that

$$a_{4,0} \geq 0 \,. \tag{4.155}$$

Analyzing the sums over the partial waves we get the following list of constraints[29]

$$\left\{ \langle \hat{\mathbf{a}}_2, i_s, i_s + 2 \rangle_{i_s \geq 2} \,, \quad \langle \hat{\mathbf{a}}_4, i_u^{(4)} + 1, i_u^{(4)} \rangle_{i_u \geq 5} \,, \quad \langle \hat{\mathbf{a}}_4, 5_u^{(4)}, 2_s \rangle \right\} \geq 0 \,. \tag{4.156}$$

These include the usual cyclic constraints, as well as an extra fixed constraint. We plot the allowed region in the as shaded (green) in Fig. 4.9. A characteristic feature of the allowed region is that it is unbounded.

In deriving the bounds above we have not used crossing symmetry which leads to improved two-sided bounds. To do that we can consider a complete set of couplings at $k = 4$, namely $\mathbf{a}_4 = (a_{4,0}, a_{4,1}, a_{4,2}, a_{4,3}, a_{4,4})$. It is then straightforward to check by inspection that the following set of constraints define the boundary region in the space of couplings:

$$\begin{aligned}
\bigl\{ &\langle \mathbf{a}_4, i_s, i_s + 2, j_s, j_s + 2 \rangle_{j > i \geq 2} \,, \quad \langle \mathbf{a}_4, i_u^{(4)}, i_u^{(4)} + 1, j_u^{(4)}, j_u^{(4)} + 1 \rangle_{j > i \geq 5} \,, \\
&\langle \mathbf{a}_4, i_s, i_s + 2, j_u^{(4)} + 1, j_u^{(4)} \rangle_{i \geq 4, j \geq 5} \,, \quad \langle \mathbf{a}_4, 2_s, 4_s, j_u^{(4)} + 1, j_u^{(4)} \rangle_{j \geq 7} \,, \\
&\langle 2_s, \mathbf{a}_4, i_s, i_s + 2, 5_u^{(4)} \rangle_{i \geq 4} \,, \quad \langle 5_u^{(4)}, \mathbf{a}_4, j_u^{(4)}, j_u^{(4)} + 1, 2_s \rangle_{j \geq 7} \,, \\
&\langle \mathbf{a}_4, 4_u^{(4)}, 5_u^{(4)}, 6_u^{(4)}, 7_u^{(4)} \rangle \,, \quad \langle \mathbf{a}_4, 2_s, 4_s, 4_u^{(4)}, 5_u^{(4)} \rangle, \langle \mathbf{a}_4, 2_s, 4_s, 7_u^{(4)}, 4_u^{(4)} \rangle \,, \\
&\langle \mathbf{a}_4, 4_u^{(4)}, 5_u^{(4)}, 7_u^{(4)}, 2_s \rangle \,, \langle 4_u^{(4)}, \mathbf{a}_4, 5_u^{(4)}, 6_u^{(4)}, 4_s \rangle, \langle 4_u^{(4)}, \mathbf{a}_4, 6_u^{(4)}, 7_u^{(4)}, 4_s \rangle \bigr\} \geq 0 \,.
\end{aligned} \tag{4.157}$$

It is easy to recover the previous constraints Eq. (4.156) from Eq. (4.157) by taking some of the spins to infinity. For example $\lim_{i_s \to \infty} \langle 2_s, \mathbf{a}_4, i_s, i_s + 2, 5_u^{(4)} \rangle_{i \geq 4} \geq 0$ reduces to $\langle \hat{\mathbf{a}}_4, 5_u^{(4)}, 2_s \rangle \geq 0$.

---

[29]By taking i_s or $i_u \to \infty$ limit in Eq. (4.156) we recover the simple bound Eq. (4.155).

A somewhat new feature of this case compared to the ones considered above that mixed $s-u$ channel boundaries come in infinite families. However, these families are again either cyclic, as in $\langle \mathbf{a}_4, i_s, i_s+2, j_u^{(4)}+1, j_u^{(4)} \rangle_{i \geq 4, j \geq 5}$ or involve low-spin partial wave only and therefore easily identifiable. We find it quite remarkable that the allowed region can be found analytically!

We then consider the section of this region by the crossing symmetry relations that take the form

$$\text{Crossing}: \quad a_{4,3} = 2(a_{4,2} - a_{4,1}), \quad a_{4,4} = a_{4,2} - a_{4,1}. \tag{4.158}$$

As a result we get the region of allowed couplings depicted in red in Fig. 4.9. To generate the plot we considered bounds Eq. (4.157) where we truncated the maximal spin to $i_{max}, j_{max}, k_{max} = 20$. We also checked explicitly that the all determinants obtained in this way are non-negative given dispersive representation for the couplings truncated to $J_{max} = 200$.

The bounds coming from imposing Eq. (4.157) together with crossing symmetry Eq. (4.158) are two-sided, both from above and from below. The theory island occupied by the known theories forms a tiny black slit inside the allowed region.

As we did for $k = 2$ we can again understand the structure of the island using the idea of LSD. To this extent we can use the null constraints coming from crossing Eq. (4.158) to derive the following rigorous bounds

$$-\frac{7.01\langle\rho_5^{+-}\rangle_4 + 20.18\langle\rho_6^{+-}\rangle_4}{\langle\rho_0^{++}\rangle_4 + \langle\rho_4^{+-}\rangle_4 + \langle\rho_5^{+-}\rangle_4 + \langle\rho_6^{+-}\rangle_4} \leq \frac{a_{4,1}}{a_{4,0}} \leq \frac{6\langle\rho_2^{++}\rangle_4 + 20\langle\rho_4^{++}\rangle_4 + 4.01\langle\rho_4^{+-}\rangle_4}{\langle\rho_0^{++}\rangle_4 + \langle\rho_4^{+-}\rangle_4 + \langle\rho_2^{++}\rangle_4 + \langle\rho_4^{++}\rangle_4},$$
$$\tag{4.159}$$

$$-\frac{20.16\langle\rho_5^{+-}\rangle_4}{\langle\rho_0^{++}\rangle_4 + \langle\rho_4^{+-}\rangle_4 + \langle\rho_5^{+-}\rangle_4 + \langle\rho_6^{+-}\rangle_4} \leq \frac{a_{4,2}}{a_{4,0}}$$
$$\leq \frac{6\langle\rho_2^{++}\rangle_4 + 90\langle\rho_4^{++}\rangle_4 + 6.43\langle\rho_4^{+-}\rangle_4 + 15.32\langle\rho_6^{+-}\rangle_4}{\langle\rho_0^{++}\rangle_4 + \langle\rho_4^{+-}\rangle_4 + \langle\rho_2^{++}\rangle_4 + \langle\rho_4^{++}\rangle_4 + \langle\rho_6^{+-}\rangle_4}. \tag{4.160}$$

Again we see that the corners of the red regions in Fig. 4.9 can be obtained from Eq. (4.159) by assuming that the sub-leading spins in the corresponding channels are dominant. This is not what happens in the physical theories and again assuming weak LSD Eq. (4.149) we can get a tighter bounds in which physical theories reside. In practice, we see that physical
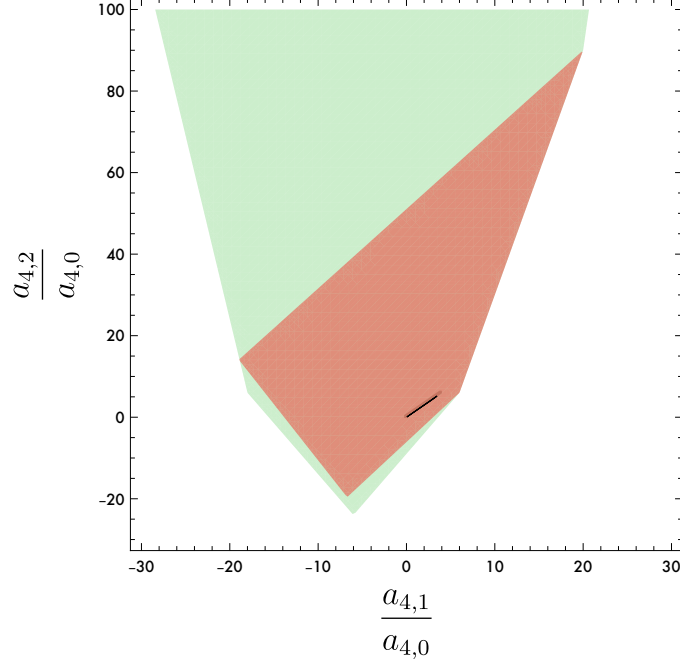
Figure 4.9: The allowed region for $(\frac{a_{4,1}}{a_{4,0}}, \frac{a_{4,2}}{a_{4,0}})$. The lightly shaded (green) region corresponds to the bounds Eq. (4.156). The darkly shaded (red) region corresponds to the bounds Eq. (4.157). The black theory island (which is so narrow that on this scale it looks like a line segment) is the region covered by known amplitudes. The small gray-shaded region that surrounds the black theory island corresponds to the LSD $\alpha = 10^2$ bounds.

theories occupy even smaller region which can be understood using the strong version of LSD Eq. (4.151).

A striking feature of Fig. 4.10 is that the known theories align closely with the straight line with the slope $3/2$. To understand this we can derive the bound analogous to Eq. (4.159) for the difference $a_{4,2} - \frac{3}{2}a_{4,1}$. It takes the following form

$$-\frac{3\langle\rho_2^{++}\rangle_4 + 15\langle\rho_5^{+-}\rangle_4}{\langle\rho_0^{++}\rangle_4 + \langle\rho_4^{+-}\rangle_4 + \langle\rho_2^{++}\rangle_4 + \langle\rho_5^{+-}\rangle_4} \leq \frac{a_{4,2} - \frac{3}{2}a_{4,1}}{a_{4,0}} \leq$$
$$\frac{60\langle\rho_4^{++}\rangle_4 + 0.47\langle\rho_4^{+-}\rangle_4 + 45.58\langle\rho_6^{+-}\rangle_4}{\langle\rho_0^{++}\rangle_4 + \langle\rho_4^{+-}\rangle_4 + \langle\rho_4^{++}\rangle_4 + \langle\rho_6^{+-}\rangle_4} . \quad (4.161)$$

We emphasize that at this point the bound Eq. (4.161) is rigorous and no additional assumptions have been made. To derive an upper bound we have considered the dispersive representation for $a_{4,2} - \frac{3}{2}a_{4,1} + \frac{1687}{7205}(a_{4,3} - 2a_{4,4}) + \frac{411}{524}(a_{4,3} - 2(a_{4,2} - a_{4,1}))$, where we made use of crossing Eq. (4.158). The lower bound follows directly from the dispersive representation
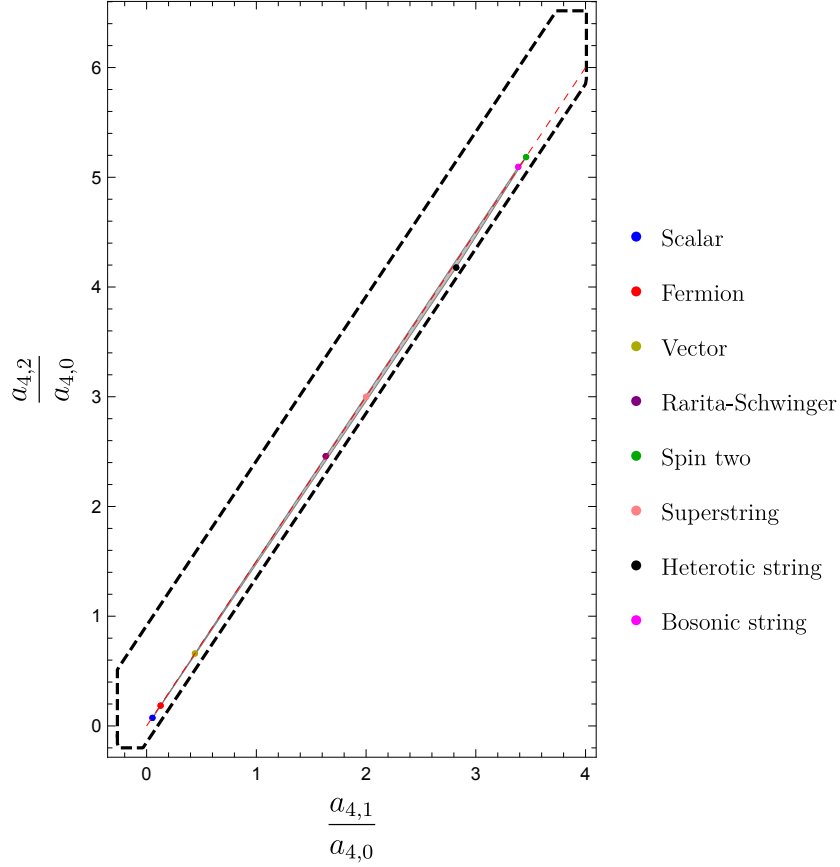
Figure 4.10: A scaled version of the theory island from Fig. 4.9. The dashed black line bounds the region which is found from Eqs. (4.159) and (4.161) using the LSD assumption Eq. (4.152) with $\alpha = 10^2$. The dashed red line $a_{4,2} = \frac{3}{2}a_{4,1}$ corresponds to $\alpha = \infty$ bound Eq. (4.163). Remarkably, all known theories lie in this small region where they populate a small region around the $\alpha = \infty$ curve.

of $a_{4,2} - \frac{3}{2}a_{4,1}$.

To make use of it, we can now assume $\alpha = 10^2$ LSD and apply it to the bounds Eq. (4.159) and Eq. (4.161). In this way we get

$$(4.159) + (4.160) + (4.161) + \mathrm{LSD}_{\alpha=10^2} : \quad -0.27 \le \frac{a_{4,1}}{a_{4,0}} \le 4.01,$$

$$-0.20 \le \frac{a_{4,2}}{a_{4,0}} \le 6.52,$$

$$-0.15 \le \frac{a_{4,2} - \frac{3}{2}a_{4,1}}{a_{4,0}} \le 0.92. \qquad (4.162)$$

We plot the result in Fig. 4.10 and again observe that the known examples neatly land in the predicted region. Moreover, it is straightforward to see that if we increase α the bound Eq. (4.161) becomes not optimal and instead we get

$$\mathrm{LSD}_{\alpha\to\infty} : \quad \frac{a_{4,2} - \frac{3}{2}a_{4,1}}{a_{4,0}} = 0, \quad 0 \le \frac{a_{4,1}}{a_{4,0}} \le 4, \quad 0 \le \frac{a_{4,2}}{a_{4,0}} \le 6. \qquad (4.163)$$

which is the line along which our explicit examples cluster. Intuitively, this result can be understood as follows: We write down explicitly the dispersive representation for the couplings $a_{4,i}$,

$$a_{4,0} = \int_{m_{\mathrm{gap}}^2}^{\infty} \frac{dm^2}{\pi} \frac{\rho_{++0}(m^2)}{(m^2)^9} + \int_{m_{\mathrm{gap}}^2}^{\infty} \frac{dm^2}{\pi} \frac{\rho_{+-4}(m^2)}{(m^2)^9} + \mathrm{h}igher\ spin\,,$$

$$a_{4,1} = 4 \int_{m_{\mathrm{gap}}^2}^{\infty} \frac{dm^2}{\pi} \frac{\rho_{+-4}(m^2)}{(m^2)^9} + \mathrm{h}igher\ spin\,,$$

$$a_{4,2} = 6 \int_{m_{\mathrm{gap}}^2}^{\infty} \frac{dm^2}{\pi} \frac{\rho_{+-4}(m^2)}{(m^2)^9} + \mathrm{h}igher\ spin\,, \qquad (4.164)$$

where 'higher spin' denotes infinitely many partial-wave contributions. Suppose that the lowest-spin partial waves in each channel dominates. Note that the leading spin $J = 0$ contribution in the ρ_{++J} channel drops out from $a_{4,1}$ and $a_{4,2}$. Notice that if we set the 'higher-spin' terms to 0 in the formulas above we get the region Eq. (4.163). A priori it is not clear that this follows from sending $\alpha \to \infty$ in Eq. (4.152) since we still have infinitely many spins that can potentially compensate for the smallness of $1/\alpha$. Crossing symmetry, however, guarantees that it is indeed the case and higher-spin contributions cannot compensate for

smallness of $1/\alpha$ as can be seen from the explicit analysis using the finite number of partial-wave bounds similar to Eq. (4.161).

Note that there are two distinct ways in which points can be close to the straight line in Fig. 4.10. First, as explained above by assuming the strong version of LSD in $a_{4,1}$ and $a_{4,2}$. Another mechanism is to have $a_{4,0} \gg a_{4,1}, a_{4,2}$ which happens when the contribution of ρ_{++0} to $a_{4,0}$ dominates over the partial waves that enter to $a_{4,1}$ and $a_{4,2}$. In this case the points appear very close to the origin on the $\left(\frac{a_{4,1}}{a_{4,0}}, \frac{a_{4,2}}{a_{4,0}}\right)$ plot and the slope defined by the ratio $\frac{a_{4,2}}{a_{4,1}}$ is not directly visible, nor does it need to be $\frac{3}{2}$. In fact, $a_{4,1}$ and $a_{4,2}$ have nontrivial higher-spin corrections in Eq. (4.164), i.e. ρ_2^{++} is sizable compared to ρ_4^{+-} and contributes ruining the $3/2$ ratio for $\frac{a_{4,2}}{a_{4,1}}$. This is precisely what happens for the scalar and fermion contributions in Fig. 4.10. In this case, by looking at Fig. 4.10 it is not apparent that Eq. (4.164) is not an accurate description of these points since they are close to the origin, which is on the line. When this happens the simple model of dropping higher-spin contributions in Eq. (4.164) is too crude. For example, consider the one-loop massive scalar amplitude which lies very close to the origin in Fig. 4.10. In this case to accurately capture $a_{4,1}$ we also need to include $\rho_2^{++}(m^2)$ (which is comparable to $\rho_4^{+-}(m^2)$ in this case) in the formulas Eq. (4.164). For $a_{4,2}$ to get 1% precision $\rho_4^{++}(m^2)$ required as well. We re-iterate that in deriving the bounds using LSD we did not make any assumptions about the contributions of infinitely many higher-spin terms in Eq. (4.164) and instead used crossing symmetry to derive rigorous and tight bounds based on Eq. (4.152). In contrast, when we use Eq. (4.164) and try to estimate the contribution of higher-spin partial waves we observe that depending on the model and the coupling at hand, the number of terms required to be kept in the expansion to reach good precision varies.

We observe that the relation Eq. (4.163) generates a hierarchy $\sim 10^{-2}$ between certain coefficients in the low-energy EFT. A naive low-energy observer could have been puzzled by the fact that $|a_{4,2} - \frac{3}{2}a_{4,1}| \ll a_{4,0}$. We see that this hierarchy is generated by unitarity, namely it appears due to the dominance of the dispersive integrals by the low-spin partial waves. We discuss this point further in Sect. 4.5.5.

139

k = 6:

The analysis gets more and more complicated as we go to higher k. For $k = 6$ we get the 7-dimensional coupling vector $\mathbf{a}_6 = (a_{6,0}, a_{6,1}, a_{6,2}, a_{6,3}, a_{6,4}, a_{6,5}, a_{6,6})$. Out of seven couplings only four are independent due to the crossing-symmetry relations

$$
\begin{aligned}
\text{Crossing}: \quad a_{6,4} &= 5(a_{6,1} - a_{6,2}) + 3a_{6,3}\,, \\
a_{6,5} &= 6(a_{6,1} - a_{6,2}) + 3a_{6,3}\,, \\
a_{6,6} &= 2(a_{6,1} - a_{6,2}) + a_{6,3}\,.
\end{aligned}
\tag{4.165}
$$

Working out the boundary of the coupling region is more laborious, but follows the same pattern that we observed before

$$
\begin{aligned}
&\big\{ \langle \mathbf{a}_6, i_s, i_s + 2, j_s, j_s + 2, k_s, k_s + 2 \rangle_{k>j>i\geq 2}\,, \\
&\quad \langle \mathbf{a}_6, i_u^{(6)} + 1, i_u^{(6)}, j_u^{(6)}, j_u^{(6)} + 1, k_u^{(6)}, k_u^{(6)} + 1 \rangle_{k>j>i\geq 5}\,, \\
&\quad \langle \mathbf{a}_6, 5_u^{(6)}, 4_u^{(6)}, 6_u^{(6)}, 7_u^{(6)}, 8_u^{(6)}, 9_u^{(6)} \rangle\,, \quad \text{mixed } s\text{–}u \text{ constraints} \big\} \geq 0\,,
\end{aligned}
\tag{4.166}
$$

where we list the explicit mixed constraints that we found in Appendix 4.C. After the boundaries are identified we take the crossing-symmetric slice Eq. (4.165). The resulting region of allowed couplings is plotted in Fig. 4.11. The region covered by the known theories is again a small island in the space of couplings.

As in the analysis above the island occupied by the explicit examples can be understood using the idea of strong LSD. As before the first step is to derive a set of rigorous bounds in terms of the low-spin partial waves. We do not present the complete analysis here but only
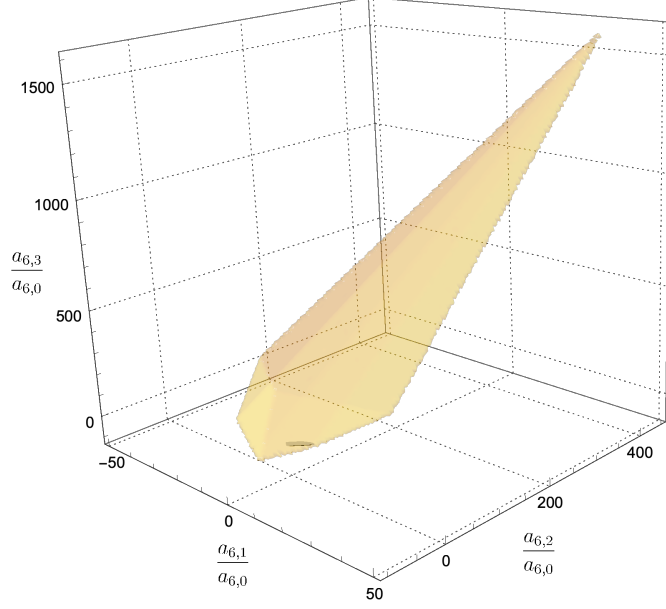
Figure 4.11: The allowed region for couplings $\left(\frac{a_{6,1}}{a_{6,0}}, \frac{a_{6,2}}{a_{6,0}}, \frac{a_{6,3}}{a_{6,0}}\right)$ derived from constraints Eq. (4.166). The black little island (barely visible) is the space occupied by known perturbative amplitudes. The small gray shaded region that surrounds it corresponds to the LSD $\alpha = 10^2$ bound. The details on how the plot was generated can be found in Appendix 4.C.

present some of the relevant bounds

$$
-\frac{9\langle\rho_2^{++}\rangle_6 + 25\langle\rho_5^{+-}\rangle_6}{\langle\rho_0^{++}\rangle_6 + \langle\rho_4^{+-}\rangle_6 + \langle\rho_2^{++}\rangle_6 + \langle\rho_5^{+-}\rangle_6} \leq \frac{a_{6,2} - \frac{5}{2}a_{6,1}}{a_{6,0}}
$$

$$
\leq \frac{40\langle\rho_4^{++}\rangle_6 + 315\langle\rho_6^{++}\rangle_6 + 32.56\langle\rho_6^{+-}\rangle_6 + 220.41\langle\rho_7^{+-}\rangle_6}{\langle\rho_0^{++}\rangle_6 + \langle\rho_4^{+-}\rangle_6 + \langle\rho_4^{++}\rangle_6 + \langle\rho_6^{++}\rangle_6 + \langle\rho_6^{+-}\rangle_6 + \langle\rho_7^{+-}\rangle_6},
$$

$$(4.167)$$

$$
-\frac{20\langle\rho_2^{++}\rangle_6 + 66.67\langle\rho_5^{+-}\rangle_6}{\langle\rho_0^{++}\rangle_6 + \langle\rho_4^{+-}\rangle_6 + \langle\rho_2^{++}\rangle_6 + \langle\rho_5^{+-}\rangle_6} \leq \frac{a_{6,3} - \frac{10}{3}a_{6,1}}{a_{6,0}}
$$

$$
\leq \frac{73.34\langle\rho_4^{++}\rangle_6 + 1540\langle\rho_6^{++}\rangle_6 + 163.49\langle\rho_6^{+-}\rangle_6 + 495.64\langle\rho_7^{+-}\rangle_6}{\langle\rho_0^{++}\rangle_6 + \langle\rho_4^{+-}\rangle_6 + \langle\rho_4^{++}\rangle_6 + \langle\rho_6^{++}\rangle_6 + \langle\rho_6^{+-}\rangle_6 + \langle\rho_7^{+-}\rangle_6}.
$$

$$(4.168)$$

From the formulas above and a similar analysis for $a_{6,i}$ we also see that

$$\text{LSD}_{\alpha\to\infty} : \qquad \frac{a_{6,2} - \frac{5}{2}a_{6,1}}{a_{6,0}} = 0\,, \qquad \frac{a_{6,3} - \frac{10}{3}a_{6,1}}{a_{6,0}} = 0\,,$$

$$0 \le \frac{a_{6,1}}{a_{6,0}} \le 6\,, \qquad 0 \le \frac{a_{6,2}}{a_{6,0}} \le 15\,,$$

$$0 \le \frac{a_{6,3}}{a_{6,0}} \le 20\,. \tag{4.169}$$

As for $k = 4$ we can understood the result above by simply dropping higher-spin contributions in the dispersive representations for the couplings and keeping only the lowest-spin partial waves in each channel

$$a_{6,0} = \int_{m_{gap}^2}^{\infty} \frac{dm^2}{\pi} \frac{\rho_{++0}(m^2)}{(m^2)^{11}} + \int_{m_{gap}^2}^{\infty} \frac{dm^2}{\pi} \frac{\rho_{+-4}(m^2)}{(m^2)^{11}} + \text{higher spin}, \tag{4.170}$$

$$a_{6,1} = 6 \int_{m_{gap}^2}^{\infty} \frac{dm^2}{\pi} \frac{\rho_{+-4}(m^2)}{(m^2)^{11}} + \text{higher spin}, \tag{4.171}$$

$$a_{6,2} = 15 \int_{m_{gap}^2}^{\infty} \frac{dm^2}{\pi} \frac{\rho_{+-4}(m^2)}{(m^2)^{11}} + \text{higher spin}, \tag{4.172}$$

$$a_{6,3} = 20 \int_{m_{gap}^2}^{\infty} \frac{dm^2}{\pi} \frac{\rho_{+-4}(m^2)}{(m^2)^{11}} + \text{higher spin}. \tag{4.173}$$

We emphasize again that while dropping infinitely many terms is not justified, the bound Eq. (4.169) is rigorous.

Assuming the strong version of the LSD and using Eq. (4.167) we again find the small region around the island occupied by the explicit examples, as shown in Fig. 4.11 and Fig. 4.12.

k = 8:

For $k = 8$ we do not perform the analysis of finding the allowed region but simply report on the data in the specific theories. There are five independent couplings at this level which we choose to be $a_{8,0\le j\le 4}$. Other couplings $a_{8,5\le j\le 8}$ can be obtained by crossing. The
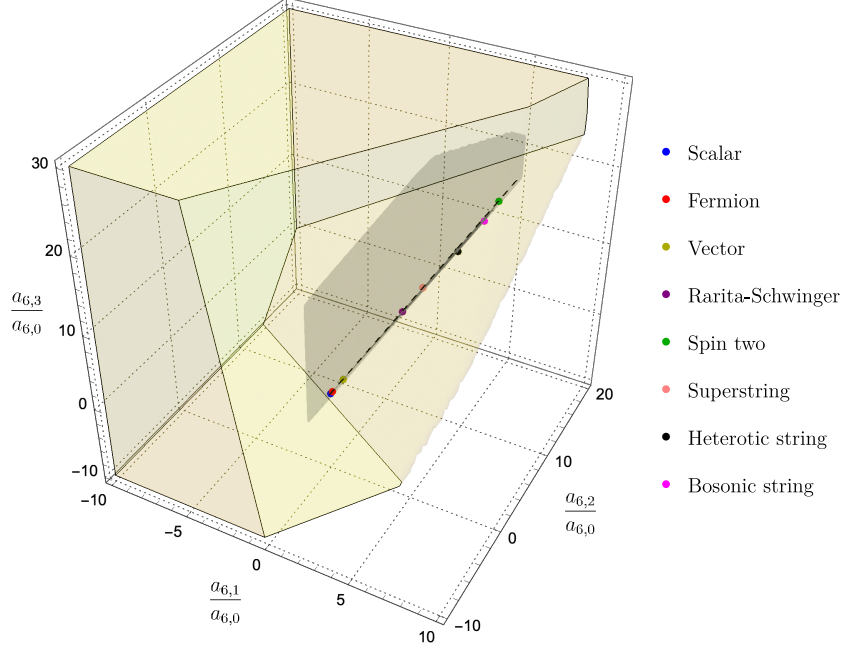
Figure 4.12: The scaled version of the theory island from Fig. 4.11. The gray region is derived using the bounds Eq. (4.167) (and similar bounds for $a_{6,i}$ which we do not write down explicitly) and the LSD assumption Eq. (4.152) with $\alpha = 10^2$. The dashed black line $\frac{a_{6,2}}{a_{6,1}} = \frac{5}{2}$ and $\frac{a_{6,3}}{a_{6,1}} = \frac{10}{3}$ corresponds to LSD$_{\alpha\to\infty}$ bounds given in Eq. (4.169).

dispersive representation of the couplings take the following form

$$a_{8,0} = \int_{m_{\text{gap}}^2}^{\infty} \frac{dm^2}{\pi} \frac{\rho_{++0}(m^2)}{(m^2)^{13}} + \int_{m_{\text{gap}}^2}^{\infty} \frac{dm^2}{\pi} \frac{\rho_{+-4}(m^2)}{(m^2)^{13}} + \mathrm{h}igher\ spin\,,$$

$$a_{8,1} = 8 \int_{m_{\text{gap}}^2}^{\infty} \frac{dm^2}{\pi} \frac{\rho_{+-4}(m^2)}{(m^2)^{13}} + \mathrm{h}igher\ spin\,,$$

$$a_{8,2} = 28 \int_{m_{\text{gap}}^2}^{\infty} \frac{dm^2}{\pi} \frac{\rho_{+-4}(m^2)}{(m^2)^{13}} + \mathrm{h}igher\ spin\,,$$

$$a_{8,3} = 56 \int_{m_{\text{gap}}^2}^{\infty} \frac{dm^2}{\pi} \frac{\rho_{+-4}(m^2)}{(m^2)^{13}} + \mathrm{h}igher\ spin\,,$$

$$a_{8,4} = 70 \int_{m_{\text{gap}}^2}^{\infty} \frac{dm^2}{\pi} \frac{\rho_{+-4}(m^2)}{(m^2)^{13}} + \mathrm{h}igher\ spin\,, \tag{4.174}$$

where we keep the leading spin contributions in both channels. To visualize the data we consider two 3-dimensional slices of the space of couplings with coordinates $\left(\frac{a_{8,1}}{a_{8,0}}, \frac{a_{8,2}}{a_{8,0}}, \frac{a_{8,3}}{a_{8,0}}\right)$ and $\left(\frac{a_{8,2}}{a_{8,0}}, \frac{a_{8,3}}{a_{8,0}}, \frac{a_{8,4}}{a_{8,0}}\right)$. Formulas Eq. (4.174) define a line in this space upon neglecting the higher-spin partial wave contributions. We depict the result in Fig. 4.13 and it is again

completely analogous to our observations for lower k's. It would be interesting to extend the analysis done for lower k to this case as well.
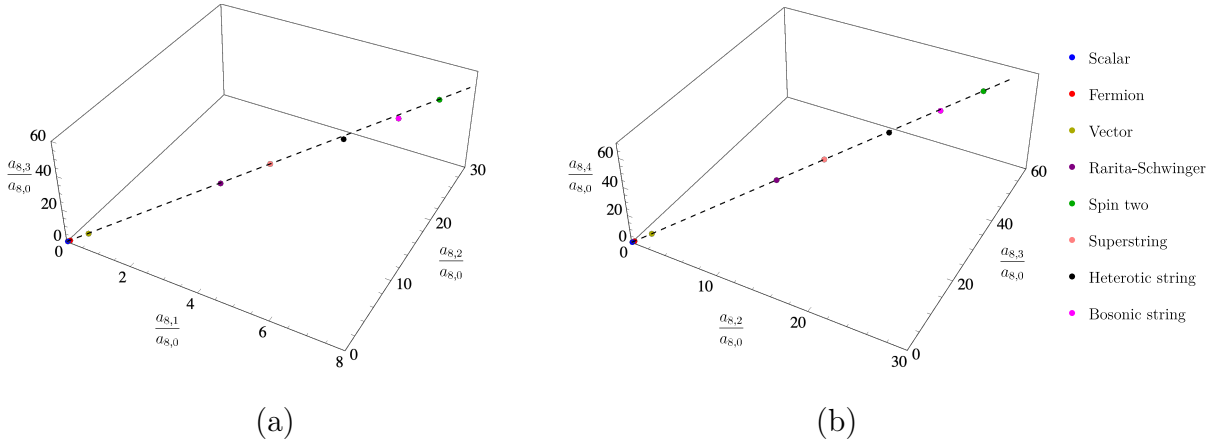
Figure 4.13: A plot for the data for $a_{8,j}$ in various theories. In panel a) we plot $\left(\frac{a_{8,1}}{a_{8,0}}, \frac{a_{8,2}}{a_{8,0}}, \frac{a_{8,3}}{a_{8,0}}\right)$ and in panel b) $\left(\frac{a_{8,2}}{a_{8,0}}, \frac{a_{8,3}}{a_{8,0}}, \frac{a_{8,4}}{a_{8,0}}\right)$. The dashed line corresponds to the low-spin dominant line defined by Eq. (4.174) upon neglecting the higher-spin contributions to the partial-wave expansion.

4.5.3 Crossing-symmetric dispersive representation of low-energy couplings

We can also analyze the same amplitude using dispersive representation with a different pair of channels. We start by recalling that

$$\mathcal{M}_4(1^+, 2^-, 3^-, 4^+) = (\langle 23 \rangle [14])^4 \, f(s, u) \,. \tag{4.175}$$

We would like to use dispersion relations at fixed t to derive the dispersive representation for the low-energy couplings. For this purpose it is natural to introduce the following parameterization of the low-energy expansion of $f(s, u)$

$$f\left(z - \frac{t}{2}, -z - \frac{t}{2}\right) = \left(\frac{\kappa}{2}\right)^2 \frac{1}{t(\frac{t^2}{4} - z^2)} + |\beta_{R^3}|^2 \frac{(\frac{t^2}{4} - z^2)}{t} - |\beta_\phi|^2 \frac{1}{t}$$

$$+ \sum_{k \geq q \geq 0}^{\infty} \tilde{a}_{k,q} z^{k-q} t^q, \qquad z = s + \frac{t}{2}, \qquad k - q \in 2\mathbb{Z}_{\geq 0} \,. \tag{4.176}$$

Crossing symmetry $f(s, u) = f(u, s)$ acts as $z \to -z$ and therefore constrains $k - q$ to be even.

144

To derive the bounds we can try to use dispersive representation for $\tilde{a}_{k,q}$, where we keep t fixed and deform the z integral

$$\tilde{a}_{k,q} = \frac{1}{q!}\partial_t^q \oint \frac{dz}{2\pi i}\frac{1}{z^{k-q+1}}$$

$$\left[f(z-\frac{t}{2},-z-\frac{t}{2}) - \left(\frac{\kappa}{2}\right)^2 \frac{1}{t(\frac{t^2}{4}-z^2)} - |\beta_{R^3}|^2\frac{(\frac{t^2}{4}-z^2)}{t} + |\beta_\phi|^2\frac{1}{t}\right]\Bigg|_{t=0}, \qquad (4.177)$$

where the contour integral encircles the origin and we explicitly subtracted the contributions that are singular at $t = 0$. As discussed in the previous section, unitarity constrains the form of the discontinuity of $f(z-\frac{t}{2}, -z-\frac{t}{2})$. Therefore, in evaluating Eq. (4.177) we can open the contour and assuming we can drop the arcs at infinity to arrive at the following representation

$$\tilde{a}_{k,q} = \frac{2}{q!}\partial_t^q \int_{m_{gap}^2}^\infty \frac{dm^2}{\pi} \sum_{J=4}^\infty \frac{\rho_J^{+-}(m^2)}{(m^2+\frac{t}{2})^{k-q+1}}\frac{(-1)^J d_{4,-4}^J\left(1+\frac{2t}{m^2}\right)}{t^4}\Bigg|_{t=0}, \qquad k-q\in 2\mathbb{Z}_{\geq 0}\,.$$

$$(4.178)$$

The factor of 2 originates from the sum over the s-channel and the u-channel discontinuities. For odd $k-q$ they cancel each other and we get zero. An important factor $1/t^4$ originates from the fact that unitarity constraints are formulated in terms of $\mathcal{M}_{+--+}$ which includes the prefactor $(\langle 23\rangle[14])^4$—see Sect. 4.4.2 for details. The factor $(-1)^J$ can be understood from the fact that with a given choice of helicity the discontinuity is positive for the forward limit $u = 0$ (as opposed to $t = 0$).[30] In using the representation (4.178) we should not forget that it was derived assuming that the Regge behavior of the amplitude is such that the arcs at infinity can be dropped. In particular, given that $f(z-\frac{t}{2}, -z-\frac{t}{2}) \sim z^{J_0}$ for large $|z|$, and taking into account the subtractions of terms that are singular at $t = 0$ the representation (4.178) is valid only for $k-q > max\{J_0, 2\}$. As opposed to the previous section all $\tilde{a}_{k,q}$, whose dispersive representation is given in Eq. (4.178), are independent and there are no extra constraints coming from crossing.

The presence of $(-1)^J$ in the sum Eq. (4.178) prevents us from deriving useful bounds from the representation Eq. (4.178). We, however, present the data for $\tilde{a}_{k,q}$ obtained from

---

[30]Consistency between Eq. (4.133) and Eq. (4.178), namely matching of the ρ_J^{+-} discontinuities, requires that $d_{4,4}^J(x) = (-1)^J d_{4,-4}^J(-x)$, which is indeed the case.

the explicit amplitudes since it reveals an interesting aspect of the discussion in the previous section.

For example, consider $k = 6$. The mapping between $a_{6,j}$ and $\tilde{a}_{6,j}$ takes the following form

$$\tilde{a}_{6,0} = 2(a_{6,1} - a_{6,2}) + a_{6,3} \,,$$

$$\tilde{a}_{6,2} = \frac{1}{4}(-10a_{6,1} + 10a_{6,2} - 3a_{6,3}) \,,$$

$$\tilde{a}_{6,4} = \frac{1}{16}(30a_{6,1} - 14a_{6,2} + 3a_{6,3}) \,, \tag{4.179}$$

and we will not need $\tilde{a}_{6,6}$ for our purposes. The remarkable fact about $\tilde{a}_{6,j}$ is that the dashed LSD line from Fig. 4.12 maps to the point $(\frac{15}{4}, \frac{15}{16})$ in the $(\frac{\tilde{a}_{6,2}}{\tilde{a}_{6,0}}, \frac{\tilde{a}_{6,4}}{\tilde{a}_{6,0}})$ plane, which can also be found by keeping the lowest-spin contribution in Eq. (4.178)

$$\text{LSD}_{\alpha \to \infty} : \quad \left(\frac{\tilde{a}_{6,2}}{\tilde{a}_{6,0}}, \frac{\tilde{a}_{6,4}}{\tilde{a}_{6,0}}\right) = \left(\frac{15}{4}, \frac{15}{16}\right) \simeq (3.75, 0.94) \,. \tag{4.180}$$

Therefore, the plane $(\frac{\tilde{a}_{6,2}}{\tilde{a}_{6,0}}, \frac{\tilde{a}_{6,4}}{\tilde{a}_{6,0}})$ happens to be precisely orthogonal to the line in Fig. 4.12 and it is well-suited to study the fine structure of the distribution of points around the line.

Looking at the plot 4.12, we see that both the scalar and the fermion lie pretty far from the naive LSD point. The reason we did not detect this on Fig. 4.12 is that for the scalar and fermion: $a_{6,0} \gg a_{6,1}, a_{6,2}, a_{6,3}$. In this way both points are very close to the LSD line in Fig. 4.12, but for the trivial reason of being close to the origin. In Fig. 4.14 we resolve the origin by switching to variables Eq. (4.179) that do not depend on $a_{6,0}$.

Working with $\tilde{a}_{k,q}$ emphasizes an important aspect of LSD. While assuming strong LSD leads to much tighter bounds on ratios $\frac{a_{k,j}}{a_{k,0}}$ it does not lead to improved bounds for $\frac{\tilde{a}_{k,q}}{\tilde{a}_{k,0}}$. The reason can be understood as follows: For any large, but finite α, the admissible range for $\frac{a_{k,j}}{a_{k,0}}$ includes 0 and a small part of the negative axis. It is then easy to see from the definition Eq. (4.179) that arbitrarily small vicinity of the origin in the $\frac{a_{k,j}}{a_{k,0}}$ includes all possible values for $\frac{\tilde{a}_{k,q}}{\tilde{a}_{k,0}}$. This precludes using LSD to derive stronger bounds on $\frac{\tilde{a}_{k,q}}{\tilde{a}_{k,0}}$. This simple fact highlights the point that not all EFT coupling bases are equally illuminating for understanding the underlying structure.

A similar analysis can be performed for $k = 8$. By switching to the $(\frac{\tilde{a}_{8,2}}{\tilde{a}_{8,0}}, \frac{\tilde{a}_{8,4}}{\tilde{a}_{8,0}}, \frac{\tilde{a}_{8,6}}{\tilde{a}_{8,0}})$ coordinates we note that the line from Fig. 4.13 maps to a single point. The same point can
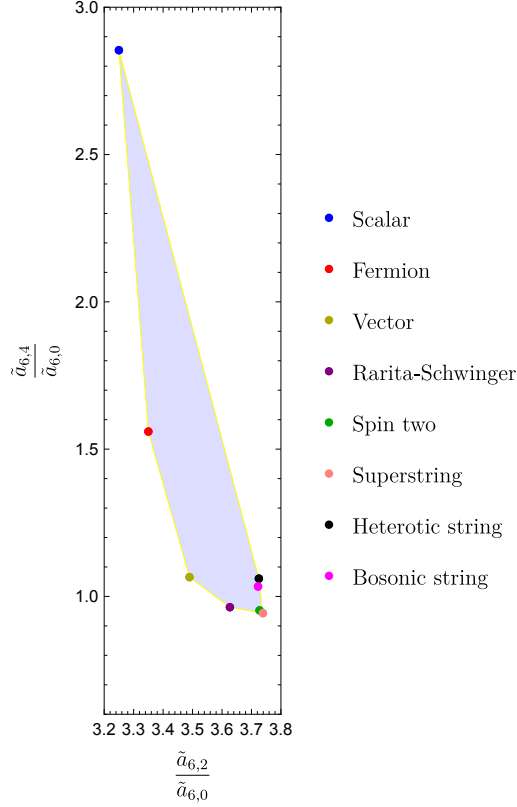
Figure 4.14: The transverse view of the theory island from Fig. 4.12. We indicate various theories that form the vertices of the island. To reach a particular point inside the UV island we need to take a superposition of various amplitudes.

be obtained by keeping only $J = 4$ contribution in (4.178)

$$\text{LSD}_{\alpha \to \infty}: \quad \left(\frac{\tilde{a}_{8,2}}{\tilde{a}_{8,0}}, \frac{\tilde{a}_{8,4}}{\tilde{a}_{8,0}}, \frac{\tilde{a}_{8,6}}{\tilde{a}_{8,0}}\right) = \left(7, \frac{35}{8}, \frac{7}{16}\right) = (7, 4.375, 0.4375). \tag{4.181}$$

Therefore by plotting the data in these coordinates we can resolve the points close to the origin in Fig. 4.13 which were located there due to the fact that $a_{8,0} \gg a_{8,i>0}$. One can check again that $\left(\frac{\tilde{a}_{8,2}}{\tilde{a}_{8,0}}, \frac{\tilde{a}_{8,4}}{\tilde{a}_{8,0}}, \frac{\tilde{a}_{8,6}}{\tilde{a}_{8,0}}\right)$ is independent of $a_{8,0}$ and therefore this suppression does not take place anymore. The result is depicted in Fig. 4.15.

4.5.4 Spectral densities and low-spin dominance

In the discussion above we considered various bounds that follow from the dispersive representation of the low-energy couplings and observed the phenomenon of LSD in the known
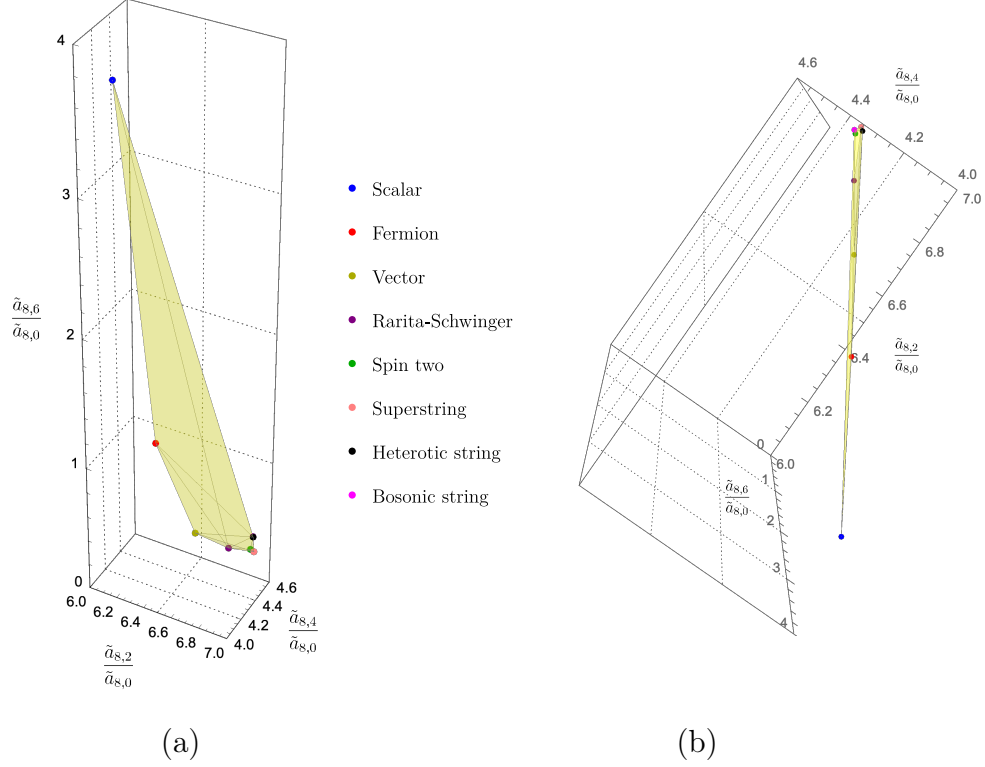
Figure 4.15: Various data points for $(\frac{\tilde{a}_{8,2}}{\tilde{a}_{8,0}}, \frac{\tilde{a}_{8,4}}{\tilde{a}_{8,0}}, \frac{\tilde{a}_{8,6}}{\tilde{a}_{8,0}})$. Panels a) and b) present the same plot as seen from different vantage points. In particular, panel b) makes it clear that the points essentially lie on a plane.

physical theories. It manifests itself in the fact that the low-energy couplings occupy a very small region in the space of couplings allowed on general grounds. To see this phenomenon more clearly it is instructive to look at the spectral densities of the amplitudes directly.

Given a known expression for the amplitude it is not hard to compute various spectral densities. Indeed, it amounts to taking a discontinuity of the amplitude and integrating it against the proper Wigner d-function. These satisfy a familiar orthogonality relation

$$\int_{-1}^{1} dx\, d^{J}_{\lambda,\lambda'}(x) d^{\tilde{J}}_{\lambda,\lambda'}(x) = \frac{2}{2J+1}\delta_{J,\tilde{J}}\,. \tag{4.182}$$

For tree-level amplitudes the spectral density is a sum of delta-functions which correspond to the masses of exchanged particles. For the one-loop amplitudes the discontinuity has a continuous support above the two-particle threshold $4m^2$. In this case we perform the integration Eq. (4.182) numerically. We focus on the first few spin spectral densities in

148

both ρ_J^{++} and ρ_J^{+-} channels. To go from spectral densities to the coefficients in the low-energy expansion we need to compute the moments as in Eqs. Eq. (4.164), Eq. (4.170), and Eq. (4.174).
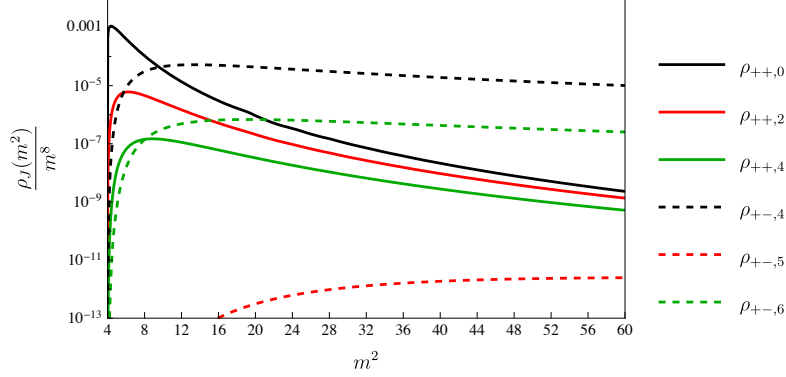
Figure 4.16: Spectral densities for the one-loop minimally-coupled scalar. We observe that $\rho_0^{++} \gg \rho_{J\geq4}^{+-}, \rho_{J\geq2}^{++}$ and that $\rho_4^{+-} \sim \rho_2^{++}$ close to the two-particle threshold. This is fully consistent with the features of the plots for various couplings in the previous section.
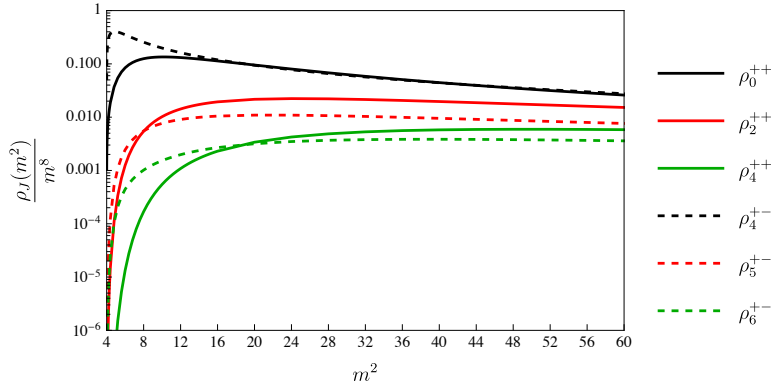
Figure 4.17: Spectral densities for the one-loop minimally coupled spin-2 particle. We observe that $\rho_4^{+-} \gg \rho_{J>4}^{+-}, \rho_{J\geq2}^{++}$ and that $\rho_4^{+-} \sim \rho_0^{++}$. Therefore in the space of couplings this amplitude is expected to lie on the low-spin dominance line.

The results for a few selected cased are listed in Fig. 4.16-4.19. In all cases we see that the minimal-spin partial waves dominate in the corresponding channel. It is also instructive to plot the moments $\langle \rho_J \rangle_k$ which we present in Fig. 4.20. The moments clearly satisfy LSD used in the previous section to derive stronger bounds.
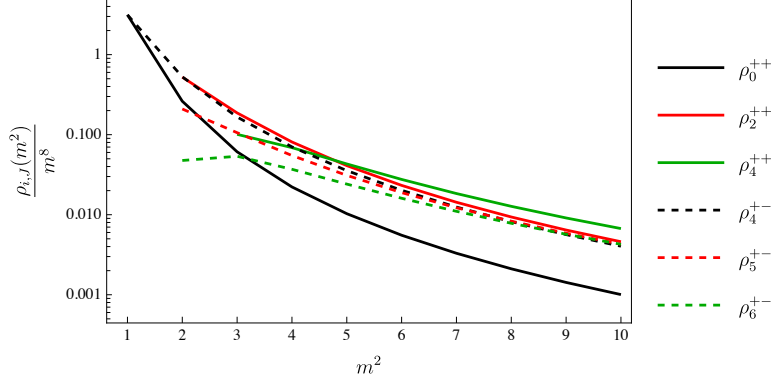
Figure 4.18: Spectral densities for the tree-level scattering of gravitons in the superstring theory. We observe that $\rho_4^{+-} \gg \rho_{J>4}^{+-}, \rho_{J\geq2}^{++}$ and that $\rho_4^{+-} \sim \rho_0^{++}$. Therefore in the space of couplings this amplitude is expected to lie on the low-spin dominance line.

In fact the moments of spectral density $\langle\rho_J\rangle_k$ in the examples we consider not only exhibit the dominance of the lowest-spin partial waves but also rapid decay at higher J. This latter feature is expected to be completely general. Indeed, the convergence of the sum rules Eq. (4.134) requires that $\langle\rho_J\rangle_k$ decay faster than any polynomial at large J. This latter decay can be traced to locality of scattering in the impact-parameter space.

Indeed, in the perturbative regime at large J we have

$$\rho_J(s) \sim \text{Im}\,\delta(s,b), \qquad b = \frac{2J}{\sqrt{s}}, \tag{4.183}$$

where $\delta(s,b)$ is the phase shift and b is the impact parameter. For fixed s and large impact parameters we expect to have

$$\text{Im}\delta(s,b) \sim e^{-m_{\text{gap}}b}, \qquad m_{\text{gap}}b \gg 1, \tag{4.184}$$

which controls decay of $\rho_J(s)$ at large J. In string theory the leading-order behavior is different and is controlled by the transverse spreading of strings $\text{Im}\,\delta(s,b) \sim e^{-\frac{b^2}{2\alpha'\log\frac{s\alpha'}{4}}}$ —see Ref. [354].

A priori the large impact parameter discussion is not necessarily relevant for understanding the large-J behavior of $\langle\rho_J\rangle_k$ which involves computing the moment Eq. (4.148) over all energies (as opposed to keeping s fixed as we take the large-J limit). However, in analyzing

150
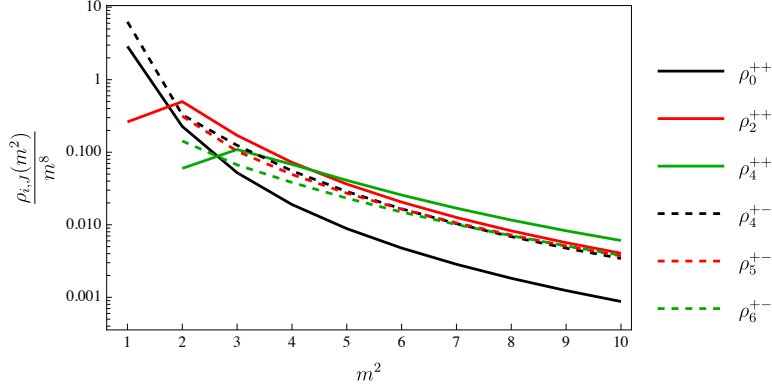
Figure 4.19: Spectral densities for the tree-level scattering of gravitons in the heterotic string theory. We observe that $\rho_4^{+-} \gg \rho_{J>4}^{+-}, \rho_{J\geq 2}^{++}$ and that $\rho_4^{+-} \sim \rho_0^{++}$. Therefore in the space of couplings this amplitude is expected to lie on the LSD line.

$\langle \rho_J \rangle_k$ for the amplitudes considered in the present paper we experimentally observed that the integral over energies is peaked at energies

$$\langle \rho_J \rangle_k : \quad \frac{s_*}{m_{gap}^2} \sim J. \tag{4.185}$$

Plugging this into the formula for the impact parameter Eq. (4.183) we find that the dominant impact parameters are $m_{gap}b_* \sim J^{1/2} \gg 1$ and therefore the large-J behavior of the moments $\langle \rho_J \rangle$ is still controlled by large impact-parameter physics. We tested this picture against the data presented in Fig. 4.20 and found a qualitative agreement. It would be interesting to study the large-J limit of $\langle \rho_J \rangle_k$ more systematically. Of course, this discussion does not explain the fact that the hierarchical structure among partial waves continues all the way to the lowest spins in the examples we analyzed. It is this latter fact was crucial for the analysis in the previous section.

An important question is to understand how general is the picture that we observed in the tree-level string amplitudes and one-loop matter amplitudes. A priori these amplitudes look very different from each other, but at the level of the partial-wave analysis discussed in this section they exhibit remarkably similar behavior and strong version of LSD. This suggests that the hierarchical structures we observed in this paper could be a general property of consistent weakly-coupled gravitational S-matrices, but we do not have a proof yet.

151
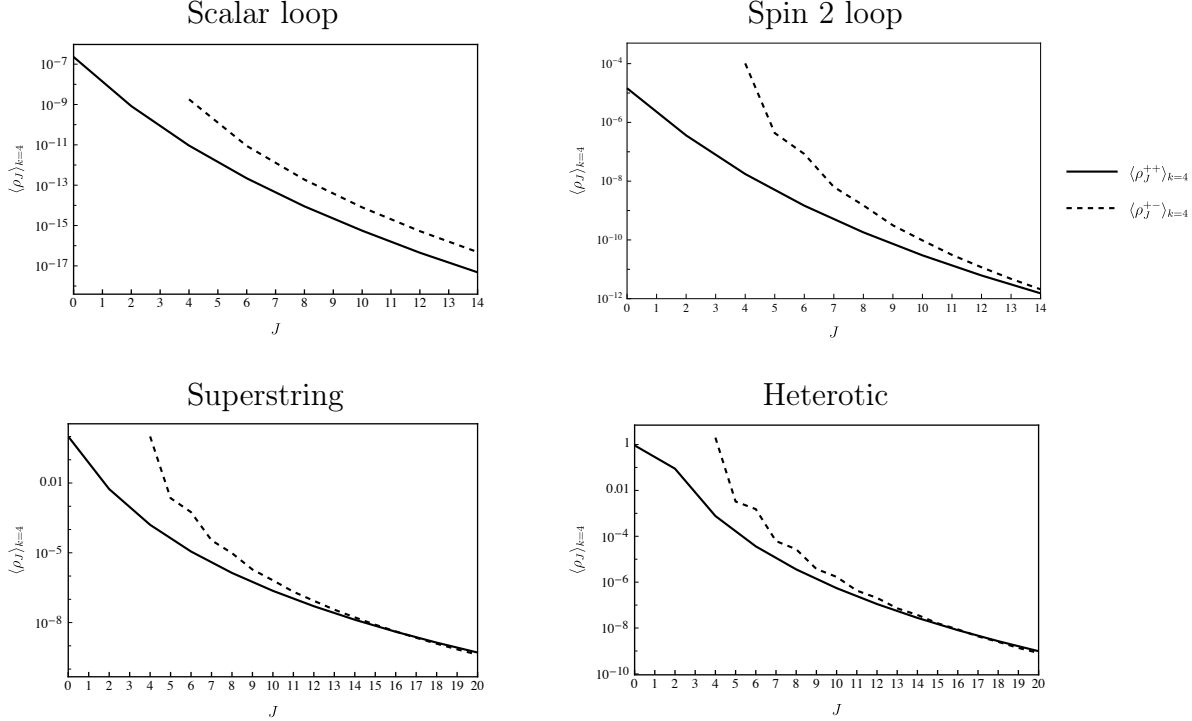
Figure 4.20: Moments of the spectral density $\langle \rho_J \rangle_4$ Eq. (4.148) as a function of spin J for various examples. For the scalar one loop result ρ_J^{+-} with J being odd are negligible and are not presented in the figure. The line in the corresponding panel is obtained by connecting the even spin values of the spectral density moments.

4.5.5 A hierarchy from unitarity

The LSD discussion above illustrates an interesting phenomenon of emergent hierarchy between EFT coefficients in the absence of an underlying symmetry. Consider for example $D^8 R^4$ type corrections discussed in the $k = 4$ section above. In writing down the relevant correction to the amplitude an EFT practitioner guided by the considerations of the supersymmetric decomposition Eq. (4.32) can write the following ansatz

$$f_{D^8 R^4}(t, u) = c_0 \left(s^2 + t^2 + u^2\right)^2 + c_1 \, s^4 + c_{\text{rest}} \left(t^2 + u^2\right)^2 . \tag{4.186}$$

The first term, which is proportional to c_0, is the completely crossing-symmetric term of the type that appears in the new spin-2 part of the amplitude given in Eq. (4.298), corresponding to a massive $\mathcal{N} = 8$ supersymmetric multiplet, obtained, for example, by dimensional
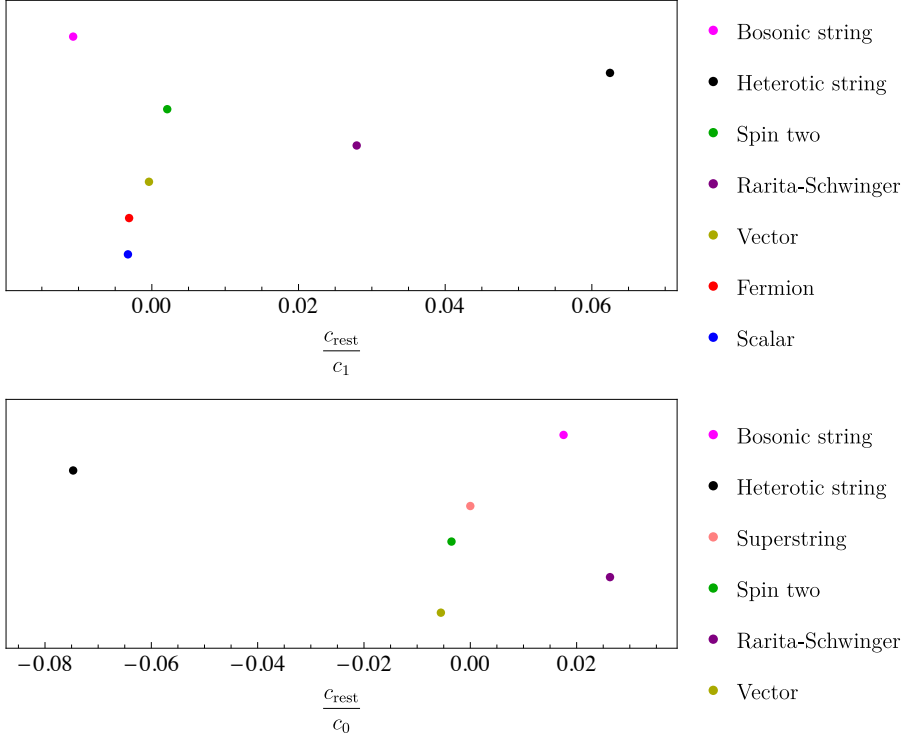
Figure 4.21: Examples of a hierarchy from unitarity. The horizontal axis shows illustrates that the dominance of low-spin spectral densities naturally introduces a 10^{-2} hierarchy between various EFT coefficients in the absence of any symmetry. The vertical axis carries no meaning other than separating the points.

reduction from five dimensions. In the $\mathcal{N} = 8$ theory the full crossing symmetry of such terms is a consequence of $\mathcal{N} = 8$ supersymmetric Ward identities [321, 322, 323, 324]. The c_1 term corresponds to the additional terms needed in the new spin-3/2 part of the amplitude Eq. (4.297) beyond the fully crossing symmetric terms already appearing in the new spin-2 part of the amplitude. Finally, the third term containing c_{rest} is the remaining independent term with t–u crossing symmetry. This term is distinguished from the c_1 term by its differing behavior for $t \to \infty$ with s fixed.

We then express the coefficient above in terms of more familiar $a_{k,j}$ defined in Eq. (4.131)

and used in the discussion of various bounds. We get the following result

$$c_0 = \frac{1}{4}\left(2a_{4,1} - a_{4,2}\right),$$

$$c_1 = \frac{1}{4}\left(4a_{4,0} - 5a_{4,1} + 2a_{4,2}\right),$$

$$c_{\text{rest}} = \frac{1}{2}\left(a_{4,2} - \frac{3}{2}a_{4,1}\right). \tag{4.187}$$

Remarkably, we see that c_{rest} vanishes along the low-spin dominance line that follows from Eq. (4.164). Plugging in the values of $a_{k,j}$ for the theories discussed here we find a 10^{-2} hierarchy with $c_{\text{rest}} \ll c_1$ in the absence of any symmetry, as shown in Fig. 4.21. For spin $S = 1, \frac{3}{2}, 2$ particle in the loop we also have $c_{\text{rest}} \ll c_0$.

4.6 Deriving bounds: multiple polarizations

In this section we consider dispersion relations that combine information from the different helicity configurations. More precisely, we consider dispersive sum rules Eq. (4.121) which we apply to the matrices built out of various scattering amplitudes Eq. (4.110), Eq. (4.111). We derive bounds on the inelastic amplitudes (single-minus and all-plus amplitudes) in terms of the elastic double-minus amplitude.

4.6.1 $s = 0$

The simplest bounds comes from setting $s = 0$ in Eq. (4.122). The relevant equation takes the form

$$\oint_{t_0} \frac{dt}{2\pi i} \mathcal{M}_h(s, t) \frac{1}{t} \frac{1}{(t(s+t))^k}\Big|_{s=0} = \int_{m_{\text{gap}}^2}^{\infty} \frac{dt}{\pi} \frac{2}{t^{2k+1}} Disc_t \mathcal{M}_h(0, t) \succeq 0. \tag{4.188}$$

By plugging the low-energy expansion of the amplitude in the LHS of the equation above and requiring that its eigenvalues are non-negative we get

$$2f_{2k-4,0} \geq |h_{2k,0}|, \quad k = 2, 4, 6, \ldots . \tag{4.189}$$

The combination above for different k form a set of moments as can be seen from the RHS of (4.188). The difference compared to the recent analysis in Ref. [353] is that in our case we

have a positive semi-definite spectral density matrix instead of a function. By contracting such matrix moments with an arbitrary polarization vector reduces the problem to the one considered in Ref. [353].

The situation simplifies in the parity preserving case when $h^*(s, u) = h(s, u)$. In this case the eigenvectors $\mathcal{M}_{h,\pm}(s, t)$ given in Eq. (4.117) generate the low-energy expansion that satisfies the moment problem conditions considered in great detail in Ref. [353]. More precisely, we define a set of moments as $\mu_{k-1} \equiv 2f_{2k-4,0} - h_{2k,0}$ and consider the Hankel matrix $H_{ij} = \mu_{i+j-1}$.

Using the results in Appendix 4.H for the one-loop amplitude due to minimally-coupled scalar in the loop the first five moments take the following form

$$
H^{S=0} = \frac{1}{140} \left(\frac{\kappa}{2} \right)^4 \frac{1}{(4\pi)^2}
\begin{pmatrix}
\frac{1}{135m^4} & \frac{1}{24024m^8} & \frac{1}{1969110m^{12}} \\[2mm]
\frac{1}{24024m^8} & \frac{1}{1969110m^{12}} & \frac{1}{109745064m^{16}} \\[2mm]
\frac{1}{1969110m^{12}} & \frac{1}{109745064m^{16}} & \frac{1}{4833678850m^{20}}
\end{pmatrix}.
\tag{4.190}
$$

In agreement with the general prediction the one-loop moment matrix has nonnegative minors.

4.6.2 Away from $s = 0$: first derivative

We can use Eq. (4.113) to derive the bounds by taking the derivative of $B_k^+(s)$ with respect to s before setting $s = 0$. For example let us consider the first derivative with respect to s. In this way we get

$$
\partial_s \oint_{t_0} \frac{dt}{2\pi i} \mathcal{M}_{h,g}(s, t) \frac{1}{t} \frac{1}{(t(s+t))^k} \Big|_{s=0}
$$
$$
= \int_{m_{gap}^2}^{\infty} \frac{dt}{\pi} \frac{1}{t^{2k+2}} \left(-(2k+1) \mathrm{Disc}_t \mathcal{M}_{h,g}(0, t) + 2t\, \partial_s \mathrm{Disc}_t \mathcal{M}_{h,g}(0, t) \right).
\tag{4.191}
$$

The RHS is not positive semi-definite and therefore we cannot derive the bound on the LHS in a similar fashion. We can, however, consider the following linear combination

$$\frac{2k+1}{2m_{\text{gap}}^2} \oint_{t_0} \frac{dt}{2\pi i} \mathcal{M}_{h,g}(s,t) \frac{1}{t} \frac{1}{(t(s+t))^k} + \partial_s \oint_{t_0} \frac{dt}{2\pi i} \mathcal{M}_{h,g}(s,t) \frac{1}{t} \frac{1}{(t(s+t))^k}\bigg|_{s=0}$$
$$= \int_{m_{\text{gap}}^2}^{\infty} \frac{dt}{\pi} \frac{1}{t^{2k+2}} \left(\left[\frac{t}{m_{\text{gap}}^2} - 1 \right] (2k+1) \text{Disc}_t \mathcal{M}_{h,g}(0,t) + 2t \, \partial_s \text{Disc}_t \mathcal{M}_{h,g}(0,t) \right) \succeq 0 \,.$$

$$(4.192)$$

We now apply Eq. (4.192) to $\mathcal{M}_h$. By plugging the low-energy expansion (see Eqs. (4.98) and (4.68)) in the LHS of the formula above and imposing that the eigenvalues of the resulting matrix are nonnegative we can derive various bounds. Let us consider for example $k = 2$. We get the following bound on the inelastic amplitude in terms of the elastic one

$$\left| h_{5,1} + \frac{5}{2} \frac{h_{4,0}}{m_{\text{gap}}^2} \right| \le 5 \left(f_{1,0} + \frac{f_{0,0}}{m_{\text{gap}}^2} \right) - 2|\beta_{R^3}|^2 \,. \tag{4.193}$$

To apply the dispersive sum rule above to the bosonic string amplitude we first subtracted the contribution of the tachyon exchange to get $\delta f^{(\text{bs})}(s,u) = f^{(\text{bs})}(s,u) + \left(\frac{\kappa}{2}\right)^2 \frac{1}{1+t}$ and $\delta h^{(\text{bs})}(s,u) = h^{(\text{bs})}(s,u) + \left(\frac{\kappa}{2}\right)^2 \left(\frac{s^4}{1+s} + \frac{t^4}{1+t} + \frac{u^4}{1+u} \right)$. The resulting functions satisfy all the properties needed to apply Eq. (4.192) for $k = 2$. We then get, using the formulas from App. 4.B,

$$\delta f_{0,0}^{(\text{bs})} = \left(\frac{\kappa}{2}\right)^2 \left(3 + 2\zeta(3) \right), \qquad \delta f_{1,0}^{(\text{bs})} = \left(\frac{\kappa}{2}\right)^2 (-3),$$
$$\delta h_{4,0}^{(\text{bs})} = \left(\frac{\kappa}{2}\right)^2 2, \qquad \delta h_{5,1}^{(\text{bs})} = \left(\frac{\kappa}{2}\right)^2 (-3), \qquad |\beta_{R^3}^{(\text{bs})}|^2 = \left(\frac{\kappa}{2}\right)^2 . \tag{4.194}$$

which indeed satisfy Eq. (4.193) where $m_{\text{gap}}^2 = 1$ in the string case.

For the one-loop minimally coupled scalar $|\beta_{R^3}|^2 \sim \kappa^6$ and appears only at two loops. For other coefficients that enter into Eq. (4.193) we get, using Eq. Eq. (4.86) and Eq. Eq. (4.91),

$$f_{0,0}^{S=0} = \left(\frac{\kappa}{2}\right)^4 \frac{1}{(4\pi)^2} \frac{1}{6300 m^4}, \qquad f_{1,0}^{S=0} = -\left(\frac{\kappa}{2}\right)^4 \frac{1}{(4\pi)^2} \frac{1}{41580 m^6},$$
$$h_{4,0}^{S=0} = \left(\frac{\kappa}{2}\right)^4 \frac{1}{(4\pi)^2} \frac{1}{3780 m^4}, \qquad h_{5,1}^{S=0} = -\left(\frac{\kappa}{2}\right)^4 \frac{1}{(4\pi)^2} \frac{1}{7920 m^6}, \tag{4.195}$$

so that, together with $m_{\text{gap}}^2 = 4m^2$, Eq. (4.193) is again satisfied.

More generally, the formula above bounds the correction to the three-point function of the graviton β_{R^3} from above in terms of the EFT data. To make it more manifest we can rewrite the above

$$2|\beta_{R^3}|^2 \le 5\left(f_{1,0} + \frac{f_{0,0}}{m_{\text{gap}}^2}\right) - \left|h_{5,1} + \frac{5}{2}\frac{h_{4,0}}{m_{\text{gap}}^2}\right| \le \frac{10 f_{0,0}}{m_{\text{gap}}^2}, \tag{4.196}$$

where in the last inequality we used the fact that $|f_{1,0}| \le \frac{1}{m_{\text{gap}}^2} f_{0,0}$ which readily follows from Eqs. (4.132) and (4.134). We can restate it more succinctly in terms of the Wilson coefficients of the gravitational EFT

$$|\beta_{R^3}|^2 \le 5\frac{\beta_{R^4}^+}{m_{\text{gap}}^2}, \tag{4.197}$$

where m_{gap}^2 denotes the mass gap at which the massive degrees of freedom that induce the higher-derivative corrections appear. Recall that $f_{0,0} = \beta_{R^4}^+$ was defined in Eq. (4.84). Bounds similar to Eq. (4.196) can be derived by considering the superconvergence sum rules for $k > 2$. We do not list them here.

In fact it is not difficult to strengthen the bound Eq. (4.197) by considering the following unsubtracted dispersive sum rule (analogous to $k = 0$ in Eq. (4.121))

$$\oint_{\infty} \frac{dt}{2\pi i}\frac{1}{t}f(s, -s-t) = 0. \tag{4.198}$$

The universal tree-level gravitational piece $\left(\frac{\kappa}{2}\right)^2\frac{1}{stu}$, which is singular at $s = 0$, does not contribute to Eq. (4.198) therefore we can consider

$$\left(\frac{1}{m_{\text{gap}}^2} + \partial_s\right)Eq. \text{ (4.198)}\Big|_{s=0} : \quad \frac{\beta_{R^4}^+}{m_{\text{gap}}^2} - |\beta_{R^3}|^2 =$$
$$\int_{m_{\text{gap}}^2}^{\infty}\frac{dt}{\pi}\frac{1}{t}\left(\left[\partial_s + \frac{1}{m_{\text{gap}}^2}\right]\text{Disc}_t f + \left[\partial_s + \frac{t - m_{\text{gap}}^2}{m_{\text{gap}}^2 t}\right]\text{Disc}_u f\right)\Big|_{s=0} \ge 0, \tag{4.199}$$

where nonnegativity of the RHS can be readily checked for each partial wave separately by plugging the discontinuities of $f(s, u)$, given in Eq. (4.133), into the formula above.[31] In this

---

[31]More precisely, it follows from $\partial_s^n\left(\frac{d_{4,4}^J(1 + \frac{2s}{m^2})}{(m^2 + s)^4}\right)\Big|_{s=0} > 0$ for $n = 0, 1$ which can be readily checked using formulas from Appendix 4.E.

way we immediately get a bound

$$\left|\beta_{R^3}\right|^2 \le \frac{\beta_{R^4}^+}{m_{gap}^2} \, .$$

(4.200)

The bound Eq. (4.200) is a step towards making the analysis of Ref. [241] quantitatively precise. At least for the R^3 correction to the graviton three-point coupling which is considered here, it translates the problem to bounding the coefficient $\beta_{R^4}^+$ in terms of G/m_{gap}^2.[32] This problem was beautifully solved recently in Ref. [271] for $D = 10$ maximal supergravity in a perturbative setting similar to ours, and it was addressed nonperturbatively in Ref. [282]. The method used in Ref. [271] is not directly applicable in four dimensions due to the IR divergences, but at least in $D \ge 5$ where the $2 \to 2$ amplitude is nonperturbatively well-defined it is natural to expect that one will be able to get a bound on $\beta_{R^4}^+$ in terms of G/m_{gap}^2. It would be very interesting to demonstrate it explicitly.

Indeed, assuming the nonperturbative Regge bound Eq. (4.119), we can consider the (-2) subtracted dispersion relations for $f(s, u)$ which expresses $-8\pi G/s$ in terms of the contribution of heavy states, cf. equation (3.37) in Ref. [271]. Existence of such a dispersion relation in the absence of supersymmetry is crucially due to the fact that we consider gravitons as external states.

4.6.3 Away from $s = 0$: second derivative

Using exactly the same technique as above one can check that

$$\frac{2k^2 - 1}{4} \oint_{t_0} \frac{dt}{2\pi i} \mathcal{M}_{h,g}(s, t) \frac{1}{t} \frac{1}{(t(s+t))^k} + \frac{2k+1}{2t_0} \partial_s \oint_{t_0} \frac{dt}{2\pi i} \mathcal{M}_{h,g}(s, t) \frac{1}{t} \frac{1}{(t(s+t))^k}$$
$$+ \partial_s^2 \oint_{t_0} \frac{dt}{2\pi i} \mathcal{M}_{h,g}(s, t) \frac{1}{t} \frac{1}{(t(s+t))^k} \Big|_{s=0} \succeq 0 \, .$$

(4.201)

Consider $k = 2$ and plug the low-energy expansion of $\mathcal{M}_g(s, t)$ in the formula above. We get a matrix whose eigenvalues should be non-negative. In this way we can bound the

---

[32]Recall from Eq. (4.15) that $(\kappa/2)^2 = 8\pi G$.

constant term in the $++-+$ amplitude

$$\boxed{|g_{0,0}| \le \frac{7}{4}\frac{f_{0,0}}{(m_{\text{gap}}^2)^2} + \frac{5}{4}\frac{5f_{1,0} - 4|\beta_{R^3}|^2}{m_{\text{gap}}^2} + \frac{3}{2}\left(f_{2,0} + 3f_{2,1}\right).}$$ (4.202)

As in the previous section we can check Eq. (4.202) in the bosonic string theory. The extra data compared to the previous section takes the form

$$g_{0,0}^{(\text{bs})} = \left(\frac{\kappa}{2}\right)^2 \left(2\zeta_3\right), \quad \delta f_{2,0}^{(\text{bs})} = \left(\frac{\kappa}{2}\right)^2 \left(3 + 2\zeta(5)\right),$$
$$\delta f_{2,1}^{(\text{bs})} = \left(\frac{\kappa}{2}\right)^2 \left(2 + 4\zeta(3) + 2\zeta(5)\right).$$ (4.203)

Plugging Eq. (4.203) into Eq. (4.202) we see that it is indeed satisfied.

For the one-loop minimally coupled scalar we get correspondingly

$$g_{0,0}^{S=0} = \left(\frac{\kappa}{2}\right)^4 \frac{1}{(4\pi)^2} \frac{1}{6306300m^8}, \qquad f_{2,0}^{S=0} = \left(\frac{\kappa}{2}\right)^4 \frac{1}{(4\pi)^2} \frac{3}{560560m^8},$$
$$f_{2,1}^{S=0} = \left(\frac{\kappa}{2}\right)^4 \frac{1}{(4\pi)^2} \frac{31}{9081072m^8}.$$ (4.204)

Again, we checked that Eq. (4.202) is satisfied, where we set $m_{\text{gap}}^2 = 4m^2$.

Using the bounds from the previous section and Eq. (4.202) we can bound $g_{0,0}$ in terms of $\beta_{R^4}^+$ defined in Eq. (4.66) as follows

$$|g_{0,0}| \le \frac{815}{44} \frac{\beta_{R^4}^+}{m_{\text{gap}}^4}.$$ (4.205)

In deriving Eq. (4.205) we first expressed $f_{i,j}$, defined in Eq. (4.98), in terms of $a_{k,j}$, defined in Eq. (4.131), and then used Eqs. (4.138) and (4.146). Assuming LSD we get a stronger bound

$$\text{LSD}_{\alpha\to\infty}: \qquad |g_{0,0}| \le \frac{25}{4} \frac{\beta_{R^4}^+}{m_{\text{gap}}^4},$$ (4.206)

where in deriving this we used the stronger LSD bound Eq. (4.154).

4.7 Conclusions

Our paper naturally consisted of two parts with the first part providing theoretical data that we interpreted in the second part in terms of bounds on coefficients of gravitational

EFTs. In the first part, using amplitudes methods, we obtained the one-loop four-graviton amplitude with a minimally-coupled massive particle of spin up to $S = 2$ circulating in the loop. By series expanding these amplitude in large mass, we obtain theoretical data for Wilson coefficients which we analyze in the second part. Combining this data with similar theoretical data obtained from tree-level string-theory amplitudes we found that the Wilson coefficients fall on small islands compared to the general bounds coming from consistency of $2 \to 2$ scattering determined along the lines of Refs. [267, 268, 269]. It is quite striking that the EFT coefficients derived from both string-theory and one-loop-massive amplitudes land on the same small islands. Remarkably this can be explained as a consequence of low-spin dominance in the partial-wave expansions.

4.7.1 Obtaining one-loop amplitudes

In order to compute the one-loop amplitudes used to generate EFT data we applied standard amplitudes methods, including spinor helicity [6, 7, 8, 9, 10], generalized unitarity [19, 20, 22], the double copy [33, 35, 34] and integration by parts [325, 245, 246]. Using generalized unitarity we obtained all integral coefficients except for a few whose integrals have no unitarity cuts in any channel. We fixed the coefficients of the latter integrals by using the known ultraviolet properties of the amplitude. To fully utilize this information we made use of overcomplete integral basis that contains higher-dimensional integrals, but whose coefficients do not depend on the spacetime dimension or equivalently the dimensional-regularization parameter ϵ. In addition, we also demonstrated that these coefficients do not depend on the mass m of the particles circulating in the loops. The existence of such a basis imposes constraints that makes it reasonably straightforward to determine any pieces not captured by the s, t and u channel unitarity cuts. In this basis we used the fact that the coefficient of the potential $1/\epsilon$ logarithmic ultraviolet divergence is zero [320] to completely fix the remaining integral coefficients. A basis without ϵ-dependent coefficients always exists for one-loop problems [355], however the lack of m-dependence appears to be special to our case of a closed massive loop with external massless particles.

It would of course be interesting whether there is some way to generalize our approach to more complicated situations with external legs of differing masses. To generalize our approach to the generic case of a massive one-loop amplitude one could use information from the higher-than-logarithmic divergences which are accessible in dimensional regularization by shifting the dimension downwards as discussed in Sect. 4.2.5. We showed that knowledge of all these divergences is sufficient to fully constrain the remaining ambiguities, something we expect to be true more generally. We expect constraints from ultraviolet divergences and from requiring proper decoupling in the large mass limit to be sufficient to remove any ambiguities in terms that are not fixed by the unitarity cuts, up to the usual ambiguities tied to scheme choices and renormalization. This may provide an alternative method for obtaining complete one-loop amplitudes using on-shell techniques [284].

We exposed a useful supersymmetric decomposition for graviton amplitudes with a massive particle in the loop. A similar decomposition exists in gauge theory [302]. This decomposition expressed the amplitude with a particle of spin S in the loop in terms of amplitudes with lower-spin particles and simpler to calculate pieces. These pieces correspond to amplitudes with a massive BPS multiplet circulating in the loop.

Having constructed the one-loop four-graviton amplitudes with massive particles in the loop, it was then straightforward to expand in large mass, generating amplitudes matching those from a gravitational EFT. Because the original amplitudes are sensible, satisfying appropriate Regge behavior and unitarity, this EFT is also sensible and can be used to test the constraints derived from dispersion relations.

Besides using these results in our study of bounds on EFT coefficients, we also noted a simple relations between ultraviolet divergences in higher dimensions and the coefficients in the $1/m$ expansion. This relation requires a particular analytic continuation of the amplitude to higher dimensions where we keep the number of physical states at their four-dimensional values. It would be interesting to see if similar relations hold more generally, including higher loops, and whether this connection can be exploited in studies of bounds on EFT coefficients.

4.7.2 EFT bounds

In order to derive bounds on the Wilson coefficients, we first reviewed in Sect. 4.4 the basic properties of unitarity, crossing, and bounds on the Regge limit in the context of perturbative $2 \to 2$ scattering of gravitons in four dimensions. These allowed us to study dispersion relations and derive bounds on the Wilson coefficients.

In Sect. 4.5 we focused on the double-minus amplitude and derived bounds on the Wilson coefficients along the lines of Ref. [267, 268, 269]. We expressed the low-energy expansion coefficients as dispersive integrals in Eq. (4.134). We then identified the two-sided bounds on the coefficients following the observation in Ref. [269] that the boundaries of the allowed region inherit the cyclicity property from the one channel dispersion relation. In this way, by explicitly extracting the mixed constraints from the mixed s–u channel partial waves we identified the new boundaries of the allowed region. We do not rigorously prove that our identification of the bounds is optimal, and we leave filling this gap for future work. We then introduced the idea of LSD which expresses a relationship between moments of the spectral functions of various spins, and we used crossing symmetry or null constraints [268] to derive rigorous bounds in terms of a few low-spin partial waves. We found that all the amplitudes considered in this paper lie on small islands whose location and shape can be determined using the *low-spin dominance* principle.

In Sect. 4.6 we studied dispersion relations for the graviton amplitudes of various helicities. The key observation is that we can apply dispersion relations to matrices Eq. (4.102), composed of the different helicity amplitudes, whose discontinuity is positive semi-definite. Applying dispersive sum rules along the lines of Ref. [268] to these matrices we derived constraints on the Wilson coefficients which appear in the single-minus and all-plus gravitational scattering amplitudes. Notably we placed a bound on the R^3 coefficient that corrects the graviton three-point amplitude in terms of the R^4 coefficient, making a step towards making the analysis of Ref. [241] quantitatively precise.

The idea that the set of possibilities to UV complete gravity is much sparser than one naively would have thought lies at the heart of the swampland program [356, 357, 358, 359,

360]. Usually this sparseness is associated with non-perturbative aspects of the UV completion. In the present paper we analyzed the problem in a perturbative setting. By minimally coupling low-spin matter to gravity we generated S-matrices which we expect should satisfy the axioms of causality and unitarity up to an arbitrary order in G and in an arbitrary n-point amplitude. We can ask therefore a weaker version of the swampland question: what is the set of perturbatively consistent weakly-coupled gravitational S-matrices? It is in the framework of this question that the analysis of the present work can be placed. Unexpectedly, we found that in known examples of perturbatively consistent gravitational S-matrices the low-energy couplings lie in regions much smaller than predicted on general grounds of causality and positivity of $2 \rightarrow 2$ graviton scattering. Looking at the amplitudes for tree-level string theory and minimally coupled one-loop matter it is not a priori obvious at all that they should be "close" to each other. Dispersive representation of the low-energy expansion of both makes this similarity apparent. Indeed, as discussed in Sect. 4.5 both amplitudes satisfy strong versions of LSD that localizes their low-energy data to regions that are much smaller than indicated by the general analysis of unitarity and crossing.

An obvious question is: how general is this universality? We motivated it by pointing out that the examples considered in the present paper define consistent S-matrices for any $n \rightarrow m$ scattering, whereas the bounds were derived by considering $2 \rightarrow 2$ scattering only. To answer this question we would need to better understand the landscape of consistent gravitational amplitudes, including any unitary perturbative or nonperturbative QFT coupled to gravity, as well as amplitudes in theories with extra dimensions. In particular, it would be very interesting to understand if and how consistency of $n \rightarrow m$ scattering can be used to rigorously establish stronger bounds on $2 \rightarrow 2$ scattering, potentially bringing us closer to the small theory islands observed in the present work. It would also be very interesting to understand the example of large-N QCD coupled to gravity [279].

In this paper, we only considered the leading-order effect from integrating out massive degrees of freedom. We did not address the question of bounds that can be applied to IR-safe observables in four dimensions, nor have we included the loops of massless particles which

generate more general logarithmic corrections in the low-energy expansion of the amplitude. We leave these important questions to future work. The logarithmic running was discussed in Refs. [353, 281, 269], with the basic idea being that instead of expanding the amplitude around $s, t = 0$ one considers dispersive representations of the EFT couplings defined at some scale. To deal with the IR divergences we may consider dressed states (see e.g. Ref. [343, 342] for a recent discussion), for which the full implications of unitarity and crossing are still to be fully understood. Another interesting problem is to repeat the analysis of the present paper in the context of AdS_4/CFT_3 where the problem of IR divergences does not arise, but dispersive techniques discussed in the present paper still hold [361, 362, 363, 364, 280].

In summary, motivated by low-energy theoretical data obtained from one-loop field-theory and tree-level string-theory amplitudes, we put forward the idea that EFTs that describe sensible weak gravitational theories live on small islands that can be understood in terms of partial-wave low-spin dominance. It will be important to understand the extent to which this can be extended to constrain gravitational theories.

4.A   Minimal Coupling

In this appendix we present in more detail our definition of minimal coupling of gravity to a massive spinning particle. For massive spinning particles, the requirement of general-coordinate invariance and mass-dimension-4 operators leaves an ambiguity for integer spin-particles in defining the minimal coupling to gravity. In this appendix we discuss this ambiguity and the choice we make in this paper. Our choice corresponds to the one that does not violate the unitarity and causality constraints of Refs. [19, 20, 299, 365, 276, 242]. We start by reviewing the case of electromagnetism (EM) where a similar situation exists, before we move on to consider the gravitational case.

This issue appears only for integer-spin particles. The source of the ambiguity is the existence of a gauge-invariant operator that has the same mass dimension as the kinetic term. For half-integer-spin particles, the corresponding operator is of higher-mass dimension and hence would not count as minimal coupling. Therefore, the cases that require attention are the coupling of a spin-1 or spin-2 particle to gravity. Since the analysis of the coupling of a spin-1 particle to EM is similar, we start by reviewing this case.

Here we fix the ambiguity by requiring that the interactions smoothly match onto the massless limit. To explain our choice, it suffices to evaluate the three-point amplitude between two massive spinning particles and a photon or a graviton.[33] Specifically, we demand that by taking the massless limit of these amplitudes and identifying the spin-1 particles as gauge bosons and the spin-2 particles as gravitons, we recover the corresponding amplitudes in Yang-Mills and pure gravity. The former is indeed realized for the coupling of the W boson to the photon [366]. The double-copy construction used in this paper is smooth in the massless limit, and hence selects the above prescription.

For this discussion, we follow the formalism of Refs. [59, 46, 46], which allows us to

---

[33]In calculating this amplitude one implicitly uses complex kinematics.
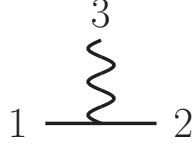
Figure 4.A.1: The three-point amplitude necessary to study minimal coupling. The straight lines represent massive spinning particles, while the wiggly line denotes either a photon or a graviton.

discuss particles of arbitrary spin.[34] After obtaining the relevant three-point amplitudes, we specialize to the cases of interest. The part of the Lagrangian we give is just the one necessary to obtain the three-point amplitudes relevant for this discussion. We emphasize that these Lagrangians would need to be modified with auxiliary-field terms in order to reproduce our one-loop calculation.

For the case of a massive spinning particle ϕ coupled to EM we have

$$\mathcal{L} = -\frac{1}{4}F_{\mu\nu}F^{\mu\nu} + D^\dagger_\mu\bar{\phi}D^\mu\phi - m^2\bar{\phi}\phi + e(g-1)F_{\mu\nu}\,\bar{\phi}M^{\mu\nu}\phi + \dots\,, \qquad (4.207)$$

where e is the charge of the particle, g is the gyromagnetic ratio and the ellipsis denote possible auxiliary-field terms. For the Lorentz generator M in the representation of ϕ we may use

$$(M^{\mu\nu})_{c(s)}{}^{d(s)} = 2is\delta^{[\mu}_{(c_1}\eta^{\nu](d_1}\delta^{d_2}_{c_2}\dots\delta^{d_s)}_{c_s)}\,, \qquad (4.208)$$

where the indices $c(s)$ and $d(s)$ stand for the symmetrized sets of vector indices $\{c_1,\dots,c_s\}$ and $\{d_1,\dots,d_s\}$ and symmetrizations include division by the number of terms.

We may now obtain the three-point amplitude between two massive spinning particles and a photon, depicted in Fig. 4.A.1. Neglecting the overall normalization we find

$$\mathcal{A}_3^{\text{EM}-s} \sim \varepsilon_1 \cdot \varepsilon_2\,\varepsilon_3 \cdot p_1 + i(g-1)\varepsilon_1 \cdot M[\varepsilon_3, p_3] \cdot \varepsilon_2\,, \qquad (4.209)$$

where labels 1 and 2 denote the massive spinning particles, while particle 3 is a photon. We

---

[34]Descriptions of higher-spin particles date back to Pauli and Fierz [367].

use the notation

$$A \cdot M[p,q] \cdot B \equiv p_\mu q_\nu (M^{\mu\nu})_{c(s)}{}^{d(s)} A^{c(s)} B_{d(s)} \,. \tag{4.210}$$

Plugging in the spin-1 representation for M we find

$$\mathcal{A}_3^{\text{EM}-1} \sim \varepsilon_1 \cdot \varepsilon_2 \, \varepsilon_3 \cdot p_1 + (g-1)\Big(\varepsilon_3 \cdot \varepsilon_1 \, \varepsilon_2 \cdot p_3 - \varepsilon_2 \cdot \varepsilon_3 \, \varepsilon_1 \cdot p_3\Big) \,. \tag{4.211}$$

Identifying all three particles as gauge bosons in the massless limit, i.e. demanding $\mathcal{A}_3^{\text{EM}-1} = \mathcal{A}_3^{\text{YM}}$, fixes $g = 2$.

The case of a massive spinning particle coupled to gravity is similar. In this case, we have

$$\mathcal{L} = -\frac{1}{16\pi G}R + \frac{1}{2}g^{\mu\nu}\nabla_\mu \phi \nabla_\nu \phi - \frac{1}{2}m^2 \phi\phi + \frac{\text{H}}{8}R_{\kappa\lambda\mu\nu}\,\phi M^{\kappa\lambda}M^{\mu\nu}\phi + \dots \,, \tag{4.212}$$

where H is an arbitrary dimensionless coefficient and we again denote possible auxiliary-field terms by the ellipsis. Plugging in the spin-1 representation we see that the Riemann tensor in the term proportional to H contracts into the Ricci tensor or scalar which under the equations of motion is equivalent to a ϕ^2 term. Therefore, the H term may be replaced by using an appropriate field redefinition by a ϕ^4-type term, which is not relevant for our discussion. Looking at the spin-2 representation and taking the massless limit, we recover the background-field-gauge gravitational Lagrangian of Ref. [368] for H $= 1$ upon identifying the spin-2 particle with the graviton.

We may alternatively reach the same conclusions by looking at the three-point amplitude between two massive spinning particles and a graviton. This amplitude, shown in Fig. 4.A.1, is given by

$$\mathcal{M}_3^{\text{GR}-s} \sim -\varepsilon_1 \cdot \varepsilon_2 (\varepsilon_3 \cdot p_1)^2 + i(\varepsilon_3 \cdot p_1)\varepsilon_1 \cdot M[\varepsilon_3, p_3] \cdot \varepsilon_2 + \frac{\text{H}}{2}\varepsilon_1 \cdot M[\varepsilon_3, p_3] \cdot M[\varepsilon_3, p_3] \cdot \varepsilon_2 \,. \tag{4.213}$$

For the spin-1 representation of M we observe that the last term vanishes. For the spin-2 representation we have

$$\begin{aligned}
\mathcal{M}_3^{\text{GR}-2} \sim &-\varepsilon_1 \cdot \varepsilon_2 (\varepsilon_3 \cdot p_1)^2 - 2\,\varepsilon_1^{\mu\kappa}\varepsilon_{2,\kappa}^\nu (\varepsilon_{3,\mu}p_{3,\nu} - \varepsilon_{3,\nu}p_{3,\mu})(\varepsilon_3 \cdot p_1) \\
&- \text{H}\,\varepsilon_1^{\mu\nu}\varepsilon_2^{\alpha\beta}(\varepsilon_{3,\mu}p_{3,\nu} - \varepsilon_{3,\nu}p_{3,\mu})(\varepsilon_{3,\alpha}p_{3,\beta} - \varepsilon_{3,\beta}p_{3,\alpha}) \,. \tag{4.214}
\end{aligned}$$

Identifying the spin-2 particles with gravitons, i.e. setting $\mathcal{M}_3^{\text{GR}-2}$ equal to the three-point amplitude in pure gravity, we find H = 1.

With this choice our one-loop amplitudes do not violate unitarity or causality constraints [19, 20, 276, 242, 241]. Hence, they serve as toy models of causal UV completions.

4.B   Tree-level string amplitudes

Here we collect the relevant string four-graviton tree-level amplitudes [33]

$$
\mathcal{M}_4^{(\text{ss})}(1^+, 2^-, 3^-, 4^+) = -\left(\frac{\kappa}{2}\right)^2 (\langle 23\rangle [14])^4 \frac{\Gamma(-s)\Gamma(-t)\Gamma(-u)}{\Gamma(1+s)\Gamma(1+t)\Gamma(1+u)} ,
$$

$$
\mathcal{M}_4^{(\text{hs})}(1^+, 2^-, 3^-, 4^+) = -\left(\frac{\kappa}{2}\right)^2 (\langle 23\rangle [14])^4 \frac{\Gamma(-s)\Gamma(-t)\Gamma(-u)}{\Gamma(1+s)\Gamma(1+t)\Gamma(1+u)} \left(1 - \frac{su}{t+1}\right) ,
$$

$$
\mathcal{M}_4^{(\text{bs})}(1^+, 2^-, 3^-, 4^+) = -\left(\frac{\kappa}{2}\right)^2 (\langle 23\rangle [14])^4 \frac{\Gamma(-s)\Gamma(-t)\Gamma(-u)}{\Gamma(1+s)\Gamma(1+t)\Gamma(1+u)} \left(1 - \frac{su}{t+1}\right)^2 ,
$$

$$(4.215)$$

where we set the closed string tension $\alpha' = 4$ and (ss), (hs), (bs) stand for superstring, heterotic string and bosonic string respectively. In the case of the bosonic string we have additional independent nonvanishing helicity configurations,

$$
\mathcal{M}_4^{(\text{bs})}(1^+, 2^+, 3^-, 4^+) = -\left(\frac{\kappa}{2}\right)^2 ([12][14]\langle 13\rangle)^4 \frac{\Gamma(-s)\Gamma(-t)\Gamma(-u)}{\Gamma(1+s)\Gamma(1+t)\Gamma(1+u)} ,
$$

$$
\mathcal{M}_4^{(\text{bs})}(1^+, 2^+, 3^+, 4^+) = -\left(\frac{\kappa}{2}\right)^2 \left(\frac{[12][34]}{\langle 12\rangle\langle 34\rangle}\right)^2 \frac{4s^2t^2u^2(1 - \frac{stu}{2})^2}{(1+s)^2(1+t)^2(1+u)^2}
$$
$$
\times \frac{\Gamma(-s)\Gamma(-t)\Gamma(-u)}{\Gamma(1+s)\Gamma(1+t)\Gamma(1+u)} . \qquad (4.216)
$$

In Sect. 4.5 we considered the dispersive representation of $f(s, u)$ and used it to derive various bounds on the Wilson coefficients. We focused on the polynomial expansion of the amplitudes at low energies around $s = t = 0$ which are generated by exchanges of massive states above a certain gap m_{gap}^2. To focus on such contributions let us write down explicitly the part of the amplitude due to the exchange by light states (in the case of strings these

are tachyon, dilaton, graviton)

$$f^{(\text{ss})}(s,u) = -\left(\frac{\kappa}{2}\right)^2 \frac{\Gamma(-s)\Gamma(-t)\Gamma(-u)}{\Gamma(1+s)\Gamma(1+t)\Gamma(1+u)} = \left(\frac{\kappa}{2}\right)^2 \frac{1}{stu} + \delta f^{(\text{ss})}(s,u)\,,$$

$$f^{(\text{hs})}(s,u) = -\left(\frac{\kappa}{2}\right)^2 \frac{\Gamma(-s)\Gamma(-t)\Gamma(-u)}{\Gamma(1+s)\Gamma(1+t)\Gamma(1+u)}\left(1 - \frac{su}{t+1}\right) = \left(\frac{\kappa}{2}\right)^2 \left(\frac{1}{stu} - \frac{1}{t}\right) + \delta f^{(\text{hs})}(s,u)\,,$$

$$f^{(\text{bs})}(s,u) = -\left(\frac{\kappa}{2}\right)^2 \frac{\Gamma(-s)\Gamma(-t)\Gamma(-u)}{\Gamma(1+s)\Gamma(1+t)\Gamma(1+u)}\left(1 - \frac{su}{t+1}\right)^2$$

$$= \left(\frac{\kappa}{2}\right)^2 \left(\frac{1}{stu} - \frac{1}{t+1} + \frac{su-2}{t}\right) + \delta f^{(\text{bs})}(s,u)\,, \tag{4.217}$$

where Disc $\delta f(s,u)$ is nonzero only for $s,t,u \geq m_{gap}^2 = 1$ and $\delta f(s,u)$ admits the low-energy expansion Eq. (4.98) with the dispersive representation of the couplings Eq. (4.134).

To write the dispersive representations for string amplitudes let us recall their Regge limit behavior. In the t-channel we have

$$\lim_{|t|\to\infty} |f^{(\text{ss,hs,bs})}(s,u)| \leq \frac{\text{const}}{|t|^2}\,, \qquad s \leq 0\,. \tag{4.218}$$

Therefore, we can write dispersion representation for $f(s,u)$ without subtractions and $\delta f(s,u)$ will take the form Eq. (4.133) and the corresponding bounds of Sect. 4.5.2 apply to $\delta f(s,u)$.

The situation is different in the s-channel relevant for Sect. 4.5.3. In this case we have

$$\lim_{|s|\to\infty} |f^{(\text{ss})}(s,u)| \leq \frac{\text{const}}{|s|^2}\,, \qquad t \leq 0\,, \tag{4.219}$$

$$\lim_{|s|\to\infty} |f^{(\text{hs})}(s,u)| \leq \text{const}\,, \qquad t \leq 0\,, \tag{4.220}$$

$$\lim_{|s|\to\infty} |f^{(\text{bs})}(s,u)| \leq \text{const}|s|^2\,, \qquad t \leq 0\,. \tag{4.221}$$

Therefore, for the heterotic and bosonic strings we would need to consider dispersion relations with subtractions. In Sect. 4.5.3 instead we directly considered the dispersive representation of the relevant couplings Eq. (4.177) in the expansion of $\delta f(s,u)$. As can be seen from Eq. (4.217) the s-channel Regge limit of $\delta f(s,u)$ coincides with the ones of the corresponding $f(s,u)$. In particular, the set of couplings that can admit a dispersive representation in the s-channel in the three cases correspond to $J_0^{(\text{ss})} = -2$, $J_0^{(\text{hs})} = 0$, $J_0^{(\text{bs})} = 2$, where J_0 is the Regge intercept see the discussion after Eq. (4.178).

In Sect. 4.6 we consider superconvergence relations applied to various helicity amplitudes. The relevant Regge limits for $g^{(\text{bs})}(s,u)$ and $h^{(\text{bs})}(s,u)$ can be easily read off from Eq. (4.216) and take the following form

$$\lim_{|t|\to\infty} |g^{(\text{bs})}(s,u)| \le \frac{\text{const}}{|t|^2}, \qquad s \le 0\,, \tag{4.222}$$

$$\lim_{|t|\to\infty} |h^{(\text{bs})}(s,u)| \le \text{const}|t|^2, \qquad s \le 0\,. \tag{4.223}$$

All the Regge bounds discussed in this section are in agreement with the general tree-level Regge bound Eq. (4.118).

4.C Bounding the coupling space at $k = 6$

In the main body of the paper we did not list the complete set of linear constraints that characterizes the space of admissible couplings in the case of $k = 6$. For completeness we list full set of constraints that we did not present in the main text. To reduce cluttering we avoid writing the subindices that we used in main text and specify which channel should be used in evaluating the determinant explicitly. The constraints are:

$\langle suuuuu\rangle$:

$$\begin{aligned}
\big\{ &\langle 2,4,5,6,7,9\rangle,\ \langle 4,4,5,7,8,9\rangle,\ -\langle 6,4,5,6,7,8\rangle,\ -\langle 6,4,5,6,8,9\rangle,\ -\langle 6,4,6,7,8,9\rangle,\\
&-\langle 2,5,6,7,k,k+1\rangle_{k\ge 9},\ -\langle 2,5,j,j+1,k,k+1\rangle_{k>j\ge 9},\ -\langle 4,5,7,8,k,k+1\rangle_{k\ge 9}, \quad (4.224)\\
&-\langle 4,5,8,9,k,k+1\rangle_{k\ge 10}\big\} \ge 0\,.
\end{aligned}$$

$\langle ssuuuu\rangle$:

$$\begin{aligned}
\big\{ &-\langle 2,4,5,7,k,k+1\rangle_{k\ge 9},\ -\langle 2,4,4,5,6,7\rangle,\ -\langle 2,4,4,5,7,9\rangle,\ -\langle 2,6,4,5,8,9\rangle,\\
&-\langle 4,6,4,5,6,7\rangle,\ -\langle 4,6,4,5,7,8\rangle,\ -\langle 4,6,5,6,7,8\rangle,\ \langle 2,4,4,5,8,9\rangle,\ \langle 2,6,4,5,6,9\rangle,\\
&\langle 2,6,4,6,7,9\rangle,\ \langle 4,6,4,7,8,9\rangle,\ \langle 4,8,5,6,7,8\rangle,\ \langle 2,4,5,9,k,k+1\rangle_{k\ge 10},\ \langle 2,6,6,7,k,k+1\rangle_{k\ge 9},\\
&\langle 2,6,5,6,k,k+1\rangle_{k\ge 9},\ \langle 6,8,5,6,k,k+1\rangle_{k\ge 8},\ \langle 2,4,j,j+1,k,k+1\rangle_{k>j\ge 9},\\
&\langle 4,6,j,j+1,k,k+1\rangle_{k>j\ge 7},\ \langle 6,8,j,j+1,k,k+1\rangle_{k>j\ge 6},\\
&\langle i,i+2,j,j+1,k,k+1\rangle_{i\ge 8;k>j\ge 5}\big\} \ge 0\,. \quad (4.225)
\end{aligned}$$

$\langle sssuuu \rangle$:

$$\big\{ -\langle 2,4,6,4,5,6 \rangle, \ -\langle 2,4,6,4,6,7 \rangle, \ -\langle 2,4,6,4,7,9 \rangle, \ \langle 2,4,6,4,5,8 \rangle, \ \langle 2,4,6,4,8,9 \rangle,$$

$$\langle 2,4,8,5,6,7 \rangle, \ \langle 4,6,8,5,6,8 \rangle, \ \langle 4,6,8,6,7,8 \rangle, \ \langle 2,4,6,7,k,k+1 \rangle_{k \geq 9},$$

$$\langle 2,i,i+2,5,j,j+1 \rangle_{i \geq 8; j \geq 6}, \ \langle 4,i,i+2,5,7,8 \rangle_{i \geq 8} \big\} \geq 0 \,. \tag{4.226}$$

$\langle ssssuu \rangle$:

$$\big\{ \langle 2,4,6,8,5,6 \rangle, \ -\langle 2,4,j,j+2,5,8 \rangle_{6 \leq j \leq 14}, \ \langle 2,4,j,j+2,5,7 \rangle_{j \geq 8}, \ -\langle 2,4,j,j+2,8,9 \rangle_{6 \leq j \leq 14},$$

$$-\langle 2,4,j,j+2,6,7 \rangle_{8 \leq j \leq 24}, \ -\langle 2,6,j,j+2,5,6 \rangle_{j \geq 8}, \ -\langle 2,4,j,j+2,k,k+1 \rangle_{j \geq 6, k \geq 9},$$

$$-\langle 4,6,j,j+2,k,k+1 \rangle_{j \geq 8, k \geq 6}, \ -\langle i,i+2,j,j+2,k,k+1 \rangle_{j > i \geq 6, k \geq 5} \big\} \geq 0 \,. \tag{4.227}$$

$\langle sssssu \rangle$:

$$\big\{ -\langle 2,4,6,j,j+2,6 \rangle_{j \geq 8}, \ -\langle 2,i,i+2,j,j+2,5 \rangle_{j > i \geq 6} \big\} \geq 0 \,. \tag{4.228}$$

In the above formulas, s indicates that in evaluating the determinant one should use i_s vectors in the corresponding position, whereas u means that the corresponding vector should be $j_u^{(6)}$. Note also that i_s take only even integer values. To summarize, the precise meaning of $\langle sssuuu \rangle : \langle 2,4,6,7,k,k+1 \rangle_{k \geq 9} \geq 0$ is

$$\langle \mathbf{a}_6, 2_s, 4_s, 6_s, 7_u^{(6)}, k_u^{(6)}, k_u^{(6)} + 1 \rangle_{k \geq 9} \geq 0 \,. \tag{4.229}$$

On the crossing-symmetric slice we found that the strongest constraints arise from the $\langle ssuuuu \rangle$ case. To generate Fig. 4.11 the maximal spin in the $\langle ssuuuu \rangle$ bounds above is set to $i_{max}, j_{max}, k_{max} = 20$. We used dispersive representations for the couplings truncated to $J_{max} = 100$ to check that all the determinants are non-negative. We found that the final allowed region for the couplings is not sensitive to the precise value of k_{max}.

4.D Amplitude with an accumulation point in the spectrum

In this appendix we analyze a toy model that violates the LSD property. Nevertheless, we find that the model still winds up on the LSD island. Consider the amplitude function

$$f(t,u) = -\frac{1}{(t-m_1^2)(u-m_1^2)(s-m_2^2)} \tag{4.230}$$
$$= \frac{1}{t-m_1^2}\frac{1}{m_1^2+m_2^2+t}\left(\frac{1}{s-m_2^2}+\frac{1}{u-m_1^2}\right),$$

where in the second line we rewrote the amplitude in the dispersive representation using partial fractions. For scattering of external scalars, a similar model with $m_1 = m_2$ was considered in [268]. This amplitude saturates the tree-level Regge bound and it has an accumulation point in its spectrum, by which we mean that the residue of the amplitude at either m_1 or m_2 involves infinitely many particles of all spins in the partial-wave expansion. Such models should not be considered physical, but nevertheless it is useful to illustrate features when LSD is violated.

Expanding the s- and u-channel residues in the corresponding partial waves we find that the amplitude is unitary for

$$m_2 \geq m_1. \tag{4.231}$$

Let us therefore set $m_1 = 1$ and study the model as a function of $m_2 \geq 1$.

It is easy to find $\rho_J^{++}(m_2^2)$ explicitly with the following result

$$-\frac{1}{t-1}\frac{1}{1+m_2^2+t}\bigg|_{t=-\frac{m_2^2}{2}(1-x)} = \sum_{J=0}^{\infty}\rho_J^{++}(m_2^2)\,d_{0,0}^J(x)\,, \tag{4.232}$$

where

$$\rho_J^{++}(m_2^2) = \frac{4(2J+1)}{m_2^2(2+m_2^2)}Q_J\left(\frac{2+m_2^2}{m_2^2}\right), \tag{4.233}$$

is determined by projecting the left-hand-side of Eq. (4.232) onto the Legendre polynomials. The function $Q_J(z)$ is the four-dimensional Legendre Q-function[35] that can be found in

---

[35]Note that the Mathematica LegendreQ function is defined somewhat differently. The precise relation is $Q_J(z) = \text{LegendreQ}[J, z+i0] - i\frac{\pi}{2}\text{LegendreP}[J, z]$ for $z > 1$.

Eq. (2.44) of Ref. [369]. By increasing m_2 we can make the spectral densities of non-minimal spin dominant. One way to understand this is by noting that the LHS of Eq. (4.232) develops a singularity at $x = \pm 1$ when $m_2 = \infty$ which translates into enhancement of higher-spin contributions. Therefore, Eq. (4.230) is an explicit example where LSD does not hold.

In the other channel we have

$$-\frac{1}{t-1}\frac{1}{1+m_2^2+t}\Big|_{t=-\frac{1}{2}(1-x)} = \sum_{J=4}^{\infty} \frac{\rho_J^{+-}(1)}{(\frac{1+x}{2})^4}d_{4,4}^J(x).$$
(4.234)

It is then straightforward to check that $\rho_J^{+-}(1)$ satisfies LSD with $\alpha \simeq 10$ for any value of m_2.

Curiously, if we now consider the values of the couplings $a_{k,j}$ for various values of m_2 they all end up being located at the LSD islands. For m_2 close to 1 it is manifest in the properties of the spectral densities described above. At large values of m_2 when the s-channel spectral density $\rho_J^{++}(m_2^2)$ violates the LSD property the reason is that its contribution to the low-energy couplings $a_{k,j}$ is suppressed by an extra factor of $\left(\frac{1}{m_2^2}\right)^{k-j}$ coming from the expansion of $\frac{1}{s-m_2^2}$ at small s, compared to the u-channel contribution that does satisfy $\alpha \simeq 10$ LSD. In other words, for $m_2 \gg 1$ we have $\langle \rho_J^{+-} \rangle_k \gg \langle \rho_J^{++} \rangle_k$.

To summarize, while Eq. (4.230) with an accumulation point in the spectrum does provide an example of an amplitude function which violates the LSD assumption at $\frac{m_2}{m_1} \gg 1$, from the low-energy couplings point of view it still ends up in the LSD island region because the $\rho_J^{++}(m_2^2)$ spectral function that violates the LSD property ends up being irrelevant. While this model should not be considered physical, it does illustrate the idea that potential violations of the LSD principle do not affect the location of the island if there is a separation of scales between the lowest-mass state and higher-mass physics that sources the violation.

4.E Wigner d-matrices

Here we list convenient formulas for Wigner d-matrices used in bulk of the paper

$$d_{4,4}^{J}(x) = 2^{-J}(x+1)^{J} \, _2F_1\left(-J-4, 4-J; 1; \frac{x-1}{x+1}\right), \tag{4.235}$$

$$d_{4,-4}^{J}(x) = \frac{2^{-J-7}}{315}\frac{\Gamma(J+5)}{\Gamma(J-3)}(1-x)^4(x+1)^{J-4}\, _2F_1\left(4-J, 4-J; 9; \frac{x-1}{x+1}\right), \tag{4.236}$$

$$d_{4,0}^{J}(x) = \frac{2^{-J-3}}{3}\sqrt{\frac{\Gamma(J+5)}{\Gamma(J-3)}}(1-x)^2(x+1)^{J-2}\, _2F_1\left(4-J, -J; 5; \frac{x-1}{x+1}\right), \tag{4.237}$$

$$d_{0,0}^{J}(x) = \, _2F_1\left(-J, J+1; 1; \frac{1-x}{2}\right). \tag{4.238}$$

By expanding the formulas above around $x = 1$ it is easy to check formulas Eq. (4.114), Eq. (4.115), and Eq. (4.116) for the first few n's. In Mathematica notation the $d_{\lambda_1,\lambda_2}^{J}(x)$ functions are given by WignerD$[\{J, \lambda_2, \lambda_1\}, \text{ArcCos}[x]]$. For a detailed derivation of the partial-wave expansion for spinning external particles see Ref. [341].

4.F Explicit values of one-loop four-graviton amplitudes

In this appendix we collect the final results for the integrated one-loop amplitudes. For the double-minus configuration, we give the results for the $\mathcal{M}_4^{\{S\}}$ defined in Eq. (4.32). The supersymmetric decomposition Eq. (4.32) directly gives the amplitude for any massive particle up to spin 2 circulating in the loop. For the single-minus and all-plus helicity configurations, we present the amplitude with a scalar particle circulating in the loop. The amplitudes with a higher-spin particle circulating in the loop are all proportional to this one as shown in Eq. (4.34). In this appendix we give the results for the amplitudes in terms of scalar integral functions whose values we cite in Appendix 4.G.

4.F.1 The double-minus configuration

We first give our results formally to all orders in the dimensional-regularization parameter ϵ. We write them in terms of an overcomplete basis that contains higher-dimensional integrals

as we find this form to be the most concise. This basis is chosen so that the coefficients of the integrals are free of both ϵ and m. As we explained in Appendix 4.G.2, using dimension-shifting relations the higher-dimension integrals are directly expressible in terms of standard $(4-2\epsilon)$-dimensional ones. We collect the explicit values of the $(4-2\epsilon)$-dimensional integrals to leading orders in ϵ [370, 371, 372, 373, 374, 375, 376, 377, 378, 379] in Appendix 4.G.1.

We manifest Bose symmetry under a $2 \leftrightarrow 3$ relabeling (which implies $s \leftrightarrow u$) by writing the amplitudes as

$$\mathcal{M}_4^{\{S\}}(1^+, 2^-, 3^-, 4^+) = -\frac{1}{(4\pi)^{2-\epsilon}} \left(\frac{\kappa}{2}\right)^2 \mathcal{M}_4^{\text{tree}}\left(F_1^{\{S\}}(s, u) + F_2^{\{S\}}(s, u) + F_2^{\{S\}}(u, s)\right),$$

(4.239)

where $F_1^{\{S\}}(s, u) = F_1^{\{S\}}(u, s)$ with kinematics in the Euclidean region, and the tree-level amplitude $\mathcal{M}_4^{\text{tree}}$ is given in Eq. (4.55).

For the $\mathcal{M}_4^{\{0\}}$ pieces we have

$$
\begin{aligned}
F_1^{\{0\}}(s, u) &= \frac{13s^4 + 52s^3 u + 75s^2 u^2 + 52su^3 + 13u^4}{96t^4} I_1 \\
&\quad - \frac{8s^4 + 40s^3 u + 55s^2 u^2 + 40su^3 + 8u^4}{8sut^3} I_1^{6-2\epsilon} \\
&\quad - \frac{(s^2 - su + u^2)^2 t}{64s^2 u^2} I_2(t) + \frac{1}{32}\left(16 - \frac{7s}{u} - \frac{7u}{s}\right) I_2^{6-2\epsilon}(t) - \frac{45}{16t} I_2^{8-2\epsilon}(t) \\
&\quad + \frac{s^8 + s^7 u + su^7 + u^8}{128s^3 u^3} I_3(t) - \frac{5(s^5 + u^5)}{64s^2 u^2} I_3^{6-2\epsilon}(t) + \frac{25(s^2 - su + u^2)}{32su} I_3^{8-2\epsilon}(t) \\
&\quad + \frac{105}{16t} I_3^{10-2\epsilon}(t) - \frac{s^5 u^5}{256t^7} I_4(s, u) + \frac{7s^4 u^4}{32t^6} I_4^{6-2\epsilon}(s, u) - \frac{105s^3 u^3}{32t^5} I_4^{8-2\epsilon}(s, u) \\
&\quad + \frac{105s^2 u^2}{8t^4} I_4^{10-2\epsilon}(s, u) - \frac{105su}{16t^3} I_4^{12-2\epsilon}(s, u),
\end{aligned}
$$

(4.240)

$$F_2^{\{0\}}(s,u) = -\frac{s^3(s^2 + 2su + 2u^2)(s^4 + 4s^3u + 5s^2u^2 + 2su^3 + u^4)}{64u^2t^6} I_2(s)$$

$$-\frac{s^2(7s^4 + 30s^3u + 50s^2u^2 + 40su^3 - 12u^4)}{32ut^5} I_2^{6-2\epsilon}(s)$$

$$-\frac{45s^4 + 118s^3u + 294s^2u^2 + 96su^3 + 16u^4}{16st^4} I_2^{8-2\epsilon}(s)$$

$$+\frac{s^6(s^6 + 7s^5u + 21s^4u^2 + 35s^3u^3 + 35s^2u^4 + 21su^5 + 7u^6)}{128u^3t^7} I_3(s)$$

$$+\frac{s^4(5s^5 + 25s^4u + 50s^3u^2 + 50s^2u^3 + 25su^4 + 32u^5)}{64u^2t^6} I_3^{6-2\epsilon}(s)$$

$$+\frac{5s^3(5s^3 + 15s^2u + 15su^2 - 32u^3)}{32ut^5} I_3^{8-2\epsilon}(s) + \frac{3s^2(35s + 128u)}{16t^4} I_3^{10-2\epsilon}(s)$$

$$-\frac{s^5t}{256u^3} I_4(s,t) - \frac{s^4}{32u^2} I_4^{6-2\epsilon}(s,t) - \frac{9s^3}{32tu} I_4^{8-2\epsilon}(s,t) - \frac{15s^2}{8t^2} I_4^{10-2\epsilon}(s,t)$$

$$-\frac{105su}{16t^3} I_4^{12-2\epsilon}(s,t). \tag{4.241}$$

For the $\mathcal{M}_4^{\{1/2\}}$ pieces we have

$$F_1^{\{1/2\}}(s,u) = \frac{4s^2 + 7su + 4u^2}{8t^2} I_1 + \frac{(s-u)^2t}{16su} I_2(t) + \frac{3}{4} I_2^{6-2\epsilon}(t) + \frac{(s^5 + u^5)t}{32s^2u^2} I_3(t)$$

$$+\frac{s^3 + u^3}{4su} I_3^{6-2\epsilon}(t) - \frac{15}{8} I_3^{8-2\epsilon}(t) - \frac{s^4u^4}{64t^5} I_4(s,u) + \frac{15s^3u^3}{32t^4} I_4^{6-2\epsilon}(s,u)$$

$$-\frac{45s^2u^2}{16t^3} I_4^{8-2\epsilon}(s,u) + \frac{15su}{8t^2} I_4^{10-2\epsilon}(s,u), \tag{4.242}$$

$$F_2^{\{1/2\}}(s,u) = \frac{s^3(s + 2u)(s^2 + 2su + 2u^2)}{16ut^4} I_2(s) + \frac{3s^3 + 7s^2u + 12su^2 + 2u^3}{4t^3} I_2^{6-2\epsilon}(s)$$

$$-\frac{s^4(s + 2u)(s^4 + 3s^3u + 4s^2u^2 + 2su^3 + u^4)}{32u^2t^5} I_3(s)$$

$$-\frac{s^3(2s^3 + 6s^2u + 6su^2 - 5u^3)}{8ut^4} I_3^{6-2\epsilon}(s) - \frac{3s^2(5s + 16u)}{8t^3} I_3^{8-2\epsilon}(s)$$

$$+\frac{s^4t}{64u^2} I_4(s,t) + \frac{3s^3}{32u} I_4^{6-2\epsilon}(s,t) + \frac{9s^2}{16t} I_4^{8-2\epsilon}(s,t) + \frac{15su}{8t^2} I_4^{10-2\epsilon}(s,t). \tag{4.243}$$

For the $\mathcal{M}_4^{\{1\}}$ pieces we have

$$F_1^{\{1\}}(s,u) = -\frac{t}{4} I_2(t) + \frac{s^4 + s^3u + su^3 + u^4}{8su} I_3(t) + \frac{3t}{4} I_3^{6-2\epsilon}(t) - \frac{s^3u^3}{16t^3} I_4(s,u)$$

$$+\frac{3s^2u^2}{4t^2} I_4^{6-2\epsilon}(s,u) - \frac{3su}{4t} I_4^{8-2\epsilon}(s,u), \tag{4.244}$$

176

$$F_2^{\{1\}}(s,u) = -\frac{s(s^2+2su+2u^2)}{4t^2} I_2(s) + \frac{s^4(s^2+3su+3u^2)}{8ut^3} I_3(s) + \frac{s^2(3s+8u)}{4t^2} I_3^{6-2\epsilon}(s)$$

$$-\frac{s^3 t}{16u} I_4(s,t) - \frac{s^2}{4} I_4^{6-2\epsilon}(s,t) - \frac{3su}{4t} I_4^{8-2\epsilon}(s,t). \tag{4.245}$$

For the $\mathcal{M}_4^{\{3/2\}}$ pieces we have

$$F_1^{\{3/2\}}(s,u) = -\frac{t^2}{2} I_3(t) - \frac{s^2 u^2}{4t} I_4(s,u) + \frac{su}{2} I_4^{6-2\epsilon}(s,u), \tag{4.246}$$

$$F_2^{\{3/2\}}(s,u) = -\frac{s^2(s+2u)}{2t} I_3(s) + \frac{s^2 t}{4} I_4(s,t) + \frac{su}{2} I_4^{6-2\epsilon}(s,t). \tag{4.247}$$

Finally, for the $\mathcal{M}_4^{\{2\}}$ pieces we have

$$F_1^{\{2\}}(s,u) = -stu\, I_4(s,u), \tag{4.248}$$

$$F_2^{\{2\}}(s,u) = -stu\, I_4(s,t). \tag{4.249}$$

We note that the progression of the new pieces from more complicated contributions to simpler ones as the spin increases is a direct consequence of the supersymmetric decomposition Eq. (4.32). As the spin increases the new pieces have lower and lower power counts corresponding to increasing supersymmetry. The final pieces Eq. (4.248) and Eq. (4.249) correspond to $D = (4 - 2\epsilon)$ scalar box integrals with no powers of loop momentum in the numerator. This may be compared to the $\mathcal{M}_4^{\{0\}}$ contribution which has 8 powers of loop momentum in the numerator. This high power count results in, for example, the $D = (12 - 2\epsilon)$ box integrals appearing in Eqs. (4.240) and (4.241).

Next we expand the above results to leading order in the dimensional-regularization parameter ϵ. Using Eq. (4.285) we express the higher-dimensional integrals in terms of $(4-2\epsilon)$-dimensional ones whose explicit values through $\mathcal{O}(\epsilon^0)$ are collected in Appendix 4.G.1. In the following expressions, the integrals are understood as truncated to this order.

Both $F_1^{\{S\}}$ and $F_2^{\{S\}}$ are ultraviolet divergent. However, when put together in Eq. (4.239), the ultraviolet divergence cancels as expected [326]. We expose this cancellation by separating the bubble integral in Eq. (4.277) into a divergent part $I_2(0)$ and a finite part defined in Eq. (4.279). After canceling the $1/\epsilon$-pole we write the amplitude as

$$\mathcal{M}_4^{\{S\}}(1^+, 2^-, 3^-, 4^+) = -\frac{1}{(4\pi)^2}\left(\frac{\kappa}{2}\right)^2 \mathcal{M}_4^{\text{tree}}(f_1^{\{S\}}(s,u) + f_2^{\{S\}}(s,u) + f_2^{\{S\}}(u,s)), \tag{4.250}$$

where $f_1^{\{S\}}(s,u) = f_1^{\{S\}}(u,s)$ and $f_{1,2}^{\{S\}}$ are ultraviolet finite.

For the $\mathcal{M}_4^{\{0\}}$ pieces corresponding to Eqs. (4.240) and (4.241) we have

$$f_1^{\{0\}}(s,u) = -\frac{1}{360t^5}\Big(540m^4 sut^2 + su(2s^4 + 23s^3 u + 222s^2 u^2 + 23su^3 + 2u^4)$$

$$- 2m^2 t(8s^4 + 5s^3 u - 366s^2 u^2 + 5su^3 + 8u^4)\Big)$$

$$-\frac{su}{2t^7}\Big(s^4 u^4 + 8m^2 s^3 u^3 t + 20m^4 s^2 t^2 u^2 + 16m^6 sut^3 + 2m^8 t^4\Big)I_4(s,u), \quad (4.251)$$

$$f_2^{\{0\}}(s,u) = \frac{u}{60st^6}\Big(2m^4 t^2(73s^3 - 147s^2 u - 48su^2 - 8u^3)$$

$$+ 2m^2 st(9s^4 + 78s^3 u - 105s^2 u^2 - 28su^3 - 4u^4)$$

$$+ s^2(s-u)(s^4 + 9s^3 u + 46s^2 u^2 + 9su^3 + u^4)\Big)I_2^{fin}(s)$$

$$-\frac{s^2 u}{t^7}(su + 2m^2 t)(s^2 u^2 + 4m^2 stu + 2m^4 t^2)\, I_3(s) - \frac{m^8 su}{t^3}I_4(s,t), \quad (4.252)$$

where the integrals are defined in Eqs. Eq. (4.277), Eq. (4.280) and Eq. (4.281). For the $\mathcal{M}_4^{\{1/2\}}$ pieces corresponding to Eqs. (4.242) and (4.243) we have

$$f_1^{\{1/2\}}(s,u) = -\frac{(s^2 + 14su + u^2 + 24m^2 t)su}{24t^3}$$

$$-\frac{(su + 2m^2 t)(s^2 u^2 + 4m^2 stu + m^4 t^2)su}{2t^5}I_4(s,u), \quad (4.253)$$

$$f_2^{\{1/2\}}(s,u) = \frac{\Big((s-u)(s^2 + 8su + u^2)s + 4m^2(-4s^3 + 2s^2 u + 7su^2 + u^3)\Big)u}{12t^4}I_2^{fin}(s)$$

$$-\frac{(su + 3m^2 t)(su + m^2 t)s^2 u}{t^5}I_3(s) - \frac{m^6 su}{t^2}I_4(s,t). \quad (4.254)$$

For the $\mathcal{M}_4^{\{1\}}$ pieces corresponding to Eqs. (4.244) and (4.245) we have

$$f_1^{\{1\}}(s,u) = -\frac{su}{2t} - \frac{(s^2 u^2 + 4m^2 stu + 2m^4 t^2)su}{2t^3}I_4(s,u), \quad (4.255)$$

$$f_2^{\{1\}}(s,u) = \frac{(s-u)su}{2t^2}I_2^{fin}(s) - \frac{(su + 2m^2 t)s^2 u}{t^3}I_3(s) - \frac{m^4 su}{t}I_4(s,t). \quad (4.256)$$

For the $\mathcal{M}_4^{\{3/2\}}$ pieces corresponding to Eqs. (4.246) and (4.247) we have

$$f_1^{\{3/2\}}(s,u) = -\frac{(su + 2m^2 t)su}{2t}I_4(s,u), \quad (4.257)$$

$$f_2^{\{3/2\}}(s,u) = -\frac{s^2 u}{t}I_3(s) - m^2 su\, I_4(s,t). \quad (4.258)$$

Finally, for the $\mathcal{M}_4^{\{2\}}$ pieces corresponding to Eqs. (4.248) and (4.249) we have

$$f_1^{\{2\}}(s,u) = -\,stu\,I_4(s,u)\,,\tag{4.259}$$

$$f_2^{\{2\}}(s,u) = -\,stu\,I_4(s,t)\,.\tag{4.260}$$

4.F.2 The all-plus configuration

As noted in Eq. (4.34), the result for particles of any spin $0 \leq S \leq 2$ circulating in the loop is proportional to the $S = 0$ case. The all-orders-in-ϵ form of this amplitude using the higher-dimensional integral basis is

$$\mathcal{M}_4^{S=0}(1^+,2^+,3^+,4^+) = \frac{1}{(4\pi)^{2-\epsilon}} \left(\frac{\kappa}{2}\right)^4 \left(\frac{[12][34]}{\langle 12\rangle\langle 34\rangle}\right)^2 \frac{1}{2}(F_3(s,t,u)\tag{4.261}$$

$$+\, F_4(s,t) + F_4(t,u) + F_4(u,s))\,,$$

where

$$F_3(s,t,u) = \frac{(s^2+t^2+u^2)^2}{64stu}\,I_1 - \frac{15}{4}\,I_1^{6-2\epsilon}\,,\tag{4.262}$$

$$\begin{aligned}F_4(s,t) = {}& \frac{u^2(s^3+t^3)^2}{32s^3t^3}\,I_2(u) + \frac{u^3(7s^2-16st+7t^2)}{16s^2t^2}\,I_2^{6-2\epsilon}(u) + \frac{45u^2}{8st}\,I_2^{8-2\epsilon}(u)\\
&+ \frac{u^4(s^7+t^7)}{64s^4t^4}\,I_3(u) + \frac{5u^3(s^5+t^5)}{32s^3t^3}\,I_3^{6-2\epsilon}(u) + \frac{25u^2(s^3+t^3)}{16s^2t^2}\,I_3^{8-2\epsilon}(u)\\
&- \frac{105u^2}{8st}\,I_3^{10-2\epsilon}(u) + \frac{s^4t^4}{128u^4}\,I_4(s,t) + \frac{s^3t^3}{16u^3}\,I_4^{6-2\epsilon}(s,t) + \frac{9s^2t^2}{16u^2}\,I_4^{8-2\epsilon}(s,t)\\
&+ \frac{15st}{4u}\,I_4^{10-2\epsilon}(s,t) + \frac{105}{8}\,I_4^{12-2\epsilon}(s,t)\,.\end{aligned}\tag{4.263}$$

There is no corresponding tree-level amplitude for the all-plus helicity. Instead, we choose the above spinor-helicity combination to be completely Bose symmetric. Given this choice, the combination in the parenthesis also has this property. Furthermore, we arrange our functions such that F_3 is completely Bose symmetric, while $F_4(s,t) = F_4(t,s)$.

The expression simplifies significantly if we expand in ϵ and drop the $\mathcal{O}(\epsilon)$ pieces. We

179

have

$$\mathcal{M}_4^{S=0}(1^+, 2^+, 3^+, 4^+) = \frac{1}{(4\pi)^2} \left(\frac{\kappa}{2}\right)^4 \left(\frac{[12][34]}{\langle 12 \rangle \langle 34 \rangle}\right)^2 \frac{1}{2} \left(-\frac{1}{120}(120m^4 + s^2 + t^2 + u^2) \right.$$

$$\left. + 2m^8(I_4(s,t) + I_4(t,u) + I_4(u,s)) + \mathcal{O}(\epsilon) \right). \quad (4.264)$$

Because the corresponding tree-level amplitude vanishes this amplitude is infrared finite. As for the other helicities it is ultraviolet finite because of the lack of a viable counterterm [326]. Another interesting property is that for $m \to 0$ it has no logarithms. The all-minus amplitude follows from parity and is given by swapping angle and square brackets.

4.F.3   The single-minus configuration

As for the all-plus case, for the single-minus configuration we only need the $S = 0$ case. The single-minus amplitude in a form valid to all orders in ϵ is

$$\mathcal{M}_4^{S=0}(1^+, 2^+, 3^-, 4^+) = \frac{1}{(4\pi)^{2-\epsilon}} \left(\frac{\kappa}{2}\right)^4 ([12]\langle 13 \rangle [14])^4 \frac{1}{2}(F_5(s,t,u) \quad (4.265)$$

$$+ F_6(s,t) + F_6(t,u) + F_6(u,s)).$$

We choose the little group combination to have complete Bose symmetry. The function F_5 is completely Bose symmetric, while $F_6(s,u) = F_6(u,s)$. We find

$$F_5(s,t,u) = \frac{(s^2 + t^2 + u^2)^2}{64(stu)^3} I_1 + \frac{246(stu)^2 - 9(s^2 + t^2 + u^2)^3}{4(stu)^4} I_1^{6-2\epsilon}, \quad (4.266)$$

$$F_6(s,u) = \frac{s^6 + u^6}{32 s^5 u^5} I_2(t) - \frac{s^4 + 2s^3 u - 2s^2 u^2 + 2su^3 + u^4}{16 s^4 u^4 t} I_2^{6-2\epsilon}(t)$$

$$- \frac{3(9s^4 + 22s^3 u + 42s^2 u^2 + 22su^3 + 9u^4)}{8 s^3 u^3 t^4} I_2^{8-2\epsilon}(t)$$

$$+ \frac{s^9 + 2s^8 u + s^7 u^2 + s^2 u^7 + 2su^8 + u^9}{64 s^6 u^6} I_3(t)$$

$$+ \frac{3(s^6 + s^5 u + su^5 + u^6)}{32 s^5 u^5} I_3^{6-2\epsilon}(t)$$

$$+ \frac{31s^6 + 93s^5 u + 93s^4 u^2 + 126 s^3 u^3 + 93 s^2 u^4 + 93 su^5 + 31 u^6}{16 s^4 u^4 t^3} I_3^{8-2\epsilon}(t)$$

$$+ \frac{3(29s^4 + 52s^3 u - 18s^2 u^2 + 52su^3 + 29u^4)}{8 s^3 u^3 t^4} I_3^{10-2\epsilon}(t) + \frac{s^2 u^2}{128 t^6} I_4(s,u)$$

$$- \frac{su}{16 t^5} I_4^{6-2\epsilon}(s,u) - \frac{15}{16 t^4} I_4^{8-2\epsilon}(s,u) - \frac{15}{4 sut^3} I_4^{10-2\epsilon}(s,u) + \frac{105}{8 s^2 t^2 u^2} I_4^{12-2\epsilon}(s,u).$$

$$(4.267)$$

Next, we expand the above amplitude to leading order in ϵ. We write

$$\mathcal{M}_4^{S=0}(1^+, 2^+, 3^-, 4^+) = \frac{1}{(4\pi)^2} \left(\frac{\kappa}{2}\right)^4 ([12]\langle 13\rangle [14])^4 \frac{1}{2}(f_5(s,t,u) \tag{4.268}$$

$$+ f_6(s,t) + f_6(t,u) + f_6(u,s)).$$

As in the double-minus configuration, we extract the ultraviolet poles from the bubble integrals in order to manifest the ultraviolet-divergence cancellation. In this way we may express the amplitude in terms of the ultraviolet-finite functions f_5 and f_6. We choose these functions such that f_5 is completely Bose symmetric and $f_6(s,u) = f_6(u,s)$. We have

$$f_5(s,t,u) = \frac{1}{360(stu)^4} \left((s^2 + t^2 + u^2)(stu)^2 - 15m^2(stu)(s^2 + t^2 + u^2)^2 \right.$$

$$\left. + m^4 \left(90(s^2 + t^2 + u^2)^3 - 2520(stu)^2 \right) \right), \tag{4.269}$$

and

$$f_6(s, u) = \frac{m^4}{s^3 u^3 t^4} \left(2s^4 + 5s^3 u + 5su^3 + 2u^4 \right) I_2^{\text{fin}}(t)$$

$$+ \frac{2m^4}{s^4 t^4 u^4} \Big(s^7 + 4s^6 u + 6s^5 u^2 + 4s^4 u^3 + 4s^3 u^4 + 6s^2 u^5 + 4su^6 + u^7$$

$$- m^2 (2s^5 u + 6s^4 u^2 + 6s^3 u^3 + 6s^2 u^4 + 2su^5) \Big) I_3(t)$$

$$+ \frac{m^4}{s^2 u^2 t^4} \left(s^2 u^2 + 4m^2 (stu) + 2m^4 t^2 \right) I_4(s, u). \tag{4.270}$$

As for the all-plus amplitude amplitude, because there is no corresponding tree-level ampli-tude there are no infrared singularities and again in the $m \to 0$ limit the expression is free of logarithms. The single-plus helicity configuration follows from parity.

4.F.4 Pure gravity

For completeness, we also give the corresponding one-loop amplitude with a massless graviton circulating in the loop. We obtain this result by taking the massless limit of the amplitude with a massive spin-2 particle circulating in the loop, after accounting for the additional states (see Eq. (4.29)). Our results match the ones previously obtained in Ref. [283].

Referring to this amplitude as $\mathcal{M}_4^{\text{GR}}$, for the all-plus configuration we have

$$\mathcal{M}_4^{\text{GR}}(1^+, 2^+, 3^+, 4^+) = \frac{-1}{(4\pi)^2} \left(\frac{\kappa}{2} \right)^4 \left(\frac{[12][34]}{\langle 12 \rangle \langle 34 \rangle} \right)^2 \frac{s^2 + t^2 + u^2}{120}, \tag{4.271}$$

while for the single-minus configuration we find [368]

$$\mathcal{M}_4^{\text{GR}}(1^+, 2^+, 3^-, 4^+) = \frac{1}{(4\pi)^2} \left(\frac{\kappa}{2} \right)^4 ([12]\langle 13 \rangle [14])^4 \frac{s^2 + t^2 + u^2}{360(stu)^2}. \tag{4.272}$$

182

For the double-minus configuration the amplitude takes the form

$$\mathcal{M}_4^{\mathrm{GR}}(1^+, 2^-, 3^-, 4^+) = \frac{r_\Gamma}{(4\pi)^{2-\epsilon}} \left(\frac{\kappa}{2}\right)^2 stu \mathcal{M}_4^{\mathrm{tree}} \left[\vphantom{\frac{4s^6}{t^8}} \right.$$

$$\frac{2}{\epsilon} \frac{1}{stu} \left(s \log\left(\frac{-s}{\mu^2}\right) + t \log\left(\frac{-t}{\mu^2}\right) + u \log\left(\frac{-u}{\mu^2}\right) \right)$$

$$+ \frac{2}{stu} \left(u \log\left(\frac{-t}{\mu^2}\right) \log\left(\frac{-s}{\mu^2}\right) + t \log\left(\frac{-s}{\mu^2}\right) \log\left(\frac{-u}{\mu^2}\right) + s \log\left(\frac{-t}{\mu^2}\right) \log\left(\frac{-u}{\mu^2}\right) \right)$$

$$+ \frac{4s^6 + 14s^5 u + 28s^4 u^2 + 35s^3 u^3 + 28s^2 u^4 + 14su^5 + 4u^6}{t^8} \left(\log^2\left(\frac{s}{u}\right) + \pi^2 \right)$$

$$+ \frac{(s-u)(261s^4 + 809s^3 u + 1126s^2 u^2 + 809su^3 + 261u^4)}{30t^7} \log\left(\frac{s}{u}\right)$$

$$+ \left. \frac{1682s^4 + 5303s^3 u + 7422s^2 u^2 + 5303su^3 + 1682u^4}{180t^6} \right], \tag{4.273}$$

where

$$r_\Gamma = \frac{\Gamma(1+\epsilon)\Gamma^2(1-\epsilon)}{\Gamma(1-2\epsilon)}. \tag{4.274}$$

Here μ is an infrared dimensional regularization scale. Since massless gravitons circulate in the loop there is an infrared divergence. On the other hand there is no ultraviolet divergence because there is no available counterterm [326]. In this expression we use the four-dimensional helicity scheme [286, 287]. For the massless case the analytic continuation from the Euclidean region to the physical one is simple and accomplished by taking $\log(-s) \to \log(s) - i\pi$. We have explicitly verified that our results for the graviton in the loop match the ones calculated in Ref. [283], up to the opposite sign for the $\mathcal{M}_4^{\{1/2\}}$ piece already noted in Ref. [329].

4.G   Values of one-loop integrals

In this appendix we give the values of the integrals appearing in the amplitudes collected in Appendix 4.F. We first present the $(4-2\epsilon)$-dimensional integrals and then discuss the higher-dimensional integrals. Furthermore, we provide an algorithmic procedure for obtaining an expression for the amplitudes with no ϵ or mass dependence in the integral coefficients.

4.G.1 Explicit values of one-loop integrals

We now collect the values for the integrals appearing in the above amplitudes [370, 371, 372, 373, 374, 375, 376, 377, 378, 379]. We present the integrals in the unphysical Euclidean region where $s, t, u < 0$ and then discuss the analytic continuation to the physical region. We define a generic D-dimensional n-point integral by

$$I_n^D = i(-1)^{n+1}(4\pi)^{D/2} \int \frac{d^D p}{(2\pi)^D} \frac{1}{(p^2 - m^2)((p-p_1)^2 - m^2) \cdot ((p - p_{n-1})^2 - m^2)}, \quad (4.275)$$

where the p_i's are linear combinations of the external momenta. The integral I_n^D is also labeled by the specific choice of the p_i's. For example, we use $I_2^D(s)$ for a D-dimensional bubble integral that has an invariant mass square of $s = (k_1 + k_2)^2$ flowing through its external legs. Similarly, we use $I_3^D(s)$ and $I_4^D(s,t)$ for a D-dimensional triangle and box respectively, where we use all scales that may appear in the integral as arguments of the corresponding function. When dealing with a $(4 - 2\epsilon)$-dimensional integral we suppress the superscript writing $I_n^{4-2\epsilon} \equiv I_n$.

For the purposes of this paper it is sufficient to present the explicit expressions for the $(4 - 2\epsilon)$-dimensional, one- through four-point integrals up to $\mathcal{O}(\epsilon^0)$. The tadpole (one-point) integral takes the form

$$I_1 = m^{2-2\epsilon} \frac{\Gamma(1 + \epsilon)}{\epsilon(\epsilon - 1)}. \quad (4.276)$$

The bubble (two-point) integral with a kinematic invariant s is given by

$$I_2(s) = I_2(0) + I_2^{fin}(s) + \mathcal{O}(\epsilon), \quad (4.277)$$

where

$$I_2(0) = m^{-2\epsilon} \frac{\Gamma(1 + \epsilon)}{\epsilon} = \frac{1}{\epsilon} + \mathcal{O}(\epsilon^0), \quad (4.278)$$

and

$$I_2^{fin}(s) = 2 + x^{(s)} \log \left(\frac{x^{(s)} - 1}{x^{(s)} + 1} \right), \quad (4.279)$$

184

with $x^{(s)} \equiv \sqrt{1 - 4m^2/s}$. The triangle (three-point) integral is

$$I_3(s) = -\frac{1}{2s} \log^2 \left(\frac{x^{(s)} + 1}{x^{(s)} - 1} \right) + \mathcal{O}(\epsilon) \,. \tag{4.280}$$

Finally, the box (four-point) integral is given by

$$I_4(s,t) = \frac{2}{stx^{(st)}} \left[2\log^2 \left(\frac{x^{(st)} + x^{(s)}}{x^{(st)} + x^{(t)}} \right) + \log \left(\frac{x^{(st)} - x^{(s)}}{x^{(st)} + x^{(s)}} \right) \log \left(\frac{x^{(st)} - x^{(t)}}{x^{(st)} + x^{(t)}} \right) - \frac{\pi^2}{2} \right.$$
$$\left. + \sum_{i=s,t} \left(2\text{Li}_2 \left(\frac{x^{(i)} - 1}{x^{(st)} + x^{(i)}} \right) - 2\text{Li}_2 \left(-\frac{x^{(st)} - x^{(i)}}{x^{(i)} + 1} \right) - \log^2 \left(\frac{x^{(i)} + 1}{x^{(st)} + x^{(i)}} \right) \right) \right] \,,$$

$$\tag{4.281}$$

where $x^{(st)} \equiv \sqrt{1 - 4m^2/s - 4m^2/t}$. To evaluate the expressions in physical regions, e.g. $s > 0$, $t, u < 0$, we need to account for the $i\epsilon$ prescription which for all our integrals is obtained by shifting the mass by $m^2 \to m^2 - i\epsilon$.

In order to match to the low-energy EFT, we expand the above integrals in the large-mass limit. It is straightforward to expand the tadpole, bubble and triangle integrals in this limit.

For the box integral we use

$$I_4(s,t) = \frac{1}{6m^4} + \frac{s+t}{60m^6} + \frac{2s^2 + st + 2t^2}{840m^8} + \frac{(s+t)(3s^2 - 2st + 3t^2)}{7560m^{10}}$$
$$+ \frac{12s^4 + 3s^3t + 2s^2t^2 + 3st^3 + 12t^4}{166320m^{12}} + \frac{(s+t)(10s^4 - 8s^3t + 9s^2t^2 - 8st^3 + 10t^4)}{720720m^{14}}$$
$$+ \frac{60s^6 + 10s^5t + 4s^4t^2 + 3s^3t^3 + 4s^2t^4 + 10st^5 + 60t^6}{21621600m^{16}}$$
$$+ \frac{105s^7 + 15s^6t + 5s^5t^2 + 3s^4t^3 + 3s^3t^4 + 5s^2t^5 + 15st^6 + 105t^7}{183783600m^{18}}$$
$$+ \frac{280s^8 + 35s^7t + 10s^6t^2 + 5s^5t^3 + 4s^4t^4 + 5s^3t^5 + 10s^2t^6 + 35st^7 + 280t^8}{2327925600m^{20}}$$
$$+ \frac{252s^9 + 28s^8t + 7s^7t^2 + 3s^6t^3 + 2s^5t^4 + 2s^4t^5 + 3s^3t^6 + 7s^2t^7 + 28st^8 + 252t^9}{9777287520m^{22}}$$
$$+ \frac{1}{449755225920m^{24}}\Big(2520s^{10} + 252s^9t + 56s^8t^2 + 21s^7t^3 + 12s^6t^4 + 10s^5t^5$$
$$+ 12s^4t^6 + 21s^3t^7 + 56s^2t^8 + 252st^9 + 2520t^{10}\Big)$$
$$+ \frac{1}{1873980108000m^{26}}\Big(2310s^{11} + 210s^{10}t + 42s^9t^2 + 14s^8t^3 + 7s^7t^4 + 5s^6t^5$$
$$+ 5s^5t^6 + 7s^4t^7 + 14s^3t^8 + 42s^2t^9 + 210st^{10} + 2310t^{11}\Big)$$
$$+ \frac{1}{101194925832000m^{28}}\Big(27720s^{12} + 2310s^{11}t + 420s^{10}t^2 + 126s^9t^3 + 56s^8t^4$$
$$+ 35s^7t^5 + 30s^6t^6 + 35s^5t^7 + 56s^4t^8 + 126s^3t^9$$
$$+ 420s^2t^{10} + 2310st^{11} + 27720t^{12}\Big)$$
$$+ \mathcal{O}(m^{-30}). \tag{4.282}$$

4.G.2 Higher-dimension integrals

In constructing the amplitudes we used an overcomplete basis of integrals containing both $(4-2\epsilon)$- and higher-dimensional integrals, which as we noted has the advantage of removing ϵ and m dependence from the integral coefficients. We now explain the construction of this form of the amplitudes and how one returns to the usual integral basis containing only the $(4-2\epsilon)$-dimensional scalar integrals introduced in Eq. (4.7). In the $(4-2\epsilon)$-dimension form the coefficients of the integrals have explicit ϵ and m dependence. As we discussed in Sect. 4.2.6, the basis including higher-dimension integrals is useful for exploiting known

properties of the amplitude in order to fix the coefficients a_0 and b_0 in Eq. (4.7), which we cannot obtain from the generalized-unitarity cuts.

Higher-dimension integrals occur naturally in the course of evaluating the loop integrands. Integrals with powers of the higher-dimensional components of loop momentum μ (defined in Eq. (4.42)) in the numerator may be expressed directly in terms of higher-dimensional integrals. Following Ref. [22] we have,

$$\int \frac{d^4\ell}{(2\pi)^4} \frac{d^{-2\epsilon}\mu}{(2\pi)^{-2\epsilon}} \frac{(\mu^2)^r}{D_{abcd}} = \mathcal{P}(\epsilon, r)(4\pi)^r \int \frac{d^{4+2r-2\epsilon}L}{(2\pi)^{4+2r-2\epsilon}} \frac{1}{D_{abcd}}, \qquad (4.283)$$

where the loop momentum on the right-hand side is integrated over a $(4+2r-2\epsilon)$-dimensional space, D_{abcd} is defined in Eq. (4.23), and

$$\mathcal{P}(\epsilon, 0) = 1, \qquad \mathcal{P}(\epsilon, r) = -\epsilon(1-\epsilon)(2-\epsilon)\dots(r-1-\epsilon), \quad r > 0. \qquad (4.284)$$

The resulting higher-dimensional integrals may be expressed in terms the $(4-2\epsilon)$-dimensional ones using the dimension-shifting formula [380, 290, 290]:

$$I_n^{D+2} = \frac{1}{(n-D-1)c_0}\left[2I_n^D - \sum_{i=1}^{n} c_i I_{n-1}^{D(i)}\right], \qquad (4.285)$$

which holds for any spacetime dimension D and $n \le 5$. I_n^D refers to an n-gon integral in D dimensions, defined in Eq. (4.275). We use $I_{n-1}^{D(i)}$ for the integral obtained by I_n^D by removing the propagator between legs $(i-1)$ and i. The c_i are combinations of kinematic factors given by

$$c_i = \sum_{j=1}^{n} S_{ij}^{-1}, \qquad c_0 = \sum_{i=1}^{n} c_i, \qquad (4.286)$$

where the matrix S for the cases of interest to us is given by

$$S_{ij} = m^2 - \frac{1}{2}p_{ij}^2, \qquad \text{with} \qquad p_{ij} = p_{i-1} - p_{j-1}. \qquad (4.287)$$

For example, a $(6-2\epsilon)$-dimensional box integral is expressed in terms of a $(4-2\epsilon)$-dimensional box and four $(4-2\epsilon)$-dimensional triangles, illustrated in Fig. 4.G.1.

Using Eq. (4.285), we can reduce an expression that contains higher-dimensional integrals to one that does not. For the reverse process, i.e. in order to eliminate all ϵ and m dependence
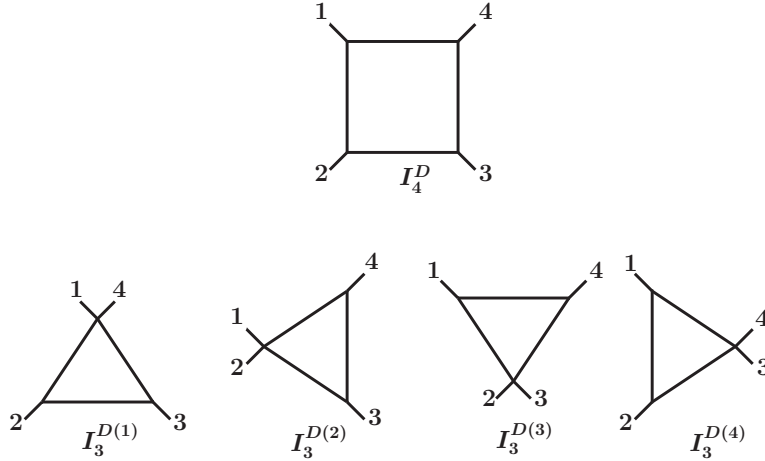
Figure 4.G.1: The D-dimensional box integral and its four triangle-integral daughters.

in a one-loop amplitude $\mathcal{M}_4^{\text{1-loop}}$, we adopt the following strategy: We start by inspecting the coefficients of the boxes, which take the following schematic form

$$\mathcal{M}_4^{\text{1-loop}} = \frac{P(\epsilon)Q(s,t,m)}{(4-(4-2\epsilon)-1)(4-(6-2\epsilon)-1)(4-(8-2\epsilon)-1)(4-(10-2\epsilon)-1)}I_4$$
$$+ \dots$$

(4.288)

where $P(\epsilon)$ is at most an order-four polynomial in ϵ that does not cancel any of the poles of the expression and $Q(s,t,m)$ is some rational function. The maximum degree in ϵ is directly tied to the maximal power of loop momentum that can appear in the numerator for minimally-coupled gravity. Here we assume the highest possible power of loop momentum, which corresponds to a spin-0 particle circulating in the loop. I_4 in Eq. (4.288) stands for a box integral in our amplitude, whose arguments we do not specify since we are being schematic. This discussion applies to all box integrals in our amplitude. The ellipsis contains other master integrals and their coefficients. Looking at Eq. (4.285), we may identify this term as coming from the $I_4^{12-2\epsilon}$ integral,

$$\mathcal{M}_4^{\text{1-loop}} = P(\epsilon)Q'(s,t,m)I_4^{12-2\epsilon} + \dots,$$

(4.289)

where $Q'(s,t,m)$ is some new rational function. Note that the ellipsis also changes as dictated

188

by Eq. (4.285). Now we may set $D = 4 - 2\epsilon$ in Eq. (4.285) and rewrite it as follows,

$$\epsilon I_n^{6-2\epsilon} = \frac{1}{2c_0}[2I_n - \sum_{i=1}^{n} c_i I_{n-1}^{(i)} - c_0(n-5)I_n^{6-2\epsilon}], \qquad (4.290)$$

where $I_n^{4-2\epsilon} \equiv I_n$. Similarly, setting $D = 6 - 2\epsilon$ in Eq. (4.285) we get

$$\epsilon I_n^{8-2\epsilon} = \frac{1}{2c_0}[2I_n^{6-2\epsilon} - \sum_{i=1}^{n} c_i I_{n-1}^{6-2\epsilon(i)} - c_0(n-7)I_n^{8-2\epsilon}], \qquad (4.291)$$

etc. Combining the two we may trade for example $\epsilon^2 I_n^{8-2\epsilon}$ for an expression containing $I_n^{8-2\epsilon}$, $I_n^{6-2\epsilon}$, I_n and lower-point integrals with ϵ dependence only in the coefficients of the lower-point integrals. In this fashion we turn Eq. (4.289) into

$$\mathcal{M}_4^{\text{1-loop}} = \sum_{r=0}^{4} Q_r(s,t) I_4^{4+2r-2\epsilon} + \dots \qquad (4.292)$$

with some different rational functions $Q_r(s,t)$. In this way we eliminate all explicit ϵ and m dependence in the coefficients of the boxes (we discuss the m dependence momentarily). Only after this step is completed, the poles in ϵ in the coefficients of the triangles have a similar interpretation, i.e. as coming from higher-dimensional triangles. This is because there is a feed down from the coefficients of the boxes to those of the triangles due to Eq. (4.285). The fact that the poles of the triangles align correctly is a nontrivial check of our calculation. We repeat this process sequentially for all lower-point integrals to completely remove the explicit ϵ and m dependence in the coefficients.

This procedure always succeeds. The reason is that there exists an alternative process of reducing the integrals to master integrals that does not introduce any explicit ϵ dependence, but instead introduces these higher-dimensional integrals (for an extensive discussion we refer the reader to Appendix I of Ref. [355]). The existence of such a process guarantees the success of a procedure like the one outlined above. In addition, we may understand why there is no m dependence in the coefficients of the master integrals in this basis as follows: We imagine performing the calculation in a covariant gauge, in which all propagators in the integrals have the canonical form $(p^2 - m^2)$, and there are no other poles in the loop momentum or the mass. We use

$$m^2 = L^2 - (L^2 - m^2), \qquad \mu^2 = -L^2 + \ell^2 \qquad (4.293)$$

189

to trade all m and μ dependence in the coefficients for tensor integrals and lower-point integrals. Once all m and μ dependence has been eliminated in this way, we may reduce the tensor integrals using the IBP reduction procedure described in Appendix I of Ref. [355]. The resulting expression contains higher-dimensional integrals without ϵ or m dependence.

4.H   High-order expansion of the one-loop four-graviton amplitudes in the large-mass limit

In this appendix, we present the large-mass expansion of our one-loop four-graviton amplitudes through $\mathcal{O}(m^{-20})$. We give the amplitudes in terms of loop integrals in Appendix 4.F. We obtain the results of this appendix by expanding the ones of Appendix 4.F in the large-mass limit. We give the values and expansion of the integrals in Appendix 4.G.1. The present representation corresponds to low-energy effective description of the gravitational theories under consideration.

The data contained here should be useful for systematic investigations at higher orders in the $1/m$ expansion than carried out in this paper. The examples in Sects. 4.5-4.6 based on low orders in the expansion suggest that Wilson coefficients in physical theories lie on small islands in the allowed parameter space. Rather strikingly, these islands are one dimensional to a good approximation, which is due to the LSD property. Rather remarkably the string-theory data we use also satisfy similar properties, so the Wilson coefficients obtained from string theory also populate these islands. We hope that the data presented here will facilitate further investigations of these features.

Using the amplitudes expanded in the large-mass limit one may obtain the low-energy effective description of the theory, along the lines of Sect. 4.3. Besides the operators present in the action of Eq. (4.66), one should include operators of the schematic form $D^{2k}R^4$. The operators $D^{2k}R^4$ correspond to the terms of $\mathcal{O}(m^{-(4+2k)})$.

We organize the amplitudes in a supersymmetric decomposition Eq. (4.32) in terms of the new contributions for a given spin, $\mathcal{M}_4^{\{S\}}$. We may then assemble these pieces into

the contributions for a particle of a given spin circulating in the loop using Eq. (4.32). Regarding the double-minus configuration, starting with the spin-0 contribution and moving to the additional new pieces through spin 2, we have,

$$f^{\{0\}}(s,u) = \mathcal{K}\left(\frac{1}{6300m^4} + \frac{t}{41580m^6}\right.$$

$$+ \frac{81(s^2+u^2)+155su}{15135120m^8} + \frac{t\left(161(s^2+u^2)+324su\right)}{151351200m^{10}}$$

$$+ \frac{3556(s^4+u^4)+14035(s^3u+su^3)+21030s^2u^2}{15437822400m^{12}}$$

$$+ \frac{t\left(2052(s^4+u^4)+8218(s^3u+su^3)+12287s^2u^2\right)}{41902660800m^{14}}$$

$$+ \frac{4634(s^6+u^6)+27650(s^5u+su^5)+69026(s^4u^2+s^2u^4)+91987s^3u^3}{430200650880m^{16}}$$

$$+ \frac{t\left(87780(s^6+u^6)+526770(s^5u+su^5)+1314684(s^4u^2+s^2u^4)+1752653s^3u^3\right)}{37104806138400m^{18}}$$

$$+ \frac{2551824(s^8+u^8)+20357964(s^7u+su^7)+71183961(s^6u^2+s^2u^6)}{4823624797992000m^{20}}$$

$$+ \left.\frac{142285437(s^5u^3+s^3u^5)+177823240s^4u^4}{4823624797992000m^{20}}\right), \tag{4.294}$$

$$f^{\{1/2\}}(s,u) = \mathcal{K}\left(\frac{1}{1120m^4} + \frac{t}{8400m^6}\right.$$

$$+ \frac{15(s^2+u^2)+28su}{554400m^8} + \frac{t\left(153(s^2+u^2)+313su\right)}{30270240m^{10}}$$

$$+ \frac{665(s^4+u^4)+2596(s^3u+su^3)+3890s^2u^2}{605404800m^{12}}$$

$$+ \frac{t\left(581(s^4+u^4)+2345(s^3u+su^3)+3495s^2u^2\right)}{2572970400m^{14}}$$

$$+ \frac{29106(s^6+u^6)+172676(s^5u+su^5)+430955(s^4u^2+s^2u^4)+574230s^3u^3}{586637251200m^{16}}$$

$$+ \frac{t\left(34440(s^6+u^6)+207564(s^5u+su^5)+517436(s^4u^2+s^2u^4)+690109s^3u^3\right)}{3226504881600m^{18}}$$

$$+ \frac{39270(s^8+u^8)+312240(s^7u+su^7)+1091604(s^6u^2+s^2u^6)}{16491024950400m^{20}}$$

$$+ \left.\frac{2181716(s^5u^3+s^3u^5)+2726549s^4u^4}{16491024950400m^{20}}\right), \tag{4.295}$$

$$f^{\{1\}}(s,u) = \mathcal{K}\left(\frac{1}{180m^4} + \frac{t}{1680m^6} \right.$$

$$+ \frac{22(s^2+u^2)+39su}{151200m^8} + \frac{t\big(20(s^2+u^2)+43su\big)}{831600m^{10}}$$

$$+ \frac{825(s^4+u^4)+3125(s^3u+su^3)+4684s^2u^2}{151351200m^{12}}$$

$$+ \frac{t\big(315(s^4+u^4)+1308(s^3u+su^3)+1930s^2u^2\big)}{302702400m^{14}}$$

$$+ \frac{1036(s^6+u^6)+6027(s^5u+su^5)+15036(s^4u^2+s^2u^4)+20030s^3u^3}{4410806400m^{16}}$$

$$+ \frac{t\big(7056(s^6+u^6)+43316(s^5u+su^5)+107555(s^4u^2+s^2u^4)+143715s^3u^3\big)}{146659312800m^{18}}$$

$$+ \frac{11760(s^8+u^8)+92232(s^7u+su^7)+322372(s^6u^2+s^2u^6)}{1075501627200m^{20}}$$

$$+ \left. \frac{644205(s^5u^3+s^3u^5)+805050s^4u^4}{1075501627200m^{20}} \right), \tag{4.296}$$

$$f^{\{3/2\}}(s,u) = \mathcal{K}\left(\frac{1}{24m^4} + \frac{t}{360m^6} \right.$$

$$+ \frac{9(s^2+u^2)+14su}{10080m^8} + \frac{t\big(8(s^2+u^2)+21su\big)}{75600m^{10}}$$

$$+ \frac{10(s^4+u^4)+34(s^3u+su^3)+51s^2u^2}{332640m^{12}}$$

$$+ \frac{t\big(225(s^4+u^4)+1075(s^3u+su^3)+1518s^2u^2\big)}{50450400m^{14}}$$

$$+ \frac{105(s^6+u^6)+558(s^5u+su^5)+1391(s^4u^2+s^2u^4)+1852s^3u^3}{86486400m^{16}}$$

$$+ \frac{t\big(224(s^6+u^6)+1533(s^5u+su^5)+3729(s^4u^2+s^2u^4)+5035s^3u^3\big)}{1102701600m^{18}}$$

$$+ \frac{5292(s^8+u^8)+38416(s^7u+su^7)+134211(s^6u^2+s^2u^6)}{97772875200m^{20}}$$

$$+ \left. \frac{268122(s^5u^3+s^3u^5)+335050s^4u^4}{97772875200m^{20}} \right), \tag{4.297}$$

$$f^{\{2\}}(s,u) = \mathcal{K}\left(\frac{1}{2m^4} + \frac{s^2 + su + u^2}{120m^8}\right.$$

$$+ \frac{stu}{504m^{10}} + \frac{(s^2 + su + u^2)^2}{3780m^{12}} + \frac{(s^2 + su + u^2)stu}{7920m^{14}}$$

$$+ \frac{75(s^6 + u^6) + 225(s^5u + su^5) + 559(s^4u^2 + s^2u^4) + 743s^3u^3}{7207200m^{16}}$$

$$+ \frac{3(s^2 + su + u^2)^2 stu}{400400m^{18}}$$

$$\left. + \frac{(s^2 + su + u^2)(56(s^6 + u^6) + 168(s^5u + su^5) + 557(s^4u^2 + s^2u^4) + 834s^3u^3)}{122522400m^{20}}\right).$$

$$(4.298)$$

We give the relation between $\mathcal{M}_4(1^+, 2^-, 3^-, 4^+)$ and $f(s,u)$ in Eq. (4.68) and define $\mathcal{K}$ in Eq. (4.87).

For the all-plus and single-minus configurations it suffices to give the result for the spin-0 contribution since we obtain the remaining amplitudes via Eq. (4.34). For the all-plus

configuration we have

$$
h^{S=0}(s,u) = \mathcal{K}\left(\frac{stu}{504m^2} + \frac{(s^2+su+u^2)^2}{3780m^4} \right.
$$

$$
+ \frac{(s^2+su+u^2)stu}{7920m^6} + \frac{75(s^6+u^6)+225(s^5u+su^5)+559(s^4u^2+s^2u^4)+743s^3u^3}{7207200m^8}
$$

$$
+ \frac{3(s^2+su+u^2)^2stu}{400400m^{10}}
$$

$$
+ \frac{(s^2+su+u^2)\bigl(56(s^6+u^6)+168(s^5u+su^5)+557(s^4u^2+s^2u^4)+834s^3u^3\bigr)}{122522400m^{12}}
$$

$$
+ \frac{\bigl(392(s^6+u^6)+1176(s^5u+su^5)+2481(s^4u^2+s^2u^4)+3002s^3u^3\bigr)stu}{888844320m^{14}}
$$

$$
+ \frac{(s^2+su+u^2)^2\bigl(105(s^6+u^6)+315(s^5u+su^5)+1412(s^4u^2+s^2u^4)+2299s^3u^3\bigr)}{4888643760m^{16}}
$$

$$
+ \frac{(s^2+su+u^2)\bigl(150(s^6+u^6)+450(s^5u+su^5)+1049(s^4u^2+s^2u^4)+1348s^3u^3\bigr)stu}{5766092640m^{18}}
$$

$$
+ \frac{1}{33731641944000m^{20}}\Bigl(35640(s^{12}+u^{12})
$$

$$
+ 213840(s^{11}u+su^{11})+1174365(s^{10}u^2+s^2u^{10})+3911625(s^9u^3+s^3u^9)
$$

$$
\left. + 8797526(s^8u^4+s^4u^8)+14072594(s^7u^5+s^5u^7)+16416696s^6u^6\Bigr)\right),
$$

$$(4.299)$$

while for the single-minus configuration we find

$$
g^{S=0}(s,u) = \mathcal{K}\left(\frac{1}{5040m^2stu} + \frac{1}{6306300m^8} \right.
$$

$$
+ \frac{(s^2+su+u^2)}{441080640m^{12}} + \frac{stu}{2715913200m^{14}} + \frac{(s^2+su+u^2)^2}{22406283900m^{16}} + \frac{(s^2+su+u^2)stu}{64250746560m^{18}}
$$

$$
\left. + \frac{\bigl(27(s^6+u^6)+81(s^5u+su^5)+197(s^4u^2+s^2u^4)+259s^3u^3\bigr)}{25057791158400m^{20}} \right).
$$

$$(4.300)$$

The relation of $\mathcal{M}_4(1^+,2^+,3^+,4^+)$ and $\mathcal{M}_4(1^+,2^+,3^-,4^+)$ to $h(s,u)$ and $g(s,u)$ is found in Eq. (4.68).

CHAPTER 5

Effective Field Theory Islands from Perturbative and Nonperturbative Four-Graviton Amplitudes

Theoretical data obtained from physically sensible field and string theory models suggest that gravitational Effective Field Theories (EFTs) live on islands that are tiny compared to current general bounds determined from unitarity, causality, crossing symmetry, and a good high-energy behavior. In this work, we present explicit perturbative and nonperturbative $2 \to 2$ graviton scattering amplitudes and their associated low-energy expansion in spacetime dimensions $D \geq 4$ to support this notion. Our new results include a first nonperturbative example consisting of a $D = 4$, $\mathcal{N} = 1$ supersymmetric field theory that is coupled weakly to gravity. We show that this nonperturbative model lies on the same islands identified using four-dimensional perturbative models based on string theory and minimally-coupled matter circulating a loop. Furthermore, we generalize the previous four-dimensional perturbative models based on string theory and minimally-coupled massive spin-0 and spin-1 states circulating in the loop to D dimensions. Remarkably, we again find that the low-energy EFT coefficients lie on small islands. These results offer a useful guide towards constraining possible extensions of Einstein gravity.

5.1   Introduction

The language of effective field theory (EFT) is a widely accepted framework in which to formulate the physical laws at a certain energy scale (often referred to as the infrared (IR) scale). Typically, this language is used in the context of current and near-future high-energy

physics experiments [381, 382], but has also found applications in a variety of topics including hydrodynamics [383], inflation [384], the large scale structure of the Universe [385], and the description of binary motion in general relativity [64], among many others. In EFTs, the relevant physics is parameterized by independent local operators that capture all relevant physical degrees of freedom and are consistent with the known symmetries of the problem. Examples of such symmetries include Lorentz invariance and possibly gauge or global symmetries. The unknown physics at high energy or ultraviolet (UV) physics is then systematically parameterized by successively including higher-dimension operators that capture corrections to low-energy observables. Naively, the (Wilson) coefficients of such higher-dimension operators are undetermined and can take on arbitrary values. However, desirable properties of the underlying theory such as causality (analyticity) and unitarity impose nontrivial constraints or bounds on the allowed values of the low-energy couplings [252, 241]. A way to expose these bounds is to study the connection of the $2 \to 2$ scattering amplitude in the IR and the UV by means of *dispersion relations* which relate low-energy Wilson coefficients to the discontinuities of the UV amplitude by a contour deformation subject to certain assumptions about the Regge growth of amplitudes at large energies in the complex plane, see e.g. Refs. [386, 387, 345, 388]. In recent years this basic philosophy has been systematized to extract various nontrivial constraints [353, 269, 4, 389, 390, 391, 392].

It is critical to understand the full implications of these constraints and whether sensible physical theories must necessarily lie in small regions of the EFT parameter space. Ref. [4] observed that the Wilson coefficients of two distinct classes of gravitational effective field theories derived from models of UV physics populate small *theory islands* in the larger space allowed by current dispersive arguments. The first class are string theories, which are ultraviolet complete, and the second class comes from integrating out minimally coupled matter circulating in loops. In both instances gravity is assumed to be weakly coupled so that only the leading order contributions are required, corresponding to tree level in string theory and one loop in the field-theory models. While the field-theory models are not full UV completions, they can be interpreted as intermediate-scale theories, which satisfy all the

196

assumptions used to derive bounds on the EFT coefficients. The fact that such dissimilar models land on the same small theory island suggests that sensible theories should obey much stronger constraints than have been found as yet from the general arguments. The observed small islands were interpreted as being related to *low spin dominance*—essentially the property that the spectral density in these models is dominated by the lowest spin partial waves.

While suggestive, an obvious question is whether the appearance of small islands is an artifact of the special theories that were considered or whether they are generic for physically sensible theories. Here we provide evidence towards the latter by obtaining data from two new classes of theories. The first is a nonperturbative strongly coupled $\mathcal{N} = 1$ supersymmetric gauge theory which is then weakly coupled to gravity and the second is matter minimally coupled to gravity in $D > 4$ spacetime dimensions. Specifically, we present explicit results in $D = 6, 10$ dimensions with further data and evaluation routines available in the ancillary files. The well known string-theory amplitudes in $D > 4$ provide a third class of EFT data. We use this data to support the notion that small theory islands are not a special feature of $D = 4$ perturbative examples, but indeed generalize beyond the cases analyzed in Ref. [4]. It remains a challenge to find the tightest bounds that physically sensible EFTs must satisfy. Some recent progress on improving bounds is found in Refs. [390, 391].

One of the key lessons of the modern scattering amplitudes program is to focus on gauge- and field-redefinition-invariant quantities. In this spirit, as in Refs. [353, 269, 4, 389, 390], we focus on the low-energy expansions of scattering amplitudes directly, rather than Wilson coefficients in a Lagrangian that are subject to field-redefinition and integration-by-parts ambiguities. Assuming that gravity couples weakly, we can work to tree-level accuracy in the EFT. There is then a one-to-one map between S-matrix elements in the IR and Wilson coefficients in any given basis of operators, see e.g. [393]. In this way, the low-energy amplitude can be schematically expanded in the form[1]

---

[1]Below, we denote amplitude coefficients by their monomial term, e.g. $a[s^{k-q}t^q]$. For the sake of compactness, here we simply use $a_{k,q}$ which will have a different meaning for a particular $4D$ helicity amplitude.

$$\mathcal{M}_{\mathrm{IR}}(s,t) \sim \text{light exchange} + \sum_{k \geq q \geq 0} a_{k,q} \, s^{k-q} t^q \,, \tag{5.1}$$

where the Mandelstam invariants are $s = (p_1 + p_2)^2$, $t = (p_1 + p_4)^2$, and $u = (p_1 + p_3)^2$. As usual, for massless external states, they satisfy the relation $u = -s-t$. The terms denoted by "light exchange" correspond to low-energy *poles* from massless or light (relative to the scale of Mandelstam invariants) exchange of states that are within the low-energy EFT. Finally, the $a_{k,q}$ parameterize new four-point contact interactions graded by mass dimension k.

In the ultraviolet, it is convenient to parameterize the unknown physics in terms of the partial-wave expansion of the amplitude, involving the spectral density and some characteristic polynomial of the scattering angle $\cos\theta = 1 + 2t/s$ (for massless external states in the s-channel center of mass) that encodes the Poincaré-invariance properties akin to conformal partial waves in conformal-field-theory (CFT) correlation functions [394, 395, 396, 397]. For external scalars, these are the Gegenbauer polynomials (see e.g. [269]) in general D and the Wigner-d matrices for spinning external states in $D = 4$, see e.g. Refs. [398, 341].

The simplest incarnation of the bounds on the coefficients $a_{k,q}$ in Eq. (5.1) is relatively easy to understand. In the presence of some elastic channel where the 'out' state is the same as the 'in' state, in the forward limit (i.e. $t \to 0$) the discontinuity of the amplitude becomes an absolute square which then implies positivity constraints on EFT amplitude coefficients [252]:

$$a_{k,0} \sim \langle \mathrm{in} | T^\dagger T | \mathrm{in} \rangle = \left| T | \mathrm{in} \rangle \right|^2 \geq 0 \,. \tag{5.2}$$

Such bounds have first appeared in the context of chiral Lagrangians and pion scattering [399, 400, 401], before experiencing a revival inspired by the seminal works of Refs. [252, 241]. Recently, similar bounds [257, 260, 263, 264, 353, 270, 402, 403] were organized into a novel geometric structure termed the EFT-hedron [269] (see also Ref. [404, 391, 4]), related to the Weak Gravity Conjecture [258, 405, 406], the analytic bootstrap in AdS/CFT [280, 389], and applied to the Standard Model EFT and pion scattering [253, 407, 408, 409]. Furthermore, these bounds were refined away from the forward limit [268, 271, 390] in order to handle cases with gravitational couplings where the t-channel graviton exchange causes difficulties with

some of the naive forward limit bounds. Cases with different external helicity configurations, which individually cannot be considered as elastic scattering, were also considered in Refs. [4, 390, 391], in a spirit similar to Refs. [410, 351, 411]. A key feature, common to all presently known bounds is the appearance of the demarcation of allowed and disallowed regions in the space of low-energy couplings $a_{k,q}$.

As already noted above, in previous four-dimensional studies, explicit string- and field-theory data suggest that physical EFTs live on small theory islands [4]. In contrast to the four-dimensional case, and for the D-dimensional scattering of scalar particles, the spinning partial-wave decomposition that enter the UV part of the dispersion relations are not presently analyzed for the scattering of D-dimensional spinning states (see however our "note added" below and the upcoming work of Ref. [412]). Nevertheless, independently of the availability of precise bounded regions, we can ask where do explicit data lie in order to guide further explorations. Here, we address the question of whether similar islands are observed for more general models than the ones considered in [4]. We do so by obtaining new explicit examples of UV models, including nonperturbative matter and cases outside of four dimensions, from which we extract the low-energy expansion coefficients for gravitational scattering amplitudes. Our analysis further supports the notion that small theory islands are a robust feature of gravitational EFTs. Our example of nonperturbative matter in gravitational $2 \rightarrow 2$ scattering opens up a new class of possible theories to analyze in the future. Higher dimensions are interesting for various reasons, including that they allow for analyses of bounds that avoid complications with IR singularities [271] and because 10 dimensions is natural for addressing the question of where does string theory lie in the space of possible UV completions [282].

The remainder of this paper is organized as follows: In section 5.2 we summarize our kinematic conventions for D-dimensional graviton scattering including a parametrization of the center-of-mass momenta and the polarization states of the external gravitons. In section 5.3, we use supersymmetric arguments to generate a first four-dimensional example of nonperturbative matter for gravitational $2 \rightarrow 2$ scattering. In section 5.4 we discuss the

straightforward case of tree-level four-graviton string-theory amplitudes in general spacetime dimensions. Our results for one-loop minimally-coupled graviton amplitudes in D dimensions, from which we extract nontrivial EFT data, is presented in section 5.5. We consider the cases of minimally-coupled massive spin-0 and spin-1 matter circulating in the loop. We also briefly summarize the well-known amplitudes techniques such as generalized unitarity and integration tools used to evaluate and manipulate such expressions. In section 5.6 we give a summary of our data by plotting some of the obtained low-energy amplitude coefficients that should serve as a useful guide for any near-future attempts to place dispersive bounds on higher-dimensional graviton scattering. We supply the relevant amplitudes and their low-energy expansion in a computer-readable form as ancillary files to this paper. We close with conclusions and a future outlook in section 5.7.

5.2   External kinematics

To describe $2 \rightarrow 2$ graviton scattering in D dimensions we introduce external momenta p_i, where $i = 1, \ldots, 4$ labels the external graviton in question, and work in an all-incoming convention. To capture scattering of all possible external states, we use formal polarization tensors for the gravitons

$$\varepsilon_i^{\mu\nu} = \varepsilon_i^\mu \varepsilon_i^\nu \,, \quad \text{with} \quad p_i \cdot \varepsilon_i = 0 \quad \text{and} \quad \varepsilon_i \cdot \varepsilon_i = 0 \,. \tag{5.3}$$

We express gravitational polarization tensors in terms of transverse, null polarization vectors ε_i^μ. Note that there are $D-2$ such independent null vectors in D spacetime dimensions, while there are $D(D-3)/2$ independent symmetric traceless tensors. The expressions in terms of the above tensors capture the entire space of states for the D-dimensional gravitons. Indeed, a generic polarization tensor $E^{\mu\nu} \equiv \varepsilon^\mu \tilde{\varepsilon}^\nu + \tilde{\varepsilon}^\mu \varepsilon^\nu$ may always be written in terms of linear combinations of factorized tensors, e.g. [413, 339]

$$\varepsilon^\mu \tilde{\varepsilon}^\nu + \tilde{\varepsilon}^\mu \varepsilon^\nu = (\varepsilon + \tilde{\varepsilon})^\mu (\varepsilon + \tilde{\varepsilon})^\nu - \varepsilon^\mu \varepsilon^\nu - \tilde{\varepsilon}^\mu \tilde{\varepsilon}^\nu \,, \tag{5.4}$$

where we take $\varepsilon \cdot \tilde{\varepsilon} = 0$ to ensure tracelessness.

To study specific examples, we introduce explicit momenta and polarization tensors. We consider scattering in the center-of-mass frame, where

$$p_1^\mu = \sqrt{\frac{s}{2}} \begin{pmatrix} +1 \\ -1 \\ 0 \\ \vec{0}_{D-3} \end{pmatrix}, \qquad p_2^\mu = \sqrt{\frac{s}{2}} \begin{pmatrix} +1 \\ +1 \\ 0 \\ \vec{0}_{D-3} \end{pmatrix},$$

$$p_3^\mu = \sqrt{\frac{s}{2}} \begin{pmatrix} -1 \\ -\cos\theta \\ -\sin\theta \\ \vec{0}_{D-3} \end{pmatrix}, \qquad p_4^\mu = \sqrt{\frac{s}{2}} \begin{pmatrix} -1 \\ \cos\theta \\ \sin\theta \\ \vec{0}_{D-3} \end{pmatrix}, \tag{5.5}$$

and the scattering angle θ is related to the Mandelstam invariants via $\cos\theta = 1 + \frac{2t}{s}$, with $s > 0$, and $-s < t < 0$ for physical s-channel scattering. In all examples analyzed in this paper, we consider external polarization tensors of the factorized form in Eq. (5.3). Different cases can also be obtained straightforwardly as explained above. Focusing on even D, given a set of spatial unit vectors $e_a^\mu = \delta_a^\mu$, with $a = 1, \ldots, D$, we define (see e.g. Ref. [413])

$$\varepsilon_{1,2n\pm}^\mu = \frac{1}{\sqrt{2}}(e_{2n-1}^\mu \pm \mathrm{i}\, e_{2n}^\mu), \qquad n = 2, \ldots \frac{D}{2}. \tag{5.6}$$

We obtain the polarization vectors for the other three gravitons using appropriate rotations. More details on the polarization choices are included in the ancillary files with explicit evaluation code for all Lorentz products for graviton polarizations similar to the ones discussed here. Note that for $D = 4$ ($n = 2$) the polarizations in Eq. (5.6) describe helicity states. Indeed, for this choice our results reproduce the ones obtained in Ref. [4] using spinor-helicity methods.

5.3   Non-perturbative data

To gain some direct indication on nonperturbative low-energy effective actions, we consider a matter-coupled $\mathcal{N} = 1$ supersymmetric gauge theory which we couple to gravity. This

gauge theory confines in flat space at some scale Λ, whose specific relation to the high-energy couplings will not be important. We assume that Λ is relatively high and that the the low-energy theory is described by the glueball superfield which is much lighter than the confinement scale. This can be arranged by adjusting the couplings of the high-energy theory. We then focus our discussion on energies below the mass m_s of the glueball superfield. Thus we can ignore terms $\mathcal{O}(p^2/\Lambda^2)$, but we cannot ignore terms $\mathcal{O}(p^n/m_S^n)$.

The Wilsonian effective action below the confinement scale for an $\mathcal{N} = 1$ supersymmetric gauge theory with (holomorphic) tree-level superpotential $W_{\text{tree}}(\phi, Q, \bar{Q})$ depending on some chiral superfields ϕ in the adjoint representation and other superfields $Q, \bar{Q}$ in the fundamental representation, has the standard form

$$\mathcal{L} = \int d^4\theta \, K_{\text{eff}}(S, \bar{S}, G, \bar{G}) + \int d^2\theta \, W_{\text{eff}}(S, G) + \text{h.c.} \,, \tag{5.7}$$

where S is the glueball (chiral) superfield, G is the Weyl superfield and K_{eff} and W_{eff} are the effective Kähler potential and superpotential respectively. The latter is completely non-perturbative [414], while the former receives both perturbative and nonperturbative contributions. The Weyl superfield G, capturing the induced coupling of the effective theory with gravity, carries left-handed spinor indices and its first two components are the self-dual gravitino field strength and the self-dual Riemann tensor respectively.

While the effective Kähler potential is largely unconstrained, the effective superpotential is stringently constrained by symmetry and holomorphy arguments and instanton calculations [415, 416, 417]. Refs. [418, 419] argued that the effective superpotential has the form

$$W_{\text{eff}} = \frac{\partial \mathcal{F}_0}{\partial S} + \frac{\partial^2 \mathcal{F}_0}{\partial S^2} G^{\alpha\beta\gamma} G_{\alpha\beta\gamma} + \mathcal{O}\big((G^{\alpha\beta\gamma} G_{\alpha\beta\gamma})^2\big) \,, \tag{5.8}$$

where $\mathcal{F}_0$ is a holomorphic function of the glueball superfield S.[2] Given a tree-level superpotential W_{tree}, the nonperturbative effective potential W_{eff} can be computed algorithmically, including its gravitational couplings, either via a symmetry and holomorphy analysis

---

[2]We do not include a detailed expression of the higher-order terms because they contribute only to higher-point gravitational amplitudes, so we do not need them.

[415, 416], or through matrix-model methods [418, 419, 420, 421, 422, 423, 424, 425]. For our purpose here we do not need its detailed form.

In the latter approach most terms in W_{eff} are evaluated perturbatively, and the glueball superfield S enters initially in the form of the gauge invariant bilinear $S \propto Tr[W^\alpha W_\alpha]$, where W is the vector superfield, whose lowest component is the gluino. The nonperturbative nature of the superpotential comes from interpreting this superfield as a fundamental field, and from the inclusion in $\mathcal{F}_0$ of the Veneziano-Yankielovicz superpotential [426], which accounts for the chiral anomaly.

The critical point of the G-independent part of the effective superpotential, which is a solution of $\partial^2 \mathcal{F}_0 / \partial S^2 = 0$, fixes a vacuum expectation value, $S = S_*$, of the glueball superfield. This breaks chiral symmetry and determines the non-normalized mass of this superfield as $\tilde{m}_S = \partial^3 \mathcal{F}_0 / \partial S^3|_{S=S_*}$.[3] It also implies that among the terms with two Weyl-superfields there exists a linear coupling to $(S - S_*)$, $m_S(S - S_*)G^{\alpha\beta\gamma}G_{\alpha\beta\gamma}$, which is also proportional to the mass of these fields. Evaluating the integral over Grassmann variables in Eq. (5.8), integrating out the the auxiliary fields and normalizing the quadratic term for φ leads to

$$\int d^2\theta W_{\text{eff}} + h.c. = |m_S|^2 \bar{\varphi}\varphi + M\,\varphi\,R_{\alpha\beta\gamma\delta}R^{\alpha\beta\gamma\delta} + M^*\,\bar{\varphi}\,R_{\dot\alpha\dot\beta\dot\gamma\dot\delta}R^{\dot\alpha\dot\beta\dot\gamma\dot\delta} + \text{fermions} \ , \qquad (5.9)$$

where $M = \tilde{m}_S/(\partial_S\partial_{\bar S}K_{\text{eff}}|_{S=S_*})^{1/2}$, $\varphi = (S - S_*)|_{\theta=0}$ is the scalar in the glueball superfield and $R^{\alpha\beta\gamma\delta}$ and $R^{\dot\alpha\dot\beta\dot\gamma\dot\delta}$ are the self-dual and anti-self-dual parts of the Riemann tensor, containing the negative- and positive-helicity gravitons respectively. Thus, the nonperturbative superpotential couples the fluctuation φ of the glueball scalar around its expectation value S_* with two gravitons of the same helicity,

$$(5.10)$$

---

[3]The mass m_S depends on the details of the Kähler potential. On dimensional and holomorphy grounds one may expect that up to numerical factors, $m_S \propto S_*^{4/3}\tilde{m}_S$.

Setting aside the exchange of gravitons, the leading-order terms in the four-graviton amplitude come from tree-level exchange of φ. There are three possible contributions: two vertices from the superpotential, two vertices from the Kähler potential, and a contact term from the Kähler potential. Since extracting gravitons out of the G superfield requires only one Grassmann derivative, it follows that the third field in a vertex with two gravitons is acted upon by two Grassmann derivatives, so it must be the auxiliary field of the glueball superfield. Thus, the Kähler potential can contribute only contact terms at tree level. We graphically denote superpotential contributions by circles and Kähler potential contributions by boxes. The corresponding graphs are:

$$\begin{array}{ccc} \text{(diagram)} & \text{(diagram)} & \text{(diagram)} \end{array} \tag{5.11}$$

We first focus on the superpotential contributions and argue later that under certain circumstances the Kähler potential contributions do not affect the conclusions.

Four-graviton tree-level diagrams with vertices from the superpotential are very simple. Eq. (5.9) implies that, for a fixed graviton helicity configuration, the amplitude receives contributions from a single exchange diagram. For example, if gravitons 1 and 2 have negative helicity and gravitons 3 and 4 have positive helicity, the only diagram that contributes is:

$$\mathcal{M}(1^-, 2^-, 3^+, 4^+) \quad \sim \quad \text{(diagram)} \tag{5.12}$$

This diagram depends on the scalar-field propagator, which in turn depends on the Kähler potential.[4] The Källén-Lehmann representation of massive two-point functions identifies this propagator as some function f of the momentum with a simple pole at $p^2 = m_S^2$ where m_S is the physical mass of the field φ. In particular, this implies that it has a regular expansion

---

[4]A dimensional-analysis-based suggestion was put forth in Ref. [426], $K(S) \propto (\bar{S}S)^{1/3}$.

around vanishing momentum, i.e.

$$f(s) = \sum_{n \geq 0} a_n s^n \ . \tag{5.13}$$

Then, the amplitude $\mathcal{M}(1^-, 2^-, 3^+, 4^+)$ is given by

$$\mathcal{M}(1^-, 2^-, 3^+, 4^+) = \langle 12 \rangle^4 [34]^4 \, f(s) \ , \tag{5.14}$$

with other helicity configurations, $\mathcal{M}(1^-, 2^+, 3^+, 4^-)$ and $\mathcal{M}(1^-, 2^+, 3^-, 4^+)$, obtained by relabeling. This implies that

$$\frac{a_{n,j}}{a_{n,0}} = 0 \, , \quad \text{for all } j > 0 \, , \tag{5.15}$$

which puts the nonperturbative contributions from the superpotential on the small islands of physical EFTs and the low-spin-dominance lines in $D = 4$ discussed in Ref. [4].

Consider now briefly the consequences of including Kähler-potential contributions to leading-order gravitational amplitudes. As we saw earlier, these contributions can come only from contact terms which arise either from terms of the type $\int d^4\theta f(S, \bar{S}) G^2 \bar{G}^2$ in K_{eff} in Eq. (5.7), or from terms with two Weyl multiplets in K_{eff} upon integrating out the auxiliary field in the glueball superfield.

Nonperturbative contributions to K_{eff} necessarily depend on the confinement scale Λ; moreover, if they are dependent on momenta, then dimensional analysis suggests that they depend on p^2/Λ^2 which, according to our initial assumption, is negligible at the energy scale $p^2 \ll \Lambda^2$ that we are focusing on. Thus, the contributions of such Kähler potential terms to amplitudes are essentially constant (up to the helicity-dependent factor), and therefore they affect only a limited number of $a_{n,j}$ coefficients, perhaps only $a_{0,0}$, leading to effectively no changes to Eq. (5.15).

One may wonder if the expansion around the nonvanishing expectation value for the glueball superfield S may enhance these terms suppressed by the ratio p^2/Λ^2. The expectation of a smooth limit in which the high-energy theory is trivial (i.e. that the tree-level superpotential is zero) suggests that the momentum dependence cannot be enhanced for

small values of the parameters of the high-energy theory. While this argument suggests that the nonperturbative momentum dependence could be enhanced at large values of these parameters, naively of the order of Λ^2/p^2, there remains a comfortable range of parameters of the high-energy theory for which inclusion of the purely nonperturbative terms in the Kähler potential does not affect Eq. (5.15).

Extension of this discussion to the perturbative and mixed part of the Kähler potential is difficult because of their detailed dependence on the parameters of the high-energy theory. Using however the identity

$$x \leq \frac{a_{n,j}^{(1)}}{a_{n,0}^{(1)}}, \frac{a_{n,j}^{(2)}}{a_{n,0}^{(2)}} \leq y \quad \implies \quad x \leq \frac{a_{n,j}^{(1)} + a_{n,j}^{(2)}}{a_{n,0}^{(1)} + a_{n,0}^{(2)}} \leq y \ , \tag{5.16}$$

if all $a_{n,j} > 0$ together with the results of Ref. [4] and those discussed in later sections, we expect that the complete nonperturbative four-graviton amplitude in the class of theories discussed here belongs to the EFT island for $p^2/\Lambda^2 \ll 1$. Further study and explicit calculations are necessary to fully settle this issue and to extend our analysis to scales $p^2 \lesssim \Lambda^2$ in which all nonperturbative contributions to the Wilsonian effective action become important.

5.4 Tree-level graviton amplitudes in string theory

Having analyzed the first nonperturbative data for four-dimensional graviton scattering via supersymmetric arguments, we now move on to more traditional perturbative amplitudes, although beyond the commonly considered four-dimensional setup. We expect that this data will provide useful guidance for any attempts to place dispersive bounds on graviton scattering in higher dimensions.

To this end, we collect the available tree-level results for the scattering of four external gravitons in superstring (ss), heterotic-string (hs), and bosonic-string (bs) theory. These closed-string amplitudes are determined by Kawai-Lewellen-Tye (KLT) relations [33] in terms of open-string ones. We take the mass of the first excited string level to be $m_s^2 = 4/\alpha'$ for all string theories and express the string-theory amplitudes in terms of gauge-invariant tensor

structures $\mathcal{T}$. We need two such structures,

$$\mathcal{T}_{\text{sYM}} = -s\,t\,(\varepsilon_1 \cdot \varepsilon_3)(\varepsilon_2 \cdot \varepsilon_2) + \cdots,$$
$$\mathcal{T}_{\text{bos}} = -\frac{s\,u}{(1 + \alpha't/4)}(\varepsilon_1 \cdot \varepsilon_4)(\varepsilon_2 \cdot \varepsilon_3) + \cdots, \tag{5.17}$$

which are normalized to have mass-dimension four. The full expression for these structures is provided in the ancillary file. We may now write the four-graviton amplitudes in a form that uniformly applies to the three string theories,

$$\mathcal{M}^{(\beta)} = -\left(\frac{\kappa}{2}\right)^2\left(\frac{\alpha'}{4}\right)^3 \mathcal{T}_\beta \frac{\Gamma\left[-\frac{\alpha's}{4}\right]\Gamma\left[-\frac{\alpha't}{4}\right]\Gamma\left[-\frac{\alpha'u}{4}\right]}{\Gamma\left[1+\frac{\alpha's}{4}\right]\Gamma\left[1+\frac{\alpha't}{4}\right]\Gamma\left[1+\frac{\alpha'u}{4}\right]}, \tag{5.18}$$

where $\beta \in \{\text{ss, hs, bs}\}$ and

$$\mathcal{T}_{\text{ss}} = \mathcal{T}_{\text{sYM}}^2, \qquad \mathcal{T}_{\text{hs}} = \mathcal{T}_{\text{sYM}}\,\mathcal{T}_{\text{bos}}, \qquad \mathcal{T}_{\text{bs}} = \mathcal{T}_{\text{bos}}^2. \tag{5.19}$$

Newton's constant G is related to κ via $\kappa^2 = 32\pi G$. As a consistency check, by specializing the polarization tensors to describe four-dimensional helicity states we recover the results collected in Appendix B of Ref. [4].

The bosonic string-theory amplitude contains the tachyon exchange. Following Ref. [4], we define a modified bosonic string-theory amplitude by subtracting this exchange and present our data within this definition. In four dimensions, this amplitude is consistent with the generic bounds and hence we expect the same to be true in higher dimensions as well. Let us, however, note that none of the conclusions drawn in the present paper change if we chose to drop the bosonic string-theory amplitude, given the undesired appearance of the tachyon.

We may also identify the massless exchanges in all three sting theories. Specifically, the superstring amplitude only contains the minimal-coupling graviton exchange. The heterotic string-theory amplitude contains both the minimal-coupling and Gauss-Bonnet graviton exchanges, as well as the dilaton exchange. Finally, the bosonic string-theory amplitude contains all the heterotic string-theory amplitude exchanges as well as those from an R^3-type coupling. Subtracting these exchange contributions is possible but not necessary in order for the amplitudes to be physical. We do not perform such a subtraction in the present work.

Furthermore, we point out that there is an inherent ambiguity in separating the non-analytic from the analytic part (or equivalently the non-local from the local part) of the amplitude. This ambiguity is reflecting part of the freedom in writing a Lagrangian. When there are no R^3-type contributions, there is no such ambiguity. In these cases, a simple powercounting argument shows that dilaton and Gauss-Bonnet contributions do not mix with $D^n R^4$-type (contact) operators. In contrast, when R^3-type operators are present, terms of the form $R^2 \times R^3$ and $R^3 \times R^3$ contribute at the same order as R^4-type and $D^2 R^4$-type operators respectively. Hence, in order to obtain the coefficients of the latter, one needs to calculate the low-energy amplitudes starting from a Lagrangian (or define in a different way a scheme for separating the non-analytic from the analytic part of the amplitude). For the complete analysis of the inherent ambiguity in mapping amplitude coefficients to Lagrangian coefficients one has to also include massless loop effects [353, 403]. In this work we neglect massless loop effects, and plot coefficients of $D^n R^4$-type operators with $n > 2$ which do not mix with the massless exchange contributions.

5.5 Loop-level graviton amplitudes in quantum field theory

Besides the tree-level string theory amplitudes discussed in the previous section, we are also interested in field-theory models where we allow massive states circulating in the loop as a D-dimensional extension of the four-dimensional analysis of Ref. [4]. Such models should not be viewed as proper UV completions, but should instead be viewed as intermediate-energy theories. Because they satisfy all input assumptions used to derive bounds on the low-energy EFTs they provide useful guidance on where physically sensible theories live. Here we opt to construct the full amplitudes for a simple reason: In the derivation of EFT bounds one needs the Regge behavior to determine the validity of bounds which rely on knowing (or assuming) the high-every behavior. With the exact amplitudes in hand it is straightforward to extract the high-energy behavior. A side benefit in having the full one-loop amplitudes computed is that they may be useful for purposes other that studying low-energy EFTs.

5.5.1 Maximally supersymmetric massive matter in the loop

The simplest loop-level data we can consider originates from a massive deformation of the maximally supersymmetric gravity amplitude at one-loop, where we give a common mass to the supermultiplet circulating in the loop. This is accomplished by taking the original massless one-loop four-point amplitude written in terms of scalar box integrals [427],

$$\mathcal{M}^{(\mathcal{N}=8)} = \left(\frac{\kappa}{2}\right)^4 \mathcal{T}_{\mathrm{ss}} \left[I_{\mathrm{box}}^{(D)}(s,t) + I_{\mathrm{box}}^{(D)}(s,u) + I_{\mathrm{box}}^{(D)}(u,t) \right] . \tag{5.20}$$

and replacing the loop propagators by massive ones. This may be interpreted as dimensionally-reducing a higher-dimensional maximal supergravity and integrating out a Kaluza-Klein mode whose mass is the extra-dimensional momentum. The polarization information is encoded in the tree-level superstring tensor $\mathcal{T}_{\mathrm{ss}}$ and the integrals are defined e.g. as

$$I_{\mathrm{box}}^{(D)}(s,t) = \int \frac{d^D \ell}{(2\pi)^D} \prod_{n=0}^{3} \frac{1}{(\ell + \sum_{i=1}^{n} p_i)^2 - m^2} . \tag{5.21}$$

The UV divergences that are present for $D \geq 8$ are straightforward to extract. In fact, the UV expansion of the amplitude and its large-mass expansion are intimately related: both are equivalent to an expansion around small external momenta yielding massive tadpoles, as can be easily seen from the interpretation of the mass as Kaluza-Klein momentum. We will return shortly to the large-mass expansion.

5.5.2 Non-supersymmetric massive matter in the loop
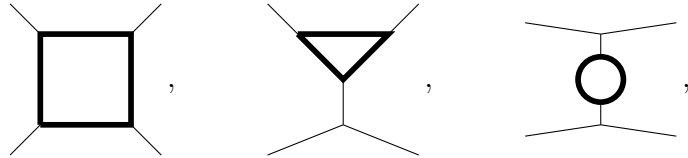
We obtained the four-graviton amplitude with a maximally supersymmetric massive multiplet circulating in the loop by simply replacing formerly massless propagators by massive ones in the known representation of the one-loop amplitude [427]. We are also interested in D-dimensional one-loop amplitudes with massive scalars and massive spin-1 fields running in the loop. We do not explicitly consider massive fermions, gravitinos, or massive spin-2 states here for the sake of brevity even though there is no conceptual problem to construct these amplitudes as well. The workflow of our construction uses a number of modern scattering-amplitude methods.

We start by constructing the amplitude's loop integrand via generalized unitarity [19, 20, 166] from the knowledge of tree-level amplitudes. We find it most convenient to directly match two-particle cuts

$$,\tag{5.22}$$

where the external states are gravitons (denoted by wiggly lines) and the massive states propagating inside the loop are generically denoted by a solid line (which can represent either massive spin-0 or spin-1 states). Since we are interested in expressions that are valid in arbitrary spacetime dimension D, we utilize tree-level gravitational Compton amplitudes (grey 'blobs' in (5.22)) in terms of formal (traceless symmetric) polarization tensors $\varepsilon_i^{\mu\nu} = \varepsilon_i^\mu \varepsilon_i^\nu$ of the gravitons that can be found e.g. in Ref. [46]. The unitarity cuts involve a sum over physical states. For the massive spin-1 circulating in the loop, the relevant states are selected out by inserting the physical state projector $\Pi^{\mu\nu}(p, m) = \eta^{\mu\nu} - \frac{p^\mu p^\nu}{m^2}$ for each cut leg. From the resulting expressions, we extract the kinematic numerators of the cubic diagrams

$$,\tag{5.23}$$

which are functions of the following Lorentz invariants: $\varepsilon_i \cdot p_j$, s, t, $p_i \cdot \ell$, and $\varepsilon_i \cdot \ell$. For the massive spin-1 exchange, it is convenient to split the numerators into a 'spin-0' part and a 'spin-1' remainder akin to the supersymmetric decomposition of the four-dimensional amplitudes in Ref. [4]:

$$N^{\text{spin}-1} = \overline{N}^{\text{spin}-1} + (D_s - 1)N^{\text{spin}-0}, \tag{5.24}$$

where $D_s = \eta^\mu_\mu$ is the state-counting parameter. This separation effectively eliminates the terms of highest degree in the loop momentum ℓ from $N^{\text{spin}-1}$.

At one loop, all contractions between the loop momentum ℓ and the external momenta p_i can be written in terms of inverse propagators, see e.g. [428], but contractions of the loop-momentum with polarization vectors ε_i require the evaluation of tensor integrals. Such

integrals are well known from e.g. Refs. [429, 430] where one converts tensor integrals into dimension-shifted [431, 432, 433] scalar integrals, see also Ref. [434]. The relevant dimension shifts can be derived algorithmically with the help of integration-by-parts relations [435, 436, 437, 438], implemented in modern computer codes such as `FIRE` [245, 246].

We find it convenient to organize the resulting amplitudes in a special basis of scalar integrals where all integral coefficients are independent of the mass of the state in the loop and of the spacetime dimension D. This closely follows the discussion of the four-dimensional amplitude construction of Ref. [4] and can be likewise achieved by judiciously using dimension-shifting relations [431, 432, 433].

The attentive reader might have noticed that our amplitudes construction via the two-particle cut in Eq. (5.22) is not yet complete as we could be missing contributions from bubble integrals with a single massless line on one side (sometimes referred to a 'snail integrals'), or from tadpole integrals. These contributions are determined along the lines of Ref. [22] by demanding that the amplitudes considered here remain IR-finite in the massless limit and by requiring that the UV divergences are mass-independent.[5] At the end of our construction, we find that all one-loop four-point amplitudes due to massive spin-S exchange considered in this work can be expressed in terms of 42 independent (possibly dimension shifted) integrals that are multiplied by gauge-invariant tensors involving only the Mandelstam invariants and contractions between polarization vectors and external momenta,

$$\mathcal{M}^{(\mathrm{S})} = \sum_k \mathcal{T}_k^{(\mathrm{S})}(\varepsilon, p) \, I_k(s, t, D, m^2) \,. \tag{5.25}$$

We include the explicit expressions of the amplitudes in the representation of (5.25) in computer readable form with explicit rules for the $\mathcal{T}_k^{(\mathrm{S})}$ in terms of Lorentz products of the external data.

In view of our goal to provide explicit expressions for the low-energy gravitational EFT amplitudes once the massive state is integrated out, it is highly advantageous to organize

---

[5]The latter requirement is equivalent to demanding that the corresponding counterterm has a local expression in terms of Riemann tensors.

the amplitudes as in Eq. (5.25). Indeed, since only the scalar (dimension-shifted) integrals, $I_k(s, t, D, m^2)$, depend on the mass, we only need to find their large-mass expansion. This can be achieved by dimension shifting all integrals back to $D = 4$ and using the known polylogarithmic expressions, conveniently collected in Ref. [439], and expanding them for $m^2 \gg |s|, |t|$. Alternatively, the same expressions can be obtained by expanding the integrand along the lines of the 'method of regions' [440] for $|\ell| \sim m \ll |p_i|$, leading effectively to tadpole integrals which are known exactly in D. We find the latter method computationally much more efficient. We provide the expansion of all one-loop integrals that appear in (5.25) to sufficiently high order in $1/m^2$ in the attached ancillary file.

As a further consistency check on our computation, we can evaluate our D-dimensional scattering amplitudes for $D = 4 - 2\epsilon$ and for specific choices of polarization vectors ε_i^μ that correspond to four-dimensional helicity states, thereby reproducing all earlier results from Ref. [4], e.g.

$$\mathcal{M}^{(0)}(1_{4+}2_{4+}3_{4+}4_{4+}) = \frac{stu}{504m^2} + \frac{(s^2 + st + t^2)^2}{3780m^4} + \dots , \tag{5.26}$$

where 1_{4+} refers to the polarization vector $\varepsilon_{1,4+}^\mu$, etc. (See our conventions in Eq. (5.6)).

Using our scattering amplitudes we may now probe the richer space of states of the graviton in $D > 4$. We consider examples of elastic amplitudes of the form $\mathcal{M}(1_{a-}2_{b-}3_{b+}4_{a+})$ for various values of a and b.

As mentioned above, generally, in order to ensure the validity of EFT bounds it is crucial to know the behavior of our amplitudes in the Regge limit, $|s| \gg -t$, $|s| \gg m^2$. Since our field theory data are only stand-in models for a intermediate UV completion of gravitational scattering, their behavior is generically worse than expected from quantum Regge bounds [345, 346, 388]. The exact behavior of the amplitudes in the Regge limit depends on the graviton polarizations, but using the explicit expressions for the amplitudes we have checked that the worst behavior is saturated by the spin-2 exchange (inside the $\mathcal{N} = 8$ amplitude) with a scaling (in even spacetime dimension D) of the form

$$\mathcal{M} \sim s^{D-1} , \tag{5.27}$$

which recovers the s^3 behavior in $D = 4$ explored in Ref. [4].

Similarly to the string-theory cases, the non-supersymmetric examples we consider here contain massless exchanges that would need to be taken into account in mapping the amplitude coefficients to Lagrangian coefficients.

5.6 Data summary and plots

Having discussed the relevant computations of the new explicit models of UV completions, we now proceed to explore the associated values of the low-energy couplings in the large-mass expansion of the amplitudes. Our analysis supports the notion that physical theories lie on small islands. Interestingly, if we choose the external states to be $4_\pm$ (which may be thought of as polarization tensors restricted to a four-dimensional subspace), we find that the projective data points remain on the same four-dimensional islands independent of the spacetime dimension.

5.6.1 Sample data in $D = 4$

To confirm our D-dimensional setup, we first reproduce the data points in Fig. 10 of Ref. [4] by specializing to $D = 4$. To do so we select four-dimensional helicity states for the external gravitons corresponding to $\mathcal{M}(1_{4-}2_{4-}3_{4+}4_{4+}) = s^4 f(t, u)$ (see Eq. (5.6) for our polarization conventions), where $f(t, u)$ admits the low-energy expansion

$$f(t, u) = \sum_{k \geq q \geq 0} a_{k,q} \, s^{k-q} t^q \,. \tag{5.28}$$

Additionally, as explained in section 5.3, we add a new data point for our nonperturbative results for the four-graviton scattering generated from the effective superpotential of a $\mathcal{N} = 1$ matter-coupled supersymmetric gauge theory further coupled to gravity. In this special case, f is a function of s only so that the sum truncates and the only nonzero coefficients are the $a_{k,0}$.

In Fig. 5.6.1 and the following, our labeling conventions are as follows: NP Matter $\equiv$
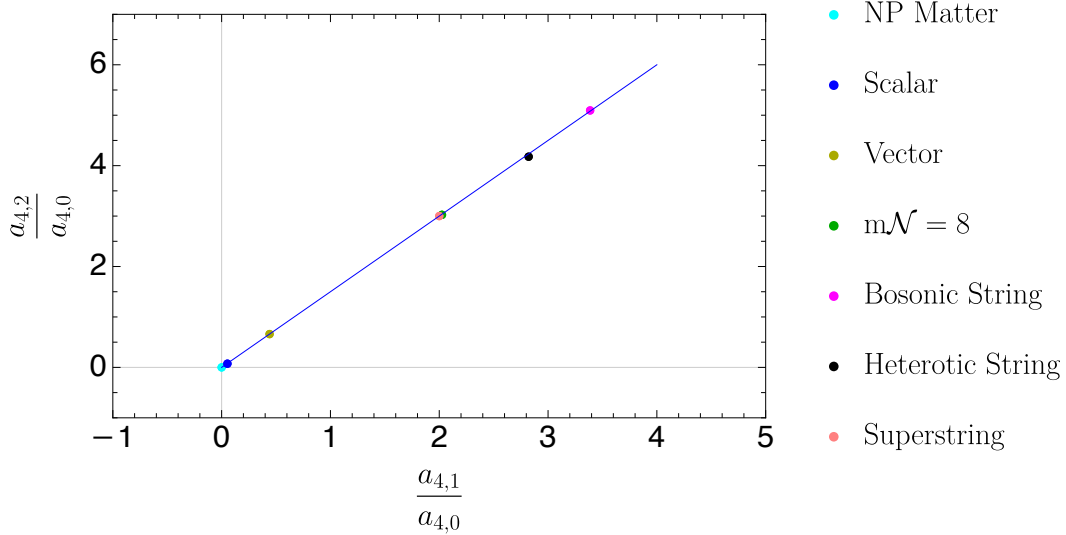
Figure 5.6.1: The $D = 4$ EFT data for various models for $a_{4,1}/a_{4,0}$ and $a_{4,2}/a_{4,0}$. A line with slope $3/2$ is added. The data points do not land perfectly on this line.

nonperturbative matter-coupled $\mathcal{N} = 1$ supersymmetric gauge theory, Scalar $\equiv$ massive spin-0 running in the loop, Vector $\equiv$ massive spin-1 running in the loop, $m\mathcal{N}=8 \equiv$ massive $\mathcal{N} = 8$ supermultiplet in the loop. The new data points further emphasize the main observation of Ref. [4], that explicit data lies on small 'theory islands' in the space allowed by unitarity, causality, and crossing constraints (this larger space is not indicated in Fig. 5.6.1 and is the red-shaded region in Fig. 9 of Ref. [4]).

5.6.2 Sample data in $D = 6$

To showcase some features of our amplitude data, we generate similar data plots for graviton polarizations that are outside the four-dimensional helicity setup. To this end, we first consider scattering of gravitons in $D = 6$ with the polarization choice $\mathcal{M}(1_{6-}2_{6-}3_{6+}4_{6+})$ where all polarizations are outside the four-dimensional subspace. (See Eq. (5.6) for our conventions of the graviton polarization states.) We consider the coefficients of the $1/m^2$ terms in Fig. 5.6.2 which are polynomials in s, t of degree four. The particular helicity choice renders the amplitude $t \leftrightarrow u$ symmetric and we denote the amplitude coefficients by their corresponding monomial in the Mandelstams. Unlike for the $D = 4$ examples considered

214

previously, it is not always possible to factor out some overall powers of Mandelstams.
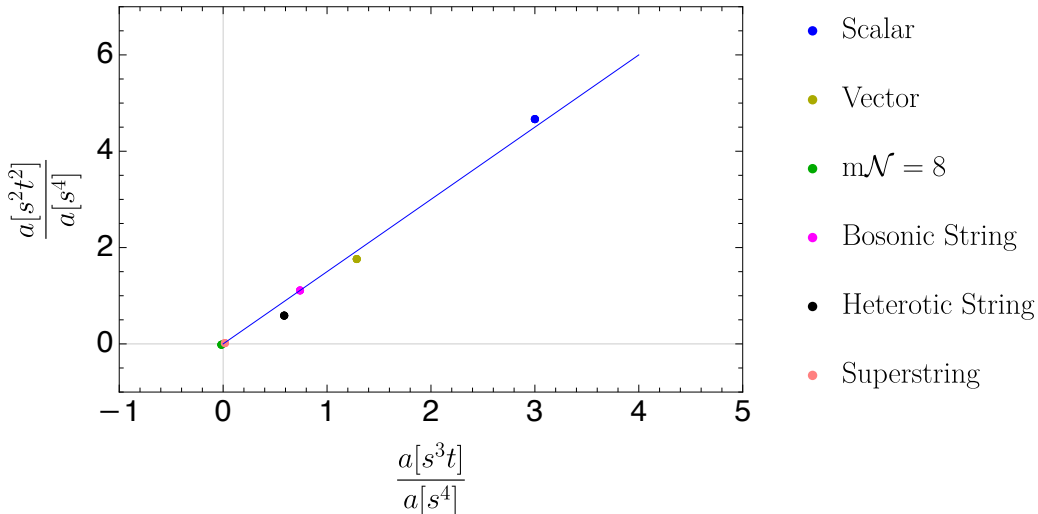
Figure 5.6.2: The $D = 6$ EFT data for various models for $a[s^3t]/a[s^4]$ and $a[s^2t^2]/a[s^4]$. A line with slope $3/2$ is added to guide the eye. Here $a[x]$ stands for the coefficient of the monomial x in the Taylor expansion of the amplitude.

It is fascinating to observe that, similarly to four-dimensional theories, the data points of the various models lie on an almost straight line and their spread from the line is much smaller than the extend of the line itself, giving us a concrete first example of small theory islands beyond $D = 4$.

We should, however, stress that not all extra-dimensional data falls on such perfect lines. To see this, let us investigate a three-dimensional section of the coefficient space at mass-level $1/m^6$ where we have degree-6 polynomials in s and t. We summarize our results in Fig. 5.6.3. As seen in a rotated viewpoint shown in Fig. 5.6.4, this data essentially lies in a plane. While it appears that the virtual scalar EFT lies somewhat off a line formed by the other models, it is difficult to assess the broader significance of this departure vis-à-vis the parameter space allowed by causality, unitarity and crossing constraints, which is currently not known beyond $D = 4$.

Figure 5.6.3: The $D = 6$ EFT data for various models for the ratios of low-energy amplitude coefficients $a[s^5t]/a[s^6]$, $a[s^4t^2]/a[s^6]$, and $a[s^3t^3]/a[s^6]$. We add a straight line to guide the eye. As illustrated in Fig. 5.6.4 from a different viewpoint the data essentially lie in a plane.
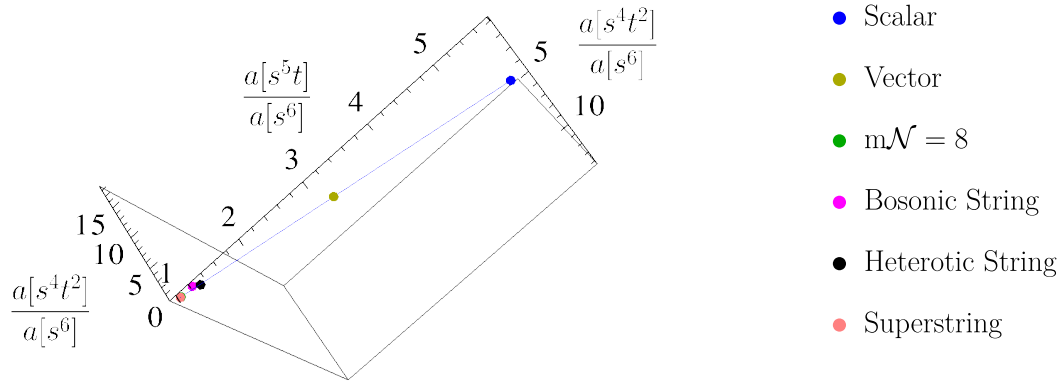
Figure 5.6.4: The same data points and line of Fig. 5.6.3 from a different viewpoint that demonstrates that the data essentially lie in a plane.

5.6.3 Sample data in $D = 10$

We proceed to analyze the data provided by perturbative calculations in $D = 10$, which is an interesting dimension from a superstring perspective. We observe that, as in lower dimen-

sions, the ratios of four-graviton amplitude coefficients again lie on a remarkably thin island. As mentioned in the introduction, this theoretical data should provide crucial guidance for future dispersive analyses analogous to those carried out in $D = 4$. Here, we only plot one particular section through our data in $D = 10$ which could eventually interplay with the search for string theory via the analysis of graviton scattering. For concreteness, we consider the amplitude $\mathcal{M}(1_{6-} 2_{10-} 3_{10+} 4_{6+})$.

Taking the large-mass expansion and evaluating all tensor structures for the specified graviton-polarization choice we collect, for example, the expansion coefficients similar to the $k = 4$ coefficients in $D = 4$. Notably, in $D = 10$ it no longer holds that we can factor out an overall helicity-dependent polynomial of the Mandelstam invariants. Therefore, the formerly $k = 4$ amplitude coefficients are associated to honest degree-8 polynomials in s, t. In the particular example we discuss, even though we do not naively have crossing symmetry due to the polarization choice, the only nontrivial contractions of polarization vectors that survive are $\varepsilon_2 \cdot \varepsilon_3$ and $\varepsilon_1 \cdot \varepsilon_4$ which is left invariant under $2 \leftrightarrow 3$ or $1 \leftrightarrow 4$. At the level of the polynomials in Mandelstam invariants, this leaves three independent degrees of freedom that we can in general bound from unitarity, causality, crossing and Regge-behavior considerations. The three independent coefficients are associated to the s^8, $s^6 t^2$ and $s^4 t^4$ terms respectively and their ratios are depicted in Fig. 5.6.5.

The data lie on an almost straight line of approximate slope 9/2. We leave to future work to establish the appropriate bounded regions of allowed parameter space from unitarity and causality constraints. However, the similarity between Figs. 5.6.1 and 5.6.5 suggests that many of the interesting features of the four-dimensional theory islands survive in higher dimensions as well.

Recently, the projective bounds between independent Wilson coefficients of the same mass-level k have been generalized to extremely interesting bounds of Wilson coefficients against e.g. Newton's constant [390, 391]. Here, we chose to plot projective data points due in part to the surprising observation that Fig. 5.6.1 in $D = 4$ does not change significantly compared to Fig. 5.6.6 in $D = 10$, where in both cases we evaluate the amplitudes for polar-
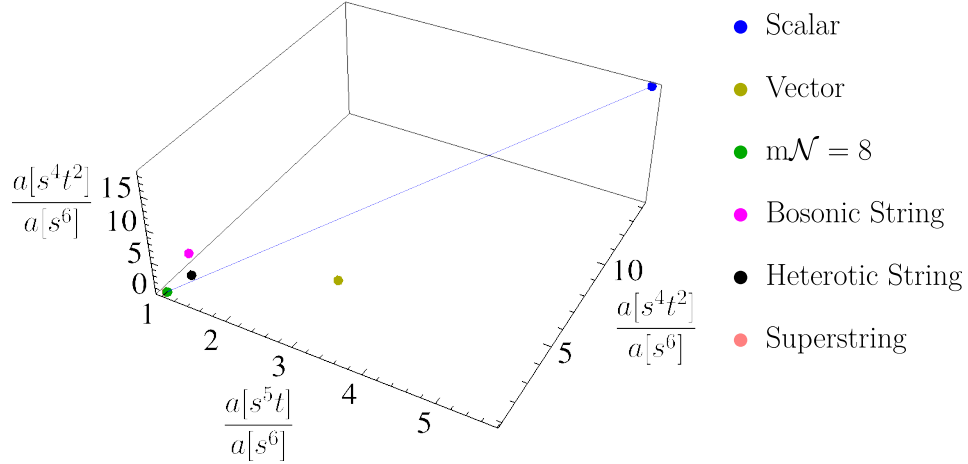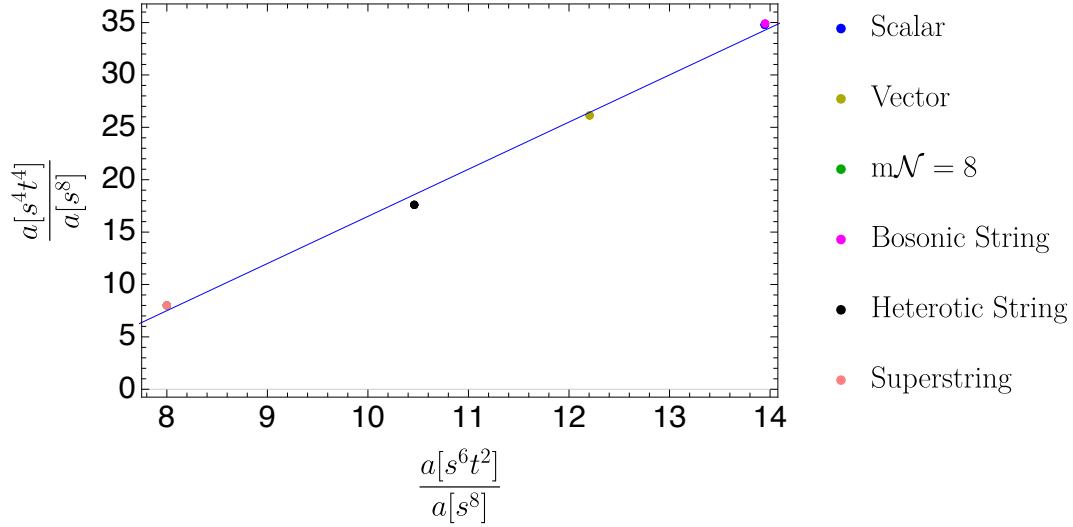
Figure 5.6.5: The $D = 10$ EFT data for various models for the ratios of low-energy amplitude coefficients $a[s^6t^2]/a[s^8]$ and $a[s^4t^4]/a[s^8]$. A line with slope $9/2$ is added to guide the eye.
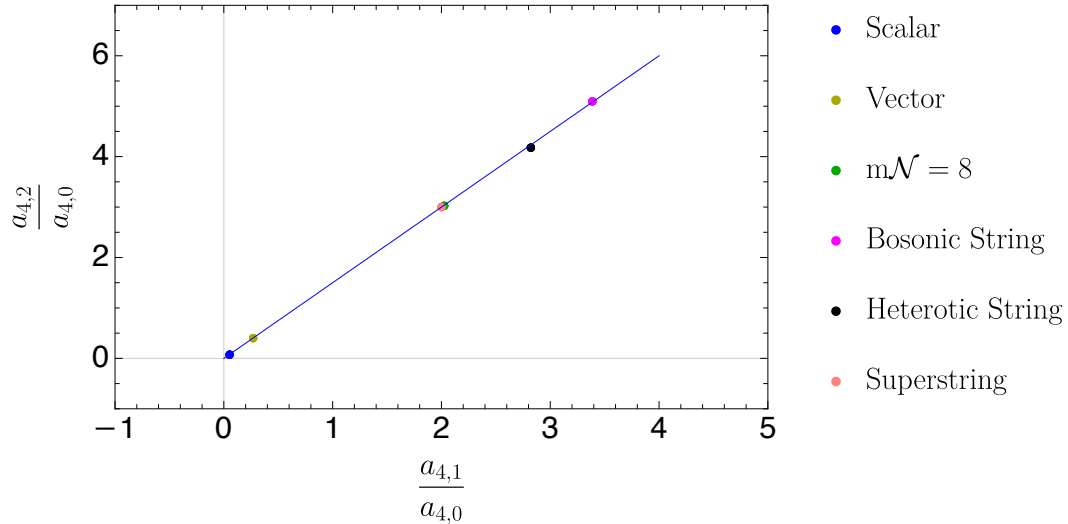
Figure 5.6.6: The $D = 10$ EFT data with four-dimensional external polarizations $4_\pm$. Here we follow the conventions of Eq. (5.28). A line with slope $3/2$ is added to guide the eye.

izations corresponding to four-dimensional helicity states. Specifically, only the "Vector" data point is D-dependent, and this dependence is solely due to the D_s appearing in Eq. (5.24). The net effect of this D-dependence is that the "Vector" data point is closer to the "Scalar" in Fig. 5.6.6 compared to Fig. 5.6.1. While we do not spell out the details, this relative unifor-

mity of the data across dimensions can be understood from the analysis of dimension-shifted scalar integrals. This is consistent with the intuition that extra-dimensional momenta in the loop can be thought of as a Kaluza-Klein mass which we effectively integrate over. This integral over the mass then drops out from the projective data.

5.7   Conclusions and Outlook

In this work we studied explicit perturbative and nonperturbative models for UV sensible four-graviton scattering amplitudes and their respective low-energy expansions. In particular, as a first example, we studied a nonperturbative $\mathcal{N} = 1$ supersymmetric gauge theory also coupled to gravity in four spacetime dimensions. Moreover, in D dimensions we considered tree-level four-graviton amplitudes in string theory and computed minimally-coupled one-loop four-graviton amplitudes with massive matter circulating in the loop.

The crucial output is the low-energy expansion of these amplitudes. As in the four-dimensional EFTs considered in Ref. [4], the low-energy coefficients of our data populate rather small theory islands compared to the naive expectation that consistent theories should fill out the full space of allowed low-energy couplings. Unlike the four-dimensional case where this feature was attributed to low-spin dominance, in general spacetime dimensions we do not currently have the same level of understanding. Nonetheless, our explicit analysis suggests that similar mechanisms are at work and it would be extremely interesting to further explore it by studying the partial-wave decomposition of our higher-dimensional amplitudes. We also anticipate that our explicit data will serve as a useful guide for any upcoming analysis of dispersive bounds on the low-energy Wilson coefficients. Further data can be found by exploiting the results of Ref. [441], in which one-loop amplitudes in theories deformed by operators induced by integrating out massive string states are computed. Similarly to the discussion in section 5.5.1, the states circulating in the loop can be rendered massive through Kaluza-Klein reduction; then, the resulting amplitudes are interpreted as those of an EFT of compactified string theory valid at scales $p^2 \sim m_{\mathrm{KK}}^2 \ll (\alpha')^{-2}$, in the same spirit as the discussion in section 5.3.

There are several further interesting directions to pursue. For one, beyond $D = 4$, gravitational scattering amplitudes are no longer plagued by infrared singularities that hamper obtaining a number of four-dimensional bounds from various approaches and can show up in the form of IR-logarithms even beyond the forward limit bounds [390]. Gravitational scattering in higher dimensions is also interesting in light of the recent attempts to find string theory [282] from an S-matrix bootstrap point of view. It would be very interesting to narrow down the range of possible extensions of gravitational UV completions in 10 spacetime dimensions beyond string theory. One could also combine the scattering matrix for different graviton states in higher dimensions into a matrix, on which nontrivial bounds can be determined, analogous to the ones found for different helicity configurations in four dimensions [4].

Additionally, the data presented here is primarily deduced from conventional gravitational scattering amplitudes, although we also presented a first example of data deduced from nonperturbative amplitudes. Recently, certain more exotic amplitudes with "accumulation point spectra" have gained some attention in e.g. Refs. [442, 443] and likewise in the model of Appendix D of Ref. [4] that in turn was inspired by Ref. [268]. It is interesting to note that while the accumulation-point model of Ref. [4] was designed to violate low-spin dominance, the associated low-energy EFT still belongs to the same theory island as the more conventional string- and field-theory data. It would be interesting to study the ultimate fate of accumulation-point amplitudes and determine whether or not they should be thought of as physical UV completions.

Along similar lines, it would be interesting to think about additional models that UV-complete gravitational scattering. Perhaps the most interesting new classes of theories involves nonperturbative physics. Here, we studied only a first example. It is possible to carry out a controlled non-perturbative analysis in the context of the AdS/CFT correspondence [444, 445, 446], generalized as in e.g. Ref. [447] or with a simple cutoff in the transverse direction [448], to describe a confining boundary theory. Indeed, bulk AdS_5 supergravity can be used to find the boundary four-dimensional correlation functions of e.g. four stress

tensors, which in turn can be interpreted as the four-graviton off-shell Green's functions. Fourier-transforming to boundary momentum space allows on-shell conditions to be imposed and leads to the boundary four-graviton amplitude due to virtual nonperturbative matter. Naively, the contribution of one bulk-exchange diagram to the amplitude is, up to a polynomial helicity-dependent factor, a function of the corresponding Mandelstam invariant. It would be very interesting to explore the consequences of these polynomial factors on the Taylor coefficients of the expansion of the amplitude at large confinement scale.[6]

In conclusion, placing bounds on gravitational scattering and analyzing explicit data in four spacetime dimensions and beyond should give us a fruitful probe of possible extensions of Einstein gravity. A key question is whether we can constrain sensible theories to live on islands as small as those suggested by the explicit theoretical data.

---

[6]At high energies the scattering process is localized in AdS space and given, up to external-state factors, by tree-level string theory amplitudes [448]. This suggests—but does not prove—that we may expect certain similarities between the properties of flat-space string-theory Taylor coefficients and those of the boundary graviton amplitudes.

REFERENCES

[1] D. Kosmopoulos, *Simplifying D-Dimensional Physical-State Sums in Gauge Theory and Gravity*, 2009.00141.

[2] D. Kosmopoulos and A. Luna, *Quadratic-in-spin Hamiltonian at $\mathcal{O}(G^2)$ from scattering amplitudes*, JHEP **07** (2021) 037 [2102.10137].

[3] Z. Bern, D. Kosmopoulos, A. Luna, R. Roiban and F. Teng, *Binary Dynamics Through the Fifth Power of Spin at $\mathcal{O}(G^2)$*, 2203.06202.

[4] Z. Bern, D. Kosmopoulos and A. Zhiboedov, *Gravitational Effective Field Theory Islands, Low-Spin Dominance, and the Four-Graviton Amplitude*, 2103.12728.

[5] Z. Bern, E. Herrmann, D. Kosmopoulos and R. Roiban, *Effective Field Theory Islands from Perturbative and Nonperturbative Four-Graviton Amplitudes*, 2205.01655.

[6] F. A. Berends, R. Kleiss, P. De Causmaecker, R. Gastmans and T. T. Wu, *Single Bremsstrahlung Processes in Gauge Theories*, Phys. Lett. B **103** (1981) 124.

[7] P. De Causmaecker, R. Gastmans, W. Troost and T. T. Wu, *Multiple Bremsstrahlung in Gauge Theories at High-Energies. 1. General Formalism for Quantum Electrodynamics*, Nucl. Phys. B **206** (1982) 53.

[8] R. Kleiss and W. J. Stirling, *Spinor Techniques for Calculating p anti-p —> W+- / Z0 + Jets*, Nucl. Phys. B **262** (1985) 235.

[9] J. F. Gunion and Z. Kunszt, *Improved Analytic Techniques for Tree Graph Calculations and the G g q anti-q Lepton anti-Lepton Subprocess*, Phys. Lett. B **161** (1985) 333.

[10] Z. Xu, D.-H. Zhang and L. Chang, *Helicity Amplitudes for Multiple Bremsstrahlung in Massless Nonabelian Gauge Theories*, Nucl. Phys. B **291** (1987) 392.

[11] A. Hodges, *Eliminating spurious poles from gauge-theoretic amplitudes*, JHEP **05** (2013) 135 [0905.1473].

[12] Z. Bern, C. Cheung, R. Roiban, C.-H. Shen, M. P. Solon and M. Zeng, *Scattering Amplitudes and the Conservative Hamiltonian for Binary Systems at Third Post-Minkowskian Order*, Phys. Rev. Lett. **122** (2019) 201603 [1901.04424].

[13] Z. Bern, C. Cheung, R. Roiban, C.-H. Shen, M. P. Solon and M. Zeng, *Black Hole Binary Dynamics from the Double Copy and Effective Theory*, JHEP **10** (2019) 206 [1908.01493].

[14] LIGO SCIENTIFIC, VIRGO collaboration, B. P. Abbott et al., *Observation of Gravitational Waves from a Binary Black Hole Merger*, Phys. Rev. Lett. **116** (2016) 061102 [1602.03837].

[15] LIGO Scientific, Virgo collaboration, B. P. Abbott et al., *GW170817: Observation of Gravitational Waves from a Binary Neutron Star Inspiral*, *Phys. Rev. Lett.* **119** (2017) 161101 [`1710.05832`].

[16] J. C. Collins, *Renormalization: An Introduction to Renormalization, The Renormalization Group, and the Operator Product Expansion*, vol. 26 of *Cambridge Monographs on Mathematical Physics*. Cambridge University Press, Cambridge, 1986, 10.1017/CBO9780511622656.

[17] Z. Bern, C. Cheung, H.-H. Chi, S. Davies, L. Dixon and J. Nohle, *Evanescent Effects Can Alter Ultraviolet Divergences in Quantum Gravity without Physical Consequences*, *Phys. Rev. Lett.* **115** (2015) 211301 [`1507.06118`].

[18] A. Cristofoli, P. H. Damgaard, P. Di Vecchia and C. Heissenberg, *Second-order Post-Minkowskian scattering in arbitrary dimensions*, *JHEP* **07** (2020) 122 [`2003.10274`].

[19] Z. Bern, L. J. Dixon, D. C. Dunbar and D. A. Kosower, *One loop n point gauge theory amplitudes, unitarity and collinear limits*, *Nucl. Phys. B* **425** (1994) 217 [`hep-ph/9403226`].

[20] Z. Bern, L. J. Dixon, D. C. Dunbar and D. A. Kosower, *Fusing gauge theory tree amplitudes into loop amplitudes*, *Nucl. Phys. B* **435** (1995) 59 [`hep-ph/9409265`].

[21] W. L. van Neerven, *Dimensional Regularization of Mass and Infrared Singularities in Two Loop On-shell Vertex Functions*, *Nucl. Phys. B* **268** (1986) 453.

[22] Z. Bern and A. G. Morgan, *Massive loop amplitudes from unitarity*, *Nucl. Phys. B* **467** (1996) 479 [`hep-ph/9511336`].

[23] Z. Bern, L. J. Dixon, D. C. Dunbar and D. A. Kosower, *One loop selfdual and N=4 superYang-Mills*, *Phys. Lett. B* **394** (1997) 105 [`hep-th/9611127`].

[24] A. Brandhuber, S. McNamara, B. J. Spence and G. Travaglini, *Loop amplitudes in pure Yang-Mills from generalised unitarity*, *JHEP* **10** (2005) 011 [`hep-th/0506068`].

[25] C. Anastasiou, R. Britto, B. Feng, Z. Kunszt and P. Mastrolia, *D-dimensional unitarity cut method*, *Phys. Lett. B* **645** (2007) 213 [`hep-ph/0609191`].

[26] C. Anastasiou, R. Britto, B. Feng, Z. Kunszt and P. Mastrolia, *Unitarity cuts and Reduction to master integrals in d dimensions for one-loop amplitudes*, *JHEP* **03** (2007) 111 [`hep-ph/0612277`].

[27] R. Britto and B. Feng, *Unitarity cuts with massive propagators and algebraic expressions for coefficients*, *Phys. Rev. D* **75** (2007) 105006 [`hep-ph/0612089`].

[28] S. D. Badger, *Direct Extraction Of One Loop Rational Terms*, *JHEP* **01** (2009) 049 [`0806.4600`].

[29] R. K. Ellis, W. T. Giele, Z. Kunszt and K. Melnikov, *Masses, fermions and generalized D-dimensional unitarity*, *Nucl. Phys. B* **822** (2009) 270 [0806.3467].

[30] R. K. Ellis, W. T. Giele, Z. Kunszt, K. Melnikov and G. Zanderighi, *One-loop amplitudes for W^+ 3 jet production in hadron collisions*, *JHEP* **01** (2009) 012 [0810.2762].

[31] S. Badger, C. Brønnum-Hansen, H. B. Hartanto and T. Peraro, *First look at two-loop five-gluon scattering in QCD*, *Phys. Rev. Lett.* **120** (2018) 092001 [1712.02229].

[32] T. Gehrmann, J. M. Henn and T. Huber, *The three-loop form factor in N=4 super Yang-Mills*, *JHEP* **03** (2012) 101 [1112.4524].

[33] H. Kawai, D. C. Lewellen and S. H. H. Tye, *A Relation Between Tree Amplitudes of Closed and Open Strings*, *Nucl. Phys. B* **269** (1986) 1.

[34] Z. Bern, J. J. M. Carrasco and H. Johansson, *New Relations for Gauge-Theory Amplitudes*, *Phys. Rev. D* **78** (2008) 085011 [0805.3993].

[35] Z. Bern, J. J. M. Carrasco and H. Johansson, *Perturbative Quantum Gravity as a Double Copy of Gauge Theory*, *Phys. Rev. Lett.* **105** (2010) 061602 [1004.0476].

[36] J. J. M. Carrasco, R. Kallosh, R. Roiban and A. A. Tseytlin, *On the U(1) duality anomaly and the S-matrix of N=4 supergravity*, *JHEP* **07** (2013) 029 [1303.6219].

[37] Z. Bern, S. Davies and J. Nohle, *Double-Copy Constructions and Unitarity Cuts*, *Phys. Rev. D* **93** (2016) 105015 [1510.03448].

[38] G. Mogull and D. O'Connell, *Overcoming Obstacles to Colour-Kinematics Duality at Two Loops*, *JHEP* **12** (2015) 135 [1511.06652].

[39] O. T. Engelund, R. W. McKeown and R. Roiban, *Generalized unitarity and the worldsheet S matrix in $AdS_n \times S^n \times M^{10-2n}$*, *JHEP* **08** (2013) 023 [1304.4281].

[40] S. Mandelstam, *Light Cone Superspace and the Ultraviolet Finiteness of the N=4 Model*, *Nucl. Phys. B* **213** (1983) 149.

[41] G. Leibbrandt, *The Light Cone Gauge in Yang-Mills Theory*, *Phys. Rev. D* **29** (1984) 1699.

[42] J. M. Cornwall, *Spontaneous Symmetry Breaking Without Scalar Mesons. 2.*, *Phys. Rev. D* **10** (1974) 500.

[43] G. Curci, W. Furmanski and R. Petronzio, *Evolution of Parton Densities Beyond Leading Order: The Nonsinglet Case*, *Nucl. Phys. B* **175** (1980) 27.

[44] D. J. Pritchard and W. J. Stirling, *QCD Calculations in the Light Cone Gauge. 1*, *Nucl. Phys. B* **165** (1980) 237.

[45] A. Koemans Collado, P. Di Vecchia and R. Russo, *Revisiting the second post-Minkowskian eikonal and the dynamics of binary black holes*, *Phys. Rev. D* **100** (2019) 066028 [1904.02667].

[46] Z. Bern, A. Luna, R. Roiban, C.-H. Shen and M. Zeng, *Spinning black hole binary dynamics, scattering amplitudes, and effective field theory*, *Phys. Rev. D* **104** (2021) 065014 [2005.03071].

[47] Z. Bern, L. J. Dixon and D. A. Kosower, *One loop amplitudes for e+ e- to four partons*, *Nucl. Phys. B* **513** (1998) 3 [hep-ph/9708239].

[48] Z. Bern, J. S. Rozowsky and B. Yan, *Two loop four gluon amplitudes in N=4 superYang-Mills*, *Phys. Lett. B* **401** (1997) 273 [hep-ph/9702424].

[49] J. J. van der Bij and E. W. N. Glover, *Z Boson Production and Decay via Gluons*, *Nucl. Phys. B* **313** (1989) 237.

[50] M. Baillargeon and F. Boudjema, *Contribution of the bosonic loops to the three photon decay of the Z*, *Phys. Lett. B* **272** (1991) 158.

[51] T. Binoth, M. Ciccolini, N. Kauer and M. Kramer, *Gluon-induced WW background to Higgs boson searches at the LHC*, *JHEP* **03** (2005) 065 [hep-ph/0503094].

[52] S. D. McDermott, H. H. Patel and H. Ramani, *Dark Photon Decay Beyond The Euler-Heisenberg Limit*, *Phys. Rev. D* **97** (2018) 073005 [1705.00619].

[53] E. W. N. Glover and A. G. Morgan, *Z boson decay into photons*, *Z. Phys. C* **60** (1993) 175.

[54] T. Binoth, E. W. N. Glover, P. Marquard and J. J. van der Bij, *Two loop corrections to light by light scattering in supersymmetric QED*, *JHEP* **05** (2002) 060 [hep-ph/0202266].

[55] E. W. N. Glover and M. E. Tejeda-Yeomans, *Two loop QCD helicity amplitudes for massless quark massless gauge boson scattering*, *JHEP* **06** (2003) 033 [hep-ph/0304169].

[56] T. Gehrmann, L. Tancredi and E. Weihs, *Two-loop QCD helicity amplitudes for $g\,g \to Z\,g$ and $g\,g \to Z\,\gamma$*, *JHEP* **04** (2013) 101 [1302.2630].

[57] Z. Bern, A. Edison, D. Kosower and J. Parra-Martinez, *Curvature-squared multiplets, evanescent effects, and the U(1) anomaly in $N = 4$ supergravity*, *Phys. Rev. D* **96** (2017) 066004 [1706.01486].

[58] Z. Bern, J. Parra-Martinez and E. Sawyer, *Structure of two-loop SMEFT anomalous dimensions via on-shell methods*, *JHEP* **10** (2020) 211 [2005.12917].

[59] L. P. S. Singh and C. R. Hagen, *Lagrangian formulation for arbitrary spin. 1. The boson case*, *Phys. Rev. D* **9** (1974) 898.

[60] LIGO Scientific, Virgo collaboration, B. P. Abbott et al., *Observation of Gravitational Waves from a Binary Black Hole Merger*, *Phys. Rev. Lett.* **116** (2016) 061102 [`1602.03837`].

[61] LIGO Scientific, Virgo collaboration, B. P. Abbott et al., *GW170817: Observation of Gravitational Waves from a Binary Neutron Star Inspiral*, *Phys. Rev. Lett.* **119** (2017) 161101 [`1710.05832`].

[62] L. Blanchet, *Gravitational Radiation from Post-Newtonian Sources and Inspiralling Compact Binaries*, *Living Rev. Rel.* **17** (2014) 2 [`1310.1528`].

[63] G. Schäfer and P. Jaranowski, *Hamiltonian formulation of general relativity and post-Newtonian dynamics of compact binaries*, *Living Rev. Rel.* **21** (2018) 7 [`1805.07240`].

[64] W. D. Goldberger and I. Z. Rothstein, *An Effective field theory of gravity for extended objects*, *Phys. Rev. D* **73** (2006) 104029 [`hep-th/0409156`].

[65] K. Westpfahl, *High-Speed Scattering of Charged and Uncharged Particles in General Relativity*, *Fortsch. Phys.* **33** (1985) 417.

[66] T. Damour, *Gravitational scattering, post-Minkowskian approximation and Effective One-Body theory*, *Phys. Rev. D* **94** (2016) 104015 [`1609.00354`].

[67] T. Damour, *High-energy gravitational scattering and the general relativistic two-body problem*, *Phys. Rev. D* **97** (2018) 044038 [`1710.10599`].

[68] T. Damour, *Classical and quantum scattering in post-Minkowskian gravity*, *Phys. Rev. D* **102** (2020) 024060 [`1912.02139`].

[69] Y. Iwasaki, *Quantum theory of gravitation vs. classical theory. - fourth-order potential*, *Prog. Theor. Phys.* **46** (1971) 1587.

[70] D. Neill and I. Z. Rothstein, *Classical Space-Times from the S Matrix*, *Nucl. Phys. B* **877** (2013) 177 [`1304.7263`].

[71] L. J. Dixon, *Calculating scattering amplitudes efficiently*, in *Theoretical Advanced Study Institute in Elementary Particle Physics (TASI 95): QCD and Beyond*, pp. 539–584, 1, 1996, `hep-ph/9601359`.

[72] H. Elvang and Y.-t. Huang, *Scattering Amplitudes*, `1308.1697`.

[73] Z. Bern, J. J. Carrasco, M. Chiodaroli, H. Johansson and R. Roiban, *The Duality Between Color and Kinematics and its Applications*, `1909.01358`.

[74] C. Cheung, I. Z. Rothstein and M. P. Solon, *From Scattering Amplitudes to Classical Potentials in the Post-Minkowskian Expansion*, *Phys. Rev. Lett.* **121** (2018) 251101 [`1808.02489`].

[75] C. Cheung and M. P. Solon, *Classical gravitational scattering at $\mathcal{O}(G^3)$ from Feynman diagrams*, *JHEP* **06** (2020) 144 [2003.08351].

[76] A. Antonelli, A. Buonanno, J. Steinhoff, M. van de Meent and J. Vines, *Energetics of two-body Hamiltonians in post-Minkowskian gravity*, *Phys. Rev. D* **99** (2019) 104004 [1901.07102].

[77] Z. Bern, J. Parra-Martinez, R. Roiban, M. S. Ruf, C.-H. Shen, M. P. Solon et al., *Scattering Amplitudes and Conservative Binary Dynamics at $\mathcal{O}(G^4)$*, *Phys. Rev. Lett.* **126** (2021) 171601 [2101.07254].

[78] D. A. Kosower, B. Maybee and D. O'Connell, *Amplitudes, Observables, and Classical Scattering*, *JHEP* **02** (2019) 137 [1811.10950].

[79] L. de la Cruz, B. Maybee, D. O'Connell and A. Ross, *Classical Yang-Mills observables from amplitudes*, *JHEP* **12** (2020) 076 [2009.03842].

[80] A. Cristofoli, N. E. J. Bjerrum-Bohr, P. H. Damgaard and P. Vanhove, *Post-Minkowskian Hamiltonians in general relativity*, *Phys. Rev. D* **100** (2019) 084040 [1906.01579].

[81] N. E. J. Bjerrum-Bohr, A. Cristofoli and P. H. Damgaard, *Post-Minkowskian Scattering Angle in Einstein Gravity*, *JHEP* **08** (2020) 038 [1910.09366].

[82] G. Kälin and R. A. Porto, *From Boundary Data to Bound States*, *JHEP* **01** (2020) 072 [1910.03008].

[83] G. Kälin and R. A. Porto, *From boundary data to bound states. Part II. Scattering angle to dynamical invariants (with twist)*, *JHEP* **02** (2020) 120 [1911.09130].

[84] G. Kälin and R. A. Porto, *Post-Minkowskian Effective Field Theory for Conservative Binary Dynamics*, *JHEP* **11** (2020) 106 [2006.01184].

[85] G. Kälin, Z. Liu and R. A. Porto, *Conservative Dynamics of Binary Systems to Third Post-Minkowskian Order from the Effective Field Theory Approach*, *Phys. Rev. Lett.* **125** (2020) 261103 [2007.04977].

[86] G. Mogull, J. Plefka and J. Steinhoff, *Classical black hole scattering from a worldline quantum field theory*, 2010.02865.

[87] S. Caron-Huot and Z. Zahraee, *Integrability of Black Hole Orbits in Maximal Supergravity*, *JHEP* **07** (2019) 179 [1810.04694].

[88] Z. Bern, H. Ita, J. Parra-Martinez and M. S. Ruf, *Universality in the classical limit of massless gravitational scattering*, *Phys. Rev. Lett.* **125** (2020) 031601 [2002.02459].

[89] J. Parra-Martinez, M. S. Ruf and M. Zeng, *Extremal black hole scattering at $\mathcal{O}(G^3)$: graviton dominance, eikonal exponentiation, and differential equations*, *JHEP* **11** (2020) 023 [2005.04236].

[90] F. Loebbert, J. Plefka, C. Shi and T. Wang, *Three-Body Effective Potential in General Relativity at 2PM and Resulting PN Contributions*, 2012.14224.

[91] P. Di Vecchia, C. Heissenberg, R. Russo and G. Veneziano, *Universality of ultra-relativistic gravitational scattering*, *Phys. Lett. B* **811** (2020) 135924 [2008.12743].

[92] P. Di Vecchia, C. Heissenberg, R. Russo and G. Veneziano, *Radiation Reaction from Soft Theorems*, 2101.05772.

[93] E. Herrmann, J. Parra-Martinez, M. S. Ruf and M. Zeng, *Gravitational Bremsstrahlung from Reverse Unitarity*, 2101.07255.

[94] T. Damour, *Radiative contribution to classical gravitational scattering at the third order in G*, *Phys. Rev. D* **102** (2020) 124008 [2010.01641].

[95] G. U. Jakobsen, G. Mogull, J. Plefka and J. Steinhoff, *Classical Gravitational Bremsstrahlung from a Worldline Quantum Field Theory*, *Phys. Rev. Lett.* **126** (2021) 201103 [2101.12688].

[96] K. Haddad and A. Helset, *Tidal effects in quantum field theory*, *JHEP* **12** (2020) 024 [2008.04920].

[97] R. Aoude, K. Haddad and A. Helset, *Tidal effects for spinning particles*, 2012.05256.

[98] M. Accettulli Huber, A. Brandhuber, S. De Angelis and G. Travaglini, *From amplitudes to gravitational radiation with cubic interactions and tidal effects*, 2012.06548.

[99] G. Kälin, Z. Liu and R. A. Porto, *Conservative Tidal Effects in Compact Binary Systems to Next-to-Leading Post-Minkowskian Order*, *Phys. Rev. D* **102** (2020) 124025 [2008.06047].

[100] C. Cheung and M. P. Solon, *Tidal Effects in the Post-Minkowskian Expansion*, *Phys. Rev. Lett.* **125** (2020) 191601 [2006.06665].

[101] C. Cheung, N. Shah and M. P. Solon, *Mining the Geodesic Equation for Scattering Data*, *Phys. Rev. D* **103** (2021) 024030 [2010.08568].

[102] Z. Bern, J. Parra-Martinez, R. Roiban, E. Sawyer and C.-H. Shen, *Leading Nonlinear Tidal Effects and Scattering Amplitudes*, 2010.08559.

[103] G. Faye, L. Blanchet and A. Buonanno, *Higher-order spin effects in the dynamics of compact binaries. I. Equations of motion*, *Phys. Rev. D* **74** (2006) 104033 [gr-qc/0605139].

[104] L. Blanchet, A. Buonanno and G. Faye, *Higher-order spin effects in the dynamics of compact binaries. II. Radiation field*, *Phys. Rev. D* **74** (2006) 104034 [gr-qc/0605140].

[105] T. Damour, P. Jaranowski and G. Schaefer, *Hamiltonian of two spinning compact bodies with next-to-leading order gravitational spin-orbit coupling*, Phys. Rev. D **77** (2008) 064032 [`0711.1048`].

[106] J. Steinhoff, S. Hergt and G. Schaefer, *On the next-to-leading order gravitational spin(1)-spin(2) dynamics*, Phys. Rev. D **77** (2008) 081501 [`0712.1716`].

[107] J. Steinhoff, G. Schaefer and S. Hergt, *ADM canonical formalism for gravitating spinning objects*, Phys. Rev. D **77** (2008) 104018 [`0805.3136`].

[108] R. A. Porto, *Post-Newtonian corrections to the motion of spinning bodies in NRGR*, Phys. Rev. D **73** (2006) 104031 [`gr-qc/0511061`].

[109] R. A. Porto and I. Z. Rothstein, *The Hyperfine Einstein-Infeld-Hoffmann potential*, Phys. Rev. Lett. **97** (2006) 021101 [`gr-qc/0604099`].

[110] R. A. Porto, *Absorption effects due to spin in the worldline approach to black hole dynamics*, Phys. Rev. D **77** (2008) 064026 [`0710.5150`].

[111] R. A. Porto and I. Z. Rothstein, *Next to Leading Order Spin(1)Spin(1) Effects in the Motion of Inspiralling Compact Binaries*, Phys. Rev. D **78** (2008) 044013 [`0804.0260`].

[112] M. Levi, *Next to Leading Order gravitational Spin1-Spin2 coupling with Kaluza-Klein reduction*, Phys. Rev. D **82** (2010) 064029 [`0802.1508`].

[113] R. A. Porto and I. Z. Rothstein, *Spin(1)Spin(2) Effects in the Motion of Inspiralling Compact Binaries at Third Order in the Post-Newtonian Expansion*, Phys. Rev. D **78** (2008) 044012 [`0802.0720`].

[114] R. A. Porto, *Next to leading order spin-orbit effects in the motion of inspiralling compact binaries*, Class. Quant. Grav. **27** (2010) 205001 [`1005.5730`].

[115] R. A. Porto, A. Ross and I. Z. Rothstein, *Spin induced multipole moments for the gravitational wave flux from binary inspirals to third Post-Newtonian order*, JCAP **03** (2011) 009 [`1007.1312`].

[116] M. Levi, *Next to Leading Order gravitational Spin-Orbit coupling in an Effective Field Theory approach*, Phys. Rev. D **82** (2010) 104004 [`1006.4139`].

[117] M. Levi, *Binary dynamics from spin1-spin2 coupling at fourth post-Newtonian order*, Phys. Rev. D **85** (2012) 064043 [`1107.4322`].

[118] M. Levi and J. Steinhoff, *Equivalence of ADM Hamiltonian and Effective Field Theory approaches at next-to-next-to-leading order spin1-spin2 coupling of binary inspirals*, JCAP **12** (2014) 003 [`1408.5762`].

[119] M. Levi and J. Steinhoff, *Next-to-next-to-leading order gravitational spin-orbit coupling via the effective field theory for spinning objects in the post-Newtonian scheme*, JCAP **01** (2016) 011 [1506.05056].

[120] M. Levi and J. Steinhoff, *Next-to-next-to-leading order gravitational spin-squared potential via the effective field theory for spinning objects in the post-Newtonian scheme*, JCAP **01** (2016) 008 [1506.05794].

[121] N. T. Maia, C. R. Galley, A. K. Leibovich and R. A. Porto, *Radiation reaction for spinning bodies in effective field theory I: Spin-orbit effects*, Phys. Rev. D **96** (2017) 084064 [1705.07934].

[122] N. T. Maia, C. R. Galley, A. K. Leibovich and R. A. Porto, *Radiation reaction for spinning bodies in effective field theory II: Spin-spin effects*, Phys. Rev. D **96** (2017) 084065 [1705.07938].

[123] W. D. Goldberger, J. Li and I. Z. Rothstein, *Non-conservative effects on Spinning Black Holes from World-Line Effective Field Theory*, 2012.14869.

[124] A. Antonelli, C. Kavanagh, M. Khalil, J. Steinhoff and J. Vines, *Gravitational spin-orbit coupling through third-subleading post-Newtonian order: from first-order self-force to arbitrary mass ratios*, Phys. Rev. Lett. **125** (2020) 011103 [2003.11391].

[125] A. Antonelli, C. Kavanagh, M. Khalil, J. Steinhoff and J. Vines, *Gravitational spin-orbit and aligned spin$_1$-spin$_2$ couplings through third-subleading post-Newtonian orders*, Phys. Rev. D **102** (2020) 124024 [2010.02018].

[126] R. A. Porto, *The effective field theorist's approach to gravitational dynamics*, Phys. Rept. **633** (2016) 1 [1601.04914].

[127] M. Levi, *Effective Field Theories of Post-Newtonian Gravity: A comprehensive review*, Rept. Prog. Phys. **83** (2020) 075901 [1807.01699].

[128] M. Levi, A. J. Mcleod and M. Von Hippel, *N^3LO gravitational spin-orbit coupling at order G^4*, JHEP **07** (2021) 115 [2003.02827].

[129] M. Levi, A. J. Mcleod and M. Von Hippel, *NNNLO gravitational quadratic-in-spin interactions at the quartic order in G*, 2003.07890.

[130] M. Levi, S. Mougiakakos and M. Vieira, *Gravitational cubic-in-spin interaction at the next-to-leading post-Newtonian order*, JHEP **01** (2021) 036 [1912.06276].

[131] M. Levi and F. Teng, *NLO gravitational quartic-in-spin interaction*, JHEP **01** (2021) 066 [2008.12280].

[132] D. Bini and T. Damour, *Gravitational spin-orbit coupling in binary systems, post-Minkowskian approximation and effective one-body theory*, Phys. Rev. D **96** (2017) 104038 [1709.00590].

[133] D. Bini, T. Damour and A. Geralico, *Spin-orbit precession along eccentric orbits: improving the knowledge of self-force corrections and of their effective-one-body counterparts*, *Phys. Rev. D* **97** (2018) 104046 [1801.03704].

[134] J. Vines, *Scattering of two spinning black holes in post-Minkowskian gravity, to all orders in spin, and effective-one-body mappings*, *Class. Quant. Grav.* **35** (2018) 084002 [1709.06016].

[135] J. Vines, J. Steinhoff and A. Buonanno, *Spinning-black-hole scattering and the test-black-hole limit at second post-Minkowskian order*, *Phys. Rev. D* **99** (2019) 064054 [1812.00956].

[136] N. Siemonsen and J. Vines, *Test black holes, scattering amplitudes and perturbations of Kerr spacetime*, *Phys. Rev. D* **101** (2020) 064066 [1909.07361].

[137] B. R. Holstein and A. Ross, *Spin Effects in Long Range Gravitational Scattering*, 0802.0716.

[138] V. Vaidya, *Gravitational spin Hamiltonians from the S matrix*, *Phys. Rev. D* **91** (2015) 024017 [1410.5348].

[139] A. Guevara, *Holomorphic Classical Limit for Spin Effects in Gravitational and Electromagnetic Scattering*, *JHEP* **04** (2019) 033 [1706.02314].

[140] N. Arkani-Hamed, T.-C. Huang and Y.-t. Huang, *Scattering amplitudes for all masses and spins*, *JHEP* **11** (2021) 070 [1709.04891].

[141] F. Cachazo and A. Guevara, *Leading Singularities and Classical Gravitational Scattering*, *JHEP* **02** (2020) 181 [1705.10262].

[142] A. Guevara, A. Ochirov and J. Vines, *Scattering of Spinning Black Holes from Exponentiated Soft Factors*, *JHEP* **09** (2019) 056 [1812.06895].

[143] M.-Z. Chung, Y.-T. Huang, J.-W. Kim and S. Lee, *The simplest massive S-matrix: from minimal coupling to Black Holes*, *JHEP* **04** (2019) 156 [1812.08752].

[144] B. Maybee, D. O'Connell and J. Vines, *Observables and amplitudes for spinning particles and black holes*, *JHEP* **12** (2019) 156 [1906.09260].

[145] M.-Z. Chung, Y.-T. Huang and J.-W. Kim, *Classical potential for general spinning bodies*, *JHEP* **09** (2020) 074 [1908.08463].

[146] M.-Z. Chung, Y.-t. Huang, J.-W. Kim and S. Lee, *Complete Hamiltonian for spinning binary systems at first post-Minkowskian order*, *JHEP* **05** (2020) 105 [2003.06600].

[147] A. Guevara, A. Ochirov and J. Vines, *Black-hole scattering with general spin directions from minimal-coupling amplitudes*, *Phys. Rev. D* **100** (2019) 104024 [1906.10071].

[148] N. Arkani-Hamed, Y.-t. Huang and D. O'Connell, *Kerr black holes as elementary particles*, *JHEP* **01** (2020) 046 [1906.10100].

[149] Y. F. Bautista and A. Guevara, *From Scattering Amplitudes to Classical Physics: Universality, Double Copy and Soft Theorems*, 1903.12419.

[150] M.-Z. Chung, Y.-T. Huang and J.-W. Kim, *Kerr-Newman stress-tensor from minimal coupling*, *JHEP* **12** (2020) 103 [1911.12775].

[151] A. Guevara, B. Maybee, A. Ochirov, D. O'connell and J. Vines, *A worldsheet for Kerr*, *JHEP* **03** (2021) 201 [2012.11570].

[152] W. T. Emond, Y.-T. Huang, U. Kol, N. Moynihan and D. O'Connell, *Amplitudes from Coulomb to Kerr-Taub-NUT*, 2010.07861.

[153] R. Aoude, M.-Z. Chung, Y.-t. Huang, C. S. Machado and M.-K. Tam, *Silence of Binary Kerr Black Holes*, *Phys. Rev. Lett.* **125** (2020) 181602 [2007.09486].

[154] R. Monteiro, D. O'Connell and C. D. White, *Black holes and the double copy*, *JHEP* **12** (2014) 056 [1410.0239].

[155] R. Aoude, K. Haddad and A. Helset, *On-shell heavy particle effective theories*, *JHEP* **05** (2020) 051 [2001.09164].

[156] P. H. Damgaard, K. Haddad and A. Helset, *Heavy Black Hole Effective Theory*, *JHEP* **11** (2019) 070 [1908.10308].

[157] K. Haddad and A. Helset, *The double copy for heavy particles*, *Phys. Rev. Lett.* **125** (2020) 181603 [2005.13897].

[158] D. Amati, M. Ciafaloni and G. Veneziano, *Higher Order Gravitational Deflection and Soft Bremsstrahlung in Planckian Energy Superstring Collisions*, *Nucl. Phys. B* **347** (1990) 550.

[159] S. Melville, S. G. Naculich, H. J. Schnitzer and C. D. White, *Wilson line approach to gravity in the high energy limit*, *Phys. Rev. D* **89** (2014) 025009 [1306.6019].

[160] A. Luna, S. Melville, S. G. Naculich and C. D. White, *Next-to-soft corrections to high energy scattering in QCD and gravity*, *JHEP* **01** (2017) 052 [1611.02172].

[161] R. Akhoury, R. Saotome and G. Sterman, *High Energy Scattering in Perturbative Quantum Gravity at Next to Leading Power*, *Phys. Rev. D* **103** (2021) 064036 [1308.5204].

[162] P. Di Vecchia, A. Luna, S. G. Naculich, R. Russo, G. Veneziano and C. D. White, *A tale of two exponentiations in $\mathcal{N} = 8$ supergravity*, *Phys. Lett. B* **798** (2019) 134927 [1908.05603].

[163] P. Di Vecchia, S. G. Naculich, R. Russo, G. Veneziano and C. D. White, *A tale of two exponentiations in $\mathcal{N} = 8$ supergravity at subleading level*, *JHEP* **03** (2020) 173 [`1911.11716`].

[164] Z. Bern, L. J. Dixon and D. A. Kosower, *Progress in one loop QCD computations*, *Ann. Rev. Nucl. Part. Sci.* **46** (1996) 109 [`hep-ph/9602280`].

[165] Z. Bern and Y.-t. Huang, *Basics of Generalized Unitarity*, *J. Phys. A* **44** (2011) 454003 [`1103.1869`].

[166] R. Britto, F. Cachazo and B. Feng, *Generalized unitarity and one-loop amplitudes in N=4 super-Yang-Mills*, *Nucl. Phys. B* **725** (2005) 275 [`hep-th/0412103`].

[167] M. Levi and J. Steinhoff, *Complete conservative dynamics for inspiralling compact binaries with spins at the fourth post-Newtonian order*, *JCAP* **09** (2021) 029 [`1607.04252`].

[168] J. Vines, D. Kunst, J. Steinhoff and T. Hinderer, *Canonical Hamiltonian for an extended test body in curved spacetime: To quadratic order in spin*, *Phys. Rev. D* **93** (2016) 103008 [`1601.07529`].

[169] M. Levi and J. Steinhoff, *Spinning gravitating objects in the effective field theory in the post-Newtonian scheme*, *JHEP* **09** (2015) 219 [`1501.04956`].

[170] M. Levi and J. Steinhoff, *Leading order finite size effects with spins for inspiralling compact binaries*, *JHEP* **06** (2015) 059 [`1410.2601`].

[171] J. Klauder and B. Skagerstam, *Coherent States: Applications in Physics and Mathematical Physics*. World Scientific, Singapore, 1985.

[172] V. Berestetskii, E. Lifshitz and L. Pitaevskii, *QUANTUM ELECTRODYNAMICS*, vol. 4 of *Course of Theoretical Physics*. Pergamon Press, Oxford, 1982.

[173] I. Khriplovich and A. Pomeransky, *Equations of motion of spinning relativistic particle in external fields*, *J. Exp. Theor. Phys.* **86** (1998) 839 [`gr-qc/9710098`].

[174] G. Passarino and M. J. G. Veltman, *One Loop Corrections for e+ e- Annihilation Into mu+ mu- in the Weinberg Model*, *Nucl. Phys. B* **160** (1979) 151.

[175] G. Ossola, C. G. Papadopoulos and R. Pittau, *Reducing full one-loop amplitudes to scalar integrals at the integrand level*, *Nucl. Phys. B* **763** (2007) 147 [`hep-ph/0609007`].

[176] D. Forde, *Direct extraction of one-loop integral coefficients*, *Phys. Rev. D* **75** (2007) 125019 [`0704.1835`].

[177] W. B. Kilgore, *One-loop Integral Coefficients from Generalized Unitarity*, `0711.5015`.

[178] A. Buonanno and T. Damour, *Effective one-body approach to general relativistic two-body dynamics*, *Phys. Rev. D* **59** (1999) 084006 [gr-qc/9811091].

[179] A. Buonanno and T. Damour, *Transition from inspiral to plunge in binary black hole coalescences*, *Phys. Rev. D* **62** (2000) 064015 [gr-qc/0001013].

[180] T. Damour, *Coalescence of two spinning black holes: an effective one-body approach*, *Phys. Rev. D* **64** (2001) 124013 [gr-qc/0103018].

[181] T. Damour, P. Jaranowski and G. Schaefer, *Effective one body approach to the dynamics of two spinning black holes with next-to-leading order spin-orbit coupling*, *Phys. Rev. D* **78** (2008) 024009 [0803.0915].

[182] E. Barausse and A. Buonanno, *An Improved effective-one-body Hamiltonian for spinning black-hole binaries*, *Phys. Rev. D* **81** (2010) 084024 [0912.3517].

[183] M. Khalil, J. Steinhoff, J. Vines and A. Buonanno, *Fourth post-Newtonian effective-one-body Hamiltonians with generic spins*, *Phys. Rev. D* **101** (2020) 104034 [2003.04469].

[184] Z. Liu, R. A. Porto and Z. Yang, *Spin Effects in the Effective Field Theory Approach to Post-Minkowskian Conservative Dynamics*, 2102.10059.

[185] M. Punturo et al., *The Einstein Telescope: A third-generation gravitational wave observatory*, *Class. Quant. Grav.* **27** (2010) 194002.

[186] LISA collaboration, P. Amaro-Seoane et al., *Laser Interferometer Space Antenna*, 1702.00786.

[187] D. Reitze et al., *Cosmic Explorer: The U.S. Contribution to Gravitational-Wave Astronomy beyond LIGO*, *Bull. Am. Astron. Soc.* **51** (2019) 035 [1907.04833].

[188] B. Bertotti, *On gravitational motion*, *Nuovo Cim.* **4** (1956) 898.

[189] R. P. Kerr, *The Lorentz-covariant approximation method in general relativity I*, *Nuovo Cim.* **13** (1959) 469.

[190] B. Bertotti and J. Plebanski, *Theory of gravitational perturbations in the fast motion approximation*, *Annals Phys.* **11** (1960) 169.

[191] M. Portilla, *MOMENTUM AND ANGULAR MOMENTUM OF TWO GRAVITATING PARTICLES*, *J. Phys. A* **12** (1979) 1075.

[192] K. Westpfahl and M. Goller, *GRAVITATIONAL SCATTERING OF TWO RELATIVISTIC PARTICLES IN POSTLINEAR APPROXIMATION*, *Lett. Nuovo Cim.* **26** (1979) 573.

[193] M. Portilla, *SCATTERING OF TWO GRAVITATING PARTICLES: CLASSICAL APPROACH*, *J. Phys. A* **13** (1980) 3677.

[194] L. Bel, T. Damour, N. Deruelle, J. Ibanez and J. Martin, *Poincaré-invariant gravitational field and equations of motion of two pointlike objects: The postlinear approximation of general relativity*, Gen. Rel. Grav. **13** (1981) 963.

[195] T. Ledvinka, G. Schaefer and J. Bicak, *Relativistic Closed-Form Hamiltonian for Many-Body Gravitating Systems in the Post-Minkowskian Approximation*, Phys. Rev. Lett. **100** (2008) 251101 [`0807.0214`].

[196] D. Bini and T. Damour, *Gravitational spin-orbit coupling in binary systems at the second post-Minkowskian approximation*, Phys. Rev. D **98** (2018) 044036 [`1805.10809`].

[197] G. U. Jakobsen, G. Mogull, J. Plefka and J. Steinhoff, *SUSY in the sky with gravitons*, JHEP **01** (2022) 027 [`2109.04465`].

[198] W.-M. Chen, M.-Z. Chung, Y.-t. Huang and J.-W. Kim, *The 2PM Hamiltonian for binary Kerr to quartic in spin*, `2111.13639`.

[199] B. M. Barker and R. F. O'Connell, *Derivation of the equations of motion of a gyroscope from the quantum theory of gravitation*, Phys. Rev. D **2** (1970) 1428.

[200] B. M. Barker and R. F. O'Connell, *Gravitational Two-Body Problem with Arbitrary Masses, Spins, and Quadrupole Moments*, Phys. Rev. D **12** (1975) 329.

[201] L. E. Kidder, C. M. Will and A. G. Wiseman, *Spin effects in the inspiral of coalescing compact binaries*, Phys. Rev. D **47** (1993) 4183 [`gr-qc/9211025`].

[202] L. E. Kidder, *Coalescing binary systems of compact objects to postNewtonian 5/2 order. 5. Spin effects*, Phys. Rev. D **52** (1995) 821 [`gr-qc/9506022`].

[203] H. Tagoshi, A. Ohashi and B. J. Owen, *Gravitational field and equations of motion of spinning compact binaries to 2.5 postNewtonian order*, Phys. Rev. D **63** (2001) 044006 [`gr-qc/0010014`].

[204] J. Steinhoff, S. Hergt and G. Schaefer, *Spin-squared Hamiltonian of next-to-leading order gravitational interaction*, Phys. Rev. D **78** (2008) 101503 [`0809.2200`].

[205] S. Marsat, A. Bohe, G. Faye and L. Blanchet, *Next-to-next-to-leading order spin-orbit effects in the equations of motion of compact binary systems*, Class. Quant. Grav. **30** (2013) 055007 [`1210.4143`].

[206] S. Hergt, J. Steinhoff and G. Schaefer, *Reduced Hamiltonian for next-to-leading order Spin-Squared Dynamics of General Compact Binaries*, Class. Quant. Grav. **27** (2010) 135007 [`1002.2093`].

[207] R. A. Porto, A. Ross and I. Z. Rothstein, *Spin induced multipole moments for the gravitational wave amplitude from binary inspirals to 2.5 Post-Newtonian order*, JCAP **09** (2012) 028 [`1203.2962`].

[208] S. Hergt, J. Steinhoff and G. Schaefer, *On the comparison of results regarding the post-Newtonian approximate treatment of the dynamics of extended spinning compact binaries*, *J. Phys. Conf. Ser.* **484** (2014) 012018 [1205.4530].

[209] A. Bohe, S. Marsat, G. Faye and L. Blanchet, *Next-to-next-to-leading order spin-orbit effects in the near-zone metric and precession equations of compact binaries*, *Class. Quant. Grav.* **30** (2013) 075017 [1212.5520].

[210] J. Hartung, J. Steinhoff and G. Schafer, *Next-to-next-to-leading order post-Newtonian linear-in-spin binary Hamiltonians*, *Annalen Phys.* **525** (2013) 359 [1302.6723].

[211] S. Marsat, L. Blanchet, A. Bohe and G. Faye, *Gravitational waves from spinning compact object binaries: New post-Newtonian results*, 12, 2013, 1312.5375.

[212] A. Bohé, G. Faye, S. Marsat and E. K. Porter, *Quadratic-in-spin effects in the orbital dynamics and gravitational-wave energy flux of compact binaries at the 3PN order*, *Class. Quant. Grav.* **32** (2015) 195010 [1501.01529].

[213] D. Bini, A. Geralico and J. Vines, *Hyperbolic scattering of spinning particles by a Kerr black hole*, *Phys. Rev. D* **96** (2017) 084044 [1707.09814].

[214] N. Siemonsen, J. Steinhoff and J. Vines, *Gravitational waves from spinning binary black holes at the leading post-Newtonian orders at all orders in spin*, *Phys. Rev. D* **97** (2018) 124046 [1712.08603].

[215] R. A. Porto and I. Z. Rothstein, *Comment on 'On the next-to-leading order gravitational spin(1) - spin(2) dynamics' by J. Steinhoff et al*, 0712.2032.

[216] J.-W. Kim, M. Levi and Z. Yin, *Quadratic-in-spin interactions at the fifth post-Newtonian order probe new physics*, 2112.01509.

[217] G. Cho, B. Pardo and R. A. Porto, *Gravitational radiation from inspiralling compact objects: Spin-spin effects completed at the next-to-leading post-Newtonian order*, *Phys. Rev. D* **104** (2021) 024037 [2103.14612].

[218] G. Cho, R. A. Porto and Z. Yang, *Gravitational radiation from inspiralling compact objects: Spin effects to fourth Post-Newtonian order*, 2201.05138.

[219] G. Schafer, *Acceleration-dependent lagrangians in general relativity*, *Phys. Lett. A* **100** (1984) 128.

[220] T. Damour and G. Schaefer, *Redefinition of position variables and the reduction of higher order Lagrangians*, *J. Math. Phys.* **32** (1991) 127.

[221] M. Chiodaroli, H. Johansson and P. Pichini, *Compton black-hole scattering for $s \leq 5/2$*, *JHEP* **02** (2022) 156 [2107.14779].

[222] A. Falkowski and C. S. Machado, *Soft Matters, or the Recursions with Massive Spinors*, *JHEP* **05** (2021) 238 [2005.08981].

236

[223] R. Aoude, K. Haddad and A. Helset, *Searching for Kerr in the 2PM amplitude, to appear* .

[224] Y. Iwasaki, *Fourth-order gravitational potential based on quantum field theory*, Lett. Nuovo Cim. **1S2** (1971) 783.

[225] S. N. Gupta and S. F. Radford, *IMPROVED GRAVITATIONAL COUPLING OF SCALAR FIELDS*, Phys. Rev. D **19** (1979) 1065.

[226] J. F. Donoghue, *General relativity as an effective field theory: The leading quantum corrections*, Phys. Rev. D **50** (1994) 3874 [`gr-qc/9405057`].

[227] N. E. J. Bjerrum-Bohr, J. F. Donoghue and B. R. Holstein, *Quantum gravitational corrections to the nonrelativistic scattering potential of two masses*, Phys. Rev. D **67** (2003) 084033 [`hep-th/0211072`].

[228] N. E. J. Bjerrum-Bohr, J. F. Donoghue and P. Vanhove, *On-shell Techniques and Universal Results in Quantum Gravity*, JHEP **02** (2014) 111 [`1309.0804`].

[229] A. Brandhuber, G. Chen, G. Travaglini and C. Wen, *Classical gravitational scattering from a gauge-invariant double copy*, JHEP **10** (2021) 118 [`2108.04216`].

[230] N. E. J. Bjerrum-Bohr, P. H. Damgaard, G. Festuccia, L. Planté and P. Vanhove, *General Relativity from Scattering Amplitudes*, Phys. Rev. Lett. **121** (2018) 171601 [`1806.04920`].

[231] Z. Bern, J. Parra-Martinez, R. Roiban, M. S. Ruf, C.-H. Shen, M. P. Solon et al., *Scattering Amplitudes, the Tail Effect, and Conservative Binary Dynamics at $O(G^4)$*, `2112.10750`.

[232] J. Blümlein, A. Maier, P. Marquard and G. Schäfer, *Testing binary dynamics in gravity at the sixth post-Newtonian level*, Phys. Lett. B **807** (2020) 135496 [`2003.07145`].

[233] D. Bini, T. Damour and A. Geralico, *Binary dynamics at the fifth and fifth-and-a-half post-Newtonian orders*, Phys. Rev. D **102** (2020) 024062 [`2003.11891`].

[234] D. Bini, T. Damour and A. Geralico, *Sixth post-Newtonian local-in-time dynamics of binary systems*, Phys. Rev. D **102** (2020) 024061 [`2004.05407`].

[235] D. Bini, T. Damour and A. Geralico, *Radiative contributions to gravitational scattering*, Phys. Rev. D **104** (2021) 084031 [`2107.08896`].

[236] J. Blümlein, A. Maier, P. Marquard and G. Schäfer, *The 6th post-Newtonian potential terms at $O(G_N^4)$*, Phys. Lett. B **816** (2021) 136260 [`2101.08630`].

[237] C. Dlapa, G. Kälin, Z. Liu and R. A. Porto, *Dynamics of Binary Systems to Fourth Post-Minkowskian Order from the Effective Field Theory Approach*, `2106.08276`.

[238] C. Dlapa, G. Kälin, Z. Liu and R. A. Porto, *Conservative Dynamics of Binary Systems at Fourth Post-Minkowskian Order in the Large-eccentricity Expansion*, `2112.11296`.

[239] D. Bini, T. Damour and A. Geralico, *Scattering of tidally interacting bodies in post-Minkowskian gravity*, *Phys. Rev. D* **101** (2020) 044039 [`2001.00352`].

[240] Z. Bern, L. J. Dixon, M. Perelstein and J. S. Rozowsky, *Multileg one loop gravity amplitudes from gauge theory*, *Nucl. Phys. B* **546** (1999) 423 [`hep-th/9811140`].

[241] X. O. Camanho, J. D. Edelstein, J. Maldacena and A. Zhiboedov, *Causality Constraints on Corrections to the Graviton Three-Point Coupling*, *JHEP* **02** (2016) 020 [`1407.5597`].

[242] N. Afkhami-Jeddi, S. Kundu and A. Tajdini, *A Bound on Massive Higher Spin Particles*, *JHEP* **04** (2019) 056 [`1811.01952`].

[243] C. Y. R. Chen, C. de Rham, A. Margalit and A. J. Tolley, *A cautionary case of casual causality*, *JHEP* **03** (2022) 025 [`2112.05031`].

[244] J. Vines, *et al.* unpublished.

[245] A. V. Smirnov, *Algorithm FIRE – Feynman Integral REduction*, *JHEP* **10** (2008) 107 [`0807.3243`].

[246] A. V. Smirnov and F. S. Chuharev, *FIRE6: Feynman Integral REduction with Modular Arithmetic*, *Comput. Phys. Commun.* **247** (2020) 106877 [`1901.07808`].

[247]

[248] A. Cucchieri, M. Porrati and S. Deser, *Tree level unitarity constraints on the gravitational couplings of higher spin massive fields*, *Phys. Rev. D* **51** (1995) 4543 [`hep-th/9408073`].

[249] I. Giannakis, J. T. Liu and M. Porrati, *Massive higher spin states in string theory and the principle of equivalence*, *Phys. Rev. D* **59** (1999) 104013 [`hep-th/9809142`].

[250] I. Cortese, R. Rahman and M. Sivakumar, *Consistent Non-Minimal Couplings of Massive Higher-Spin Particles*, *Nucl. Phys. B* **879** (2014) 143 [`1307.7710`].

[251] Y. Aharonov, A. Komar and L. Susskind, *Superluminal behavior, causality, and instability*, *Phys. Rev.* **182** (1969) 1400.

[252] A. Adams, N. Arkani-Hamed, S. Dubovsky, A. Nicolis and R. Rattazzi, *Causality, analyticity and an IR obstruction to UV completion*, *JHEP* **10** (2006) 014 [`hep-th/0602178`].

[253] J. Distler, B. Grinstein, R. A. Porto and I. Z. Rothstein, *Falsifying Models of New Physics via WW Scattering*, *Phys. Rev. Lett.* **98** (2007) 041601 [`hep-ph/0604255`].

[254] A. Gruzinov and M. Kleban, *Causality Constrains Higher Curvature Corrections to Gravity, Class. Quant. Grav.* **24** (2007) 3521 [`hep-th/0612015`].

[255] L. Vecchi, *Causal versus analytic constraints on anomalous quartic gauge couplings*, *JHEP* **11** (2007) 054 [`0704.1900`].

[256] I. Low, R. Rattazzi and A. Vichi, *Theoretical Constraints on the Higgs Effective Couplings*, *JHEP* **04** (2010) 126 [`0907.5413`].

[257] A. Nicolis, R. Rattazzi and E. Trincherini, *Energy's and amplitudes' positivity*, *JHEP* **05** (2010) 095 [`0912.4258`].

[258] C. Cheung and G. N. Remmen, *Infrared Consistency and the Weak Gravity Conjecture*, *JHEP* **12** (2014) 087 [`1407.7865`].

[259] D. Baumann, D. Green, H. Lee and R. A. Porto, *Signs of Analyticity in Single-Field Inflation*, *Phys. Rev. D* **93** (2016) 023523 [`1502.07304`].

[260] B. Bellazzini, C. Cheung and G. N. Remmen, *Quantum Gravity Constraints from Unitarity and Analyticity*, *Phys. Rev. D* **93** (2016) 064076 [`1509.00851`].

[261] B. Bellazzini, *Softness and amplitudes' positivity for spinning particles*, *JHEP* **02** (2017) 034 [`1605.06111`].

[262] C. Cheung and G. N. Remmen, *Positivity of Curvature-Squared Corrections in Gravity*, *Phys. Rev. Lett.* **118** (2017) 051601 [`1608.02942`].

[263] C. de Rham, S. Melville, A. J. Tolley and S.-Y. Zhou, *Positivity bounds for scalar field theories*, *Phys. Rev. D* **96** (2017) 081702 [`1702.06134`].

[264] C. de Rham, S. Melville, A. J. Tolley and S.-Y. Zhou, *UV complete me: Positivity Bounds for Particles with Spin*, *JHEP* **03** (2018) 011 [`1706.02712`].

[265] C. de Rham and A. J. Tolley, *Causality in curved spacetimes: The speed of light and gravity*, *Phys. Rev. D* **102** (2020) 084048 [`2007.01847`].

[266] D. Bai and Y.-H. Xing, *Higher Derivative Theories for Interacting Massless Gravitons in Minkowski Spacetime*, *Nucl. Phys. B* **932** (2018) 15 [`1610.00241`].

[267] A. J. Tolley, Z.-Y. Wang and S.-Y. Zhou, *New positivity bounds from full crossing symmetry*, *JHEP* **05** (2021) 255 [`2011.02400`].

[268] S. Caron-Huot and V. Van Duong, *Extremal Effective Field Theories*, *JHEP* **05** (2021) 280 [`2011.02957`].

[269] N. Arkani-Hamed, T.-C. Huang and Y.-T. Huang, *The EFT-Hedron*, *JHEP* **05** (2021) 259 [`2012.15849`].

[270] A. Sinha and A. Zahed, *Crossing Symmetric Dispersion Relations in Quantum Field Theories*, *Phys. Rev. Lett.* **126** (2021) 181601 [`2012.04877`].

[271] S. Caron-Huot, D. Mazac, L. Rastelli and D. Simmons-Duffin, *Sharp boundaries for the swampland*, *JHEP* **07** (2021) 110 [2102.08951].

[272] P. Benincasa and F. Cachazo, *Consistency Conditions on the S-Matrix of Massless Particles*, 0705.4305.

[273] S. Weinberg, *Photons and Gravitons in S-Matrix Theory: Derivation of Charge Conservation and Equality of Gravitational and Inertial Mass*, *Phys. Rev.* **135** (1964) B1049.

[274] S. Weinberg, *Photons and gravitons in perturbation theory: Derivation of Maxwell's and Einstein's equations*, *Phys. Rev.* **138** (1965) B988.

[275] Y.-t. Huang, J.-Y. Liu, L. Rodina and Y. Wang, *Carving out the Space of Open-String S-matrix*, *JHEP* **04** (2021) 195 [2008.02293].

[276] D. Meltzer and E. Perlmutter, *Beyond $a = c$: gravitational couplings to matter and the stress tensor OPE*, *JHEP* **07** (2018) 157 [1712.04861].

[277] A. Belin, D. M. Hofman and G. Mathys, *Einstein gravity from ANEC correlators*, *JHEP* **08** (2019) 032 [1904.05892].

[278] M. Kologlu, P. Kravchuk, D. Simmons-Duffin and A. Zhiboedov, *Shocks, Superconvergence, and a Stringy Equivalence Principle*, *JHEP* **11** (2020) 096 [1904.05905].

[279] J. Kaplan and S. Kundu, *Causality constraints in large N QCD coupled to gravity*, *Phys. Rev. D* **104** (2021) L061901 [2009.08460].

[280] S. Caron-Huot, D. Mazac, L. Rastelli and D. Simmons-Duffin, *Dispersive CFT Sum Rules*, *JHEP* **05** (2021) 243 [2008.04931].

[281] T. Trott, *Causality, unitarity and symmetry in effective field theory*, *JHEP* **07** (2021) 143 [2011.10058].

[282] A. Guerrieri, J. Penedones and P. Vieira, *Where Is String Theory in the Space of Scattering Amplitudes?*, *Phys. Rev. Lett.* **127** (2021) 081601 [2102.02847].

[283] D. C. Dunbar and P. S. Norridge, *Calculation of graviton scattering amplitudes using string based methods*, *Nucl. Phys. B* **433** (1995) 181 [hep-th/9408014].

[284] R. Britto and E. Mirabella, *External leg corrections in the unitarity method*, *JHEP* **01** (2012) 045 [1109.5106].

[285] M. L. Mangano and S. J. Parke, *Multiparton amplitudes in gauge theories*, *Phys. Rept.* **200** (1991) 301 [hep-th/0509223].

[286] Z. Bern and D. A. Kosower, *The Computation of loop amplitudes in gauge theories*, *Nucl. Phys. B* **379** (1992) 451.

[287] Z. Bern, A. De Freitas, L. J. Dixon and H. L. Wong, *Supersymmetric regularization, two loop QCD amplitudes and coupling shifts*, *Phys. Rev. D* **66** (2002) 085002 [`hep-ph/0202271`].

[288] Z. Bern, A. De Freitas and L. J. Dixon, *Two loop helicity amplitudes for gluon-gluon scattering in QCD and supersymmetric Yang-Mills theory*, *JHEP* **03** (2002) 018 [`hep-ph/0201161`].

[289] A. Broggio, C. Gnendiger, A. Signer, D. Stöckinger and A. Visconti, *SCET approach to regularization-scheme dependence of QCD amplitudes*, *JHEP* **01** (2016) 078 [`1506.05301`].

[290] Z. Bern, L. J. Dixon and D. A. Kosower, *Dimensionally regulated pentagon integrals*, *Nucl. Phys. B* **412** (1994) 751 [`hep-ph/9306240`].

[291] R. J. Eden, P. V. Landshoff, D. I. Olive and J. C. Polkinghorne, *The analytic S-matrix*. Cambridge Univ. Press, Cambridge, 1966.

[292] Z. Bern, L. J. Dixon and D. A. Kosower, *Two-loop g —> gg splitting amplitudes in QCD*, *JHEP* **08** (2004) 012 [`hep-ph/0404293`].

[293] Z. Bern, J. J. M. Carrasco, L. J. Dixon, H. Johansson and R. Roiban, *The Complete Four-Loop Four-Point Amplitude in N=4 Super-Yang-Mills Theory*, *Phys. Rev. D* **82** (2010) 125040 [`1008.3327`].

[294] Z. Bern, J. J. M. Carrasco, H. Johansson and R. Roiban, *The Five-Loop Four-Point Amplitude of N=4 super-Yang-Mills Theory*, *Phys. Rev. Lett.* **109** (2012) 241602 [`1207.6666`].

[295] Z. Bern, J. J. Carrasco, W.-M. Chen, A. Edison, H. Johansson, J. Parra-Martinez et al., *Ultraviolet Properties of $\mathcal{N} = 8$ Supergravity at Five Loops*, *Phys. Rev. D* **98** (2018) 086021 [`1804.09311`].

[296] C. F. Berger, Z. Bern, L. J. Dixon, F. Febres Cordero, D. Forde, H. Ita et al., *An Automated Implementation of On-Shell Methods for One-Loop Amplitudes*, *Phys. Rev. D* **78** (2008) 036003 [`0803.4180`].

[297] M. Porrati, *Massive spin 5/2 fields coupled to gravity: Tree level unitarity versus the equivalence principle*, *Phys. Lett. B* **304** (1993) 77 [`gr-qc/9301012`].

[298] S. Deser and A. Waldron, *Inconsistencies of massive charged gravitating higher spins*, *Nucl. Phys. B* **631** (2002) 369 [`hep-th/0112182`].

[299] J. Bonifacio, K. Hinterbichler, A. Joyce and R. A. Rosen, *Massive and Massless Spin-2 Scattering and Asymptotic Superluminality*, *JHEP* **06** (2018) 075 [`1712.10020`].

[300] Z. Bern, L. J. Dixon and D. A. Kosower, *One loop corrections to five gluon amplitudes*, *Phys. Rev. Lett.* **70** (1993) 2677 [`hep-ph/9302280`].

[301] Z. Bern, L. J. Dixon and D. A. Kosower, *One loop corrections to two quark three gluon amplitudes*, *Nucl. Phys. B* **437** (1995) 259 [`hep-ph/9409393`].

[302] Z. Bern and A. G. Morgan, *Supersymmetry relations between contributions to one loop gauge boson amplitudes*, *Phys. Rev. D* **49** (1994) 6155 [`hep-ph/9312218`].

[303] P. Fayet, *Spontaneous Generation of Massive Multiplets and Central Charges in Extended Supersymmetric Theories*, *Nucl. Phys. B* **149** (1979) 137.

[304] F. Quevedo, S. Krippendorf and O. Schlotterer, *Cambridge Lectures on Supersymmetry and Extra Dimensions*, `1011.1491`.

[305] R. H. Boels, *No triangles on the moduli space of maximally supersymmetric gauge theory*, *JHEP* **05** (2010) 046 [`1003.2989`].

[306] J. M. Henn, S. G. Naculich, H. J. Schnitzer and M. Spradlin, *Higgs-regularized three-loop four-gluon amplitude in N=4 SYM: exponentiation and Regge limits*, *JHEP* **04** (2010) 038 [`1001.1358`].

[307] J. M. Henn, S. G. Naculich, H. J. Schnitzer and M. Spradlin, *More loops and legs in Higgs-regulated N=4 SYM amplitudes*, *JHEP* **08** (2010) 002 [`1004.5381`].

[308] J. M. Henn, *Dual conformal symmetry at loop level: massive regularization*, *J. Phys. A* **44** (2011) 454011 [`1103.1016`].

[309] N. Craig, H. Elvang, M. Kiermaier and T. Slatyer, *Massive amplitudes on the Coulomb branch of N=4 SYM*, *JHEP* **12** (2011) 097 [`1104.2050`].

[310] M. Kiermaier, *The Coulomb-branch S-matrix from massless amplitudes*, `1105.5385`.

[311] H. Elvang, D. Z. Freedman and M. Kiermaier, *Integrands for QCD rational terms and N=4 SYM from massive CSW rules*, *JHEP* **06** (2012) 015 [`1111.0635`].

[312] A. Herderschee, S. Koren and T. Trott, *Massive On-Shell Supersymmetric Scattering Amplitudes*, *JHEP* **10** (2019) 092 [`1902.07204`].

[313] A. Herderschee, S. Koren and T. Trott, *Constructing $\mathcal{N} = 4$ Coulomb branch superamplitudes*, *JHEP* **08** (2019) 107 [`1902.07205`].

[314] L. F. Alday, J. M. Henn, J. Plefka and T. Schuster, *Scattering into the fifth dimension of N=4 super Yang-Mills*, *JHEP* **01** (2010) 077 [`0908.0684`].

[315] A. G. Morgan, *Second order fermions in gauge theories*, *Phys. Lett. B* **351** (1995) 249 [`hep-ph/9502230`].

[316] Y. M. Zinovev, *Spontaneous Symmetry Breaking in $N = 2$ Supergravity*, *Sov. J. Nucl. Phys.* **46** (1987) 540 [`hep-th/9512041`].

[317] N. Berkovits and M. M. Leite, *First massive state of the superstring in superspace*, *Phys. Lett. B* **415** (1997) 144 [`hep-th/9709148`].

[318] N. Berkovits and M. M. Leite, *Superspace action for the first massive states of the superstring*, *Phys. Lett. B* **454** (1999) 38 [`hep-th/9812153`].

[319] T. Gregoire, M. D. Schwartz and Y. Shadmi, *Massive supergravity and deconstruction*, *JHEP* **07** (2004) 029 [`hep-th/0403224`].

[320] G. 't Hooft and M. J. G. Veltman, *Regularization and Renormalization of Gauge Fields*, *Nucl. Phys. B* **44** (1972) 189.

[321] M. T. Grisaru, H. N. Pendleton and P. van Nieuwenhuizen, *Supergravity and the S Matrix*, *Phys. Rev. D* **15** (1977) 996.

[322] M. T. Grisaru and H. N. Pendleton, *Some Properties of Scattering Amplitudes in Supersymmetric Theories*, *Nucl. Phys. B* **124** (1977) 81.

[323] S. J. Parke and T. R. Taylor, *Perturbative QCD Utilizing Extended Supersymmetry*, *Phys. Lett. B* **157** (1985) 81.

[324] Z. Bern, L. J. Dixon, D. C. Dunbar, M. Perelstein and J. S. Rozowsky, *On the relationship between Yang-Mills theory and gravity and its implication for ultraviolet divergences*, *Nucl. Phys. B* **530** (1998) 401 [`hep-th/9802162`].

[325] S. Laporta, *High precision calculation of multiloop Feynman integrals by difference equations*, *Int. J. Mod. Phys. A* **15** (2000) 5087 [`hep-ph/0102033`].

[326] G. 't Hooft and M. J. G. Veltman, *One loop divergencies in the theory of gravitation*, *Ann. Inst. H. Poincare Phys. Theor. A* **20** (1974) 69.

[327] S. G. Naculich and H. J. Schnitzer, *Eikonal methods applied to gravitational scattering amplitudes*, *JHEP* **05** (2011) 087 [`1101.1524`].

[328] R. Akhoury, R. Saotome and G. Sterman, *Collinear and Soft Divergences in Perturbative Quantum Gravity*, *Phys. Rev. D* **84** (2011) 104040 [`1109.0270`].

[329] S. Abreu, F. Febres Cordero, H. Ita, M. Jaquier, B. Page, M. S. Ruf et al., *Two-Loop Four-Graviton Scattering Amplitudes*, *Phys. Rev. Lett.* **124** (2020) 211601 [`2002.12374`].

[330] P. van Nieuwenhuizen and C. C. Wu, *On Integral Relations for Invariants Constructed from Three Riemann Tensors and their Applications in Quantum Gravity*, *J. Math. Phys.* **18** (1977) 182.

[331] J. Broedel and L. J. Dixon, *Color-kinematics duality and double-copy construction for amplitudes from higher-dimension operators*, *JHEP* **10** (2012) 091 [`1208.0876`].

[332] N. Sennett, R. Brito, A. Buonanno, V. Gorbenko and L. Senatore, *Gravitational-Wave Constraints on an Effective Field-Theory Extension of General Relativity*, *Phys. Rev. D* **102** (2020) 044056 [`1912.09917`].

[333] S. Endlich, V. Gorbenko, J. Huang and L. Senatore, *An effective formalism for testing extensions to General Relativity with gravitational waves*, *JHEP* **09** (2017) 122 [1704.01590].

[334] S. A. Fulling, R. C. King, B. G. Wybourne and C. J. Cummins, *Normal forms for tensor polynomials. 1: The Riemann tensor*, *Class. Quant. Grav.* **9** (1992) 1151.

[335] D. C. Dunbar, J. H. Godwin, G. R. Jehu and W. B. Perkins, *Loop Amplitudes in an Extended Gravity Theory*, *Phys. Lett. B* **780** (2018) 41 [1711.05526].

[336] A. Brandhuber and G. Travaglini, *On higher-derivative effects on the gravitational potential and particle bending*, *JHEP* **01** (2020) 010 [1905.05657].

[337] M. Accettulli Huber, A. Brandhuber, S. De Angelis and G. Travaglini, *Eikonal phase matrix, deflection angle and time delay in effective field theories of gravity*, *Phys. Rev. D* **102** (2020) 046014 [2006.02375].

[338] W. T. Emond and N. Moynihan, *Scattering Amplitudes, Black Holes and Leading Singularities in Cubic Theories of Gravity*, *JHEP* **12** (2019) 019 [1905.08213].

[339] S. D. Chowdhury, A. Gadde, T. Gopalka, I. Halder, L. Janagal and S. Minwalla, *Classifying and constraining local four photon and four graviton S-matrices*, *JHEP* **02** (2020) 114 [1910.14392].

[340] L. Alberte, C. de Rham, S. Jaitly and A. J. Tolley, *QED positivity bounds*, *Phys. Rev. D* **103** (2021) 125020 [2012.05798].

[341] A. Hebbar, D. Karateev and J. Penedones, *Spinning S-matrix bootstrap in 4d*, *JHEP* **01** (2022) 060 [2011.11708].

[342] N. Arkani-Hamed, M. Pate, A.-M. Raclariu and A. Strominger, *Celestial amplitudes from UV to IR*, *JHEP* **08** (2021) 062 [2012.04208].

[343] A. Strominger, *Lectures on the Infrared Structure of Gravity and Gauge Theory*, 1703.05448.

[344] A. Martin, *Extension of the axiomatic analyticity domain of scattering amplitudes by unitarity. 1.*, *Nuovo Cim. A* **42** (1965) 930.

[345] J. Maldacena, S. H. Shenker and D. Stanford, *A bound on chaos*, *JHEP* **08** (2016) 106 [1503.01409].

[346] D. Chandorkar, S. D. Chowdhury, S. Kundu and S. Minwalla, *Bounds on Regge growth of flat space scattering from bounds on chaos*, *JHEP* **05** (2021) 143 [2102.03122].

[347] S. Caron-Huot, Z. Komargodski, A. Sever and A. Zhiboedov, *Strings from Massive Higher Spins: The Asymptotic Uniqueness of the Veneziano Amplitude*, *JHEP* **10** (2017) 026 [1607.04253].

[348] N. Arkani-Hamed, S. Dimopoulos and G. R. Dvali, *The Hierarchy problem and new dimensions at a millimeter*, *Phys. Lett. B* **429** (1998) 263 [`hep-ph/9803315`].

[349] L. Randall and R. Sundrum, *A Large mass hierarchy from a small extra dimension*, *Phys. Rev. Lett.* **83** (1999) 3370 [`hep-ph/9905221`].

[350] L. Randall and R. Sundrum, *An Alternative to compactification*, *Phys. Rev. Lett.* **83** (1999) 4690 [`hep-th/9906064`].

[351] C. Zhang and S.-Y. Zhou, *Convex Geometry Perspective on the (Standard Model) Effective Field Theory Space*, *Phys. Rev. Lett.* **125** (2020) 201601 [`2005.03047`].

[352] K. Yamashita, C. Zhang and S.-Y. Zhou, *Elastic positivity vs extremal positivity bounds in SMEFT: a case study in transversal electroweak gauge-boson scatterings*, *JHEP* **01** (2021) 095 [`2009.04490`].

[353] B. Bellazzini, J. Elias Miró, R. Rattazzi, M. Riembau and F. Riva, *Positive moments for scattering amplitudes*, *Phys. Rev. D* **104** (2021) 036006 [`2011.00037`].

[354] R. C. Brower, J. Polchinski, M. J. Strassler and C.-I. Tan, *The Pomeron and gauge/string duality*, *JHEP* **12** (2007) 005 [`hep-th/0603115`].

[355] Z. Bern and G. Chalmers, *Factorization in one loop gauge theory*, *Nucl. Phys. B* **447** (1995) 465 [`hep-ph/9503236`].

[356] N. Arkani-Hamed, L. Motl, A. Nicolis and C. Vafa, *The String landscape, black holes and gravity as the weakest force*, *JHEP* **06** (2007) 060 [`hep-th/0601001`].

[357] H. Ooguri and C. Vafa, *On the Geometry of the String Landscape and the Swampland*, *Nucl. Phys. B* **766** (2007) 21 [`hep-th/0605264`].

[358] T. D. Brennan, F. Carta and C. Vafa, *The String Landscape, the Swampland, and the Missing Corner*, *PoS* **TASI2017** (2017) 015 [`1711.00864`].

[359] E. Palti, *The Swampland: Introduction and Review*, *Fortsch. Phys.* **67** (2019) 1900037 [`1903.06239`].

[360] M. van Beest, J. Calderón-Infante, D. Mirfendereski and I. Valenzuela, *Lectures on the Swampland Program in String Compactifications*, `2102.01111`.

[361] A. Bissi, P. Dey and T. Hansen, *Dispersion Relation for CFT Four-Point Functions*, *JHEP* **04** (2020) 092 [`1910.04661`].

[362] D. Carmi and S. Caron-Huot, *A Conformal Dispersion Relation: Correlations from Absorption*, *JHEP* **09** (2020) 009 [`1910.12123`].

[363] D. Mazáč, L. Rastelli and X. Zhou, *A basis of analytic functionals for CFTs in general dimension*, *JHEP* **08** (2021) 140 [`1910.12855`].

[364] J. Penedones, J. A. Silva and A. Zhiboedov, *Nonperturbative Mellin Amplitudes: Existence, Properties, Applications*, *JHEP* **08** (2020) 031 [1912.11100].

[365] N. Afkhami-Jeddi, S. Kundu and A. Tajdini, *A Conformal Collider for Holographic CFTs*, *JHEP* **10** (2018) 156 [1805.07393].

[366] M. E. Peskin and D. V. Schroeder, *An Introduction to quantum field theory*. Addison-Wesley, Reading, USA, 1995.

[367] W. Pauli and M. Fierz, *On Relativistic Field Equations of Particles With Arbitrary Spin in an Electromagnetic Field*, *Helv. Phys. Acta* **12** (1939) 297.

[368] Z. Bern, D. C. Dunbar and T. Shimada, *String based methods in perturbative gravity*, *Phys. Lett. B* **312** (1993) 277 [hep-th/9307001].

[369] M. Correia, A. Sever and A. Zhiboedov, *An analytical toolkit for the S-matrix bootstrap*, *JHEP* **03** (2021) 013 [2006.08221].

[370] L. M. Brown and R. P. Feynman, *Radiative corrections to Compton scattering*, *Phys. Rev.* **85** (1952) 231.

[371] L. M. Brown, *Analytic properties of npoint loops in perturbation theory*, *Nuovo Cim.* **22** (1961) 178.

[372] B. Petersson, *Reduction of a one-loop Feynman diagram with n vertices in m-dimensional Lorentz space*, *J. Math. Phys.* **6** (1965) 1955.

[373] D. B. Melrose, *Reduction of Feynman diagrams*, *Nuovo Cim.* **40** (1965) 181.

[374] G. 't Hooft and M. J. G. Veltman, *Scalar One Loop Integrals*, *Nucl. Phys. B* **153** (1979) 365.

[375] W. L. van Neerven and J. A. M. Vermaseren, *LARGE LOOP INTEGRALS*, *Phys. Lett. B* **137** (1984) 241.

[376] R. G. Stuart, *Algebraic Reduction of One Loop Feynman Diagrams to Scalar Integrals*, *Comput. Phys. Commun.* **48** (1988) 367.

[377] G. J. van Oldenborgh and J. A. M. Vermaseren, *New Algorithms for One Loop Integrals*, *Z. Phys. C* **46** (1990) 425.

[378] A. Denner, U. Nierste and R. Scharf, *A Compact expression for the scalar one loop four point function*, *Nucl. Phys. B* **367** (1991) 637.

[379] A. I. Davydychev, *Standard and hypergeometric representations for loop diagrams and the photon-photon scattering*, in *7th International Seminar on High-energy Physics*, 5, 1993, hep-ph/9307323.

[380] Z. Bern, L. J. Dixon and D. A. Kosower, *Dimensionally regulated one loop integrals*, *Phys. Lett. B* **302** (1993) 299 [hep-ph/9212308].

[381] W. Buchmuller and D. Wyler, *CP violation, neutrino mixing and the baryon asymmetry, Phys. Lett. B* **521** (2001) 291 [hep-ph/0108216].

[382] I. Brivio and M. Trott, *The Standard Model as an Effective Field Theory, Phys. Rept.* **793** (2019) 1 [1706.08945].

[383] S. Dubovsky, L. Hui, A. Nicolis and D. T. Son, *Effective field theory for hydrodynamics: thermodynamics, and the derivative expansion, Phys. Rev. D* **85** (2012) 085029 [1107.0731].

[384] C. Cheung, P. Creminelli, A. L. Fitzpatrick, J. Kaplan and L. Senatore, *The Effective Field Theory of Inflation, JHEP* **03** (2008) 014 [0709.0293].

[385] J. J. M. Carrasco, M. P. Hertzberg and L. Senatore, *The Effective Field Theory of Cosmological Large Scale Structures, JHEP* **09** (2012) 082 [1206.2926].

[386] M. Froissart, *Asymptotic behavior and subtractions in the Mandelstam representation, Phys. Rev.* **123** (1961) 1053.

[387] A. Martin, *Unitarity and high-energy behavior of scattering amplitudes, Phys. Rev.* **129** (1963) 1432.

[388] K. Häring and A. Zhiboedov, *Gravitational Regge bounds*, 2202.08280.

[389] S. Caron-Huot, D. Mazac, L. Rastelli and D. Simmons-Duffin, *AdS bulk locality from sharp CFT bounds, JHEP* **11** (2021) 164 [2106.10274].

[390] S. Caron-Huot, Y.-Z. Li, J. Parra-Martinez and D. Simmons-Duffin, *Causality constraints on corrections to Einstein gravity*, 2201.06602.

[391] L.-Y. Chiang, Y.-t. Huang, W. Li, L. Rodina and H.-C. Weng, *(Non)-projective bounds on gravitational EFT*, 2201.07177.

[392] L.-Y. Chiang, Y.-t. Huang, L. Rodina and H.-C. Weng, *De-projecting the EFThedron*, 2204.07140.

[393] Y. Shadmi and Y. Weiss, *Effective Field Theory Amplitudes the On-Shell Way: Scalar and Vector Couplings to Gluons, JHEP* **02** (2019) 165 [1809.09644].

[394] S. Ferrara, A. F. Grillo, G. Parisi and R. Gatto, *Covariant expansion of the conformal four-point function, Nucl. Phys. B* **49** (1972) 77.

[395] S. Ferrara, R. Gatto and A. F. Grillo, *Properties of Partial Wave Amplitudes in Conformal Invariant Field Theories, Nuovo Cim. A* **26** (1975) 226.

[396] F. A. Dolan and H. Osborn, *Conformal four point functions and the operator product expansion, Nucl. Phys. B* **599** (2001) 459 [hep-th/0011040].

[397] F. A. Dolan and H. Osborn, *Conformal partial waves and the operator product expansion, Nucl. Phys. B* **678** (2004) 491 [hep-th/0309180].

247

[398] C. Itzykson and J. B. Zuber, *Quantum Field Theory*, International Series In Pure and Applied Physics. McGraw-Hill, New York, 1980.

[399] T. N. Pham and T. N. Truong, *Evaluation of the Derivative Quartic Terms of the Meson Chiral Lagrangian From Forward Dispersion Relation*, Phys. Rev. D **31** (1985) 3027.

[400] B. Ananthanarayan, D. Toublan and G. Wanders, *Consistency of the chiral pion pion scattering amplitudes with axiomatic constraints*, Phys. Rev. D **51** (1995) 1093 [hep-ph/9410302].

[401] M. R. Pennington and J. Portoles, *The Chiral Lagrangian parameters, l1, l2, are determined by the rho resonance*, Phys. Lett. B **344** (1995) 399 [hep-ph/9409426].

[402] S. D. Chowdhury, K. Ghosh, P. Haldar, P. Raman and A. Sinha, *Crossing Symmetric Spinning S-matrix Bootstrap: EFT bounds*, 2112.11755.

[403] B. Bellazzini, M. Riembau and F. Riva, *The IR-Side of Positivity Bounds*, 2112.12561.

[404] L.-Y. Chiang, Y.-t. Huang, W. Li, L. Rodina and H.-C. Weng, *Into the EFThedron and UV constraints from IR consistency*, 2105.02862.

[405] C. Cheung and G. N. Remmen, *Naturalness and the Weak Gravity Conjecture*, Phys. Rev. Lett. **113** (2014) 051601 [1402.2287].

[406] N. Arkani-Hamed, Y.-t. Huang, J.-Y. Liu and G. N. Remmen, *Causality, Unitarity, and the Weak Gravity Conjecture*, 2109.13937.

[407] A. V. Manohar and V. Mateu, *Dispersion Relation Bounds for pi pi Scattering*, Phys. Rev. D **77** (2008) 094019 [0801.3222].

[408] G. N. Remmen and N. L. Rodd, *Consistency of the Standard Model Effective Field Theory*, JHEP **12** (2019) 032 [1908.09845].

[409] G. N. Remmen and N. L. Rodd, *Signs, spin, SMEFT: Sum rules at dimension six*, Phys. Rev. D **105** (2022) 036006 [2010.04723].

[410] C. Cheung and G. N. Remmen, *Positive Signs in Massive Gravity*, JHEP **04** (2016) 002 [1601.04068].

[411] X. Li, H. Xu, C. Yang, C. Zhang and S.-Y. Zhou, *Positivity in Multifield Effective Field Theories*, Phys. Rev. Lett. **127** (2021) 121601 [2101.01191].

[412] S. Caron-Huot, D. Simmons-Duffin, J. Parra-Martinez and Y. Zhou, *Graviton partial waves and causality in higher dimensions*, to appear (2022) [2205.xxxxx].

[413] R. Boels, *Covariant representation theory of the Poincare algebra and some of its extensions*, JHEP **01** (2010) 010 [0908.0738].

[414] M. T. Grisaru, W. Siegel and M. Rocek, *Improved Methods for Supergraphs*, *Nucl. Phys. B* **159** (1979) 429.

[415] N. Seiberg, *Exact results on the space of vacua of four-dimensional SUSY gauge theories*, *Phys. Rev. D* **49** (1994) 6857 [`hep-th/9402044`].

[416] K. A. Intriligator, R. G. Leigh and N. Seiberg, *Exact superpotentials in four-dimensions*, *Phys. Rev. D* **50** (1994) 1092 [`hep-th/9403198`].

[417] I. Affleck, M. Dine and N. Seiberg, *Dynamical Supersymmetry Breaking in Chiral Theories*, *Phys. Lett. B* **137** (1984) 187.

[418] R. Dijkgraaf and C. Vafa, *A Perturbative window into nonperturbative physics*, `hep-th/0208048`.

[419] R. Dijkgraaf and C. Vafa, *Matrix models, topological strings, and supersymmetric gauge theories*, *Nucl. Phys. B* **644** (2002) 3 [`hep-th/0206255`].

[420] I. Bena and R. Roiban, *Exact superpotentials in $N = 1$ theories with flavor and their matrix model formulation*, *Phys. Lett. B* **555** (2003) 117 [`hep-th/0211075`].

[421] R. Dijkgraaf, M. T. Grisaru, C. S. Lam, C. Vafa and D. Zanon, *Perturbative computation of glueball superpotentials*, *Phys. Lett. B* **573** (2003) 138 [`hep-th/0211017`].

[422] R. Dijkgraaf, M. T. Grisaru, H. Ooguri, C. Vafa and D. Zanon, *Planar gravitational corrections for supersymmetric gauge theories*, *JHEP* **04** (2004) 028 [`hep-th/0310061`].

[423] F. Cachazo, M. R. Douglas, N. Seiberg and E. Witten, *Chiral rings and anomalies in supersymmetric gauge theory*, *JHEP* **12** (2002) 071 [`hep-th/0211170`].

[424] F. Cachazo, N. Seiberg and E. Witten, *Phases of $N=1$ supersymmetric gauge theories and matrices*, *JHEP* **02** (2003) 042 [`hep-th/0301006`].

[425] F. Cachazo, N. Seiberg and E. Witten, *Chiral rings and phases of supersymmetric gauge theories*, *JHEP* **04** (2003) 018 [`hep-th/0303207`].

[426] G. Veneziano and S. Yankielowicz, *An Effective Lagrangian for the Pure $N=1$ Supersymmetric Yang-Mills Theory*, *Phys. Lett. B* **113** (1982) 231.

[427] M. B. Green, J. H. Schwarz and L. Brink, *$N=4$ Yang-Mills and $N=8$ Supergravity as Limits of String Theories*, *Nucl. Phys. B* **198** (1982) 474.

[428] V. A. Smirnov, *Analytic tools for Feynman integrals*, vol. 250. Springer, 2012, 10.1007/978-3-642-34886-0.

[429] O. V. Tarasov, *A New approach to the momentum expansion of multiloop Feynman diagrams*, *Nucl. Phys. B* **480** (1996) 397 [`hep-ph/9606238`].

[430] O. V. Tarasov, *Generalized recurrence relations for two loop propagator integrals with arbitrary masses*, *Nucl. Phys. B* **502** (1997) 455 [`hep-ph/9703319`].

[431] O. V. Tarasov, *Connection between Feynman integrals having different values of the space-time dimension*, *Phys. Rev. D* **54** (1996) 6479 [`hep-th/9606018`].

[432] R. N. Lee, *Space-time dimensionality D as complex variable: Calculating loop integrals using dimensional recurrence relation and analytical properties with respect to D*, *Nucl. Phys. B* **830** (2010) 474 [`0911.0252`].

[433] R. N. Lee, *Calculating multiloop integrals using dimensional recurrence relation and D-analyticity*, *Nucl. Phys. B Proc. Suppl.* **205-206** (2010) 135 [`1007.2256`].

[434] C. Anastasiou and A. Daleo, *Numerical evaluation of loop integrals*, *JHEP* **10** (2006) 031 [`hep-ph/0511176`].

[435] F. V. Tkachov, *A Theorem on Analytical Calculability of Four Loop Renormalization Group Functions*, *Phys. Lett. B* **100** (1981) 65.

[436] K. Chetyrkin and F. Tkachov, *Integration by Parts: The Algorithm to Calculate beta Functions in 4 Loops*, *Nucl. Phys. B* **192** (1981) 159.

[437] S. Laporta and E. Remiddi, *The Analytical value of the electron (g-2) at order alpha**3 in QED*, *Phys. Lett. B* **379** (1996) 283 [`hep-ph/9602417`].

[438] S. Laporta, *High precision calculation of multiloop Feynman integrals by difference equations*, *Int. J. Mod. Phys. A* **15** (2000) 5087 [`hep-ph/0102033`].

[439] R. K. Ellis and G. Zanderighi, *Scalar one-loop integrals for QCD*, *JHEP* **02** (2008) 002 [`0712.1851`].

[440] M. Beneke and V. A. Smirnov, *Asymptotic expansion of Feynman integrals near threshold*, *Nucl. Phys. B* **522** (1998) 321 [`hep-ph/9711391`].

[441] A. Edison, M. Guillen, H. Johansson, O. Schlotterer and F. Teng, *One-loop matrix elements of effective superstring interactions: α'-expanding loop integrands*, *JHEP* **12** (2021) 007 [`2107.08009`].

[442] F. Figueroa and P. Tourkine, *On the unitarity and low energy expansion of the Coon amplitude*, `2201.12331`.

[443] Y.-t. Huang and G. N. Remmen, *UV-Complete Gravity Amplitudes and the Triple Product*, `2203.00696`.

[444] J. M. Maldacena, *The Large N limit of superconformal field theories and supergravity*, *Adv. Theor. Math. Phys.* **2** (1998) 231 [`hep-th/9711200`].

[445] E. Witten, *Anti-de Sitter space and holography*, *Adv. Theor. Math. Phys.* **2** (1998) 253 [`hep-th/9802150`].

[446] S. S. Gubser, I. R. Klebanov and A. M. Polyakov, *Gauge theory correlators from noncritical string theory, Phys. Lett. B* **428** (1998) 105 [`hep-th/9802109`].

[447] J. Polchinski and M. J. Strassler, *The String dual of a confining four-dimensional gauge theory*, `hep-th/0003136`.

[448] J. Polchinski and M. J. Strassler, *Hard scattering and gauge/string duality, Phys. Rev. Lett.* **88** (2002) 031601 [`hep-th/0109174`].